UNIVERSIDAD DE GRANADA

FACULTAD DE FARMACIA

Departamento de Farmacología

Programa de Doctorado en Medicina Clínica

y Salud Pública

EFFECTS OF GUT MICROBIOTA-DERIVED PRODUCTS ON CARDIOVASCULAR COMPLICATIONS OF SYSTEMIC LUPUS ERYTHEMATOSUS

Tesis Doctoral para aspirar al Grado de Doctor presentada por

Javier Moleón Moya

Bajo la dirección de los Doctores:

Juan Manuel Duarte Pérez

Miguel Romero Pérez

Granada, 2024

Editor: Universidad de Granada. Tesis Doctorales
Autor: Javier Moleón Moya
ISBN: 978-84-1195-187-6
URI: https://hdl.handle.net/10481/89495

INDEX

INDEX

FIGURE INDEX

TABLE INDEX

ABBREVIATIONS

ABBREVIATIONS

ABC
Age-associated B Cells

ACE
Acetate

Ach
Acetylcholine

ANA
Anti-nuclear antibodies

ANOVA
Two-way repeated-measures analysis of variance

ARE
Antioxidant response element

BIPES
Barcoded Illumina paired-end sequencing

BP
Blood pressure

BUT
Butyrate

CTR
Control

CVD
Cardiovascular diseases

DAPI
4,6-diamidino-2-phenylindoledichlorohydrate

DC
Dendritic cells

DHE
Dihydroethidium

DMB
3,3-dimethyl-1-butanol

DMSO
Dimethyl sulfoxide

dsDNA
Double-stranded DNA

eNOS
Endothelial NO synthase

EpRE
Electrophile response element

FFAR
Free fatty acid receptor

FMT
Faecal microbiota transplantation

GF
Germfree

GLPG
GLPG-0974

GPR
G-protein coupled receptor

HDAC
Histone deacetylase

HEPES
4-(2-hydroxyethyl)-1-piperazineethanesulfonic acid

HIF
Hypoxia-inducible factor

HO-1
Heme oxygenase-1

IFN
Interferon

IL
Interleukin

IMQ
Imiquimod

ITF
Inulin-type fructans

KEGG
Kyoto encyclopedia of genes and genomes pathways

LDA
Linear discriminant analysis

LEfSe
Linear discriminant analysis effect size

LN
Lupus nephritis

LPR
Lupus-prone MRL/Mp-Fas

LPS
Lipopolysaccharide

MBP
Mean blood pressure

MCT
Proton-coupled monocarboxylate transporter

MIX
Antibiotic cocktail

MLN
Mesenteric lymph nodes

MUC
Mucin

Myd88
Myeloid differentiation primary response 88

NADPH
Nicotinamide adenine dinucleotide phosphate

nIL-17
IL-17-neutralizing antibody

NLRP3
Nod-like receptor family pyrin domain containing 3

NO
Nitric oxide

NOX
NADPH oxidase

NQO-1
NADPH quinone oxidoreductase-1

NRF-2
Nuclear factor erythroid 2-related factor 2

NZBWF1
New Zealand black/white F1

OCT
Optimum cutting temperature

OTU
Operational taxonomy unit

PAST
Palaeontological statistics

PBS
Phosphate-buffered saline

PCA
Principal components analysis

PCR
Polymerase chain reaction

pDC
Plasmacytoid dendritic cells

PICRUSt
Phylogenetic investigation of communities by reconstruction of unobserved states

PLS-DA
Partial least square discriminant analysis

PROP
Propionate

QIIME
Quantitative insights into microbial ecology

RDP
Ribosome database project

RG
Ruminococcus (blautia) gnavus

RhoA
Ras homolog gene family member A

RLU
Relative luminescence units

ROS
Reactive oxygen species

RPL13a
Ribosomal protein L13a

RS
Resistant starch

RT- PCR
Reverse transcriptase-polymerase chain reaction

SAH
SLE-associated hypertension

SBP
Systolic blood pressure

SCFA
Short chain fatty acid

SEM
Standard error of the mean

SFB
Segmented filamentous bacteria

SLE
Systemic lupus erythematosus

SLEDAI
SLE disease activity index

SPF
Specific pathogen-free

ssRNA
Single stranded RNA

TCR
T cell receptors

Th
T helper

TJ
Tight junctions

TLR
Toll- like receptor

TLS
Tertiary lymphoid structures

TMA
Trimethylamine

TMAO
TMA N-oxide

TNF
Tumour necrosis factor

Treg
T regulatory

VANCO
Vancomycin

VIP
Variable importance in projection

ZO-1
Zonula occludens-1

ABSTRACT

ABSTRACT

In this thesis, we embark on a comprehensive exploration of the multifaceted interactions between microbiota and SLE. Through a meticulous examination of existing literature, coupled with original research endeavors, we aim to delineate the mechanistic underpinnings that govern this intricate relationship. By elucidating the key players and pathways involved, we seek to pave the way for novel therapeutic approaches that harness the potential of gut microbiota and its metabolites in the management of SLE and its consequent cardiovascular complications. Therefore, the **general objective** of this thesis was to analyse the role of gut microbiota and its bacterial by-products (TMAO, SCFA) in the development of cardiovascular complications in SLE. To achieve this aim we performed several experiments:

I) Role of gut microbiota in the development of hypertension in a TLR-7-dependent lupus mouse model

Female BALB/cJRj mice were randomly assigned to four experimental groups: an untreated control (CTR), a group treated with the TLR-7 agonist imiquimod (IMQ), IMQ-treated with vancomycin, and IMQ-treated with a cocktail of broad-spectrum antibiotics. We carried out faecal microbiota transplant (FMT) from donor CTR or IMQ mice to recipient IMQ or CTR animals, respectively. Vancomycin inhibited the increase in blood pressure, improved kidney injury, endothelial function and oxidative stress, and reduced T helper (Th)17 infiltration in aortas from IMQ-treated mice. The rise in blood pressure and vascular complications present in IMQ mice were also observed in the CTR mice recipients of IMQ microbiota. Reduced relative populations of *Sutterella* and *Anaerovibrio* were associated to high blood pressure in our animals, which were increased after stool transplantation of healthy microbiota to IMQ mice. The reduced endothelium-dependent vasodilator responses to acetylcholine induced by IMQ microbiota were normalized after interleukin-17 neutralization. In conclusion, gut microbiota plays a role in the TLR7-driven increase in Th17 cell, endothelial dysfunction, vascular inflammation and hypertension. The vascular changes induced by IMQ microbiota were initiated by Th17 infiltrating the vasculature.

II) Role of TMAO in SLE development and cardiovascular complications in a lupus mouse model induced by TLR-7 activation

Female BALB/c mice were randomly divided into 4 groups: untreated control mice, control mice treated with the trimethylamine lyase inhibitor 3,3-dimethyl-1-butanol (DMB), IMQ mice, and IMQ mice treated with DMB. The DMB-treated groups were administered in their drinking water for 8 weeks. Treatment with DMB reduced plasma levels of TMAO in mice with IMQ-induced lupus. DMB prevents the development of hypertension, reduces disease progression (plasma levels of anti-dsDNA autoantibodies, splenomegaly and proteinuria), polarization of T lymphocytes towards Th17/Th1 in secondary lymph organs and improves endothelial function in mice with IMQ-induced lupus. The deleterious vascular effects caused by TMAO appear to be associated with an increase in vascular oxidative stress generated by increased NADPH oxidase activity, derived in part from the vascular infiltration of Th17/Th1 lymphocytes, and reduced NRF-2-driven antioxidant defense. In conclusion, our findings identify the bacterial-derived TMAO as a regulator of immune system allowing the development of autoimmunity and endothelial dysfunction in SLE mice.

III) Effects of SCFA on cardiovascular complications in TLR-7-induced lupus mouse model

SCFA and dietary fibers rich in resistant starch (RS) or inulin-type fructans (ITF) effectively prevented the development of hypertension and cardiac hypertrophy. Additionally, these treatments improved aortic relaxation and mitigated vascular oxidative stress. Both SCFA treatments also contributed to the maintenance of colonic integrity, reduced endotoxemia, and decreased the proportion of Th-17 cells in MLN, blood, and aorta in TLR7-induced SLE mice. The observed changes in MLNs were correlated with increased levels of GPR43 mRNA in mice treated with acetate and increased GPR41 levels along with decreased histone deacetylase (HDAC)-3 levels in mice treated with butyrate. Notably, the effects attributed to acetate, but not butyrate, were nullified when co-administered with the GPR43 antagonist GLPG-0974. T cell priming and differentiation into Th17 cells in MLNs, as well as increased Th17 cell infiltration, were linked to aortic endothelial dysfunction and hypertension subsequent to the transfer of faecal microbiota from IMQ-treated mice to germ-free (GF) mice. These effects were counteracted in GF mice through treatment with either acetate or butyrate. To conclude, these findings underscore the potential of SCFA consumption in averting hypertension by restoring balance to the interplay between the gut, immune system, and vascular wall in TLR-7-driven SLE.

IV) Role of dietary fiber intake in the raise of BP in NZBWF1 mice

Female NZBWF1 (SLE) mice were treated with dietary fibers rich in resistant-starch (RS) or inulin-type frutans (ITF). In addition, inoculation of faecal microbiota from these experimental groups to recipient normotensive female C57Bl/6J germ-free (GF) mice was performed. Both fiber treatments, especially RS, prevented the development of hypertension, renal injury, improved the aortic relaxation induced by acetylcholine, and the vascular oxidative stress. RS and ITF treatments increased the proportion of acetate-, and butyrate-producing bacteria, respectively, improved colonic inflammation and integrity, endotoxemia, and decreased Th17 proportion in MLN, blood, and aorta in SLE mice. However, disease activity (splenomegaly and anti-ds-DNA) was unaffected by both fibers. T cell priming and Th17 differentiation in MLNs and increased Th17 infiltration was linked to aortic endothelial dysfunction and hypertension after inoculation of faecal microbiota from SLE mice to GF mice, without changes in proteinuria and autoimmunity. All these effects were lower in GF mice after faecal inoculation from fiber treated SLE mice. In conclusion, these findings support that fiber consumption prevented the development of hypertension by rebalancing of dysfunctional gut-immune system-vascular wall axis in SLE.

All of these findings suggest that gut microbiota modulation based on dietary interventions could be a novel alternative for the prevention of SLE-linked cardiovascular complications.

INTRODUCTION

INTRODUCTION

1. Systemic lupus erythematosus

1.1. Definition

Systemic lupus erythematosus (SLE) is a heterogeneous chronic inflammatory autoimmune disorder, characterized by aberrant humoral and cellular immune responses (Islam et al. 2020). Abnormal B cells produce a high number of antinuclear antibodies, especially against double stranded-DNA (ds-DNA), forming immunocomplexes and causing damage to several tissues and organs such as the kidneys, the skin or the vascular system (Tsokos 2011). As a result, this pathology is associated with several complications, including cardiovascular diseases (CVD). In general, individuals with SLE face a significantly increased risk of stroke and myocardial infarction, ranging from two to three times higher compared to the general population.

Among premenopausal women, the risk of myocardial infarction is particularly notable, surpassing traditional risk estimates. One study even reported a 52-fold increase in the incidence of myocardial infarction among women with SLE aged 35 to 44 years (Manzi et al. 1997). While traditional CVD risk factors, such as hypertension and dyslipidaemia (Frostegård 2023), are likely contributors to CVD development in individuals with SLE, they cannot completely account for the elevated CVD risk observed in SLE patients. Several SLE-specific factors may also contribute to the onset and progression of CVD in these patients, including the use of corticosteroids and immune dysregulation, both innate and adaptive that are specific to lupus, as well as metabolic dysfunction (Oliveira and Kaplan 2022).

SLE is a relatively rare condition, with a prevalence of approximately 20 to 150 cases per 100,000 individuals, depending on the population studied (Uramoto et al. 1999). The prevalence of this pathology is 9 times higher in women compared to men, especially during childbearing years (Krasselt and Baerwald 2019; Tedeschi, Bermas, and Costenbader 2013), and it displays a broad set of characteristics, which vary from patient to patient. This makes the development of SLE very difficult to predict (La Paglia et al. 2017).

The aetiology of this disease remains unknown but it seems to be a combination of genetic, epigenetic, metabolic, environmental and hormonal factors (Edwards and Costenbader 2014; Li and Mohan 2007) leading to changes in blood

pressure (BP) (Wolf and Ryan 2019). Nonetheless, the pathophysiological mechanisms behind SLE-associated hypertension (SAH) are yet to be discovered.

1.2. General features

Lupus patients cannot be considered as a common set of characteristics because they exhibit a broad range of symptoms (Kiriakidou and Ching 2020). The preliminary presentation of lupus usually mimics a viral syndrome. Constitutional symptoms, such as weight loss, fatigue, and low-grade fever, are frequent and can be accompanied by arthritis (Seibold, Wechsler, and Cammarata 1980).

1.2.1. Clinical manifestations

Common clinical features include arthritis, skin rashes (such as malar rash or discoid lesions), oral ulcers, photosensitivity, and alopecia. Organ involvement can occur in the kidneys, resulting in lupus nephritis (LN); heart, leading to pericarditis or myocarditis; lungs, causing pleuritis; and central nervous system, resulting in neuropsychiatric lupus. Hematologic abnormalities, such as anemia, leukopenia, and thrombocytopenia, are frequently observed (D'Cruz, Khamashta, and Hughes 2007; Gladman, Ibañez, and Urowitz 2002).

Up to 75%–80% of patients may experience cutaneous symptoms, which can be classified in acute, subacute, chronic, and bullous lupus (Vera-Recabarren et al. 2010). Although the typical early symptoms are fever, rash, and arthritis, sudden start with target-organ involvement is very frequent, especially in Hispanics (61%) and African Americans (45%), as opposed to whites (41%) (Alarcón et al. 1999).

In addition to the symptoms abovementioned, an assortment of cardiovascular signs can be observed in SLE patients. A higher incidence of atherosclerosis risk factors has been described as well as the presence of atherosclerotic plaque, which may form as a result of autoimmune vascular damage (Frostegård 2008; Hak et al. 2009).

These patients may also experience accelerated ischemic coronary artery disease and myocarditis at the heart level (Kaul et al. 2016; Liu and Kaplan 2018). CVD are not only prevalent in SLE, but also responsible for the most of fatalities among patients. Additionally, the main traditional risk factor for the development of renal and cardiovascular disorders is hypertension. Patients with SLE have been found to have a 3 times higher risk of fatal myocardial infarction than age- and gender-matched control subjects (Al-Herz et al. 2003).

Although a large number of studies show an enhanced prevalence of hypertension in SLE patients, mechanistic investigations for SAH are uncommon (Ryan 2009) and must be investigated in depth.

1.2.2. Diagnosis

SLE assessment must be performed whether any of these hematologic alterations is found, such as thrombocytopenia, leukopenia, lymphopenia, or anemia; respiratory symptoms, such as cough, dyspnea, hemoptysis, or pleuritic pain; renal findings, such as hematuria, proteinuria, cellular casts, or elevated serum creatinine level; or central nervous system signs, such as headache, photophobia, or focal neurologic deficits (Kiriakidou and Ching 2020).

Although diagnostic criteria may vary among countries, the American College of Rheumatology guideline has been widely accepted (Hochberg 1997). According to this, patients with 4 of the 11 criteria, the diagnosis of SLE can be made with 95% specificity and 85% sensitivity (Tunnicliffe et al. 2015).

Recently, these criteria were updated and published as a result of a collaboration between European and American rheumatology specialists (Aringer et al. 2019). Despite its broad applicability, its accuracy in juvenile SLE is not yet the best diagnostic tool (Chang et al. 2022). This diagnostic compilation emphasizes immunological abnormalities and LN, focusing on anti-dsDNA antibodies as an outcome predictor in SLE. It also highlights the complement as a possible biomarker in clinical practice since the frequency of hypocomplementemia (low C3 or C4) at diagnosis of SLE is 50%–89%. As a result, new diagnostic strategies based on measuring complement fragments and derivatives are becoming relevant (Ayano and Horiuchi 2023; Troldborg et al. 2018). To understand the relevance of these immune mediators as biomarkers in SLE detection we will tackle their role in the pathogenesis of the disease.

1.3. Pathogenesis

The onset and progression of SLE are influenced by genetic, environmental, and stochastic factors (Nandakumar and Nündel 2022). Genome-wide association studies have shown more than 40 susceptibility loci associated with this disease, mainly related with Toll-like receptor (TLR) signalling, processing of immune complexes and production of type I interferon (IFN-I) (Cui, Sheng, and Zhang 2013). Furthermore, SLE is classified as an autoimmune disorder wherein the participation of the immune system holds pivotal significance in the genesis of the pathology.

According to this, the investigation into the pathogenesis of SLE has identified two critical classes of mediators as fundamental contributors to the progression of the disease: IFN-I and autoantibodies directed against nucleic acids and nucleic acid-binding proteins (ANA) (Crow 2023).

On the one hand, IFN-I is mainly produced by plasmacytoid dendritic cells (pDC) and functions as an immunological adjuvant that fosters the activation of the entire immune system, and it especially aids in the differentiation of B cells and the synthesis of inflammatory chemokines (Eloranta and Rönnblom 2016). It might increase the threshold for B cell receptor signaling in B-cell progenitors, affecting the effectiveness of tolerance mechanisms that rely on the elimination of self-reactive cells and promoting ultimately ANA production (Sindhava et al. 2017).

On the other hand, the apparent induction of remission by anti-CD19 CAR T-cell therapy in several patients with severe SLE (Mackensen et al. 2022) suggests that autoantibodies, especially those complexed with nucleic acids in the form of immune complexes, are crucial mediators of tissue inflammation and damage in patients with SLE. ANA are mainly produced by a specific subset of B cells known as age-associated B cells (ABC) and, within its immunomodulatory functions, autoantibodies induce inflammatory mediators such as IFN-I (Savarese et al. 2006).

SLE organ damage is thus a consequence of this feedback loop where IFN-I and ANA are involved. In compliance with this idea, investigations have delineated three principal immune pathways implicated in the onset and progression of the disease (**Figure 1**):

I) The faulty clearance of cellular remnants and immune complexes (efferocytosis) is a notable phenomenon in lupus patients (Geng et al. 2022). Macrophages and monocytes from individuals with lupus exhibit a marked reduction in their phagocytic capacities. This leads to the accumulation of undigested cellular debris, which can serve as a reservoir of auto-antigens, consequently fostering the production of auto-antibodies. The removal of apoptotic cells by macrophages is imperative in averting autoimmune disorders. While the components involved in the processes of recognition and phagocytosis of apoptotic cells have been identified, the transcriptional framework governing the identification and elimination of these cells remains to be elucidated (Liu and Davidson 2012).

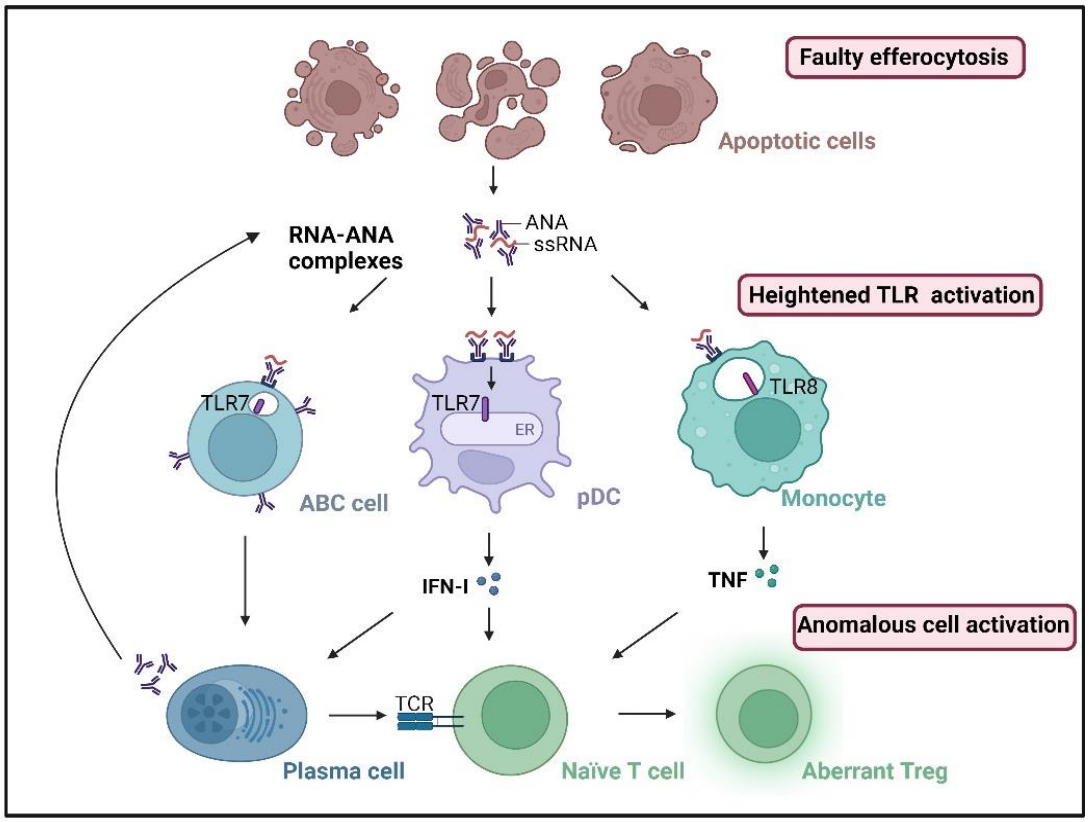

Figure 1. Principal immune pathways implicated in SLE.

Abbreviations: ANA, anti-nuclear antibody; ABC, Age-associated B cell; ER, endoplasmic reticulum; IFN-I, type I interferon; pDC, plasmacytoid dendritic cells; ssRNA, single stranded RNA; TCR, T cell receptor; TLR, Toll-like receptor; TNF, tumor necrosis factor.

II) The heightened activation of the innate immune system via TLR and IFN-α/IFN-β is noteworthy (Caielli et al. 2016; Khoryati et al. 2016). Specifically, the endosomal variants of these receptors, through the initiation of the myeloid differentiation primary response 88 (Myd88) protein signaling pathway, have been demonstrated to play a role in the overall development of SLE, as well as its associated LN (Christensen and Shlomchik 2007). This includes the notable shift in antibody isotype to IgG, a phenomenon commonly observed in SLE.

III) The anomalous activation of T and B lymphocytes, coupled with alterations observed in T, B, Natural Killer, and dendritic cells (DC) has also been recently documented (De Groof et al. 2017). Typically, aberrant B lymphocytes may display autoantibodies adhered to autoantigens on their surface. These complexes can be recognized by T cell receptors (TCR), leading to the subsequent maturation of naïve T cells. In addition, defective TCR signaling due to genetic and/or transcriptional abnormalities is known to contribute to SLE development via altered

thymic selection of self-reactive T cells, aberrant T helper (Th) cell activation, and dysfunction of T regulatory (Treg) cells (Tsokos 2020).

Despite the diverse pathways involved, all the aforementioned processes converge toward a common outcome: the production of autoantibodies, their subsequent accumulation, and deposition within target organs. As elucidated earlier, this results in several complications such as LN and hypertension (Liu and Kaplan 2018; Taylor and Ryan 2017).

1.3.1. SLE and cardiovascular complications

Hypertension is widely acknowledged as the foremost risk factor for cardiac events within lupus populations (Bartels et al. 2014). Indeed, prevalence rates ranging from 33% to 74% of SAH have been reported (Giannelou and Mavragani 2017). Despite the widespread occurrence of hypertension, the current guidelines for its management do not specifically address individuals with autoimmune disorders like SLE. This results in practitioners having to rely on existing recommendations designed for the general population (Tselios et al. 2014). Consequently, there is a deficiency of data derived from large-scale clinical trials in this specific context.

The challenge in regulating BP among patients with autoimmune disorders may stem from an incomplete understanding of the pathophysiological mechanisms. Research conducted using female New Zealand Black/White (NZBW) F1 mice, a spontaneous SLE model that mimics human disease progression and encompasses the development of SAH, has revealed a multifaceted interplay of factors contributing to the genesis of hypertension (Mathis et al. 2012). These include the inflammatory cytokine tumor necrosis factor (TNF)-α and oxidative stress. These mediators, which play a role in local inflammation and subsequent renal and vascular dysfunction, are likely downstream on the initial immune system dysregulation (Small et al. 2018; Wu et al. 2016).

The presence of hypertension in autoimmune disorders is associated with immune cell infiltration into the adventitia and periadventitial fat, along with the activation of T cells releasing proinflammatory cytokines such as interleukin (IL)-17a, IFN-γ, and TNF-α (Guzik et al. 2007; Madhur et al. 2010). In female NZBWF1 mice, hypertension is associated with low plasma renin levels and exhibits insensitivity to salt. In this SLE mouse model, treatment with anti-CD20 antibody, which reduces B cell percentages in the spleen and anti-dsDNA antibody levels in plasma, effectively prevents SAH development (Mathis et al. 2014). However, the precise roles of aberrant T and B lymphocytes in hypertension pathogenesis remain

unclear. Several studies suggest a self-perpetuating cycle linking immune cells, oxidative stress, and inflammation, significantly contributing to renal and vascular damage associated with SAH (Wu et al. 2016). T cell activation occurs both in secondary lymphoid organs and locally within target organs, particularly kidneys and blood vessels. Oxidative stress enhances neoantigen presentation in antigen-presenting cells through isoketal production, intensifying inflammatory responses (Mathis et al. 2012). Cytokine-triggered effector mechanisms encompass fibrosis, vasoconstriction, and Na+/H+ imbalance (Ryan 2013).

In both individuals with SLE and murine models, there is a significant presence of isolevuglandins, which are γ-ketoaldehydes formed through the reactive oxygen species (ROS) oxidation of fatty acids and phospholipids. These isolevuglandins are found in high levels as adducts on proteins, referred to as isolevuglandin adducts, specifically within monocytes and DC. Moreover, the binding of isolevuglandins to the transcription factor PU.1 at a crucial DNA binding site significantly inhibits the transcription of all C1q subunits. When SLE-prone mice were treated with the specific isolevuglandin scavenger 2-hydroxybenzylamine, there were noticeable improvements in various autoimmune parameters, including the reduction of plasma cell expansion, circulating IgG levels, and anti-dsDNA antibody titers. Additionally, the scavenger was able to lower BP, mitigate renal injury, and reduce the expression of inflammatory genes, particularly in DC that express C1q. Therefore, it can be concluded that ROS and isolevuglandin adducts play a pivotal role in the initiation and maintenance of systemic autoimmunity and hypertension in SLE (Patrick et al. 2022).

SAH is usually present together with endothelial dysfunction. This dysfunction manifests itself as the inability of endothelial cells to induce vasodilation through the activation of the endothelial nitric oxide synthase enzyme (eNOS) and the release of its product, nitric oxide (NO) (Deanfield et al. 2005).

High levels of IFN-I have been linked to endothelial dysfunction in patients with SLE (Somers et al. 2012). In particular, IFN-α may suppress insulin-stimulated NO generation by blocking eNOS mRNA and protein expression (Buie et al. 2017). Additionally, it has been demonstrated that TNF-α acts as a signal to reduce all eNOS activity. Furthermore, the administration of this cytokine impairs endothelial function in both human and rodent models (Chia et al. 2003; Wang, Ba, and Chaudry 1994)

Superoxide anion and other ROS are highly reactive and reduce NO bioavailability by forming peroxynitrites. These compounds have a number of detrimental effects on the structure and function of the vascular wall and are a major contributor to the development of endothelial dysfunction (Szabó,

Ischiropoulos, and Radi 2007). ROS are mainly produced by nicotinamide adenine dinucleotide phosphate (NADPH) oxidase in the vascular wall, whose activity can be increased by inflammatory cytokines such as TNF-α, IFN-γ or IL-17a (Nosalski and Guzik 2017). Treatments with either hydroxychloroquine or an antioxidant cocktail were able to inhibit superoxide anion production from the NADPH oxidase (NOX) and reduce hypertension and endothelial dysfunction in NZBWF1 mice, showing the key role of ROS in the development of endothelial dysfunction in SLE (Gómez-Guzmán et al. 2014).

In individuals with SLE there is a notable elevation in arterial stiffness when compared to control subjects (Sacre et al. 2014). This increased arterial stiffness, along with the properties of reflected pulse waves within the artery, can contribute to elevated systolic blood pressure (SBP) and pulse pressure. The primary mechanisms responsible for arterial stiffness involve endothelial dysfunction and the accumulation of collagen deposits in the extracellular matrix.

In summary, immunological cells and mediators are involved in the establishment and progression of SAH and endothelial dysfunction (**Figure 2**). Since CVD contribute to the morbidity and mortality of SLE, the control of BP in lupus patients is essential.

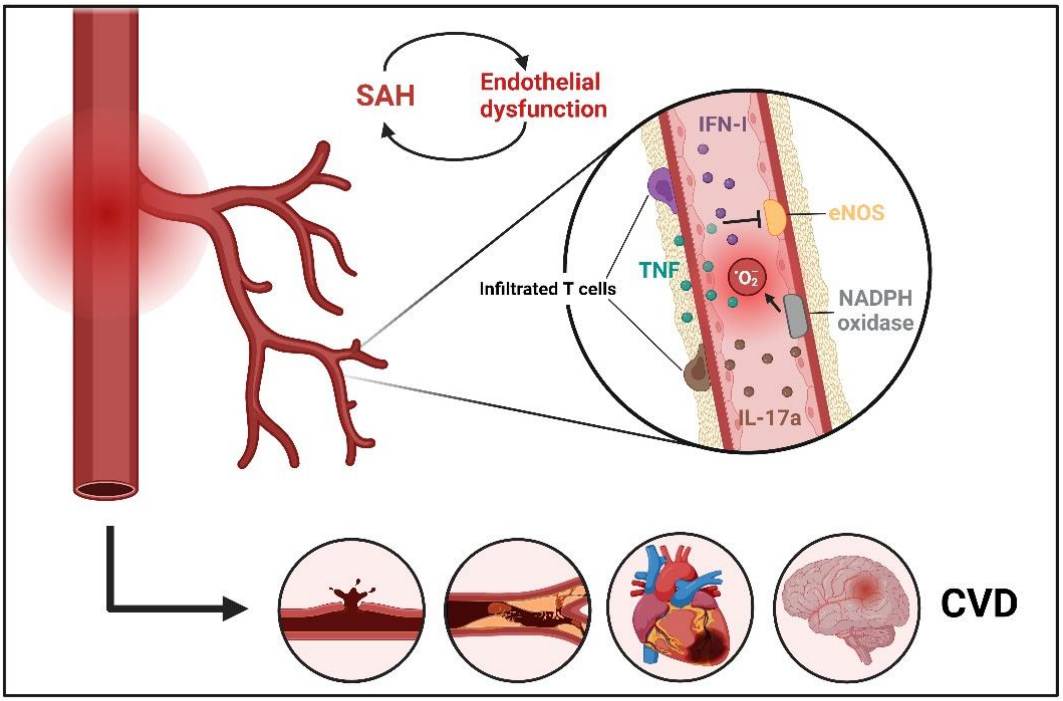

Figure 2. Immunological mediators involved in SAH and endothelial dysfunction.

Abbreviations: CVD, cardiovascular diseases; eNOS, endothelial NO synthase; IFN-I, type I interferon; IL-17a, interleukin 17a; NADPH, nicotinamide adenine dinucleotide phosphate; SAH, SLE-associated hypertension; TNF, tumor necrosis factor.

1.4. Treatments

Currently, the treatment and management of SLE primarily rely on non-steroidal anti-inflammatory drugs, glucocorticoids, hydroxychloroquine, and immunosuppressive agents (Durcan, O'Dwyer, and Petri 2019). Nevertheless, SLE management remains challenging due to the adverse effects associated with conventional therapies and the occurrence of refractory disease. Corticosteroid and azathioprine therapies, in particular, have been linked to an elevated incidence of CVD in lupus patients, worsening the SAH. Although antihypertensive medications are frequently warranted for patients with autoimmune diseases, not all of them receive the appropriate therapeutic interventions (Ikdahl et al. 2019).

Thus, there is an urgent need for new treatment approaches that can address renal and cardiovascular disorders in lupus patients without compromising their overall health. In this sense, cellular modulation of the autoimmune response is an area of great interest in lupus research (Chan et al. 2013), and one of the most promising perspectives for its study is the recently found link between the gut microbiome and the immune system (Santisteban et al. 2016).

Several studies have demonstrated that gut microbiome goes under a shift in composition in many diseases such as diabetes, inflammatory bowel disease and obesity (Gomes, Hoffmann, and Mota 2018; Iatcu, Steen, and Covasa 2021; Martel et al. 2022). These changes in the microbiota are known as dysbiosis. Notwithstanding the rising relevance of microbiome-immune system interactions, limited knowledge exists regarding the role of gut microbiota in SLE (Katz-Agranov and Zandman-Goddard 2017; Rosser and Mauri 2016).

2. SLE and microbiota

A unique set of microorganisms (viruses, archaea, bacteria and fungi) that find their niches in and on the body together with the interactions among them and the host compose the mammalian microbiome (Shanahan, Ghosh, and O'Toole 2021). One of those niches is located in the gut, and it is particularly dominated by *Firmicutes* and *Bacteroidetes*, and in lower quantities by *Actinobacteria, Proteobacteria, Synergistetes, Verrucomicrobia and Fusobacteria* (McCallum and Tropini 2023). Nonetheless, the prevalence of these bacteria can be altered due to changes in environmental factors such as hormones, diet, exercise and diseases of the host (Gentile and Weir 2018). Microbiota has emerged as a pivotal player due to its impact on host health, influencing not only gastrointestinal functions but also systemic immune responses (Belkaid and Harrison 2017). Dysregulation of microbiota parameters such as abundance, localisation or function can induce a loss of tolerance which leads to autoimmune diseases (Ruff, Greiling, and Kriegel 2020). Within this context, SLE stands as a compelling area of study.

2.1. Dysbiosis

Since gut microbiome is highly variable interindividually, it is very challenging to identify and define a standard pattern (McCallum and Tropini 2023). Due to their inverse correlation with the presence of chronic diseases, certain ecological parameters of microbial stability, such as diversity or richness, are frequently used as biomarkers for gut health rather than examining individual populations (Cotillard et al. 2013). However, the study of certain specific populations of bacteria can also be fundamental to determine the key mechanisms of dysbiosis and its link to pathological states.

2.1.1. Gut dysbiosis in humans

Initially, the first correlation between dysbiosis and SLE in human was described a few years ago (Hevia et al. 2014). The main difference observed in lupus patients in contrast with healthy subjects was the reduction of the ratio *Firmicutes/Bacteroidetes* (van der Meulen et al. 2019). Furthermore, *Firmicutes* are inversely correlated with the SLE disease activity index (SLEDAI score), which means this phyla may delay SLE progression (He et al. 2020). Nevertheless, this proportion is contradictory among countries and many factors such as sex, race, treatments and disease duration may affect it (Zhang et al. 2021).

Going deeper, at family level it is still possible to find similarities. Spanish and Chinese SLE patients display an expansion of *Prevotellaceae* (He et al. 2016; Hevia et al. 2014). At genera level, *Roseburia*, *Faecalobacterium*, *Mollicutes*, *Bifidobacterium*, *Dialister*, *Pseudobutyrivibrio*, *Lactobacillus*, *Cryptophyta* and RF39 are depleted in SLE patients, while *Blautia*, *Eubacterium*, *Klebsiella*, *Rhodococcus*, *Eggerthella*, *Prevotella* and *Flavonifractor* are increased (Luo et al. 2018).

Finally, at species level, *Streptococcus anginosus* and *Lactobacillus mucosae* appeared increased in SLE (Yao Li et al. 2019). In line with this, *Ruminococcus (blautia) gnavus* (RG) has a greater representation in SLE patients and anti-RG antibodies correlated directly with SLEDAI score and ANA levels (Azzouz et al. 2019). Furthermore, RG blooms in SLE patients are concordant with disease flare episodes (Azzouz et al. 2023).

2.1.2. Gut dysbiosis in mouse models

When focusing on animal models of SLE, it is remarkable to note the variations between human and mouse microbiota as well as the differences across other models. Looking into genetic models such as NZBWF1, Murphy Roths Large lymphoproliferative model (LPR) or TLR-7.1, all of them show an increased diversity (Zhang et al. 2014). Similar to humans, these models usually develop a reduction of the ratio *Firmicutes/Bacteroidetes* (de la Visitación et al. 2019). However, no changes in this proportion has also been described (de la Visitación et al. 2021).

Several studies describe that the microbiota from the LPR model experiences a decrease in *Lactobacillaceae* and an expansion of *Rikenellaceae, Desulfovibrionaceae, Ruminococcaceae, Lachnospiraceae*, or *Streptococcaceae* (Mu et al. 2017; Zhang et al. 2021). Focusing on genera level, *Mollicutes, Roseburia, Butyrivibrio*, and *Tenericutes* are all reported to be on the rise while *Bifidobacterium* and *Lactobacillus* were discovered to be decreased (Zhang et al. 2014). Additionally, it has been observed that the genus *Anaerostipes* was decreased in SLE mice, which is highly significant given its ability to synthesize butyrate (Kim et al. 2019).

The NZBWF1 model replicates the changes seen in LPR and humans at the phylum, family, and genus levels. Nonetheless, there is a rise in *Lactobacillus*, which has been associated with severe clinical symptoms such as systemic autoimmunity, renal function impairment, and others (Pan et al. 2021).

By comparison, the TLR-7.1 model shows an expansion in *Rikenellaceae* and *Coriobacteriaceae* families while *Clostridaceae* is decreased (Zegarra-Ruiz et

al. 2019). Regarding genera level, *Bifidobacterium*, *Anaerostipes*, *Coprobacillus* and *Turicibacter* are reduced whereas *Prevotella* and *Desulfovibrio* are augmented.

Finally, one of the most employed mouse models is the TLR-7-dependent one, induced by topical application of Imiquimod (IMQ). In this case, IMQ-treated mice show a tendence to reduce the *Firmicutes/Bacteroidetes* ratio and a significant lower α-diversity, measured by numbers of species (de la Visitación et al. 2021).

Recently, *Enterococcus gallinarum* in NZBWF1 mice (Manfredo Vieira et al. 2018) and *Lactobacillus reuteri* in TLR-7.1 (Zegarra-Ruiz et al. 2019) have been found in higher proportion and described as pathobionts, which means they can act as pathogenic bacterium under certain conditions and translocate to different organs from the gut (Pan et al. 2021). This translocation ability is partially mediated by gut epithelium, whose integrity might be compromised in autoimmune diseases (Kinashi and Hase 2021).

2.2. Microbiota as a key part

The intestinal epithelium constitutes the largest mucosal surface within the human body whose primary role is to regulate the influx of exogenous antigens and prevent the leakage of endogenous substances through the formation of tight junctions (TJ) (Peterson and Artis 2014). The mucosal barrier also includes antimicrobial peptides, mucin (MUC) and dimeric (or more polymeric) IgA secreted by several cell types (Johansson and Hansson 2016).

Conversely, the breakdown of mucosal barriers results in heightened intestinal permeability, a pathological condition recognized as leaky gut syndrome. The impairment of the intestinal barrier consists in a loss of TJ proteins such as occludin, claudin and zonula occludens (ZO)-1 (Ahmad et al. 2017). Barrier dysfunction, stemming from dysbiosis of the intestinal microbiota, leads to local or systemic disease (Mouries et al. 2019). This phenomenon is evident in various diseases, including autoimmune conditions (Christovich and Luo 2022). The mechanisms involved in this process are bacteria translocation and access of metabolites and structural components into the bloodstream, access of metabolites into the bloodstream, from where they can reach other organs (Choi et al. 2020).

Several microorganisms can pass through the intestinal barrier once leaky gut syndrome is established. As mentioned before, *E. gallinarum* has been reported as a pathobiont that is able to translocate to liver in NZBWF1 mice and induce multiple autoimmune-promoting factors such as IFN-I (Manfredo Vieira et al. 2018). Similarly, *L. reuteri* can migrate to mesenteric lymph nodes (MLN), liver and spleen in TLR-7.1 mice where it promotes pDC accumulation, IFN-I release and

splenomegaly (Zegarra-Ruiz et al. 2019). Eventually, RG, which is an obligate anaerobe commensal whose expansion is related with LN, has the potential to relocate to MLN and foster gut permeability and autoimmunity (Silverman, Deng, and Azzouz 2022).

Moreover, not only migratory pathobionts but also the whole microbiome might be critical for the progression of the disease (Choi et al. 2020). Faecal microbiota from SLE prone mice caused a considerable rise in anti-dsDNA antibodies and stimulation of the immune response in recipient germfree (GF) mice (Ma et al. 2019). These findings were evidenced after performing a similar experiment using human faeces. In this case, faecal microbiota transplantation (FMT) from SLE patients led to the development of lupus-like phenotypic features in GF mice, including an increase in serum autoimmune antibodies, an imbalance in cytokines, changes in the distribution of immune cells in mucosal and peripheral immune responses, and an upregulation of SLE-related genes (Ma et al. 2021). Overall, dysbiotic microbiota can enhance SLE pathogenesis through its interaction with the immune system.

Additionally, gut microbiota plays a role in SLE complications, such as LN and CVD, through immunological mediators. Segmented filamentous bacteria (SFB) expansion drives Th-17 cell differentiation and defective TCR signalling (Shirakashi et al. 2022), and SFB colonization in mice is related to worsening of glomerulonephritis, glomerular and tubular immune complex deposition and interstitial inflammation, causing LN (Valiente et al. 2022). In a similar fashion, transplantation of gut microbiota from hypertensive NZBWF1 mice transferred SAH and impaired endothelial function (de la Visitación et al. 2021). Interestingly, the mechanism implicated seems to be an increased proportion of Th-17 in MLN followed by a higher infiltration in aorta and ROS production (Toral et al. 2019).

Nevertheless, bacterial components and metabolites are able to generate the aforementioned effects on the host once they cross the gut barrier. TLR-4 is connected to glomerulonephritis and autoantibody synthesis in SLE (Li et al. 2013). Among its ligands, lipopolysaccharide (LPS) from Gram-negative bacteria wall might be the predominant. Once LPS binds TLR-4, Myd88 activation occurs and the subsequent downstream signaling pathway ends in pro-inflammatory cytokine production (IL-6, IFN-I and TNF-α), typically found elevated both in human patients and murine models (Lee et al. 2010).

Besides local inflammation, activation of TLR-4 in the vasculature results in increased NOX activity and ROS synthesis, facilitating endothelial dysfunction (Liang et al. 2013).

Similarly, TLR-7 selectively detects a subset of RNA sequences and promotes IFN release. Recently, a TLR-7 gain-of-function variant has been discovered in humans and it is responsible for enhancing TLR-7 activation and causing childhood-onset SLE (Brown et al. 2022). Moreover, latest investigations outlined a link between TLR-7 activation and a higher risk of rupture, myocarditis, left ventricular remodeling, and total heart block (Shafeghat et al. 2022). Hence, therapeutic manipulation of TLR is a promising target in SLE (Hennessy, Parker, and O'Neill 2010).

Finally, some bacteria have the ability to produce metabolites such as trimethylamine (TMA), which is then transformed into TMA N-oxide (TMAO) (Zhu et al. 2016), and short chain fatty acids (SCFA), which can either have harmful or positive effects on SLE when they reach the bloodstream (Arpaia et al. 2013; Luu and Visekruna 2019). In recent years, increasing evidence has shown that both TMA/TMAO and SCFA are key modulators of immune response in SLE, postulating a new field of research (Lu et al. 2022) (**Figure 3**).

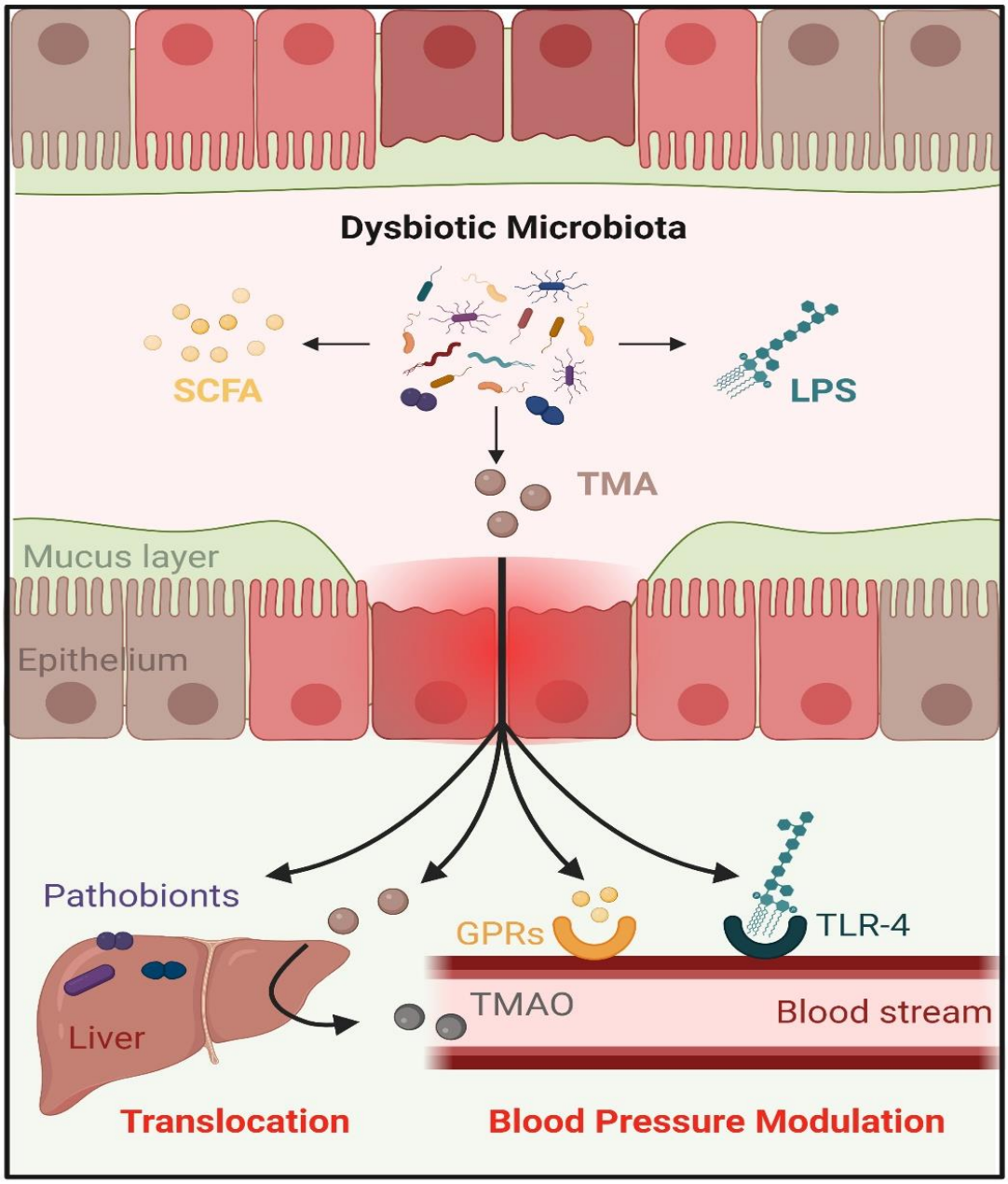

Figure 3. Microbiota pathways and metabolites implicated in SLE.

Abbreviations: GPR, G-protein coupled receptor; LPS, lipopolysaccharide; SCFA, short chain fatty acids; TLR, toll-like receptor; TMA, trimethylamine; TMAO, trimethylamine N-oxide.

2.3. TMA/TMAO

Foods high in choline, phosphatidylcholine, and carnitine, such as liver, eggs, peanuts, and dairy products, are partially metabolized by the microbiota into TMA, which is then changed into TMAO by the host hepatic flavin monooxygenases (Tang et al. 2013). Previous studies have described higher levels of plasma TMAO in SLE patients compared to healthy subjects, which is associated with the emergence of CVD (Yuhua Li et al. 2019; Wang et al. 2011; Zhu et al. 2017).

Plasmatic TMAO is able to exert an effect on the vascular wall by forming and activating nod-like receptor family pyrin domain containing 3 (NLRP3) inflammasomes in endothelial cells, causing vascular inflammation and endothelial dysfunction (Brunt et al. 2020; M.-L. Chen et al. 2017). Additionally, in allogenic graft-versus-host disease mice, TMAO increased alloreactive T-cell proliferation and differentiation into Th-1 and Th-17 (Wu et al. 2020), which are a crucial part in the vascular alterations (de la Visitación et al. 2021).

2.4. SCFA

Soluble fiber and resistant starches (RS) pass directly to the large intestine without being digested in the upper gastrointestinal tract, being called prebiotics. Once they reach the location of commensal bacteria, fibers are fermented, producing different metabolites like SCFA (Luu and Visekruna 2019). SCFA have an aliphatic tail whose length is lower than six carbon atoms, and the most studied ones are acetate (ACE), butyrate (BUT) and propionate (PROP). These substances acts as fuel for the colonic epithelium and are studied by their role in the maintenance of the intestinal barrier function and the control over BP (Asarat et al. 2016; Macia et al. 2015).

Growing evidence suggest that lack of prebiotic fiber is related to higher prevalence of elevated BP (Kaye et al. 2020; Reynolds et al. 2019). Moreover, strategies like high-fiber diets have demonstrated beneficial effects by preventing the raise in BP in hypertensive mice (Marques et al. 2017). Among fibers, RS is known to enhance SCFA-producing bacteria and restrict pathobionts translocation in SLE mice, improving autoimmunity (Zegarra-Ruiz et al. 2019). Similarly, inulin-type fructans (ITF) have the potential to prevent endothelial dysfunction in mice through microbiota modulation (Catry et al. 2018).

SCFA act as signalling molecules and they can bind to specific receptors like G-protein coupled receptor (GPR), specifically GPR41 (also known as free fatty acid receptor 3, FFAR3) and GPR43 (or FFAR2) (Tan et al. 2017).

GPR41 is predominantly expressed in endothelial cells, while GPR43 is more prevalent in immune cells (Brown et al. 2003), and both are involved in lowering the BP (Pluznick 2013). BUT exhibits stronger activity on GPR41, PROP acts as the most potent agonist for both GPR41 and GPR43, and ACE displays greater selectivity for GPR43 (Hong et al. 2005). BUT can also bind GPR109a, which induces Treg differentiation in MLN, colon and spleen (Singh et al. 2014) (**Table 1**).

Table 1. SCFA and receptor selectivity.

Receptor	Acetate	Propionate	Butyrate
GPR41 (FFAR3)	Low (Milligan, Stoddart, and Smith 2009)	High (Stoddart, Smith, and Milligan 2008)	High (Brown et al. 2003)
GPR43 (FFAR2)	High (Smith et al. 2013)	High (Stoddart et al. 2008)	Moderate (Maslowski et al. 2009)
GPR-109a	Low (Docampo et al. 2022)	Low (Singh et al. 2014)	High (Docampo et al. 2022)

Interestingly, SCFA supplementation also has an influence on the host, especially when cardiovascular features are present. For instance, chronic BUT treatment improves impaired endothelial dysfunction and attenuates hypertension induced by angiotensin II infusion in mice (Kim et al. 2018). PROP protects from vascular and cardiac damage in angiotensin II-infused apolipoprotein E knockout mice (Bartolomaeus et al. 2019) and ACE prevents the elevation of BP in hypertensive mice (Marques et al. 2017). In addition, all of them show protective effects on endothelial dysfunction in aorta from rats incubated with angiotensin II (Robles-Vera et al. 2020) and SCFA derivatives are promising treatments in hypertensive patients (Jama et al. 2023).

3. Murine models of SLE

As described before, in the study of lupus, a variety of murine models has been employed (Halkom, Wu, and Lu 2020). Most of them share the production of autoantibodies and the subsequent development of glomerulonephritis, although the degree of similarity to real human SLE varies depending on the model used and the affected organs examined (Du et al. 2015). Each model has unique characteristics that may help to explain reported variations in the composition and evolution of the gut microbiota during the pathology development. Additionally, humanized models obtained by transferring human leucocytes to immunodeficient mice are gaining relevance due to their potential for translational medicine (Chen et al. 2021). In general, SLE murine models can be divided into two groups, spontaneous and induced.

3.1. Spontaneous models

The NZBWF1 mouse is one of the most extensive models on the market, developing autoantibodies (primarily anti-dsDNA), splenomegaly, glomerulonephritis, hypertension, and occasionally vasculitis, making it possible to interpret a model of chronic lupus illness (Taylor and Ryan 2017). This model is exemplary and has been used in studies on the genetics of SLE, preclinical testing of numerous treatments used in clinical trials for lupus, and modeling CVD related to lupus (Virdis et al. 2015).

The LPR model was developed in 1976 and it is the result of the cross between LG, B6, AKR and C3H mice (Edwin D Murphy and Roths 1978). Due to the proliferation of CD4-CD8- and B220+ T-cells, hypergammaglobulinemia and high titers of ANA, these animals present a marked lymphadenopathy, which is particularly pertinent since double negative T cells are increased in SLE patients (Crispín et al. 2008).

Focusing on TLR-7 involvement, the BXSB is an inbred model characterised by secondary lymphoid node hyperplasia, hypergammaglobulinemia, monocytosis and antinuclear and anti-erythrocytic auto-antibodies (E D Murphy and Roths 1978). The unique feature of this model is the higher manifestation of the disease in male rather than female mice, due to the existence of the Y chromosome linked autoimmune accelerator (Eisenberg and Dixon 1980).

Finally, TLR-7.1 model exhibits an increase in TLR-7 expression and spontaneously develop systemic signs of SLE (Deane et al. 2007). Moreover, these mice present splenomegaly, hepatomegaly, elevated IFN-I production and gut dysbiosis, which make them a reliable preclinical subject to study SLE (Zegarra-Ruiz et al. 2019).

3.2. Induced models

One of the most popular methods to induce SLE is by injecting mineral oil pristane intraperitoneally into mice. This causes a proinflammatory response that, over several months, results in the production of ANA, arthritis, and glomerulonephritis, reason why it is the model of choice to study the mechanism of human SLE (Satoh and Reeves 1994).

Regarding TLR-7 activation, several agonists like resiquimod or IMQ have proven to enable SLE symptoms through IFN-I production after epicutaneous application (Yokogawa et al. 2014). Among its features are elevated plasma levels of anti-dsDNA autoantibodies, splenomegaly, hepatomegaly, T cell imbalance, endothelial dysfunction and SAH (Robles-Vera et al. 2020).

JUSTIFICATION AND OBJECTIVES

JUSTIFICATION AND OBJECTIVES

In accordance with all of the above, it is reasonable to investigate the leaky gut, the dysbiotic microbiota and its metabolites as a potential target for the modulation of SLE and its consequent SAH and CVD. On the one hand, multiple studies have focused on the restoration of gut dysbiosis in order to attenuate the progression of SLE (Pan et al., 2021; Rodriguez-Carrio et al., 2017). In fact, probiotic consumption has shown beneficial effects on SAH in a TLR-7-dependent mouse model (de la Visitación et al., 2021). On the other hand, there is a knowledge gap regarding microbiota-host interactions in SLE and its associated cardiovascular complications to be further explored. It is essential to understand the implication of gut microbiota and its metabolites in SLE, as the consumption of SCFA or the pharmacological inhibition of bacterial enzymes involved in the production of TMAO could exert a cardiovascular protective effect. Therefore, the general objective of this thesis was:

To analyse the role of gut microbiota and its bacterial by-products (TMAO, SCFA) in the development of cardiovascular complications in SLE

Recently, we demonstrated that TLR-7 activation causes hypertension and vascular damage in BALB/cJRj mice, and emphasizes the elevated vascular inflammation and oxidative stress, mediated in part by IL-17a, as crucial factors for cardiovascular complications (Robles-Vera et al. 2020).

New studies are showing that gut microbiota composition is linked to the pathogenesis of SLE. Intestinal microbiota may trigger symptoms and exacerbate this pathology in both murine models of SLE and patients (Hevia et al. 2014; Li et al. 2017; Luo et al. 2018; Ma et al. 2019; Mu et al. 2017). We recently demonstrated in female NZBWF1 mice that gut microbiota changes are linked to hypertension (de la Visitación et al. 2021). Interestingly, gut dysbiosis was found in TLR-7-dependent mouse models of SLE, and bacterial translocation of *L. reuteri* to secondary lymphoid tissue and liver can drive autoimmunity, which was improved with dietary RS by suppressing the pathological levels of *L. reuteri* and its translocation, through SCFA (Zegarra-Ruiz et al. 2019).

We recently demonstrated that probiotics consumption reduced BP under TLR-7 activation conditions (de la Visitación et al. 2021). In spite of all the data associating intestinal dysbiosis and autoimmunity in TLR-7-dependent lupus mice (gut microbiota depletion ameliorates the IFN pathway and autoimmunity), no information is available on the involvement of the microbiota in the pathogenesis of hypertension and vascular alterations in these animals. Previous studies on GF

mouse models demonstrated the contributory role of gut microbiota in vascular inflammation, vascular dysfunction, and BP regulation (Ascher and Reinhardt 2018; Edwards et al. 2020; Karbach et al. 2016). This was the basis for setting the first objective:

I) To study whether gut microbiota is able to enhance the predisposition to SLE onset and T cell maturation in intestinal secondary lymphoid tissues, triggering a loss of endothelial function and hypertension in a lupus model induced by epicutaneous application of the TLR-7 agonist IMQ.

Diet has been proven the most important element for gut microbiota composition. Choline-, phosphatidylcholine-, and carnitine-rich foods like liver, eggs, peanuts, dairy products, etc, are partially metabolized into TMA by the microbiota and subsequently transformed by the host hepatic flavin monooxygenases into TMAO (Zhu et al. 2016). TMAO, as a circulating intestinal microbial metabolite, can trigger vascular inflammation and endothelial dysfunction by formation and activation of NLRP3 inflammasomes in endothelial cells (Brunt et al. 2020; M.-L. Chen et al. 2017). In addition, TMAO-induced alloreactive T-cell proliferation and differentiation into Th subtypes in allogenic graft-versus-host disease mice (Wu et al. 2020). Interestingly, plasma levels of TMAO were elevated approximately 2.7 times in lupus patients in comparation to healthy individuals (Yuhua Li et al. 2019). Moreover, we have found that TMA-producing bacteria, such as *Desulfovibrio*, is increased in feces from IMQ-treated mice compared to controls, and that its reduction by vancomycin (VANCO) administration improves endothelial function and the raise in BP (de la Visitación et al. 2021). Nonetheless, whether TMAO modulates the pathophysiological process of TLR-7-driven lupus autoimmunity and its cardiovascular complications is still mostly unknown. To explore the role of this microbial metabolite, we used a structural analog of choline, 3,3-dimethyl-1-butanol (DMB), which nonlethally inhibits TMA formation and reduces the TMAO concentration in mice. This led us to our second objective:

II) To test if TMAO can boost the tendency to SLE development and T cell activation and proliferation in secondary lymph organs, causing endothelial dysfunction and hypertension in a lupus model induced by epicutaneous application of the TLR-7 agonist IMQ.

The gut microbiota and their metabolites play a critical role in regulating the host immune system. Intestinal bacteria produce LPS and SCFA, which have opposing effects on T cell polarization and inflammation, increasing, and reducing them, respectively (Chang et al. 2014). Numerous commensal gut bacteria can produce SCFA, including ACE by some bacteria, BUT by *Clostridium* species, and PROP by *Akkermansia*. However, there have been no significant findings indicating

alterations in SCFA-producing bacteria in TLR-7-induced lupus mice, suggesting that reduced levels of SCFA may not contribute to vascular dysfunction in SLE (de la Visitación et al. 2021; Zegarra-Ruiz et al. 2019). Conversely, SCFA have been shown to enhance vascular function and reduce BP in non-lupus-prone rodents (Jin et al. 2022; Kaye et al. 2020; Robles-Vera et al., 2020), as well as in humans characterized by SCFA depletion in the gut (Jama et al. 2023). Moreover, SCFA supplementation reduced plasma anti-ds-DNA in TLR7.1 Tg C57Bl/6 mice (Zegarra-Ruiz et al. 2019), which can attenuate SLE hypertension (Taylor et al. 2018). In fact, our recent study demonstrated that consuming fiber improved vascular function in a polygenetic lupus model, potentially by increasing SCFA production (Moleón et al. 2023). SCFA exert their regulatory effects on immune and endothelial function through the inhibition of histone deacetylases (HDACs) and/or the activation of GPRs, specifically GPR41 and GPR43 (Robles-Vera et al. 2020; Vinolo et al. 2011). However, the expression of GPR41 and GPR43 varies across different cell types. GPR41 is predominantly expressed in endothelial cells, while GPR43 is more prevalent in immune cells (Brown et al. 2003). BUT exhibits stronger activity on GPR41, PROP acts as the most potent agonist for both GPR41 and GPR43, and ACE displays greater selectivity for GPR43 (Hong et al. 2005). Furthermore, BUT and PROP, but not ACE, can function as HDACs inhibitors (Zheng et al. 2015). However, the expression levels of GPRs and HDACs in the gut, secondary lymph nodes, and vascular wall of TLR-7-induced lupus mice have yet to be investigated, as this may determine the response to SCFA. Thus, our third objective was:

III) To examine whether SCFA, specifically ACE and BUT, can prevent vascular dysfunction and elevated BP in TLR-7-induced lupus mice and assess the potential involvement of HDACs and/or GPRs as underlying mechanisms.

Western diet is linked to autoimmune and metabolic diseases and it is characterized by low dietary fiber intake. Some dietary fibers can be considered prebiotic if they are not digested in the upper gastrointestinal tract, passing intact to the large intestine, where they can be used by commensal bacteria in catabolic processes. Fermenting these prebiotics releases metabolites such as SCFA. Two fermentable dietary-fibers of particular interest in this respect are RS and inulin. RS is an insoluble type of cereal fiber while inulin is a soluble fiber that can be found in many types of plant foods. The patients with SLE reported a lower fiber intake than healthy humans (Elkan et al. 2012; Schäfer et al. 2021). Moreover, an inverse association between dietary fiber intake and the risk of active SLE has been

described (Minami et al. 2011). In agreement with this association, Zegarra-Ruiz *et al*. (Zegarra-Ruiz et al. 2019), using TLR-7-dependent mouse models of SLE, found that a diet high in RS leads to greater SCFA production to restrict growth of *Lactobacillus reuteri*, reducing the translocation from the gut to distal organs, and rescues lupus-prone mice from autoimmunity. Interestingly, gut bacteria thriving in the absence of prebiotic fiber is prohypertensinogenic (Kaye et al. 2020), and supplementation of RS or SCFA in diet prevented the rise of BP in rodents without genetic background of SLE (Bartolomaeus et al. 2019; Kim et al. 2018; Marques et al. 2017). However, there is no information about the role of dietary fiber in cardiovascular complications in mice with genetic susceptibility to SLE. This possibility was tackled in our last objective:

IV) To investigate the role of dietary fiber intake in the raise of BP in NZBWF1 mice and to explore the possible underlying mechanisms.

MATERIALS AND METHODS

MATERIALS AND METHODS

1. Animals and experimental groups

We adhered to the animal protocols outlined in the National Institutes of Health Guide for the Care and Use of Laboratory Animals, and we obtained approval from the Ethics Committee of Laboratory Animals at the University of Granada, Spain (Reference: 12/11/2017/164). Additionally, our procedure followed the guidelines outlined in the Transparency on Gut Microbiome Studies in Essential and Experimental Hypertension (Marques et al. 2019), as well as the ARRIVE guidelines (Percie du Sert et al. 2020).

All animals were housed in specific pathogen-free (SPF) facilities at University of Granada Biological Services Unit under standard laboratory conditions (12 hours light/dark cycle, temperature 21-22ºC, 50-70% humidity) in separate Makrolom cages (Ehret, Emmerdingen, Germany) to avoid horizontal transmission of bacteria, with dust-free laboratory bedding and enrichment. The study designs ensured equal group sizes and sufficient statistical power. Random allocation of animals into experimental groups was conducted, and the researchers remained blinded to treatments until completion of data analysis.

We employed both spontaneous (NZBWF1) and induced (TLR-7 activation with IMQ) models. We specifically opted to use female mice due to their heightened susceptibility to TLR-7-driven functional responses and autoimmunity (Souyris et al. 2019). Additionally, oestrogens are relevant elements in both SLE disease and SAH in human and murine models, further supporting our choice (Taylor and Ryan 2017).

1.1. Role of gut microbiota in the development of hypertension in a TLR-7-dependent lupus mouse model

1.1.1. Experiment 1

Seven- to nine-weeks-old female BALB/cJRj mice, were purchased from Janvier (Le Genest, France). To assess the role of gut microbiota, we reduced bacterial mass using antibiotic treatments. Mice were randomly sorted into six experimental groups of 6-8 animals each:

I. Untreated control (CTR) (n=7)
II. Control treated with vancomycin (2 g/L) (CTR-VANCO) (n=8)

III. Control treated with a broad-spectrum cocktail of antibiotics (CTR-MIX) (n=8)
IV. Imiquimod (IMQ) (n=6)
V. Imiquimod treated with vancomycin (2 g/L) (IMQ-VANCO) (n=8)
VI. Imiquimod treated with a broad-spectrum cocktail of antibiotics (IMQ-MIX) (n=7)

VANCO is a molecule that cannot be absorbed in the intestines and eliminates mainly gram-positive bacteria. In order to examine the role of VANCO-resistant bacteria in BP control we prepared a cocktail of un-absorbable antibiotics (MIX) containing VANCO (0.5 g/L; Pfizer, New York, USA), metronidazole (1 g/L; Sigma, Missouri, USA), neomycin (1 g/L; Fisher Scientific, New Hampshire, USA) and ampicillin (1 g/L; Sigma, Missouri, USA) in drinking water (Manfredo Vieira et al. 2018). In addition to the antibiotics, a sweetener (Equal, 4 g/L) was used to overcome the metallic taste of metronidazole, for control purposes, it was also added to the rest of experimental groups.

IMQ-treated mice were subjected to a total of 1.25 mg of IMQ (Zyclara® 3.75% cream) from Laboratories Meda Pharma S.A.U. (Madrid, Spain) applied to their right ears three times per week on alternate days over 8 weeks. This topical IMQ application to the skin effectively triggers the development of systemic autoimmune disease (Yokogawa et al. 2014), justifying its application to induce a murine model resembling SLE.

1.1.2. Experiment 2

For investigating whether microbiota in the IMQ model is linked to BP regulation, an FMT was carried out, following previously used protocols (Toral et al. 2019). For this reason, stool samples were freshly obtained from individual IMQ and CTR mice at 8 weeks. The samples were pooled and suspended in a 1:20 (w/v) solution in sterile phosphate-buffered saline (PBS) and superfluous faecal material was sedimented and discarded at 800 rpm for 5 min. The suspension was collected in aliquots and kept at -80ºC until used. IMQ-treated for 8 weeks and aged-matched CTR female mice were used as recipient mice. IMQ-recipient mice were also treated with IMQ cream, as described above.

These mice were administered with ceftriaxone sodium (400 mg/Kg, Normon, Madrid, Spain) daily for 5 consecutive days by oral gavage. The purpose of this antibiotic treatment was to reduce the pre-existing bacteria populations to boost the proliferation in the host of intestinal microorganisms from donor animals post-FMT. After two days from the end of the treatment with ceftriaxone, recipient mice received already prepared faecal suspensions (0.1 mL) for 3 consecutive days

through oral gavage, and later once every 3 days for a total period of 2 weeks (**Figure 4**). Animals were randomly assigned to four different groups:

I. Control with control microbiota (CTR-CTR) (n=8)
II. Control with IMQ microbiota (CTR-IMQ) (n=8)
III. IMQ with IMQ microbiota (IMQ-IMQ) (n=8)
IV. IMQ with control microbiota (IMQ-CTR) (n=8)

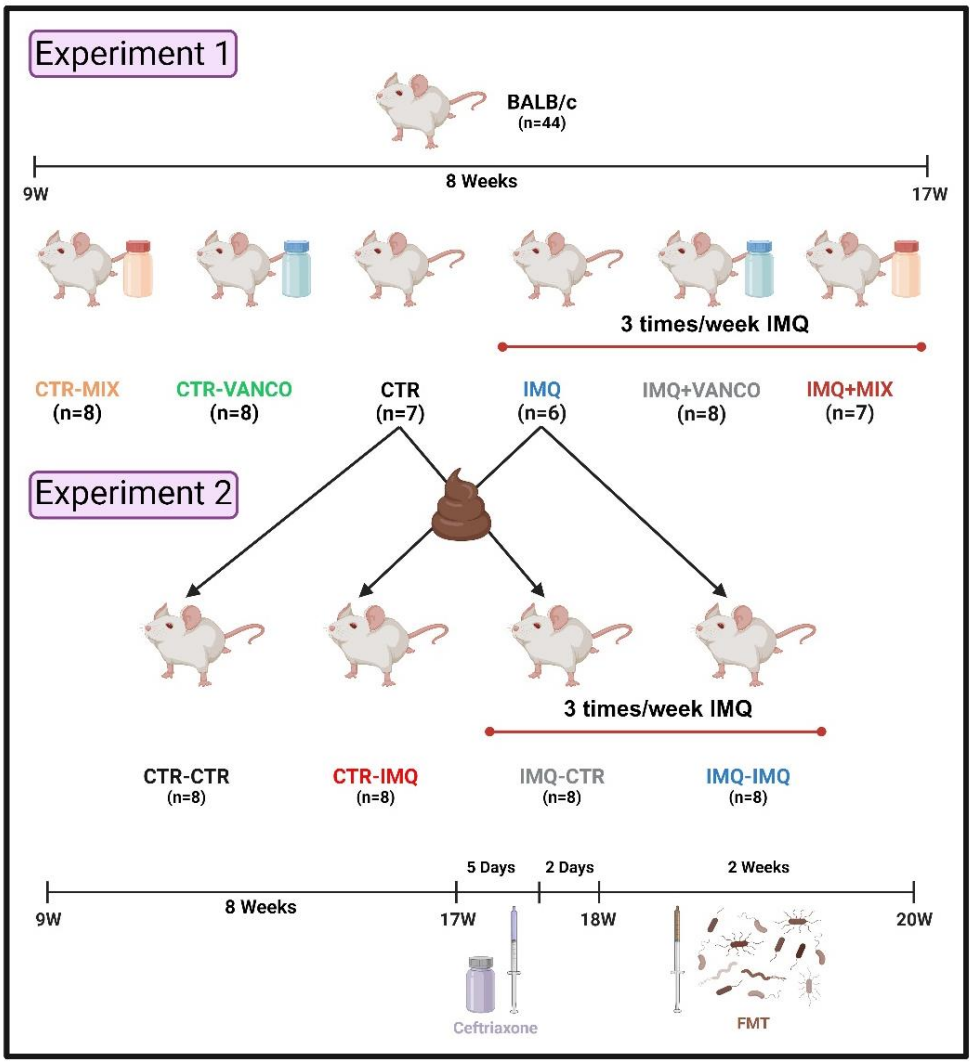

Figure 4. Experimental design of objective 1.

Abbreviations: CTR, control; FMT, faecal microbiota transplant; IMQ, imiquimod, MIX, antibiotic cocktail; VANCO, vancomycin.

1.2. Role of TMAO in SLE development and cardiovascular complications in a lupus mouse model induced by TLR-7 activation

1.2.1. Experiment 1

Seven- to nine-weeks-old female BALB/cJRj mice from Janvier (Le Genest, France), which were randomly divided into four equally-sized experimental groups (**Figure 5**):

I. Untreated control (CTR) (n=10)
II. Control treated with DMB (CTR-DMB) (n=10)
III. Imiquimod (IMQ) (n=10)
IV. Imiquimod treated with DMB (IMQ-DMB) (n=10)

All mice were fed a standard chow diet (SAFE A04, Augy, France) and randomized to receive *ad libitum* access to either normal drinking water (CTR and IMQ groups) or drinking water supplemented with 1% (v/v, DMB; Sigma, Missouri, USA). Every day fresh water bottles were provided. Water and food intake was studied and controlled daily for all groups. IMQ-treated mice were subjected to a total of 1.25 mg of IMQ (Zyclara® 3.75% cream) from Laboratories Meda Pharma S.A.U. (Madrid, Spain) applied to their right ears three times per week on alternate days over 8 weeks. Administration of IMQ to the skin effectively triggers the onset of systemic autoimmune disease (Yokogawa et al. 2014), which justifies the topical use of IMQ to induce an SLE-like autoimmune murine model. Because of their higher predisposition to TLR-7-driven functional responses and autoimmunity (Souyris et al. 2019), female experimental subjects were utilized for these experiments.

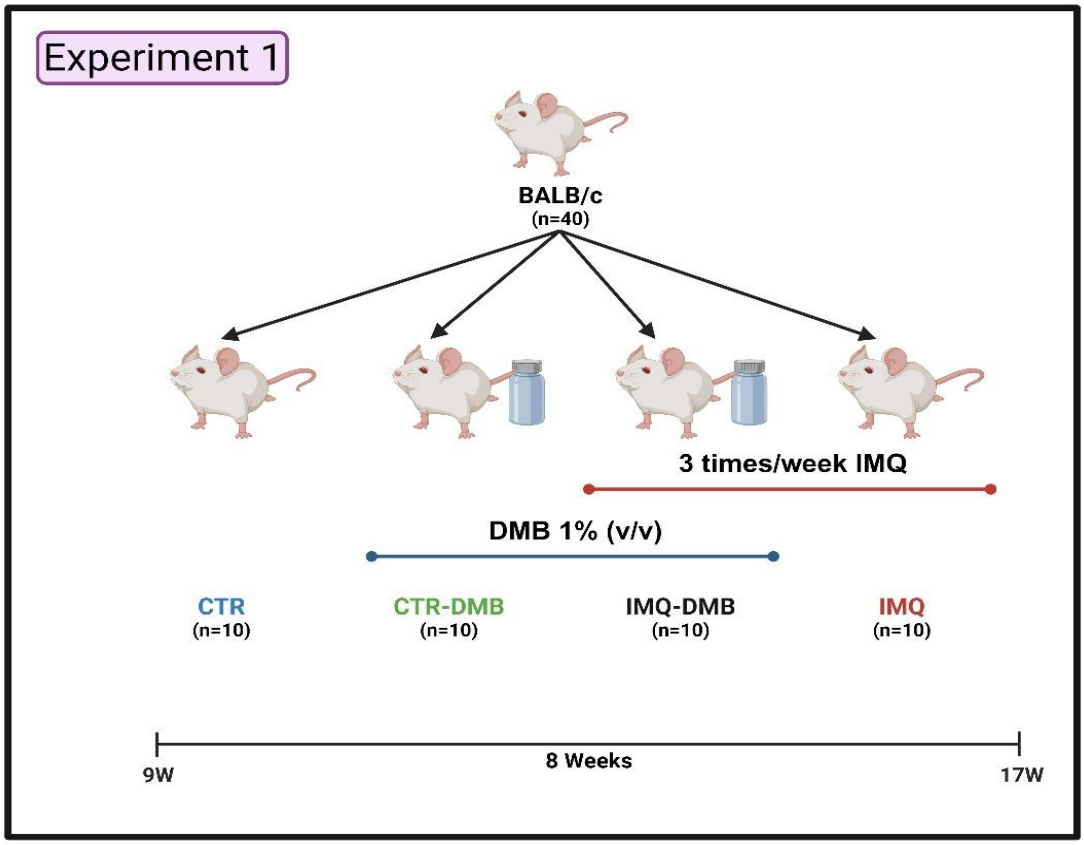

Figure 5. Experimental design of objective 2.

Abbreviations: CTR, control; DMB, 3,3-dimethyl-1-butanol; IMQ, imiquimod,

1.3. Effects of SCFA on cardiovascular complications in TLR-7-induced lupus mice

1.3.1. Experiment 1

We selected female BALB/cJRj mice aged seven to nine weeks, procured from Janvier (Le Genest, France). Mice were divided into six experimental groups (n = 8):

I. Untreated control (CTR) (n = 8)
II. Imiquimod (IMQ) (n = 8)
III. Imiquimod supplemented with magnesium acetate in drinking water (68 mM, IMQ-ACE) (n = 8)
IV. Imiquimod supplemented with sodium butyrate in drinking water (40 mM, IMQ-BUT) (n = 8)

V. Imiquimod treated with SF11-025 diet (IMQ-RS) (n = 8)
VI. Imiquimod treated with ORAFTI P95 (IMQ-ITF) (n = 8)

All mice were provided a standard chow diet (SAFE A04, Augy, France) and were randomly assigned to receive either regular drinking water (CTR and IMQ groups) or drinking water enriched with SCFA (Sigma, Missouri, USA). Considering the bitterness of butyrate, a sweetener (Equal, 4 g/l) was added to the water of all experimental groups. Freshwater bottles were replenished daily, and we monitored and controlled water and food consumption for all groups on a daily basis. IMQ-treated mice were subjected to a total of 1.25 mg of IMQ (Zyclara® 3.75% cream) from Laboratories Meda Pharma S.A.U. (Madrid, Spain) applied to their right ears three times per week on alternate days over 8 weeks. This topical IMQ application to the skin effectively triggers the development of systemic autoimmune disease (Yokogawa et al. 2014), justifying its application to induce a murine model resembling SLE.

Certain types of fiber undergo fermentation by gut microbiota, leading to the production of SCFA as byproducts. Prior studies utilizing experimental models have reported the beneficial effects of dietary fiber in reducing BP, largely attributed to SCFA (Marques et al. 2017). In our investigation of the role of dietary SCFA, we introduced two distinct fiber sources: ITF and RS, both known to yield SCFA.

Alongside the control groups, we included two sets of IMQ-treated mice: IMQ-RS (IMQ mice treated with SF11-025 diet: 72.7% insoluble fiber, sourced from Specialty Feeds, Perth, Australia) (Marques et al. 2017), and IMQ-ITF (IMQ mice treated with ORAFTI P95, a soluble fiber from Beneo, Tener, Belgium) (Catry et al. 2018). Insoluble fiber was provided as standard pellets, while soluble fiber was diluted in drinking water at a final dose of 250 mg/mouse/day.

1.3.2. Experiment 2

To investigate the role of GPR43 in the protective effects of SCFA in IMQ-induced lupus, we introduced two additional groups of IMQ mice co-treated with SCFA and the GPR43 antagonists GLPG-0974 (Tocris Bioscience, Bristol, UK) (GLPG) (Namour et al. 2016):

I. Imiquimod gavaged with vehicle (IMQ)
II. Imiquimod treated with magnesium acetate and GLPG (GLPG-IMQ-ACE) (n = 8)
III. Imiquimod treated with sodium butyrate and GLPG (GLPG-IMQ-BUT) (n = 8)

A stock solution of GLPG was prepared by dissolving it in 0.1% dimethyl sulfoxide (DMSO). GLPG (1 mg/kg body weight) was then diluted in saline and daily administered at a volume of 100 μL via oral gavage (Yang et al. 2020). The untreated IMQ group received the vehicle.

1.3.3. Experiment 3

To investigate the potential impact of the microbiota on BP regulation, we conducted a faecal inoculation study using GF female C57Bl/6J mice aged ten weeks, procured from the University of Granada, Spain (de la Visitación et al. 2021). In this process, fresh stool samples were collected individually from mice belonging to the CTR and IMQ groups in Experiment 1. These samples were combined to create a bacterial suspension by vigorous vortexing at a 1:20 ratio in sterile PBS. The suspension was then subjected to centrifugation at 800 rpm for 5 min to eliminate any debris. The resulting suspension was divided into aliquots and stored at -80ºC. Subsequently, the mice were randomly divided into four groups:

I. GF with CTR microbiota (GF-CTR) (n = 8)
II. GF with IMQ microbiota (GF-IMQ) (n = 8)
III. GF with IMQ microbiota and magnesium acetate (68 mM, GF-IMQ-ACT) (n = 8)
IV. GF with IMQ microbiota and sodium butyrate (40 mM, GF-IMQ-BUT) (n = 8)

The inoculation was carried out twice consecutively during the first week, followed by a monitoring period of 3 weeks. SCFA were supplied in drinking water. Throughout the study, all GF mice were housed under sterile conditions within a gnotobiotic facility and were provided *ad libitum* access to a standard laboratory diet. Microbiota inoculation was performed under sterile conditions in gnotobiotic facilities. After 3 weeks, stool samples were collected from all experimental groups and fully homogenized in PBS. 100μL of the resultant material were cultured in chocolate agar plates for 24h at 37°C 5% CO_2 (Lavin et al. 2018). Presence of any colony forming units (CFU) was considered as a positive transplant control. (**Figure 6**).

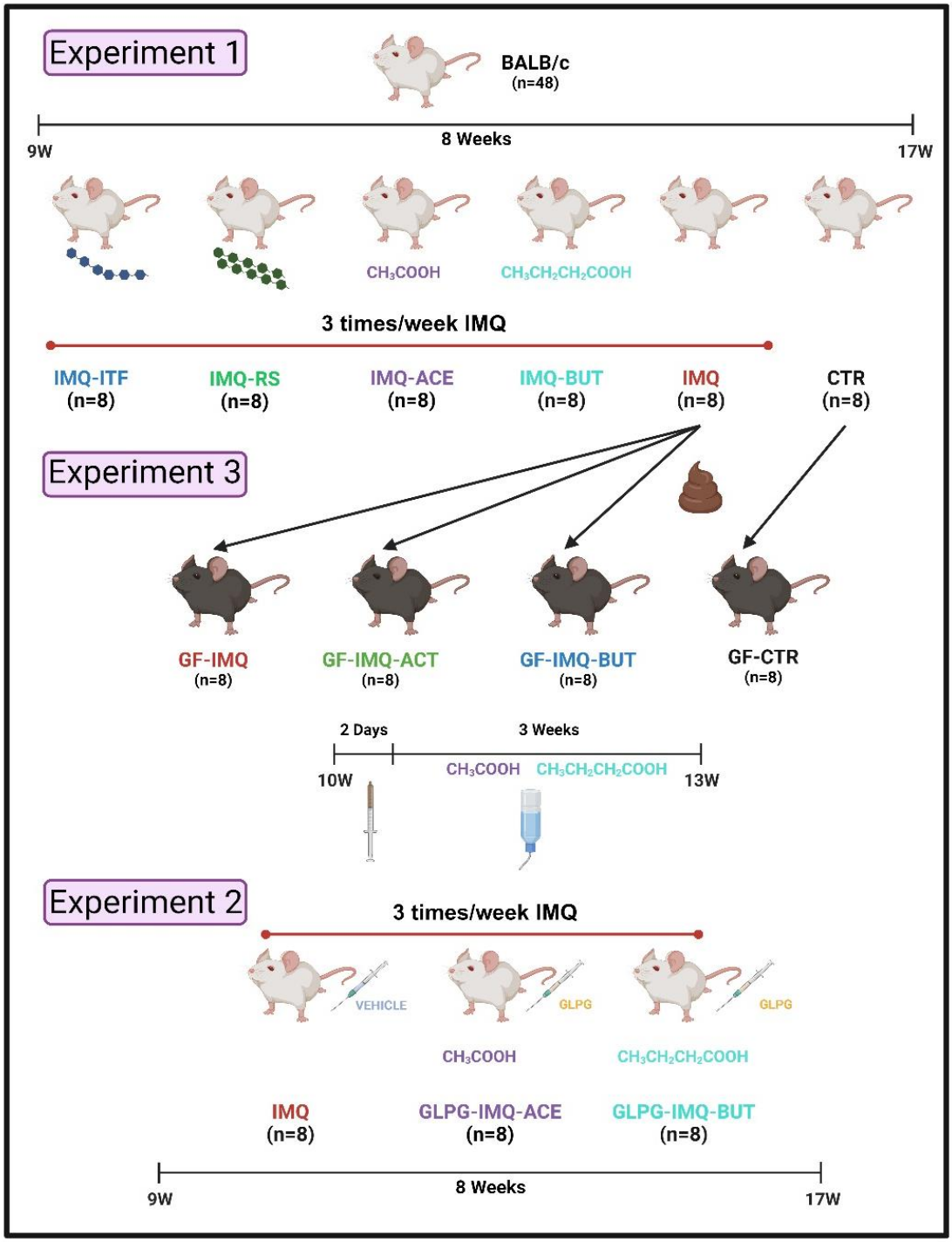

Figure 6. Experimental design of objective 3.

Abbreviations: ACE/ACT, acetate; BUT, butyrate; CTR, control; GF, germfree; GLPG, GLPG-0974; IMQ, imiquimod, ITF, inulin-type fructans; RS, resistant starch.

1.4. Role of dietary fiber intake in the raise of BP in NZBWF1 mice

1.4.1. Experiment 1

NZW/LacJ female mice and NZBWF1 25 weeks old, provided by Jackson Laboratories (Maine, USA), were used in this experiment:

I. NZW/LacJ as control group (CTR) (n=10)
II. NZBWF1 untreated (SLE) (n=10)
III. NZBWF1 treated with SF11-025 diet (RS) (n=10)
IV. NZBWF1 treated with ORAFTI P95 (ITF) (n=10)

SF11-025 diet contained 72.7% insoluble fiber (Specialty Feeds, Perth, Australia) (Marques et al. 2017) and ORAFTI P95 is a soluble fiber (Tener, Belgium) (Catry et al. 2018). The insoluble fiber was administered in the form of conventional pellets. The soluble fiber was diluted in the drinking water at a final dose of 250 mg/mouse/day. CTR, SLE and ITF mice were provided with standard laboratory diet (SAFE A04, Augy, France) *ad libitum*. Water was changed every day, and both water and food intakes were analyzed daily. When the first stages of kidney dysfunction were observed by high proteinuria (at 25-week-old) without high BP, treatment with the fiber was initiated and continued then for 8 weeks.

1.4.2. Experiment 2

To explore the involvement of microbiota in BP regulation, faecal inoculation to normotensive ten-week-old female C57Bl/6J GF mice (University of Granada, Granada, Spain) was performed (de la Visitación et al. 2021). For this, we collected and pooled fresh stool samples from individual mice from all groups in experiment 1. The samples were used to generate a bacterial suspension by vigorous vortexing 1:20 in sterile PBS and centrifuged at 60 g for 5 min to eliminate the detritus. The suspension was aliquoted and stored at -80ºC. Animals were randomly distributed among four different groups:

I. GF with CTR microbiota (GF-CTR) (n=8)
II. GF with SLE microbiota (GF-SLE) (n = 10)
III. GF with RS microbiota (GF-RS) (n = 10)
IV. GF with ITF microbiota (GF-ITF) (n = 10)

Inoculation was carried out consecutively twice in the first week. Then, mice were kept for 3 weeks. All GF mice were kept under sterile conditions at a gnotobiotic facility and were provided with standard laboratory diet *ad libitum* (**Figure 7**).

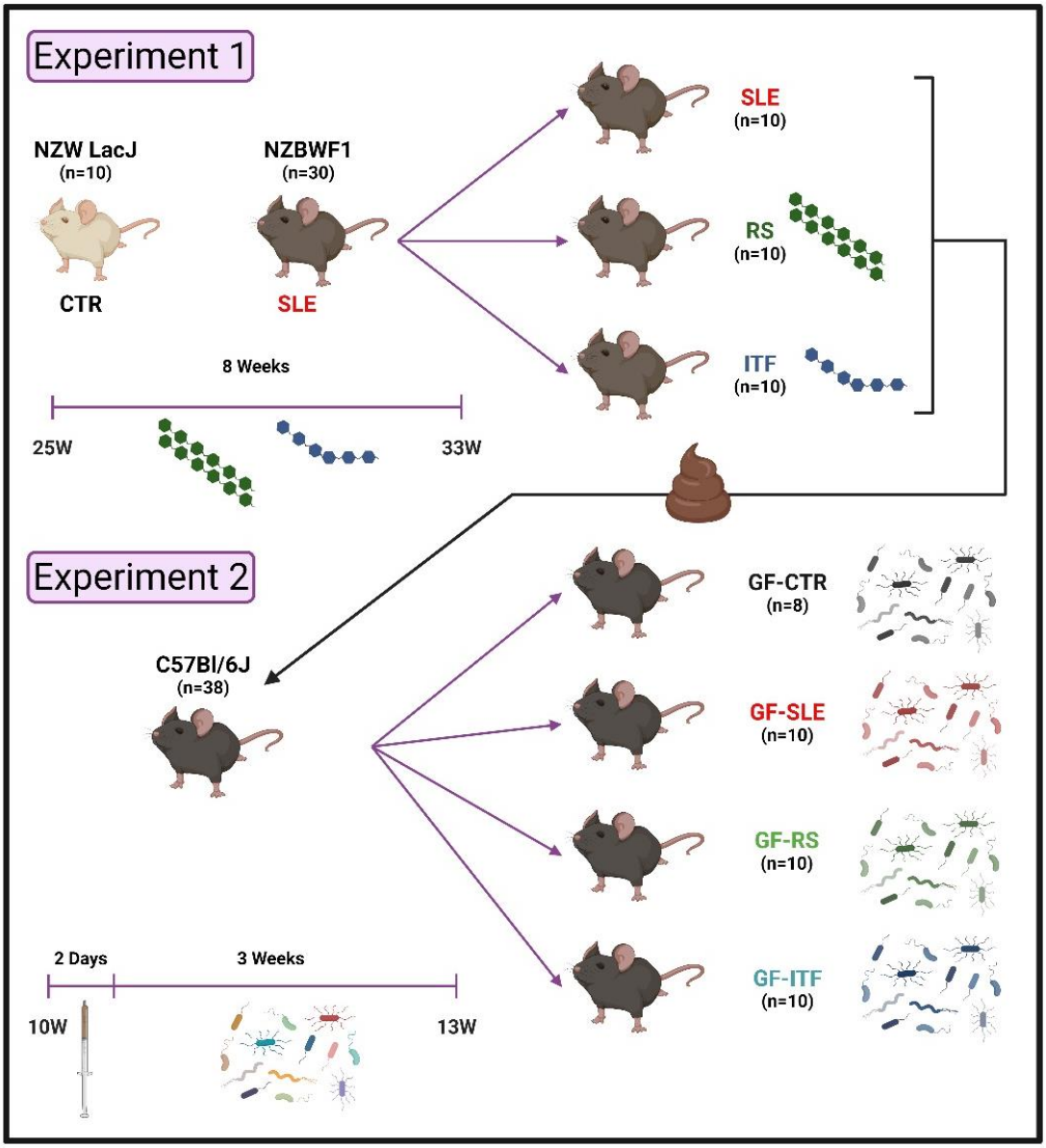

Figure 7. Experimental design of objective 4.

Abbreviations: CTR, control; GF, germfree; ITF, inulin-type fructans; RS, resistant starch; SLE, systemic lupus erythematosus.

2. Blood pressure measurements

SBP measurements were acquired from conscious mice that were pre-warmed at 35ºC for 10-15 min and gently restrained for tail-cuff plethysmography (Digital Pressure Meter, LE 5001; Letica S.A., Barcelona, Spain). Mice underwent a familiarization process, and the replication count was consistent with prior reports (de la Visitación et al. 2021).

3. Physical characteristics and organ weight indices

Body weight (in grams) was determined for all mice. After every experimental endpoint, mice were euthanized under inhalation anesthesia with 2% isoflurane. The heart, kidneys, liver, spleen and colon were excised, cleaned and weighed. The atria and the right ventricle of the heart were then discarded to obtain the weight of the left ventricle. Organ weight indices were calculated by dividing their weights by the tibia length. All samples were snap-frozen in liquid nitrogen and kept at -80ºC until used.

4. Renal injury

For histological studies, decapsulated kidneys from all groups were buffered, 10% formaldehyde-fixed, paraffin-embedded, and transversal sections in horizontal plane were stained with hematoxylin-eosin, Masson trichrome and periodic acid-Schiff stain. Histochemical stainings were interpreted and scored simultaneously by two independent investigators. The histological analysis was performed in blinded fashion on 4-micrometer sections with light microscopy, using the most appropriate stain for each lesion.

Pathological changes in the kidney were assessed by evaluating glomerular activity (glomerular, endocapillary and extracapillary proliferation, karyorrhexis/fibrinoid necrosis, hialyne thrombi, cellular crescents, floccular synechia, wire loops, hyaline deposits, and fucsinophils deposits), tubulointerstitial activity (tertiary lymphoid structures, interstitial inflammation, tubular cell necrosis, tubular casts, and flattening and tubular distension), and the chronicity of the lesions (fibrous crescents, glomerular sclerosis, tubular atrophy, and interstitial fibrosis), as previously reported (Hill et al. 2005).

Sections were scored using a 0-3 scale for glomerular activity, as follows: 0 = no lesions, 1 = lesions in, 25% of glomeruli, 2 = lesions in 25-50% of glomeruli, and 3 = lesions in >50% of glomeruli. Tubulointerstitial activity and lesion chronicity indices were scored using a 0–4 scale, as follows: 0 = no lesions, 1 = lesions in 1-10%, 2 = 11-25%, 3 = >25-50% and 4 = >50-100%. In the evaluation of mesangial sclerosis, <50% affected glomeruli were considered focal; diffuse> or equal to 50%; Segmental part of the glomerulus, and global> 50% of the glomerulus. Finally, was assessed the number of nuclei per glomerular cross-section (50 glomeruli without sclerosis per mouse). The mean scores for individual pathological features were summed to obtain the three main scores: the glomerular activity score, the tubulointerstitial activity score, and the chronic lesion score.

5. Plasma, urine, and faecal parameters

5.1. Plasma determinations

Blood samples were extracted from the left ventricle, cooled on ice and centrifuged for 10 min at 3,500 rpm at 4 ºC. Next, plasma samples were kept at -80 °C. Anti-ds-DNA antibody levels were measured in the aliquots as reported previously using an Alpha Diagnostic ELISA Kit (Alpha Diagnostic International, Texas, USA) according to the instructions of the manufacturer, as previously described (Toral et al. 2019). Additionally, we also analysed LPS contents in plasma with the Pierce™ chromogenic endotoxin quant kit (Thermo Fisher Scientific, Massachusetts, USA), following the provided instructions.

TMAO and TMA levels determination in plasma was carried out by stable isotope dilution high-performance liquid chromatography with online electrospray ionization tandem mass spectrometry on an AB SCIEX 5000 triple quadrupole mass spectrometer (SCIEX, Toronto, Canada) interfaced with a Shimadzu high-performance liquid chromatography system using a silica column (4.69250 mm, 5 lm Luna Silica; Regis) at a flow rate of 0.8 mL/min. The separation was carried out, as described previously (Wang et al. 2014).

Analysis of SCFA in mouse plasma was performed by liquid chromatography-triple quadrupole-mass spectrometry (LC-QqQ-MS) with stable-isotope internal standard calibration after chemical derivatization with dansylhydrazine (Sigma, Missouri, USA) following an optimized and validated method (Zhao and Li 2018). Analysis was carried out at CEMBIO, (Centre for Metabolomics and Bioanalysis, Madrid, Spain), with the LC Instrument 1260 Infinity series (Agilent Technologies, Madrid, Spain), coupled to a Triple Quadrupole

analyser (G6470A, Agilent Technologies, Madrid, Spain) with an electrospray ionization source in positive mode. Data was collected in dynamic multiple reaction monitoring.

5.2. Urine determinations

Combur Test strips (Roche Diagnostics, Mannheim, Germany) were utilized to determine proteinuria, depositing a drop of instant urine on top of the reactive strip and observing color changes and comparing them with the color guide provided by the manufacturer.

5.3. Faecal determinations

Concentrations of SCFA in faecal samples were measured through gas chromatography, employing a previously reported methodology (Robles-Vera et al. 2020). Stool samples were diluted in sterile PBS (1:5 w/v) and vortexed until complete homogenisation. After centrifugation 1 min 2000 rpm, supernatant was transferred to new tubes. H_2SO_4 was added for acidification and 2-methyl-valeric acid was used as internal standard (25mM, Sigma, Missouri, USA). Chloroform was added for phase separation followed by centrifugation 5 min 14000 rpm. Organic phase containing SCFA was collected for gas chromatography.

6. Vascular reactivity studies

Descending thoracic aortic samples were mounted in a wire myograph (model 610M, Danish Myo Technology, Aarhus, Denmark) containing Krebs solution (composition in mM: 118 NaCl, 4.75 KCl, 25 $NaHCO_3$, 1.2 $MgSO_4$, 2 $CaCl_2$, 1.2 KH_2PO_4 and 11 glucose). They were kept at 37ºC, gassed with 95% O_2 and 5% CO_2 (pH = 7.4) and subjected to standard conditions for isometric tension measurement, as detailed in prior publications from our research group (Toral et al. 2018). Length-tension parameters were assessed with Myodaq 2.01 software and the tissue segments were pre-tensed to a tension of 5 mN. Pre-contraction was induced using thromboxane A_2 analog U46619 (3 nM, Sigma, Missouri, USA). Serial relaxation curves were generated over 30 min, alternating between washes in the absence and presence of the specific pan-NOX inhibitor VAS2870 (10 µM, Sigma, Missouri, USA) or the Rho kinase inhibitor Y27632 (0.5 µM, Sigma, Missouri, USA). To assess the role of IL-17a, aortic rings were exposed to anti-IL-17a antibody (10 µg/mL, Invivogen, California, USA) for 6 hours prior to

constructing a relaxation-response curve with acetylcholine (Ach). Results were expressed as relaxation levels relative to pre-contraction tone.

7. NADPH oxidase activity

NOX activity was determined in vascular tissue with a lucigenin-enhanced chemiluminescence assay in intact aortic segments as previously described (Romero et al. 2017). Aortic segments from all groups were incubated for 30 min at 37 ºC in 4-(2-hydroxyethyl)-1- piperazineethanesulfonic acid (HEPES)-based solution, adding NADPH (100 µM, Sigma, Missouri, USA) to stimulate enzymatic activity. Measurements were recorded with a scintillation chamber (Lumat LB 9507, Berthold, Germany) in the presence of lucigenin (5 µM). NOX activity was expressed as relative luminescence units (RLU)/min/mg dry aortic tissue.

8. *Ex vivo* vascular ROS

Aortic segments were included in optimum cutting temperature (OCT) and stored at -80ºC. Cross-sections (5 µm) were incubated 15 min with Dihydroethidium (DHE, 10 µM, Life Technologies S.A., Madrid, Spain), a red fluorescent dye, which served as ROS sensor, as previously explained (Romero et al. 2017). Then, samples were washed with HEPES buffer (Sigma, Missouri, USA) and incubated 5 min with 4′,6-diamidino-2-phenylindole (DAPI, 500 nM, Thermo Fisher Scientific, Massachusetts, USA) for nuclear staining. Images were acquired using a Leica DMI 3000B microscope (Leica Microsystems GmbH; Wetzlar, Germany) and were processed for presentation with Photoshop (Adobe) and analyzed with ImageJ software (version 1.52a, NIH, http://rsb.info.nih/ij/).

9. RT-PCR analysis

Reverse Transcriptase-Polymerase Chain Reaction (RT-PCR) was performed in colon, MLN, and aorta following previous protocols (Robles-Vera et al. 2020). Tissues were homogenized in 0.5 mL of PRImeZOL Reagent (Canvax Biotech, S.L., Córdoba, Spain) and RNA samples were extracted using 1-bromo-3-chloropropane (Sigma, Missouri, USA) and 2-propanol (Sigma, Missouri, USA).

Quantification with NanoDrop™ (Sigma, Missouri, USA) followed by cDNA retrotranscription using standard RT-PCR methods were carried out. PCRs were executed using a PCRMax Eco 48 thermal cycler (PCRMax, Stone, Staffordshire, UK). For mRNA expression analysis, quantitative real-time RT-PCR technique was employed. Forward and reverse primers used in PCR reactions are detailed in **Table 2**. RT-PCRs were conducted as per our established protocol, with ribosomal protein L13a (RPL13a) as the reference gene. Data analysis was carried out using the ΔΔCt method (Robles-Vera et al. 2020).

Table 2. Oligonucleotides for real-time RT-PCR.

mRNA targets	Descriptions	Sense	Antisense
MCT-1	Monocarboxylate Transporter-1	GTGCAGCAGCCAAGGAGCCC	CCATGGCCAGTCCGTTGGCC
MCT-4	Monocarboxylate Transporter-4	CAGCTTTGCCATGTTCTTCA	AGCCATGAGCACCTCAAACT
Hif-1a	Hypoxia Inducible Factor-1 Alpha	ACCTTCATCGGAAACTCCAAAG	CTGTTAGGCTGGGAAAAGTTAGG
TLR-4	Toll-Like Receptor-4	GCCTTTCAGGGAATTAAGCTCC	AGATCAACCGATGGACGTGTAA
GPR41	G-protein-coupled Receptor-41	CTTCTTTCTTGGCAATTACTGGC	CCGAAATGGTCAGGTTTAGCAA
GPR43	G-protein-coupled Receptor-43	CGTTGGGGCTCAGAGGCGAC	TGCTCGGGAAGATCCGGGGG
HDAC-3	Histone Deacetylase-3	GCCAAGACCGTGGCGTATT	GTCCAGCTCCATAGTGGAAGT
Occludin	Occludin	ACGGACCCTGACCACTATGA	TCAGCAGCAGCCATGTACTC
ZO-1	Zonula Occludens-1	GGGGCCTACACTGATCAAGA	TGGAGATGAGGCTTCTGCTT
MUC-2	Mucin-2	GATAGGTGGCAGACAGGAGA	GCTGACGAGTGGTTGGTGAATG
MUC-3	Mucin-3	CGTGGTCAACTGCGAGAATGG	CGGCTCTATCTCTACGCTCTCC
IL-1β	Interleukin-1 Beta	GCTACCTGTGTCTTTCCCGT	CATCTCGGAGCCTGTAGTGC
TNF-α	Tumor Necrosis Factor-Alpha	CTACTCCCAGGTTCTCTTCAA	GCAGAGAGGAGGTTGACTTTC
CX3CR1	CX3C Chemokine Receptor-1	GAGTATGACGATTCTGCTGAGG	CAGACCGAACGTGAAGACGAG
CD80	CD80	TTCCCAGCAATGACAGACAG	CCATGTCCAAGGCTCATTCT
CD86	CD86	TCAATGGGACTGCATATCTGCC	GCCAAAATACTACCAGCTCACT
Itga4	Integrin Alpha-4	TGTGCAAATGTACACTCTCTTCCA	CTCCCTCAAGATGATAAGTTGTTCAA
Itgb7	Integrin Beta-7	AAACGGTGCTGCCCTTTGTAA	CTCTCTCTCGAAGGCTTGAGC
IL-6	Interleukin-6	CTCTGGGAAATCGTGGAAAT	TGTACTCCAGGTAGCTATGG

HO-1	Hemo-oxigenase-1	CCTCACTGGCAGGAAATCATC	CCTCGTGGAGACGCTTTACATA
NQO-1	NAD(P)H Quinone Dehydrogenase-1	TTCTCTGGCCGATTCAGAGT	GGCTGCTTGGAGCAAAATAG
IL-1β	Interleukin-1 Beta	GCTACCTGTGTCTTTCCCGT	CATCTCGGAGCCTGTAGTGC
eNOS	Endothelial Nitric Oxide Synthase	ATGGATGAGCCAACTCAAGG	TGTCGTGTAATCGGTCTTGC
NOX4	NOX4 Subunit of NOX	GGATCACAGAAGGTCCCTAGC	TTGCTGCATTCAGTTCAAGG
P47phox	P47phox Subunit of NOX	TCTTCAAAGTGCGGCCTGAT	TGCCACGGTCATCTCTGTTC
NRF-2	Nuclear Factor-erythroid 2-related Factor-2	CTGAACTCCTGGACGGGACTA	CGGTGGGTCTCCGTAAATGG
KEAP-1	Kelch-like ECH-Associated Protein-1	CCCATGAGGCATCACCGTAG	CATAGCCTCCGAGGACGTAG
NLRP3	NLR Family Pyrin Domain Containing-3	CCTGACCCAAACCCACCAGT	TTCTTTCGGATGAGGCTGCTTA
ICAM-1	Intracellular Adhesion Molecule-1	GGTTCTCTGCTCCTCCACAT	CCTTCCAGGCTTTCTCTTTG
IL-6R	Interleukin-6 Receptor	GCCACCGTTACCCTGATTTG	TCCTGTGGTAGTCCATTCTCTG
RPL13a	Ribosomal protein L13a	CCTGCTGCTCTCAAGGTTGTT	TGGTTGTCACTGCCTGGTACTT

10. Western blot analysis

We examined the content of ZO-1 and occludin in colonic homogenates by western blot analysis (González-Correa et al. 2023). These samples were homogenated 1:10 (w/v) in radio-immuno-precipitation assay (RIPA, Sigma, Missouri, USA) buffer and protein quantification was performed following bicinchoninic acid method (Walker 1994). Samples were run on a sodium dodecyl sulphate-polyacrilamide electrophoresis (20 µg of protein per lane). Next, the transference of proteins was performed to polyvinylidene difluoride membranes (Bio-Rad, California, USA). The membranes were blocked with bovine serum albumin (Sigma, Missouri, USA) and then incubated with the respective primary antibodies: rabbit polyclonal anti-occludin (Abcam, Cambridge, UK) and rabbit polyclonal anti-TJ protein ZO-1 (Novus biological, Cambridge, UK). All were incubated at 1/1000 dilution overnight at 4ºC. The membranes were then incubated 2h with secondary peroxidase-conjugated goat anti-rabbit (1/10000; Santa Cruz Biotechnology, Texas, USA). Antibody binding was detected by an ECL system (Amersham Pharmacia Biotech, Amersham, UK) and densiometric analysis was done by ImageJ software (version 1.52a, NIH, http://rsb.info.nih/ij/). Samples were re-probed for β-actin.

11. Flow cytometry

MLN, spleens, and aorta were dissected, homogenized, and filtered to eliminate tissue debris. Blood was also collected. Erythrocytes were lysed using Gey solution (BioLegend, California, USA). A protein transport inhibitor (BD GolgiPlugTM, BD Biosciences, New Jersey, USA) was used according to the manufacturer instruction for an optimum detection of intracellular cytokines by flow cytometry, together with 50 ng/mL phorbol 12-myristate 13-acetate (Sigma, Missouri, USA) and 1 µg/mL ionomycin (Sigma, Missouri, USA). Then, cells were blocked with anti-Fc-γ receptor antibodies to avoid masking by nonspecific binding (Miltenyi Biotec, Bergisch Gladbach, Germany) and incubated with a live/dead viability stain (LIVE/DEAD® Fixable Aqua Dead Cell Stain, Thermo Fisher, Massachusetts, USA), for 30 min at 4°C in PBS.

Subsequently, we proceeded to surface staining for 20 min at 4°C in the dark diluting the antibodies in flow cytometry staining buffer (PBS, 1% bovine serum albumin, Sigma, Missouri, USA). Cells were then fixed and permeabilized with the buffers A and B sequentially (Fisher Scientific, New Hampshire, USA), and

intracellular staining was carried out for 30 min at 4°C in the dark. Last, cells were resuspended in test tubes with PBS for acquisition. The cells were stained for B cells (CD45+, B220+), Th17 (CD45+, CD3+ CD4+, IL-17a+), Th1 (CD45+, CD3+ CD4+, IFN-γ+), and Treg (CD45+, CD3+, CD4+, CD25+). Key antibodies for flow cytometry are included in **Table 3**. Flow cytometric analysis was conducted on a BD FACSymphony™ A5 Cell Analyzer (BD Biosciences, New Jersey, USA), following established methods (Toral et al. 2018), with the gating strategy outlined (**Figure 8**).

Table 3. Antibodies for flow cytometry.

Antibodies	Source
anti-CD45 (RRID:AB_2727597, FITC, clone 30-F11)	Miltenyi
anti-B220 (RRID:AB_398531, APC, clone RA3-6B2)	BD Bios.
anti-CD3 (RRID:AB_2801803, PE, clone REA641)	Miltenyi
anti-CD4 (RRID:AB_1107001, PerCP-Cy5.5, clone RM4-5)	Invitrogen
anti-CD25 (RRID:AB_2784091, PE-VIO770, clone 7D4)	Miltenyi
anti-IL-17a (RRID:AB_1073235, PE-Cy7, clone eBio17B7)	eBioscience
anti-IFN-γ (RRID:AB_2738165, PE-VIO770, clone XMG1.2)	eBioscience
viability dye (LIVE/DEAD® Fixable Aqua Dead Cell Stain)	Thermo F.

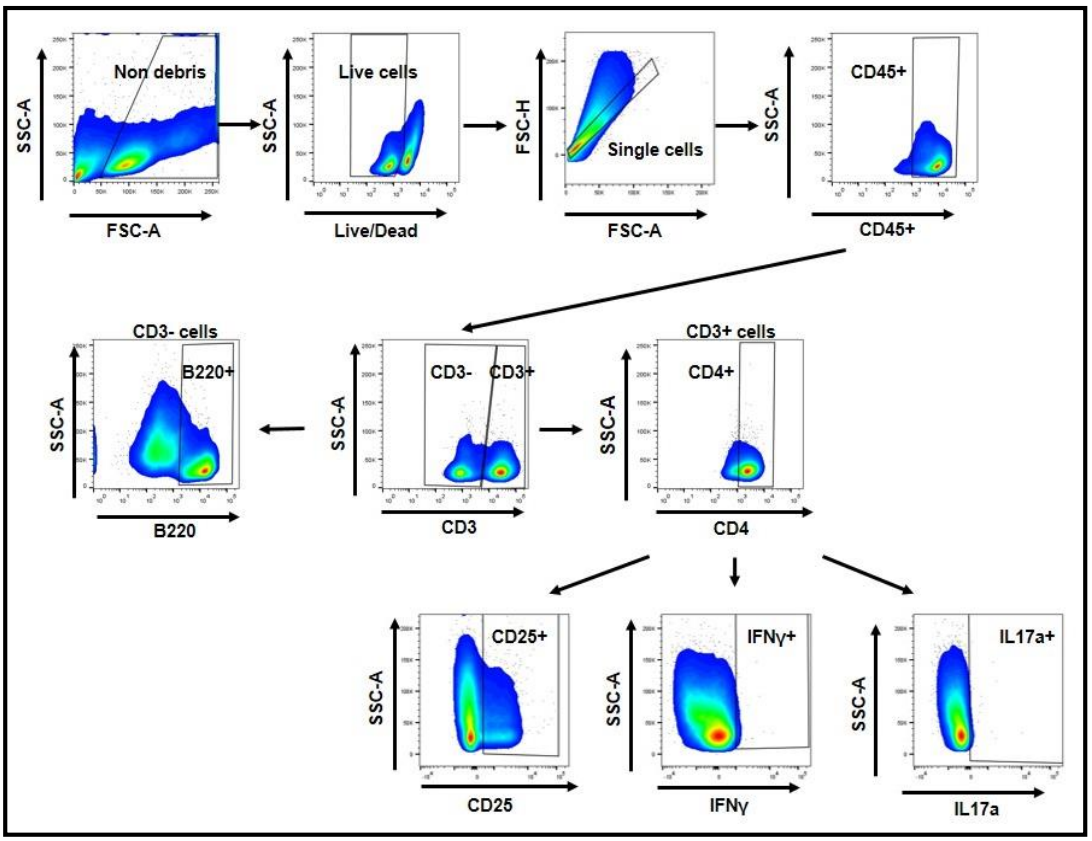

Figure 8. Gating strategy for flow cytometry.

12. Immunofluorescence

After the sacrifice, mouse colon tissues were isolated, fixed in 10% formalin overnight at 4 °C, and paraffin embedded. Paraffin cross-sections (5 µm) from fixed colons were prepared for immunofluorescence. Deparaffinized sections were rehydrated, boiled 3 min to retrieve antigens in 10 mM citrate buffer containing 0.05% Tween-20 (Sigma, Missouri, USA), pH=6, and blocked for 1 h with 10% goat serum (Thermo Fisher Scientific, Massachusetts, USA), 10% horse serum (Thermo Fisher Scientific, Massachusetts, USA), plus 4% bovine serum albumin (Sigma, Missouri, USA) in PBS. Samples were incubated with the following antibodies for immunofluorescence: rabbit monoclonal anti-FoxP3 (Cell Signaling, Massachusetts, USA), and rat monoclonal anti-ROR gamma (eBioscience, California, USA). Secondary antibodies were polyclonal Alexa-Fluor-647-conjugated goat anti-rabbit or polyclonal Alexa-Fluor-568-conjugated goat anti-rat (Molecular Probes, California, USA).

Sections were mounted with DAPI (Thermo Fisher Scientific, Massachusetts, USA) in Citifluor AF4 mounting medium (Aname, Madrid, Spain). The whole colonic cross-section was screened before taking representative pictures (minimum of three). Images were acquired at 512 × 512 pixels, 8 bits, using a Confocal TCS Leica SP5 microscope (Leica Microsystems GmbH; Wetzlar, Germany) fitted with a 40x oil-immersion objective. All images were processed for presentation with Photoshop (Adobe) and analyzed with ImageJ software (version 1.52a, NIH, http://rsb.info.nih/ij/).

13. DNA Extraction, 16S rRNA Gene Amplification, Bioinformatics

Stools from all groups were stored at -80ºC. Microbial DNA was obtained with G-spin columns (INTRON Biotechnology, Gyeonggi, South Korea) from 30 mg of faecal content in suspension with PBS, digested using proteinase K and RNAses, assessing resulting DNA concentrations with Quant-IT PicoGreen (Thermo Fischer Scientific, Massachusetts, USA) as previously documented (Dole et al. 2013).

Amplification was carried out on these samples for the V3-V4 region of the 16S rRNA gene (Caporaso et al. 2011). PCR products (approximately 450 bp) included extension tails, which allowed sample barcoding and the addition of specific Illumina sequences in a second low-cycle number PCR. Individual amplicon libraries were analyzed with a Bioanalyzer 2100 (Agilent Technologies, Madrid, Spain) and a pool of samples was made in equimolar amounts. The pool was further cleaned, quantified and the exact concentration estimated through real time PCR (Kapa Biosystems, Massachusetts, USA). Finally, the samples were sequenced on an Illumina MiSeq instrument (Illumina, California, USA) with 2 x 300 paired end read sequencing at the Unidad de Genómica (Parque Científico de Madrid, Madrid, Spain).

To process raw sequences, the barcoded Illumina paired-end sequencing (BIPES) pipeline was performed using the BIPES protocols (Zhou et al. 2011). First, the barcode primers were discarded when containing ambiguous bases or mismatches in the primer regions following BIPES protocols. Second, we eliminated all sequences found with more than one mismatch within the 40–70 bp region at each end. Third, we utilized 30 Ns to concentrate the two single-ended sequences for the downstream sequence analysis. We utilized UCHIME (implemented in USEARCH, version 6.1) to screen out and remove chimeras in the de novo mode (using-minchunk 20-xn 7-noskipgaps 2) (Edgar and Flyvbjerg 2015).

Between 90,000 and 220,000 sequences were identified in each sample. Further analyses were carried out with 16S Metagenomics (Version: 1.0.1.0) from Illumina. The sequences were subsequently clustered to an operational taxonomic unit (OTU) with USEARCH default parameters (USERACH61). The threshold distance was set to 0.03. Consequently, when similarities between 16S rRNA sequences were 97%, the sequences were classified as the same OTU. QIIME2-based alignments of representative sequences were carried out with PyNAST, and the SILVA database was used as the template file. The Ribosome Database Project (RDP) algorithm was used to classify the representative sequences into specific taxa with the default database (Zeng et al. 2019). The Taxonomy Database (National Center for Biotechnology Information) was used for classification and nomenclature. Bacteria were classified based on SCFA end-product, as previously described (Xia et al. 2021). Briefly, genera were classified into more than one group if they were defined as producers of different metabolites. Predicted metagenomes were mapped to the Kyoto Encyclopedia of Genes and Genomes pathways (KEGG) using the phylogenetic investigation of communities by reconstruction of unobserved states (PICRUSt) method. KEGG module abundance was determined by aggregating the abundance of genes annotated to the same feature. Pathway results were presented as the relative abundance of predicted functions.

14. Statistical analysis

Shannon diversity, Chao richness and Pielou evenness and observed species indexes were calculated with the PAST4.02 Palaeontological Statistics (PAST 4x). Reads in each OTU were normalized to total reads in each sample. Only taxa with a percentage of reads > 0.001% were used for the analysis. Partial least square discriminant analysis (PLS-DA) was also used on these data to determine significant taxonomic differences in two experimental groups, and variable importance in projection (VIP) scores were displayed to rank the ability of different taxa to discriminate between different groups. Principal components analysis (PCA) analyses were also performed with these data to identify significant differences between groups, using PAST 4.02. Linear discriminant analysis (LDA) scores above 3.5 were displayed, and Kruskal-Walllis test among classes and Wilcoxon test between subclasses with threshold 0.05.

Taxonomy was uploaded to the Galaxy platform (Segata et al. 2011) to generate Linear discriminant analysis effect size (LEfSe)/cladogram enrichment plots considering significant enrichment at a $P<0.05$. A volcano plot was generated by plotting $-\log10$ of the P-value against the log2 fold change of genus with the R package, ggplot2 (Ito and Murphy 2013). A quasi-likelihood F-test transformed P-value threshold ($P<0.05$) was utilized to highlight significantly differentiating data points. All data were analysed with GraphPad Prism 8. Results are expressed as means ± standard error of the mean (SEM) of measurements. The evolution of tail SBP and the concentration-response curves to Ach were analysed by two-way repeated-measures analysis of variance (ANOVA) with the Bonferroni post hoc test. The remaining variables were tested on normal distribution using Shapiro-Wilk normality test and compared using one-way ANOVA and Tukey post hoc test in case of normal distribution, or Mann-Whitney test or Kruskal-Wallis with Dunn multiple comparison test in case of abnormal distribution. $P < 0.05$ was considered statistically significant.

RESULTS

RESULTS

1. Role of gut microbiota in the development of hypertension in a TLR-7-dependent lupus mouse model

1.1. Antibiotic treatment prevented the raise of BP, renal injury, and disease activity in TLR-7-dependent SLE

Topical IMQ, a TLR-7 agonist, was used to induce lupus-like disease in mice not genetically prone to excessive TLR-7 signaling. It was administered topically three times a week in alternate days to wild-type BALB/cJRj mice (Yokogawa et al. 2014). IMQ exposition showed a high incidence of mortality (Barrat et al. 2007; Celhar and Fairhurst 2017; Crow 2014; Robles-Vera et al. 2020). The mouse mortality rate in each group treated with IMQ was the following: IMQ group, 25%, 2 dead mice out of 8; IMQ-VANCO group, 0%; and IMQ-MIX group, 12.5%, 1 dead mouse out of 8. As expected, IMQ-treated mice showed a progressive raise in SBP (**Figure 9A**), being approximately 35 mmHg higher in IMQ-treated animals than in CTR animals, at the experimental endpoint. No significant changes in heart rate were detected in the IMQ group (530.3 ± 23.9 bpm vs 540.7± 20.3 bpm, CTR and IMQ groups, respectively).

The IMQ-induced lupus model is characterized by kidney injury linked to autoimmunity (Robles-Vera et al. 2020; Yokogawa et al. 2014; Zegarra-Ruiz et al. 2019). We determined the renal function by measuring proteinuria and kidney histopathology.

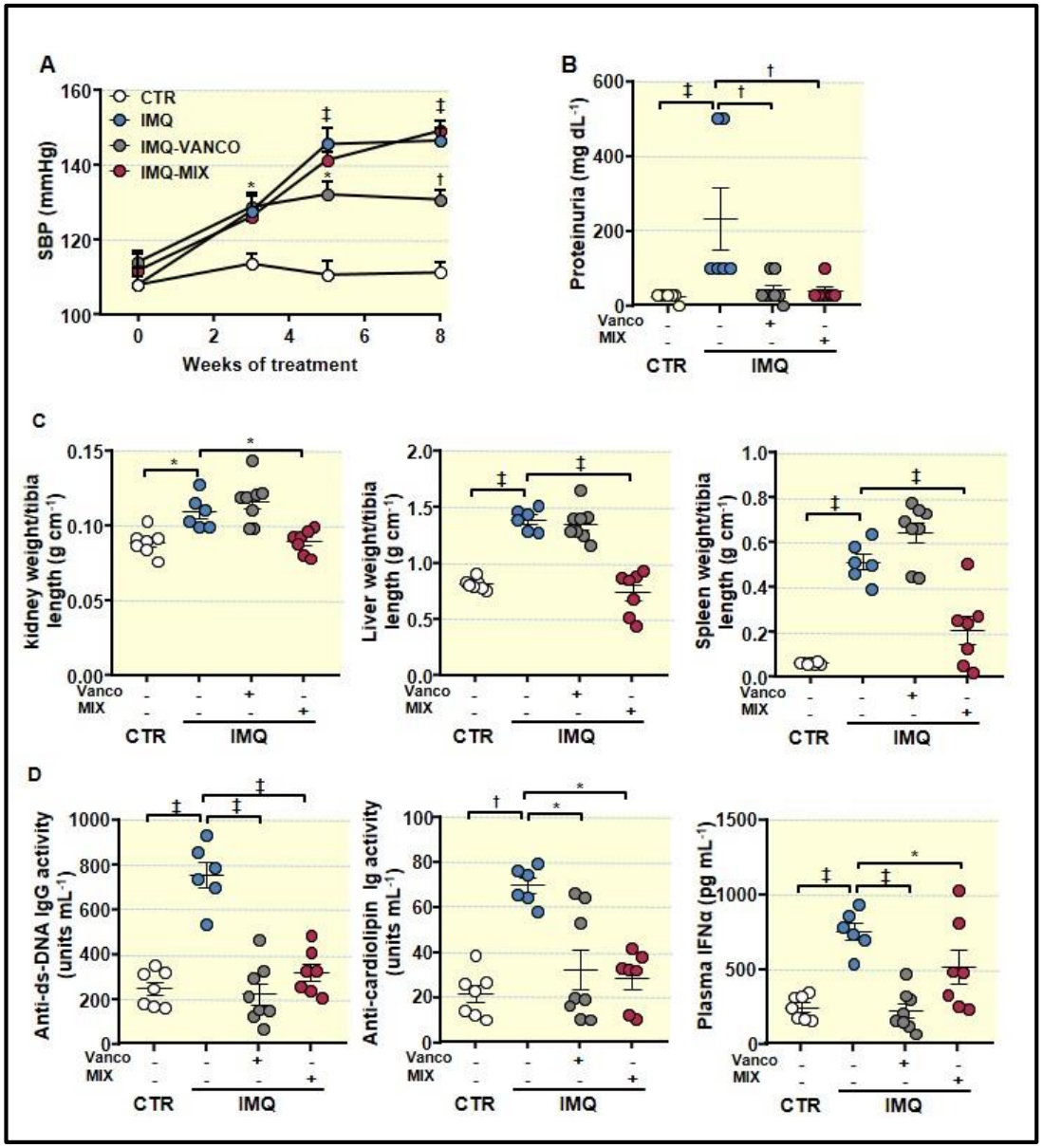

Figure 9. Effects of microbiota modification through population depletion with antibiotics on blood pressure, proteinuria, morphology, and disease activity in the imiquimod (IMQ) group.

(**A**) Systolic blood pressure (SBP) assessed with tail-cuff plethysmography, (**B**) proteinuria, (**C**) organ hypertrophy levels, (**D**) circulating double-stranded DNA (anti-ds-DNA) and anti-cardiolipin autoantibodies, and interferon (IFN)α levels in control (CTR), IMQ and IMQ-groups treated with Vancomycin (VANCO) or a cocktail of antibiotics (MIX). The data is represented as means ± SEM. The evolution of tail SBP was analysed by two-way ANOVA with the Tukey's multiple comparison test. The rest of the variables were tested with one-way ANOVA and Tukey post hoc test (morphological variables, and plasma anti-ds-DNA), or Kruskal–Wallis with Dunn's multiple comparison (proteinuria, anti-cardiolipin, plasma IFNα). * $p < 0.05$, † $p < 0.01$, ‡ $p < 0.001$ in comparison with CTR; * $p < 0.05$, † $p < 0.01$, ‡ $p < 0.001$ in comparison with IMQ.

We found significant higher protein concentration in urine (**Figure 9B**), moderate chronic perivascular and tubule-interstitial inflammatory infiltrate, mild hyaline casts in renal tubules, mild glomerular injury with extra-capillar crescent and scan immunocomplex deposits in glomerular tuft in kidney from IMQ group (**Figure 10**), showing impaired renal function. In addition, increased renal hypertrophy, hepatomegaly, and splenomegaly (**Figure 9C**) and plasma levels of anti-dsDNA and anti-cardiolipin autoantibodies, and IFNα (**Figure 9D**) were found in IMQ mice. To assess the role of the gut microbiota, we reduced the bacterial mass using VANCO and MIX. VANCO and MIX showed a reduction in total DNA levels in the colonic content by ≈ 73% and ≈ 89%, respectively (**Figure 11A**). As described previously [22], MIX treatment improved renal physiology by decreasing proteinuria (**Figure 9B**) and the inflammatory infiltrate and the glomerular injury in the kidney (**Figure 10**), it decreased splenomegaly, hepatomegaly, and renal hypertrophy (**Figure 9C**), and plasma levels of anti-dsDNA, anti-cardiolipin, and IFNα (**Figure 9D**), but did not inhibit the development of hypertension in IMQ-treated mice (**Figure 9A**). However, VANCO treatment prevented autoimmunity (reduced plasma levels of anti-dsDNA, anti-cardiolipin, and IFNα) (**Figure 9D**), proteinuria (**Figure 9B**) and renal injury histological features (**Table 4**), but also reduced the progressive increase in SBP induced by IMQ, by approximately -15 mmHg (**Figure 9A**). The effects of VANCO in SBP were independent of water consumption since mean water intake during treatments was similar among all experimental groups (mL mouse-1 day-1: CTR, 4.1 ± 0.2; IMQ, 4.3 ± 0.1; VANCO 4.2 ± 0.2; MIX 3.8 ± 0.3). Interestingly, when control mice were treated chronically with VANCO or MIX, without IMQ, no significant changes in SBP (**Figure 11B**), proteinuria (**Figure 11C**), vascular relaxation (**Figure 11D**) and NOX activity (**Figure 11E**) were observed as compared to untreated control group, showing specificity under conditions of TLR-7 activation. It also interesting to note the heterogeneity of some individual responses specific to the IMQ group observed in one or two animals. The reasons for this are unknown, but could be related to the variability in the topical administration of this drug.

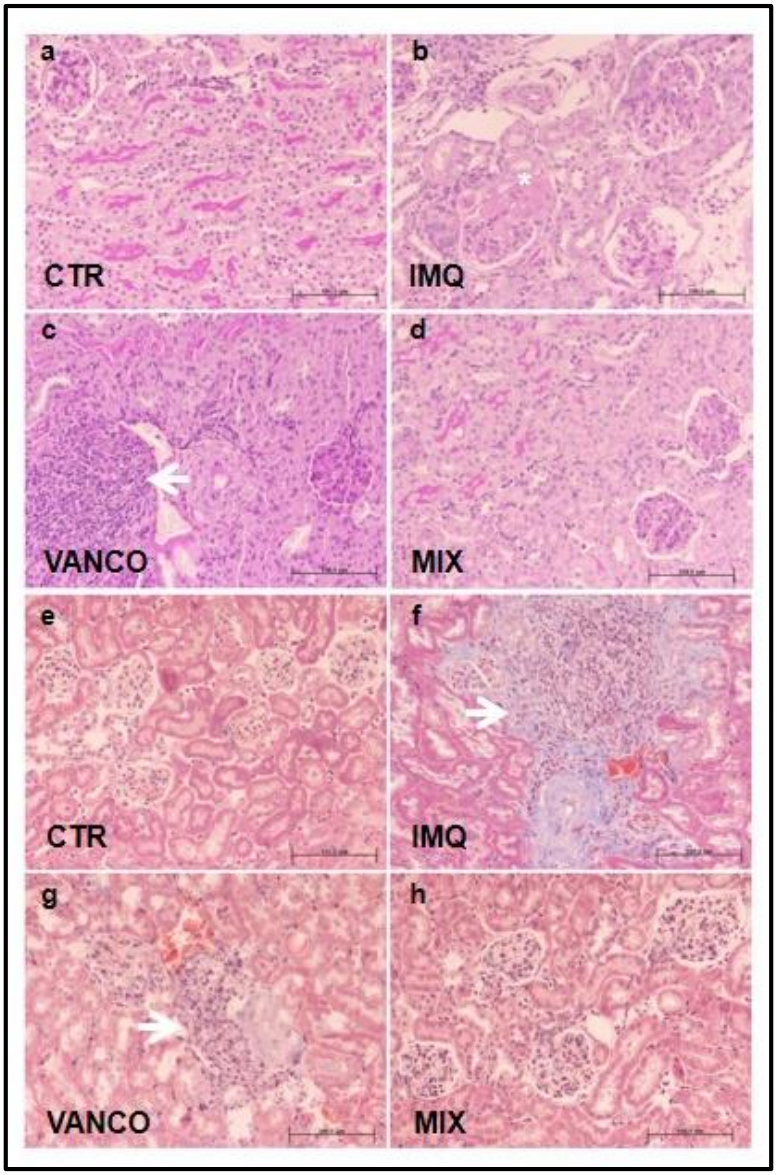

Figure 10. Effects of antibiotic treatments in renal injury in imiquimod (IMQ) mice.

Representative microphotographs of injury of mice renal cortex. Control group (CTR) with absence of tubulointerstitial lesions, preservation of the tubular brush border and normal glomerular size (a and e). IMQ group with glomerular size increase and presence of crescents (asterisk) and moderate perivascular chronic inflammatory infiltrate and mild fibrosis (arrow) (b and f). VANCO group with presence of mild perivascular chronic inflammatory infiltrate (arrow) (c and g). MIX group without tubulointerstitial or glomerular injury (d and h). (a to d, Periodic acid–Schiff stain; f to I, Masson trichrome stain). Bar scale: 100 micrometers.

Variables	CTR (n = 7)	IMQ (n = 6)	VANCO (n = 8)	MIX (n = 7)
Glomerulosclerosis (%)	0.0±0.0 [0]	0.0±0.0 [0]	0.0±0.0 [0]	0.0±0.0 [0]
Crescents (%)	0.0±0.0 [0]	23.7±6.2† [80]	4.7±3.1* [37.5]	1.0±0.7† [20]
Fuchsinophil deposits (%)	0.0±0.0 [0]	0.60±0.27* [67]	0.0±0.0* [0]	0.0±0.0* [0]
Mesangial sclerosis (%)	0.0±0.0 [0]	0.0±0.0 [0]	0.0±0.0 [0]	0.0±0.0 [0]
Cells/Glomerulus	27.8±1,3	33.7±1.7*	33.1±1.5	27.6±1.5*
Hyaline casts (0-3)	0.4±0.1 [28]	1.0±0.0* [100]	0.9±0.1 [87]	0.1±0.1† [14]
Inflammatory infiltrate (0-3)	0.0±0.0 [0]	1.8±0.2† [100]	1.1±0.2* [100]	1.0±0.2* [100]

Table 4. Quantification of renal lesions.

Values are expressed as means ± SEM of percentage of affected glomeruli (n=50/mouse). The percentage of mice with lesion is expressed in brackets [mice %]. *P<0.05, †P<0.01 compared to the CTR group; *P<0.05, †P<0.01 compared to the untreated IMQ group.

These data point to the gut microbiota being needed for TLR-7-dependent systemic autoimmunity, but only VANCO-sensitive gut microbiota was involved in the hypertensive effect induced by TLR-7 activation. We proceeded to study the gut microbial community composition derived from both antibiotic treatments, to assess potential pathobionts regulating TLR-7-dependent hypertension.

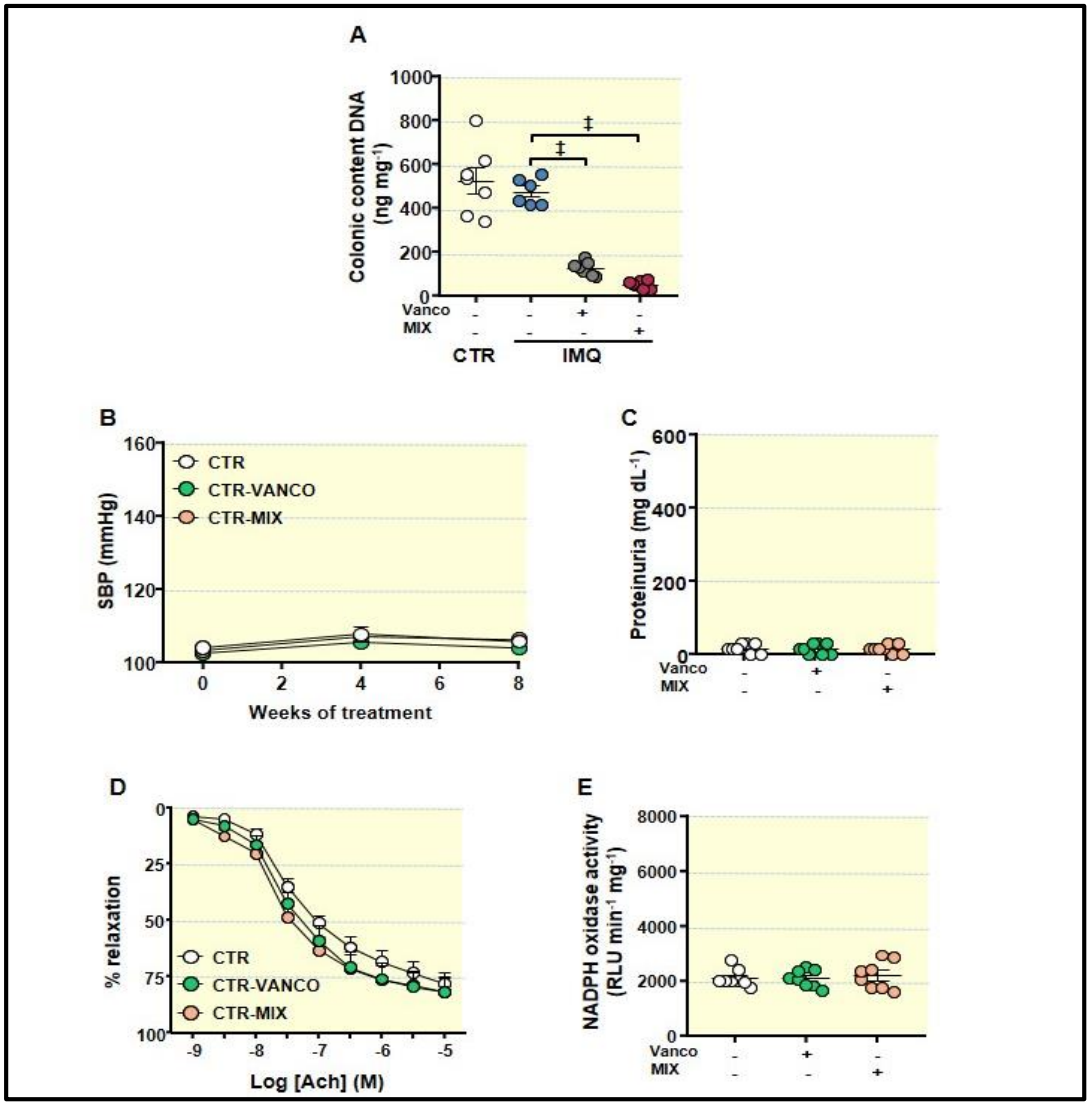

Figure 11. Effects of antibiotic treatments in DNA content of colonic microbiota in imiquimod (IMQ) mice and blood pressure, proteinuria, and endothelial function in control (CTR) mice.

(**A**) DNA content in the gut microbiota in control (CTR), IMQ and IMQ-groups treated with Vancomycin (VANCO) or a broad-spectrum antibiotic mixture (MIX). (**B**) Systolic blood pressure (SBP) measured by tail-cuff plethysmography, (**C**) proteinuria, (**D**) vascular relaxation responses induced by acetylcholine (Ach) in endothelium-intact aortas pre-contracted by U46619 (10 nM), and (**E**) aortic NADPH oxidase activity measured by lucigenin-enhanced chemiluminescence, in all experimental groups. Groups: control (CTR), and CTR-groups treated with Vancomycin (VANCO) or a broad-spectrum antibiotic mixture (MIX). Values are expressed as means ± SEM (n = 8). The concentration-response curves to Ach were analyzed by two-way ANOVA with the Tukey's multiple comparison test. The rest of the variables were tested with one-way ANOVA and Tukey post hoc test. ‡P<0.001 compared to the untreated IMQ group.

1.2. Antibiotic treatment changed colonic microbiota composition

We collected colonic content samples from mice, isolated bacterial DNA, and performed high-throughput 16S ribosomal DNA sequencing. The bacterial taxa (class, order, family, and genus) that experienced changes in IMQ mice, as indicated in our LDA, exposed that the relative abundance of 3 taxa was increased (green) and 1 taxa was decreased (red) as compared to CTR group (**Figure 12A**). No significant differences in the ecological parameters (Chao richness, Shannon diversity, Pielou evenness and numbers of species) were found between both groups (**Figure 12B**). However, increased bacteria belonging to *Actinobacteria* phylum was detected in IMQ group (**Figure 12C**). Antibiotic treatments induced profound changes in taxa as compared to IMQ group, according to the LDA (**Figure 13**). VANCO is a drug that mainly eradicates gram-positive microorganisms and cannot be absorbed in the intestines. Similar to that described in VANCO-treated female lupus prone LPR mice (Mu et al. 2020), VANCO treatment of IMQ mice reduced Shanon diversity (the combined parameter of richness and evenness) and numbers of species, while MIX showed a reduction in richness (an estimate of a total number of OTUs present in the given community), and numbers of species, but increased evenness (that shows how uniformly individuals in the community are distributed over different OTUs) (**Figure 12B**).

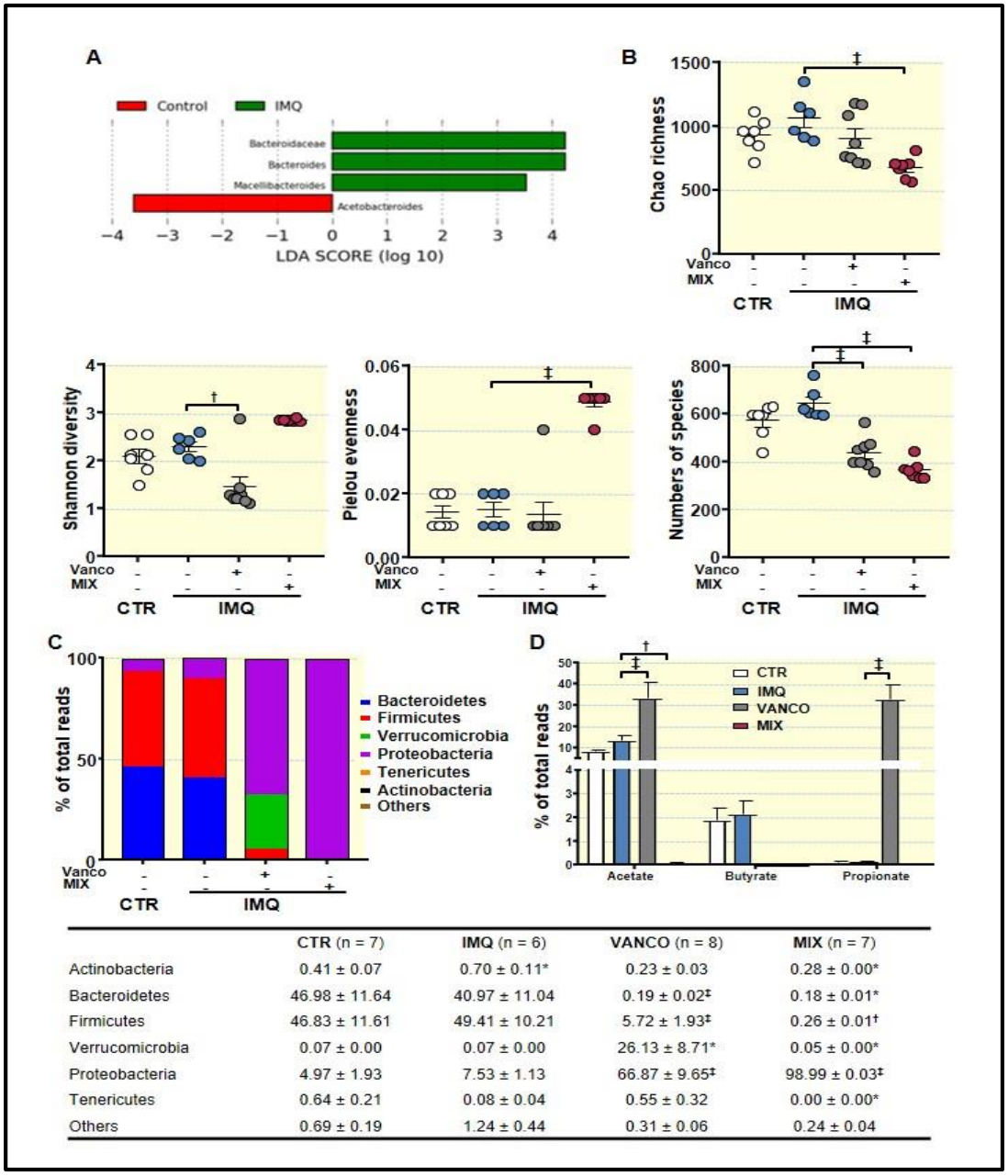

	CTR (n = 7)	IMQ (n = 6)	VANCO (n = 8)	MIX (n = 7)
Actinobacteria	0.41 ± 0.07	0.70 ± 0.11*	0.23 ± 0.03	0.28 ± 0.00*
Bacteroidetes	46.98 ± 11.64	40.97 ± 11.04	0.19 ± 0.02‡	0.18 ± 0.01*
Firmicutes	46.83 ± 11.61	49.41 ± 10.21	5.72 ± 1.93‡	0.26 ± 0.01†
Verrucomicrobia	0.07 ± 0.00	0.07 ± 0.00	26.13 ± 8.71*	0.05 ± 0.00*
Proteobacteria	4.97 ± 1.93	7.53 ± 1.13	66.87 ± 9.65‡	98.99 ± 0.03‡
Tenericutes	0.64 ± 0.21	0.08 ± 0.04	0.55 ± 0.32	0.00 ± 0.00*
Others	0.69 ± 0.19	1.24 ± 0.44	0.31 ± 0.06	0.24 ± 0.04

Figure 12. Effects of treatment with antibiotics on ecological indices and microbial phyla of in the gut from imiquimod (IMQ) mice.

(**A**) LEfSe significant differences (red bars Control enriched, green bars IMQ enriched). (**B**) Ecological parameters, (**C**) Proportion of bacterial phyla, and (**D**) Proportion of SCFAs-producing-bacteria in the microbiota from control (CTR), IMQ and IMQ-groups treated with Vancomycin (VANCO) or our cocktail of antibiotics (MIX). Data is represented as means ± SEM. Two-way ANOVA with the Tukey's multiple comparison test (SCFA-producing bacteria proportion). * $p < 0.05$ compared to CTR group; * $p < 0.05$, † $p < 0.01$, ‡ $p < 0.001$ compared to the untreated IMQ group.

Very significant shifts in phyla proportions were detected, especially in MIX (**Figure 12C**). The ratio between *Bacteroidetes* and *Firmicutes* was decreased whereas *Verrucomicrobia* and *Proteobacteria* were higher in VANCO as compared to IMQ, similar to that previously described with VANCO treatment in high fat diet-fed mice (Fujisaka et al. 2016) and in LPR mice (Mu et al. 2020). In agreement with previous report using the same mixture of broad-spectrum antibiotics in young and old mice (Brunt et al. 2019), *Proteobacteria* was the most abundant phylum in the microbiota from MIX group (≈ 99 %), with a profound depletion of *Bacteroidetes* and *Firmicutes*. Within the phylum *Firmicutes*, VANCO induced the decline of class *Clostridia*, without significant changes in *Erysipelotrichia* and *Bacilli* (not shown). Within the class *Clostridia*, every major family decreased, including *Clostridales* and *Lachnospiraceae* (not shown). This was accompanied by a significant increase of Gram negative *Proteobacteria* family *Enterobacteriaceae* (not shown). At genus level, the proportion of *Barnesiella* (*Bacteroidetes*, *Porphyromonadaceae*) and *Clostridium* XIVa (*Clostriales*) was reduced and *Escherichia*/*Shigella* (*Enterobacteriaceae*) was increased by both antibiotic treatments (**Figure 13**). By contrast, the proportion of Gram negative bacteria *Akkermansia* (*Verrucomicrobia*) and *Parasutterella* (*Proteobacteria*) was increased by VANCO but not by MIX treatment (**Figure 13**). As previously described, 16S rDNA sequencing of faecal samples from TLR-7-dependent mouse models of SLE and from SLE patients compared with healthy controls, showed Gram positive bacteria *Lactobacillus ssp*. (*Bacilli*) enrichement and translocation to internal organs (Zegarra-Ruiz et al. 2019). However, in our experimental conditions, the relative populations of Lactobacillus were not significatively different between CTR and IMQ group, which were unaffected by VANCO (consistent with the known resistance of several species of lactobacilli to VANCO) and reduced by MIX.

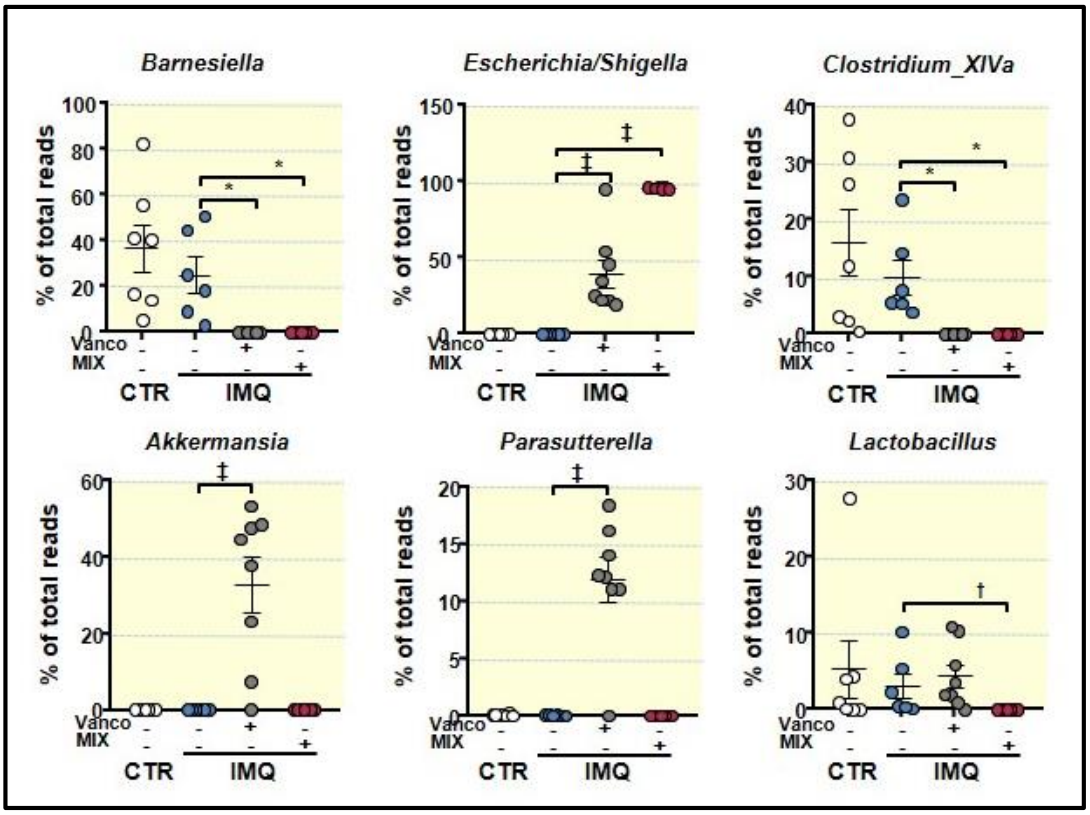

Figure 13. Effects of antibiotic treatments in the main genera proportion of gut microbiota in imiquimod (IMQ) mice.

The genera content was expressed as percentage of total reads in faeces from control (CTR), IMQ and IMQ-groups treated with Vancomycin (VANCO) or a broad-spectrum antibiotic mixture (MIX). Values are expressed as means ± SEM. One-way ANOVA and Tukey post hoc test. *P<0.05, †P<0.01, ‡P<0.001 compared to the untreated IMQ group.

SCFA are metabolites resulting from the fermentation of undigested carbohydrates in gut microbiota with known beneficial effects (Robles-Vera et al. 2020). However, no significant changes in the proportion of SCFA-producing bacteria were found between CTR and IMQ groups (**Figure 12D**). Interestingly, VANCO treatment increased ACE- and PROP-producing bacteria (**Figure 12D**). SCFA could exert certain actions on intestinal cells and on at local immune system level. We next investigated whether antibiotic treatments induced changes in immune cells in secondary lymph organs.

1.3. Antibiotic treatments attenuated T cells imbalance

An elevated production of autoantibodies and the progression of the lupus-like autoimmune pathology can be associated with an imbalance of T cells (Talaat et al. 2015) and B cell proliferation (Dar et al. 1988; Robles-Vera et al. 2020). We assessed B and T cell levels in MLN and spleens from all experimental groups.

B cell relative populations (CD3-B220+) were higher in spleen from IMQ mice than in the CTR group, but not in MLN (**Figure 14A, 14B**). VANCO and MIX treatments reduced splenic B cell populations (**Figure 14B**). The proportion of Th cells (CD3+CD4+) presented no significant differences among all experimental groups in both MLN and spleen. Treg (CD4+CD25+) and Th17 (CD4+IL-17a+) cell relative populations increased in spleen from IMQ mice (**Figure 14B**), whereas only Th17 cells where higher in lupus disease in the MLN (**Figure 14A**). VANCO treatment prevented the raise in Th17 cell content as seen in IMQ in both secondary lymph organs, being without effect in the proportion of Treg cells. By contrast, MIX treatment did not change Th17 cell population but reduced Treg content in the spleen (**Figure 14A, 14B**).

Circulating Th17 lymphocytes were increased in IMQ group compared to control mice (**Figure 14C**). In line with changes brought by treatment with the antibiotics in MLN, VANCO decreased circulating Th17 cell populations, being without effects MIX. Plasma levels of IL-17a were higher in IMQ than in CTR (**Figure 14C**), which were reduced by VANCO treatment. Taken account that IL-17a is a key factor contributing to endothelial dysfunction in this TLR-7-driven lupus autoimmunity model (Robles-Vera et al. 2020), we next examined the changes brought by the antibiotics on the observed SLE-linked endothelial dysfunction.

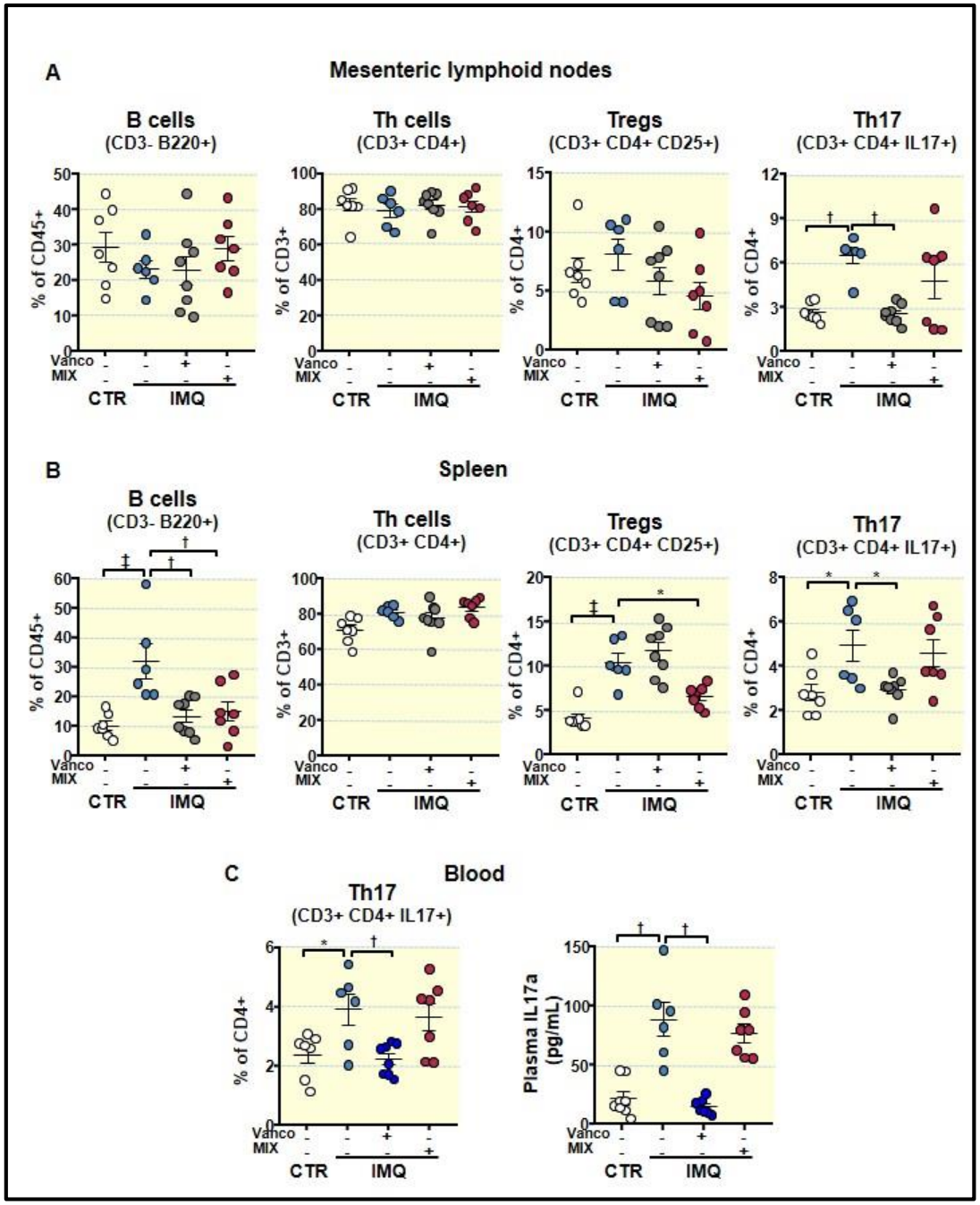

Figure 14. Effects of treatment with antibiotics on lymphocyte activation and proliferation in imiquimod (IMQ) animals.

(**A**) Total B lymphocytes, Th, Treg and Th17 cells as detected with flow cytometry in mesenteric lymph nodes, (**B**) in spleen, and (**C**) blood from control CTR, IMQ, VANCO and MIX. Data is represented as means ± SEM. The variables were tested with one-way ANOVA and Tukey post hoc test. * $p < 0.05$, † $p < 0.01$, ‡ $p < 0.001$ compared to the CTR group; * $p < 0.05$, † $p < 0.01$ compared to the untreated IMQ group.

1.4. The antibiotics prevented endothelial dysfunction, vascular oxidative stress and Th17 vascular infiltration

IMQ-treated animals presented strongly reduced endothelium-dependent vasorelation to Ach in comparison CTR animals (Emax= 39.7 ± 6.2 % and 64.1 ± 3.6 %, respectively, P<0.01) (**Figure 15A**). VANCO was able to improve this impairment, being without effect MIX. The Ach-induced response was also improved in aorta segments from IMQ-treated animals post-Y27632 incubation (a Rho kinase inhibitor) (**Figure 15A**), suggesting that the decreased relaxation with Ach is mediated, at least partially, by Rho kinase activation. The activation of RhoA/Rho kinase by ROS has already been previously described (MacKay et al. 2017). NOX is the main source of ROS in the vascular wall; thus, we tested the relaxation to Ach in the presence of the selective NOX inhibitor VAS2870, and the NOX activity in all experimental groups (**Figure 15B**). In the presence of VAS2870, improvement of endothelium-dependent relaxation to Ach was observed in aortic rings from IMQ group, being similar to that found in CTR group, which suggest the involvement of NOX activity in the endothelial dysfunction found in aortic rings from IMQ mice. In fact, the NOX activity was approximately 2-fold more elevated in segments of IMQ mice than in aortic segments of CTR animals. In agreement with this, MIX treatment, which was unable to improve the relaxation to Ach, showed a NOX activity similar IMQ rings, whereas rings from VANCO group showed lower NOX activity than IMQ group. To further explore the role of IL-17a in endothelial dysfunction induced by IMQ, we incubated for 6 hours with anti-IL-17a antibody (nIL-17). The neutralization on IL-17a improved the relaxation to Ach in rings from IMQ group, but not in control rings (**Figure 15C**). Considering that Th17 cells boosted vascular ROS synthesis, we determined aortic infiltration levels of Th17 lymphocytes. Th17 infiltration was higher in aorta from IMQ than in CTR, which was reduced by VANCO but not by MIX treatment (**Figure 15C**). Interestingly, when control mice were treated with VANCO or MIX no significant changes were observed in the relaxation to Ach (**Figure 11D**) or in the NOX activity (**Figure 11E**), as compared to untreated control mice.

Hierarchical cluster analysis (according distance measure using Pearson test correlation and clustering algorithm using ward.D) represented as heat map of the fifty most abundant bacterial genera detected among groups, showed clear separation of groups to cluster by BP and Th17 population in MLN (**Figure 16**). We subsequently examined whether the enriched gut bacterial communities partake in Th17 polarization in MLN and high BP-associated with TLR-7 activation.

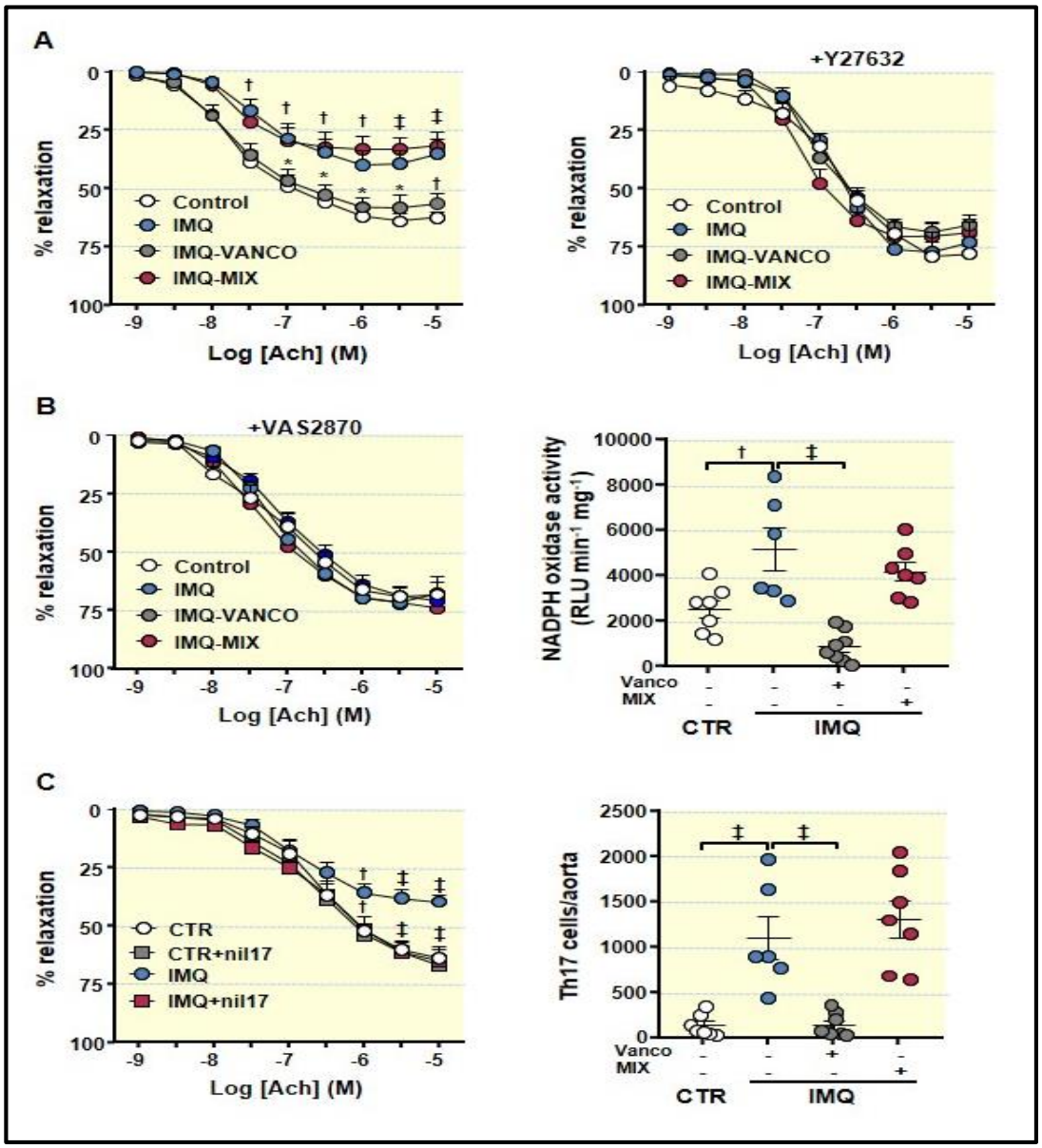

Figure 15. Effects of treatment with antibiotics on SLE-linked endothelial dysfunction, NADPH oxidase activity and immune cell aorta infiltration in imiquimod (IMQ) mice.

(**A**) Ach-induced relaxation responses in aortas pre-contracted by U46619 (10 nM), with or without the Rho kinase inhibitor Y27632 (1 μM); (**B**) Aortic responses induced by Ach in the absence or in the presence of the specific pan-NOX inhibitor VAS2870 (1 μM) and aortic NADPH oxidase activity determined using a lucigenin-enhanced chemiluminescence. (**C**) Aortic responses induced by Ach in the absence or in the presence of anti-IL-17a antibody (10 μg/mL) and aortic infiltration of Th17 assessed with flow cytometry. Data is represented as means ± SEM. The concentration-response curves to Ach were analysed by two-way ANOVA with the Tukey's multiple comparison test. The rest of the variables were tested with one-way ANOVA and Tukey post hoc test. † $p < 0.01$, ‡ $p < 0.001$ in comparison with CTR; * $p < 0.05$, † $p < 0.01$, ‡ $p < 0.001$ in comparison with IMQ.

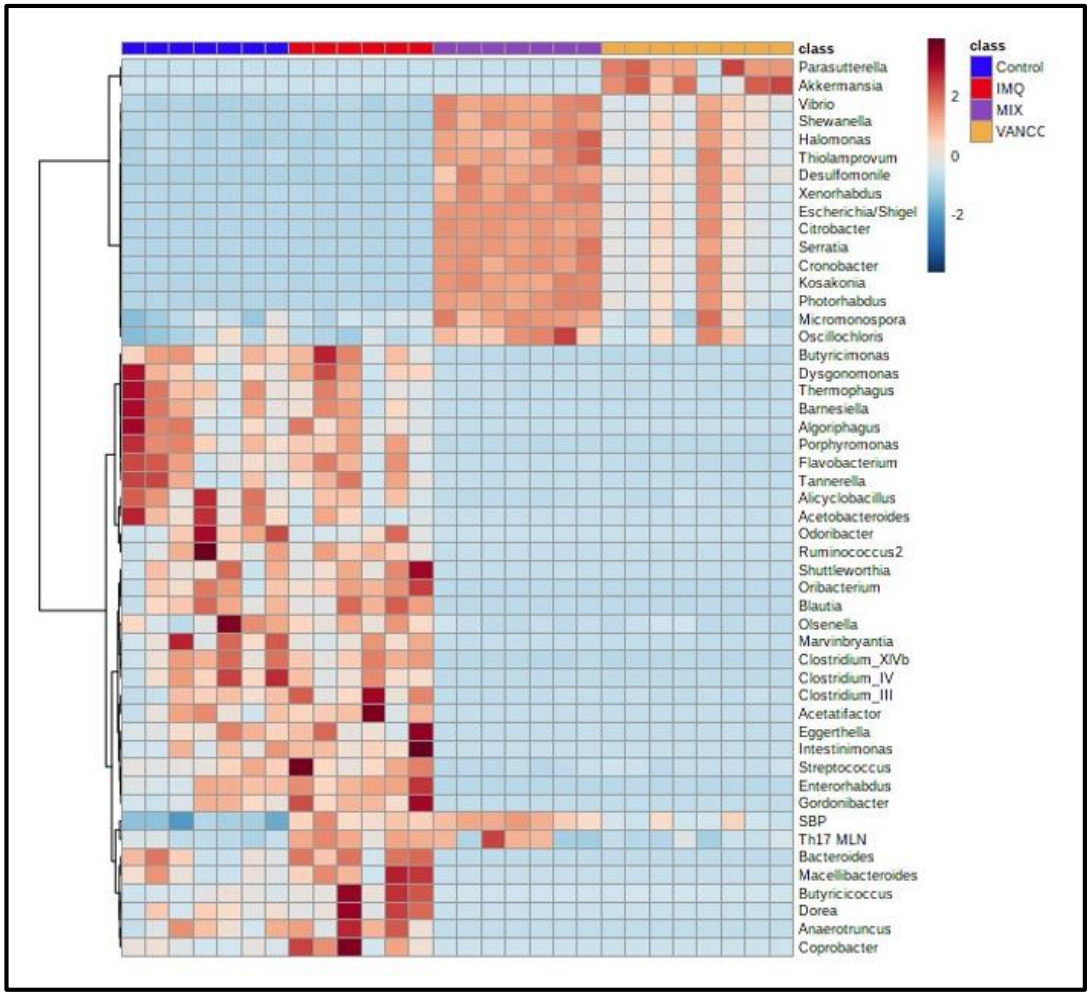

Figure 16. Effects of antibiotic treatments in the main genera proportion of gut microbiota in imiquimod (IMQ) mice associated with systolic blood pressure (SBP) and Th17 proportion in mesenteric lymph nodes (MLN).

Significantly enriched genera displayed within a heat map. The top dendrogram, and top row colored blue in control (CTR), red (IMQ), violet (IMQ-group treated with Vancomycin, VANCO), and orange (IMQ-group treated with a broad-spectrum antibiotic mixture, MIX), shows that the subjects tend to cluster by SBP and Th17 in MLN (Pearson test); abundances of the genera also cluster, dendrogram on the left. Rows are genus, columns individual mouse, and abundance is shown in individual cells on a sliding color scale.

1.5. Bacteria from IMQ-mice were transferable and induced high BP and endothelial dysfunction in control animals

To address the question whether microbiota from lupus mice induced by TLR-7 activation might affect BP and endothelial function regulation, we transplanted microbiota for 2 weeks from hypertensive IMQ or from normotensive CTR animals to recipient BALB/cJRj female mice or 8 weeks IMQ-treated mice (**Figure 17**). FMT from donor IMQ microbiota to recipient control mice increased SBP to a maximum of ≈ 22 mmHg, being without effect FMT from donor control microbiota to recipient control mice (**Figure 18A**). However, no significant change either in proteinuria (**Figure 18B**), plasma levels of anti-dsDNA and IFNα (**Figure 18C**), or B cells and Treg population in MLN (**Figure 18D**) were detected between CTR-CTR and CTR-IMQ, displaying no changes in lupus activity induced by transplant from IMQ mice. Interestingly, this microbiota increased plasma IL17 levels (**Figure 18C**), and the Th17 proportion in MLN (**Figure 18D**).

Additionally, Ach-induced endothelium-dependent relaxation in U46619-contracted segments of aorta from CTR-IMQ were decreased when compared to CTR-CTR group (Emax: 41.5 ± 4.9% vs. 63.7 ± 4.8%, $P<0.01$, respectively) (**Figure 19A**).

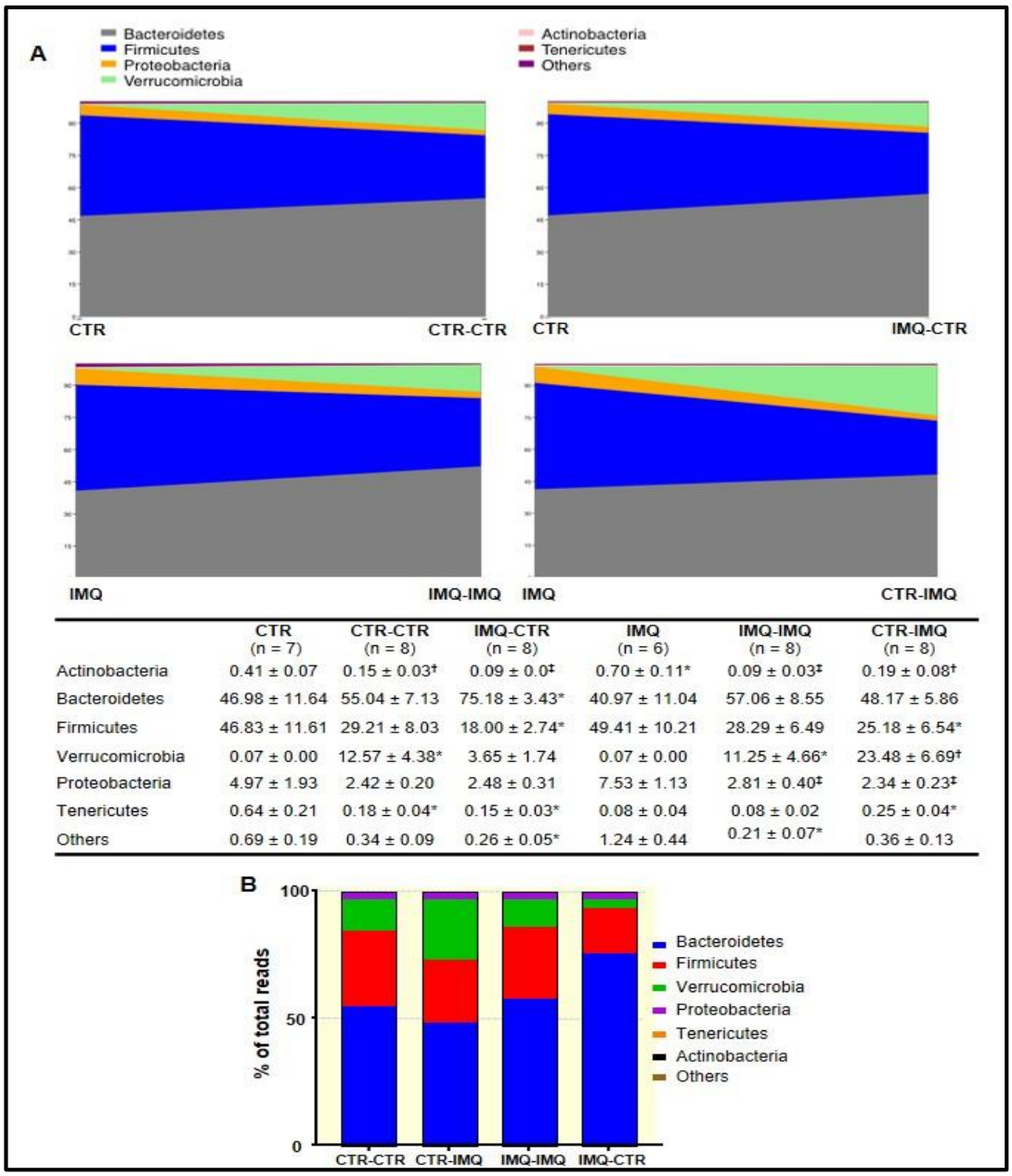

	CTR (n = 7)	CTR-CTR (n = 8)	IMQ-CTR (n = 8)	IMQ (n = 6)	IMQ-IMQ (n = 8)	CTR-IMQ (n = 8)
Actinobacteria	0.41 ± 0.07	0.15 ± 0.03†	0.09 ± 0.0‡	0.70 ± 0.11*	0.09 ± 0.03‡	0.19 ± 0.08†
Bacteroidetes	46.98 ± 11.64	55.04 ± 7.13	75.18 ± 3.43*	40.97 ± 11.04	57.06 ± 8.55	48.17 ± 5.86
Firmicutes	46.83 ± 11.61	29.21 ± 8.03	18.00 ± 2.74*	49.41 ± 10.21	28.29 ± 6.49	25.18 ± 6.54*
Verrucomicrobia	0.07 ± 0.00	12.57 ± 4.38*	3.65 ± 1.74	0.07 ± 0.00	11.25 ± 4.66*	23.48 ± 6.69†
Proteobacteria	4.97 ± 1.93	2.42 ± 0.20	2.48 ± 0.31	7.53 ± 1.13	2.81 ± 0.40‡	2.34 ± 0.23‡
Tenericutes	0.64 ± 0.21	0.18 ± 0.04*	0.15 ± 0.03*	0.08 ± 0.04	0.08 ± 0.02	0.25 ± 0.04*
Others	0.69 ± 0.19	0.34 ± 0.09	0.26 ± 0.05*	1.24 ± 0.44	0.21 ± 0.07*	0.36 ± 0.13

Figure 17. Phyla proportion after faecal microbiota transplantation (FMT) experiment.

(**A**) Evolution of phyla proportion of faecal microbiota from donor control (CTR) or imiquimod (IMQ) microbiota in recipients CTR or IMQ-treated mice. (**B**) Final gut microbiota composition, at phyla levels, after FMT. Values are expressed as means ± SEM. unpaired t-test was used to compare two groups. *P<0.05, †P<0.01, ‡P<0.001 compared to the donor CTR group; *P<0.05, †P<0.01, ‡P<0.001 compared to the donor IMQ group. CTR-CTR, Control mice transplanted with faeces from control mice; CTR-IMQ, Control mice transplanted with faeces from IMQ-treated mice; IMQ-IMQ, IMQ-treated mice transplanted with faeces from IMQ mice; and IMQCTR, IMQ-treated mice transplanted with faeces from control mice.

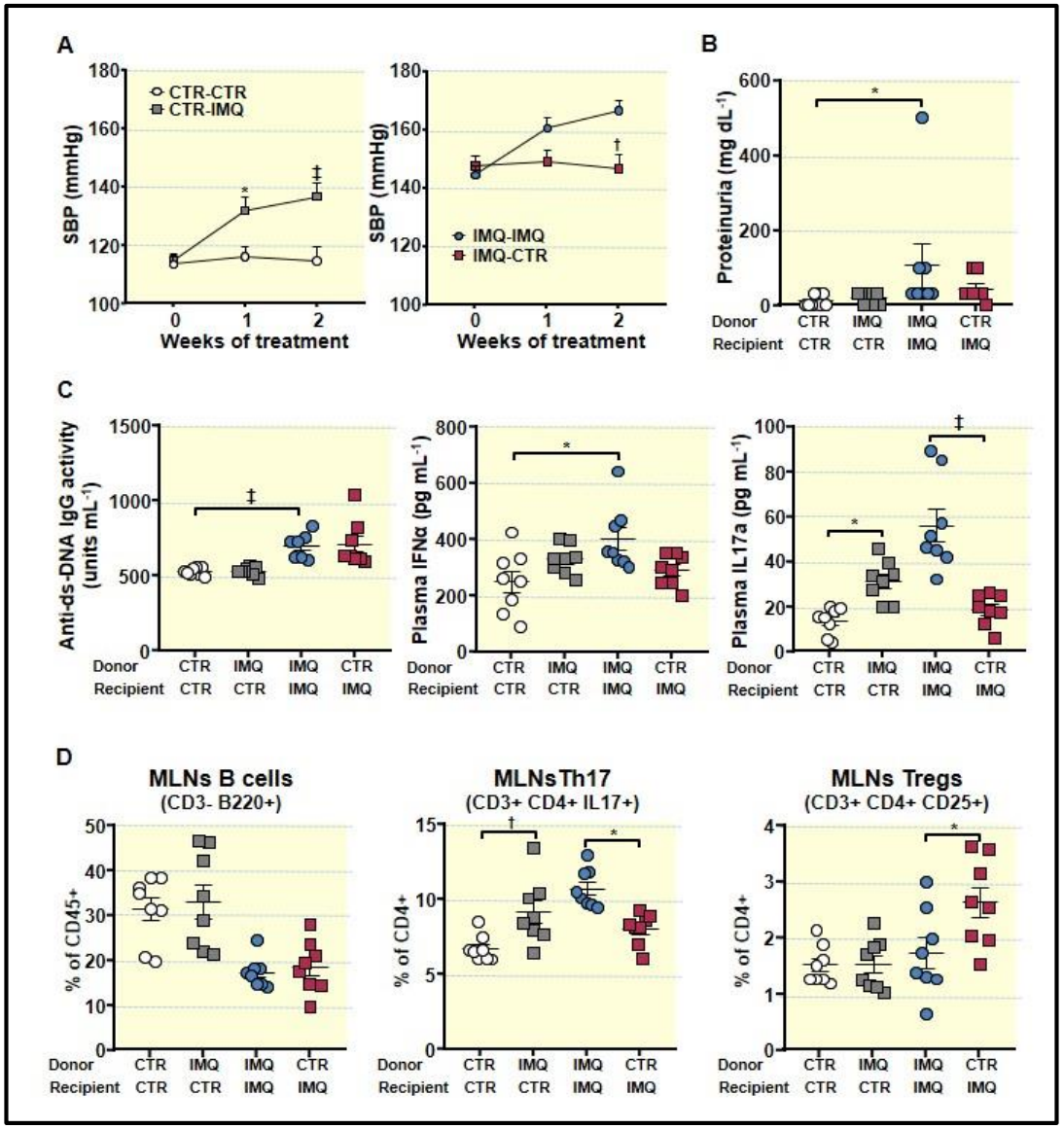

Figure 18. Effects of faecal microbiota transplants (FMT) on the progression of systolic blood pressure (SBP), proteinuria, disease activity, plasma cytokine levels, and lymphocyte proliferation in mesenteric lymph nodes.

(**A**) SBP determined via tail-cuff plethysmography. (**B**) Proteinuria, (**C**) Plasma double-stranded DNA (anti-ds-DNA) autoantibodies, interferon (IFN)α, and interleukin (IL)17a levels. (**D**) Populations of relevant lymphocytes in mesenteric lymph nodes: Total B lymphocytes, Th17, and Regulatory T cells (Treg), obtained with flow cytometry. Data is represented as means ± SEM. The evolution of tail SBP was analysed by two-way ANOVA with the Tukey's multiple comparison test. The rest of variables by unpaired t-test. * $p < 0.05$, † $p < 0.01$, ‡ $p < 0.001$ compared to the CTR-CTR group; * $p < 0.05$, † $p < 0.01$, ‡ $p < 0.001$ compared to IMQ-IMQ group. CTR-CTR, Control mice (CTR) transplanted with microbiota from CTR; CTR-IMQ, CTR mice transplanted with microbiota from imiquimod (IMQ)-treated mice; IMQ-IMQ, IMQ transplanted with microbiota from IMQ; and IMQ-CTR, IMQ transplanted with microbiota from CTR.

Incubation for 30 min with the pan-NOX inhibitor VAS2870 or with the Rho kinase inhibitor Y27632 depleted the differences between groups in relaxation to Ach, suggesting a role for NOX and Rho kinase, respectively, in this impaired relaxant response induced by IMQ microbiota. Furthermore, the transplant from IMQ raised NOX activity in aorta (**Figure 19C**), as compared to CTR-CTR. Remarkably, nIL-17 incubation increased relaxation to Ach in rings from CTR-IMQ group (**Figure 19A**), showing the role of IL17 in the impaired endothelium-dependent relaxation induced by stool transplantation with IMQ microbiota. In fact, Th17 infiltration in aorta was also higher in CTR-IMQ than in CTR-CTR (**Figure 19D**). By contrast, FMT from control mice to recipient IMQ-treated mice reduced SBP (≈ -20 mmHg) (**Figure 18A**), Th17 proportion in MLN (**Figure 18C**), plasma IL-17a levels (**Figure 18B**), aortic NOX activity (**Figure 18C**), aortic Th17 cells infiltration (**Figure 19D**), and the impaired Ach-induced relaxation as compared to IMQ-IMQ group (**Figure 19A**), confirming the key role of IL-17a in the vascular alteration induced by IMQ. In fact, neutralization of IL-17a improved endothelium-dependent relaxation in IMQ-IMQ group (**Figure 19B**) similarly to stool transplantation from control mice. However, no significant changes in proteinuria (**Figure 18B**), and plasma anti-dsDNA and IFNα (**Figure 18C**) were found between IMQ-IMQ and IMQ-CTR groups, showing a dissociation between the control of autoimmunity and SBP induced by the gut microbiota.

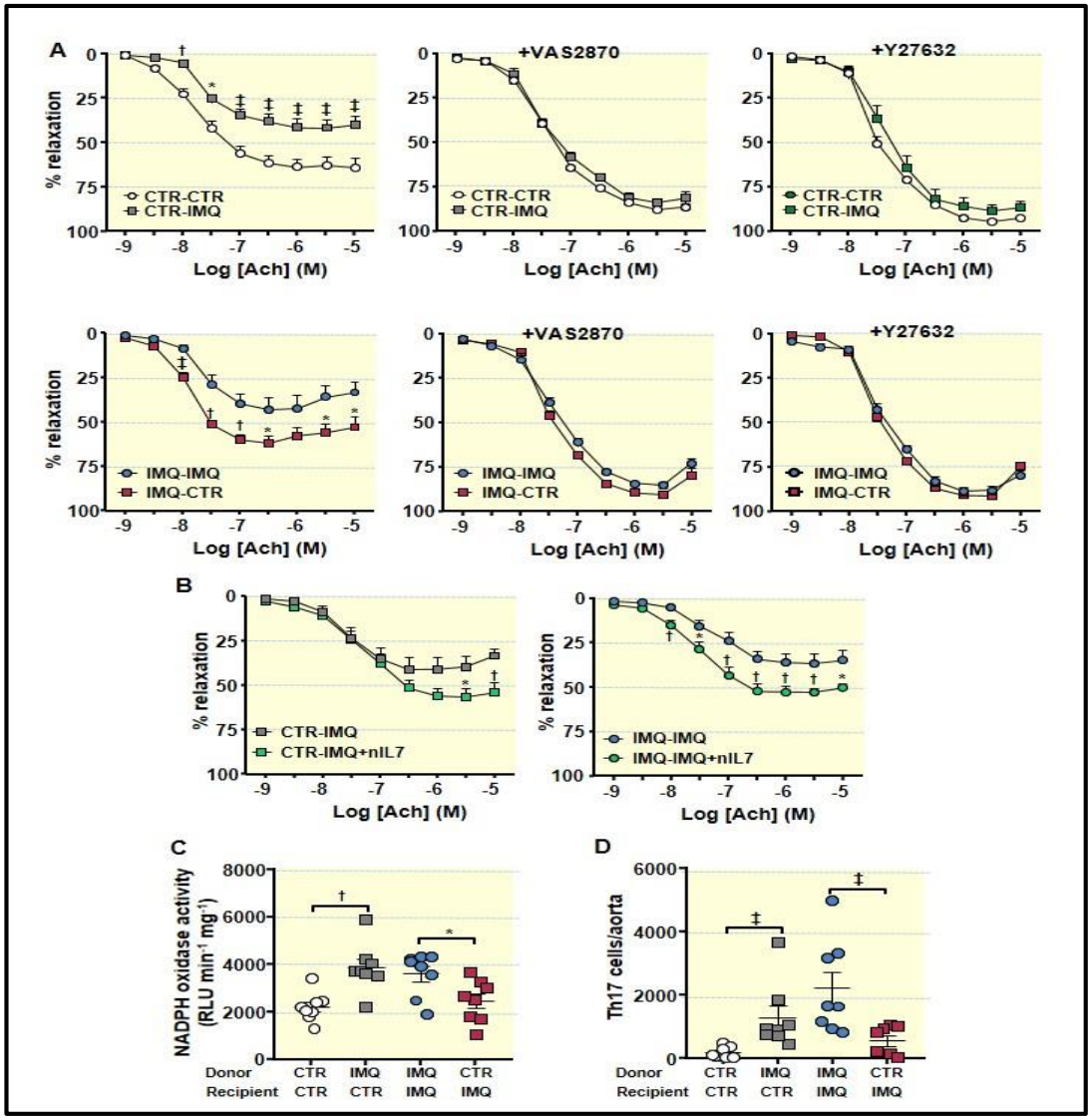

Figure 19. Effects of the microbiota transplants on endothelial function, NADPH oxidase activity and infiltration of T lymphocytes in aorta.

(**A**) Acetylcholine (Ach)-induced relaxation curves in aortas pre-contracted with U46619 (10 nM) with or without the specific pan-NOX inhibitor VAS2870 (1 μM), or the Rho kinase inhibitor Y27632 (1 μM). (**B**) Ach-induced relaxation curves with or without nIL-17a (10 μg·L) in segments from control (CTR) and Imiquimod-treated (IMQ) recipient mice, transplanted with microbiota from IMQ animals. (**C**) NOX activity determined via lucigenin-enhanced chemiluminescence. (**D**) Aortic infiltration of Th17 through flow cytometry. Values are represented as means ± SEM. The concentration-response curves to Ach were analysed by two-way ANOVA with the Tukey's multiple comparison test. The rest of the variables were tested with unpaired t-test. * $p < 0.05$, † $p < 0.01$, ‡ $p < 0.001$ compared to the CTR-CTR group; * $p < 0.05$, † $p < 0.01$, ‡ $p < 0.001$ compared to IMQ-IMQ group CTR-CTR, Control mice (CTR) transplanted with microbiota from CTR; CTR-IMQ, CTR transplanted with microbiota from imiquimod (IMQ)-treated mice; IMQ-IMQ, IMQ transplanted with microbiota from IMQ; and IMQ-CTR, IMQ transplanted with microbiota from CTR.

Next, tested the microbial composition 2 weeks post-transplant. Microbiota from donor CTR and IMQ mice changes after FMT in recipient mice (**Figure 17A**), but with minor changes depending if recipient mice were CTR or IMQ mice. At the end of FMT donor microbiota from control mice showed increased bacteria belonging to *Bacterioidetes* (75.18 ± 3.43% vs 55.06 ± 8.55%, $P<0.05$) and reduced *Actinobacteria* (0.09 ± 0.01% vs 0.15 ± 0.03%, $P<0.05$) in recipient IMQ mice in comparison with recipient CTR mice, respectively. Similarly, donor microbiota from IMQ mice showed only reduced bacteria belonging to *Tenericutes* (0.08 ± 0.02% vs 0.25 ± 0.04%, $P<0.01$) in recipient IMQ mice as compared to recipient CTR mice. We found no significant changes in phyla composition between CTR-CTR and CTR-IMQ groups (**Figure 17B**). Volcano plot showed genera clustering in CTR-CTR mice as compared to CTR-IMQ group (**Figure 20A**). There was more than 3.5-fold reduction in the genera *Sutterella* and *Anaerovibrio* (potentially protective bacteria) in mice receiving IMQ microbiota in comparison with CTR-CTR mice (**Figure 20B**).

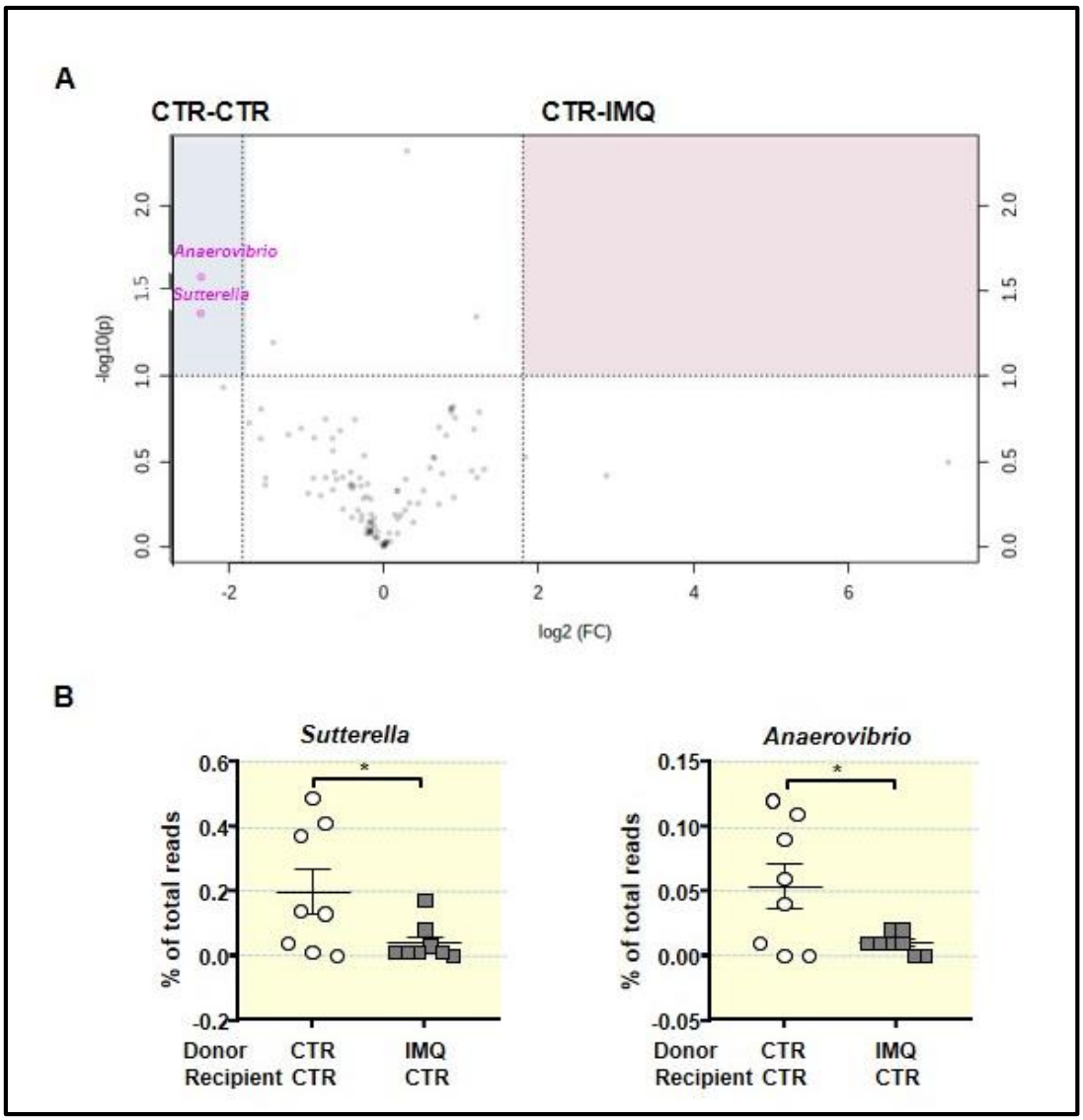

Figure 20. Effects of stool transplantation from imiquimod (IMQ)-treated mice to control mice at the genera proportion in gut microbiota.

(**A**) Volcano plot displaying significantly enriched genera in CTR-CTR group or CTR-IMQ group. The x-axis is log2 fold change and the y-axis is transformed p-value. Genera not different between cohorts are shown in black. Features selected by volcano plot with fold change threshold 3.5 and t-test with threshold 0.05. Genera more abundant in CTR-CTR are shown in the upper right, blue-shaded quadrant (**B**) Proportion of key bacterial genera expressed as percentage of total reads. Data is represented as means ± SEM. Unpaired t-test. * $p < 0.05$ compared to the CTR-CTR group. CTR-CTR, Control mice (CTR) transplanted with microbiota from CTR; CTR-IMQ, CTR transplanted with microbiota from imiquimod (IMQ)-treated mice.

By contrast, FMT of donor control faeces to IMQ-treated mice induced changes in the microbiota composition as compared to the transplantation with IMQ microbiota. The LDA score suggests that the relative abundance of 4 taxa (green) was decreased and 15 taxa (red) was increased in IMQ-CTR group when compared with IMQ-IMQ mice (**Figure 21**). The most altered genera abundances of the volcano plot showed increased proportion of *Sutterella, Anaerovibrio, Heliorestis, Sharpea, Anaerobranca*, and *Halanaerobium*, and reduced abundance of *Pseudovutyrivibrio, Moryella*, and *Streptococcus* in IMQ-treated mice transplanted with microbiota from control mice, as compared to IMQ-IMQ group (**Figure 22A, 22B**).

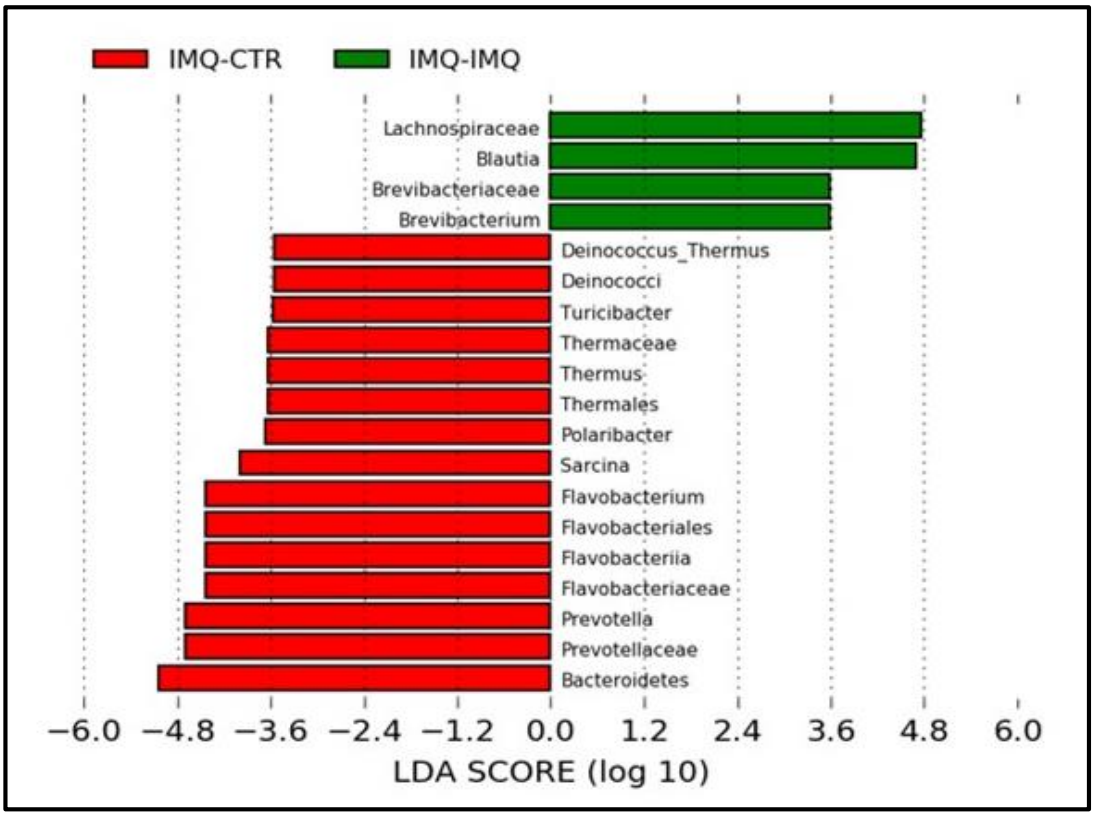

Figure 21. Effects in taxa proportion of gut microbiota after donor control (CTR) microbiota transplantation to imiquimod (IMQ)-treated mice.

Linear discriminant analysis effect size (LEfSe) identified significantly different bacterial taxa enriched in each cohort at LDA Score > 3.5, and Kruskal-Walllis test among classes and Wilcoxon test between subclases with threshold 0.05 (red bars IMQ-CTR enriched, green bars IMQ-IMQ enriched). IMQ-IMQ, IMQ-treated mice transplanted with faeces from IMQ mice; and IMQ-CTR, IMQ-treated mice transplanted with faeces from control mice.

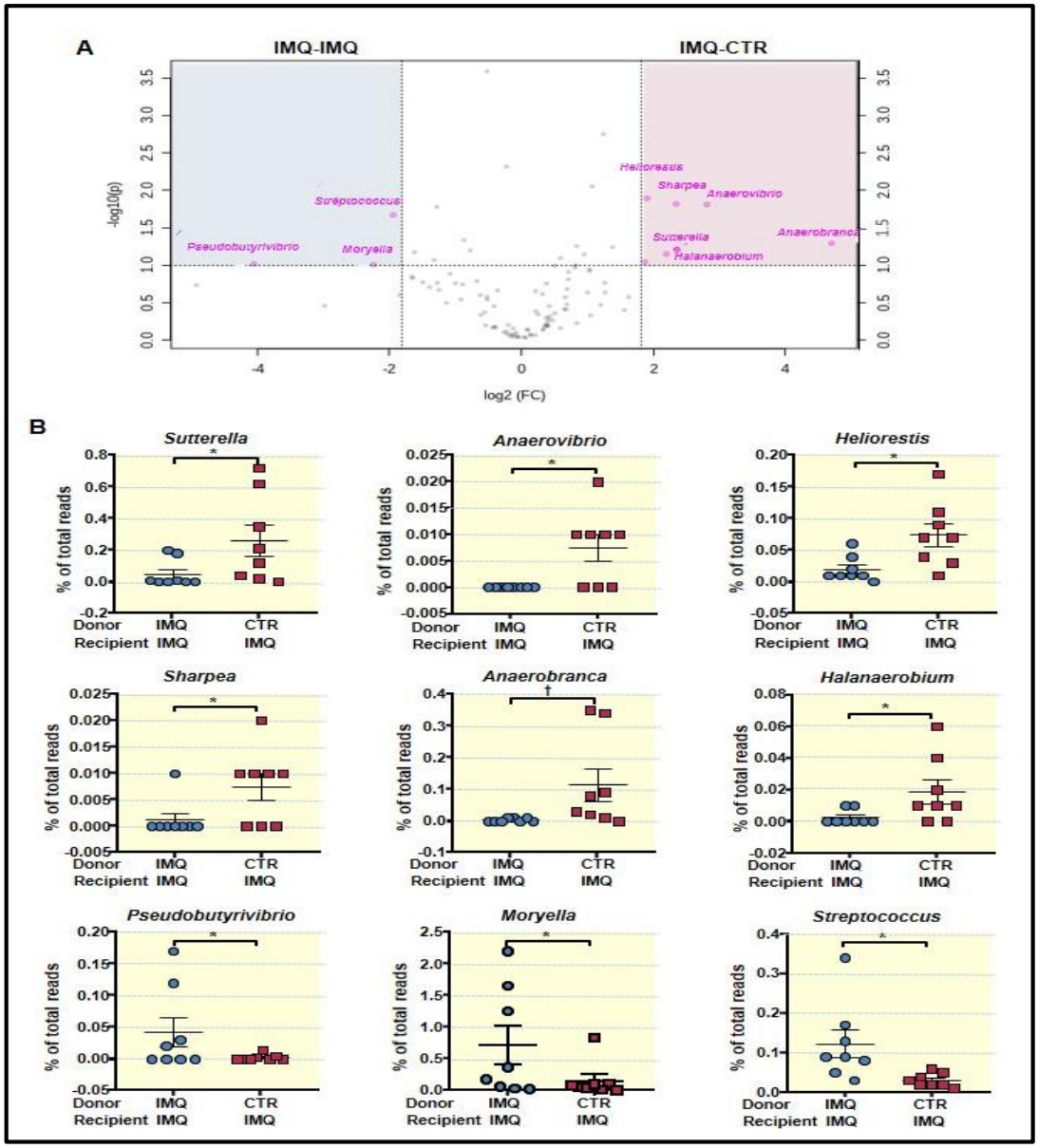

Figure 22. Effects of stool transplantation from control mice to imiquimod (IMQ)-treated mice at the genera proportion in gut microbiota.

(**A**) Volcano plot displaying significantly enriched genera in IMQ-IMQ group or IMQ-CTR group. The x-axis is log2 fold change and the y-axis is transformed P-value. Genera not different between cohorts are shown in black. Features selected by volcano plot with fold change threshold 3.5 and t-test with threshold 0.05. Genera more abundant in IMQ-IMQ are shown in the upper right, blueshaded quadrant and genera more abundant in IMQ-CTR mice in the upper left, red-shaded quadrant (**B**) Proportion of key bacterial genera expressed as percentage of total reads. Values are expressed as means ± SEM. Unpaired t-test. *P<0.05, †P<0.01 compared to IMQ-IMQ group. IMQ-IMQ, IMQ-treated mice transplanted with faeces from IMQ mice; and IMQ-CTR, IMQ-treated mice transplanted with faeces from control mice.

2. Role of TMAO in SLE development and cardiovascular complications in a lupus mouse model induced by TLR-7 activation

2.1. DMB prevented high BP, target organs damage, and proteinuria in TLR-7-dependent SLE

Topical administration three times per week in alternate days to wild-type BALB/cJRj mice of IMQ, a TLR-7 agonist, successfully induced a lupus-like pathology in our animals not genetically prone to excessive TLR-7 signaling (Yokogawa et al. 2014). As expected, IMQ-treated mice showed a gradual raise in SBP, being roughly 37 mmHg higher in IMQ than in CTR animals, at the end of the experiment. DMB prevented the development of hypertension induced by IMQ (≈ 70%), but did not affect CTR group (**Figure 23A**). We could not detect any significant differences in heart rate (537.7 ± 13.4 bpm vs 576.0± 27.9 bpm, CTR and IMQ groups, respectively), which was unchanged by DMB (**Figure 23A**). Sustained high BP is one of the most powerful determinants of the development of cardiac and renal hypertrophy. We found that both left ventricular weight/tibia length and kidney weight/tibia length were higher (≈ 12% and 73%, respectively) in IMQ-treated mice than in control mice. DMB prevented significantly left ventricular hypertrophy, but not renal hyperthophy (**Figure 23B**). This inducible model is known to present autoimmunity-linked kidney injury (López et al. 2016; Robles-Vera et al. 2020; Yokogawa et al. 2014). We found significantly higher protein levels in urine after 4 weeks of IMQ treatment, which was reduced by DMB treatment (**Figure 23C**), showing prevention of impaired renal function by DMB in IMQ group.

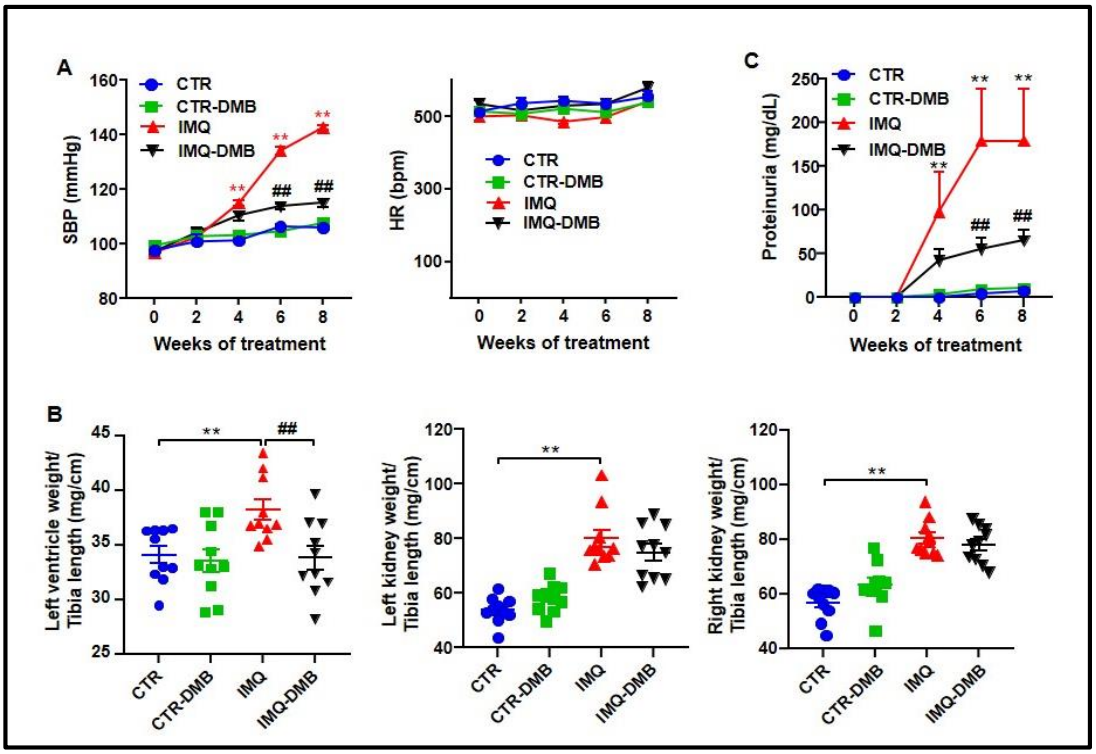

Figure 23. Effects of 3,3-dimethyl-1-butanol (DMB) treatment on blood pressure, organ morphology, and proteinuria in control (CTR) and imiquimod (IMQ) mice.

(**A**) Systolic blood pressure (SBP) as determined by tail-cuff plethysmography; (**B**) morphology data as organ weigh/tibia length ratios; and (**C**) proteinuria in CTR, CTR-group treated with DMB (CTR-DMB), IMQ, and IMQ-group treated with DMB (IMQ-DMB). The data are expressed in a means ± SEM format. Tail SBP and proteinuria were tested by two-way ANOVA with the Tukey's multiple comparison test. The morphological variables were tested with one-way ANOVA and Tukey's post hoc test, or Kruskal–Wallis test with Dunn's multiple comparisons. ** $p < 0.01$ in comparison with CTR; ## $p < 0.01$ in comparison with IMQ.

2.2. DMB prevented disease activity progression in TLR-7-dependent SLE

The IMQ model presents increased plasma levels of autoantibodies, splenomegaly, hepatomegaly, and higher type-1 IFN expression in lymph organs (Robles-Vera et al. 2020; Yokogawa et al. 2014). In the present study increased plasma levels of anti-dsDNA (**Figure 24A**), spleen weight/tibia length (**Figure 24B**), liver weight/tibia length (**Figure 24C**), and IFNα mRNA levels in MLN (**Figure 24D**), were found in IMQ mice. Interestingly, DMB treatment partially prevented the increased plasma anti-dsDNA autoantibodies (≈ 35%), splenomegaly (≈ 15%), hepatomegaly (≈ 23%), and IFNα mRNA levels (≈ 70%) in IMQ mice. We evaluated the immunomodulatory actions of TLR-7 activation by measuring the levels of B cells in spleens and blood from all experimental groups. IMQ treatment led to an increase in the percentages of both splenic and circulating B cells compared with the control group, which were prevented by DMB (**Figure 24E**). In addition, unchanged total T cells population and lower Th cells proportion were found in IMQ group as compared to CTR in spleen and blood, which were not affected by DMB treatment (**Figure 24E**).

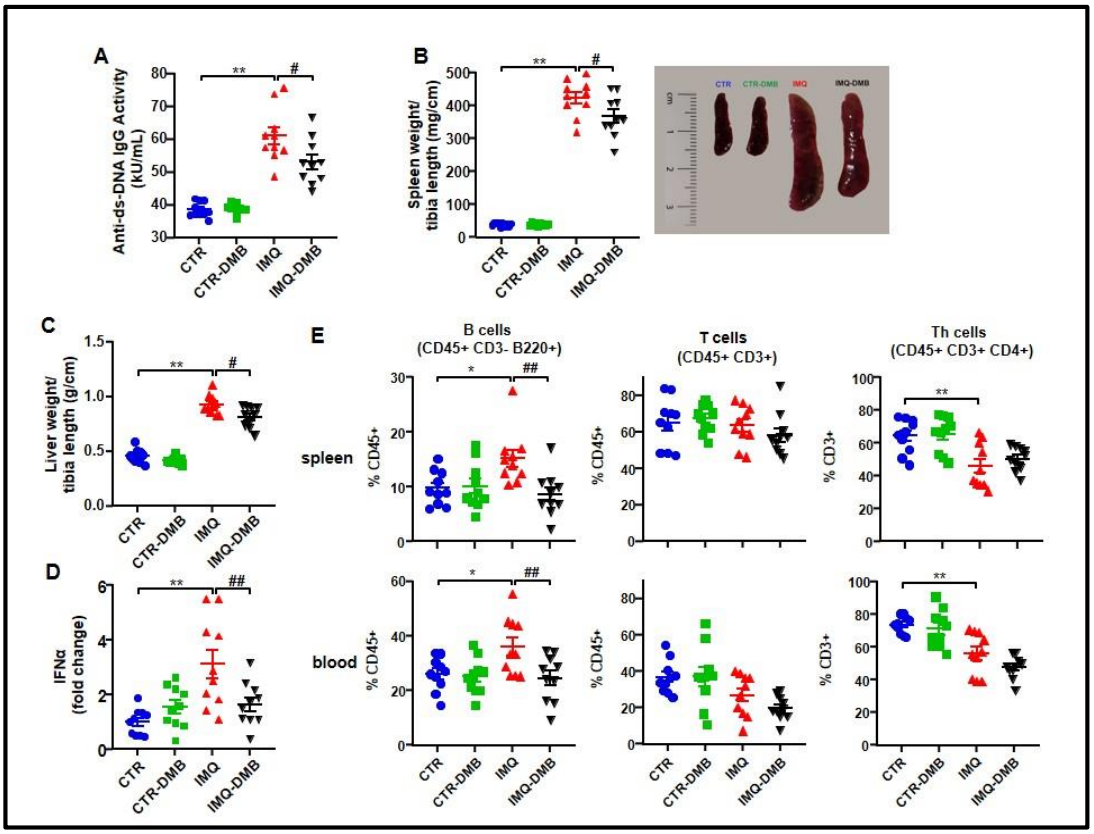

Figure 24. Effects of 3,3-dimethyl-1-butanol (DMB) treatment on disease activity signs in the imiquimod (IMQ) group.

(**A**) Circulating double-stranded DNA (anti-ds-DNA); (**B**) splenomegaly; (**C**) hepatomegaly; (**D**) IFNα mRNA levels in MLNs; and (**E**) percentage of B, T, and Th cells in spleen and blood in CTR, CTR-group treated with DMB (CTR-DMB), IMQ, and IMQ-group treated with DMB (IMQ-DMB). The data are expressed in a means ± SEM format. Comparisons between variables were performed with one-way ANOVA and Tukey's post hoc test, or Kruskal–Wallis test with Dunn's multiple comparisons. * $p < 0.05$ and ** $p < 0.01$ in comparison with CTR; # $p < 0.05$ and ##$p < 0.01$ in comparison with IMQ.

2.3. Plasma TMAO is increased in TLR-7-dependent SLE and is associated with SBP and disease activity

Fasting plasma concentrations of TMA and TMAO were measured by liquid chromatography-tandem mass spectrometry in all experimental groups. Circulating (plasma) TMA and TMAO concentrations were higher (≈ 5 and 8-fold, respectively) in IMQ group versus CTR mice (**Figure 25A**). To investigate whether increases in plasma TMAO concentrations contribute to autoimmunity and high BP in TLR-7-dependent systemic autoimmunity mice were fed a normal chow diet for 8 weeks with their drinking water either supplemented with DMB or not supplemented. DMB reduced plasma TMA (≈ 43%) and TMAO (≈ 41%) in IMQ mice, but had no effect on plasma levels in CTR animals (**Figure 25A**). We used regression analysis to determine if SBP or autoimmunity was related to circulating TMAO concentrations. Plasma TMAO level correlates positively with SBP (strong correlation, Pearson r = 0.7324) and with plasma anti-dsDNA levels (strong correlation, Pearson r = 0.6903) (**Figure 25B**).

This points to the gut microbiota-produced metabolite TMAO being required for TLR-7-dependent systemic autoimmunity, TMAO has a role in the hypertensive effect induced by TLR-7 activation. We then studied the mechanisms involved in TMAO induced TLR-7-dependent hypertension. Taken into account that Th17 infiltration in the vasculature plays a key role in the gut microbiota mediated changes in BP in TLR 7-driven lupus autoimmunity (de la Visitación et al. 2021), then our group investigated whether TMAO was able to induce a shift in immune cells in secondary lymph organs.

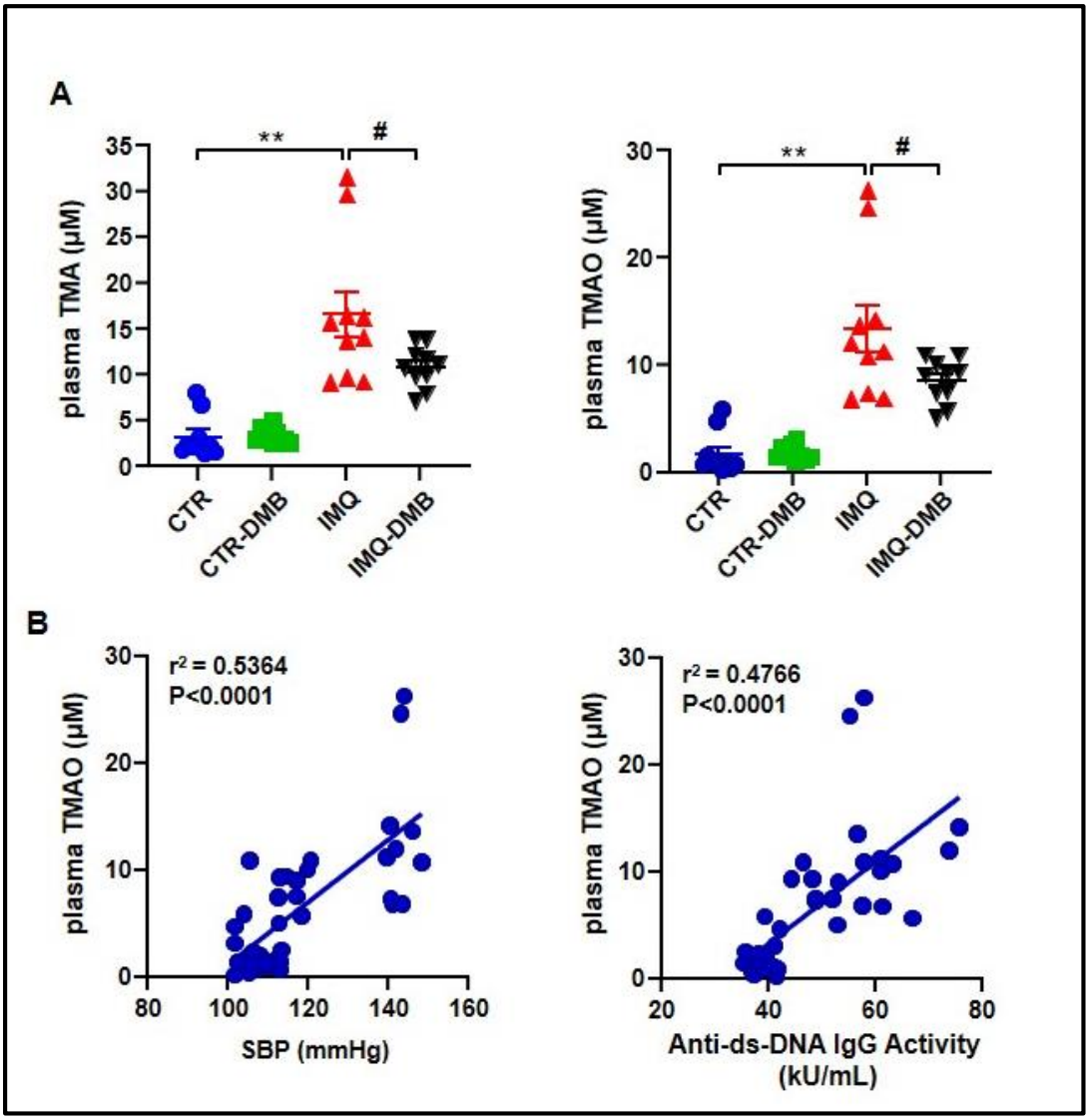

Figure 25. Plasma TMAO was correlated to systolic blood pressure and SLE disease activity.

(**A**) Plasma TMA and TMAO levels in control (CTR), CTR-group treated with 3,3-dimethyl-1-butanol (DMB) (CTR-DMB), IMQ, and IMQ-group treated with DMB (IMQ-DMB). The data are represented as means ±SEM. One-way ANOVA and Tukey's multiple comparison test were performed. ** $p < 0.01$ when compared to CTR; # $p < 0.05$ when compared to IMQ. (**B**) Pearson correlation between plasma TMAO and SBP or anti-ds-DNA activity using data from all experimental groups.

2.4. DMB treatments attenuated T cells imbalance

High autoantibody levels and the development of the lupus-like pathology can be linked to a T cell imbalance (de la Visitación et al. 2021; Robles-Vera et al. 2020; Talaat et al. 2015). We assessed T cell populations in MLN, spleens and blood from our mice. Th cell populations (CD3+CD4+) did not present any significant differences among groups in both MLN and spleen (data not shown). Th17 (CD4+IL-17a+) and Th1 (CD4+IFNγ+) cell relative populations increased in both secondary lymph nodes and in circulation from IMQ mice (**Figure 26A, 26B, 26C**), whereas Treg (CD4+CD25+) where elevated in pathological animals in the spleen and blood (**Figure 26B, 26C**). DMB prevented the increase in Th17 and Th1 seen in IMQ in both secondary lymph organs, reducing circulating levels of both type of lymphocytes, but did not seem to affect the proportion of Treg cells. Overall, this suggests that TMAO regulated T cells polarization, increasing Th17 cell population.

Considering that IL-17a is a crucial component in the mechanisms responsible for endothelial dysfunction in this TLR-7-driven lupus autoimmunity model (Robles-Vera et al. 2020), then our group focused on the possible changes induced by DMB on the SLE-linked endothelial dysfunction.

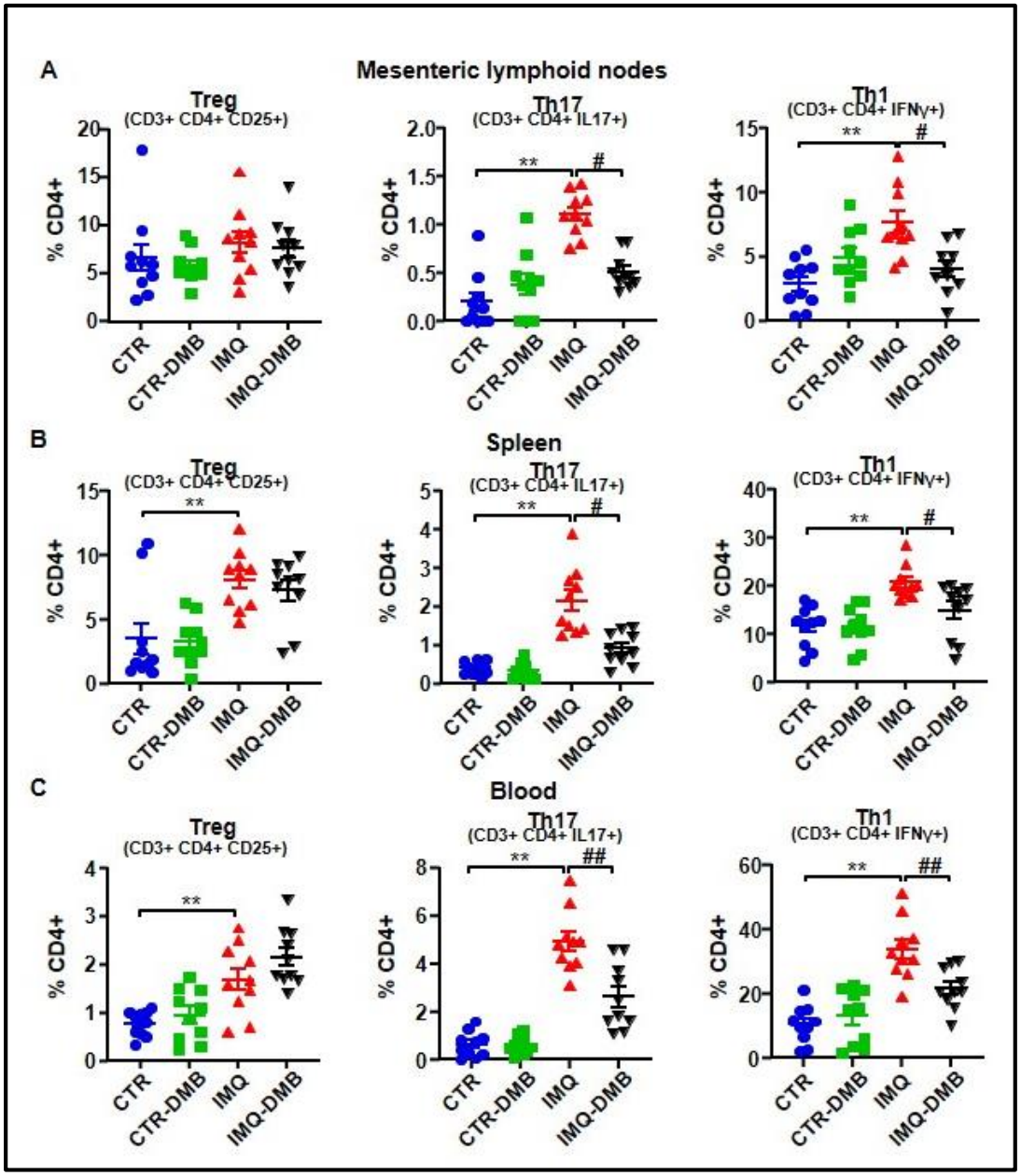

Figure 26. TMAO facilitated lymphocyte activation and proliferation in imiquimod (IMQ) animals.

(**A**) Regulatory T (Treg), Th17, and Th1 cells as analyzed through flow cytometry in mesenteric lymph nodes, (**B**) in spleen, and (**C**) blood in CTR, CTR-group treated with DMB (CTR-DMB), IMQ, and IMQ-group treated with DMB (IMQ-DMB). Data are represented as means ± SEM. One-way ANOVA and Tukey's post hoc test or Kruskal–Wallis test with Dunn's multiple comparisons were performed. ** $p < 0.01$ compared to CTR; # $p < 0.05$ and ## $p < 0.01$ compared to IMQ.

2.5. DMB prevented endothelial dysfunction, vascular oxidative stress and Th17 vascular infiltration

Aortas from IMQ group displayed markedly decreased endothelium-dependent vasorelaxation to Ach in comparison with CTR (Emax= 59.8 ± 2.7 % and 81.7 ± 2.6 %, respectively, P<0.01) (**Figure 27A**). DMB treatment restored this relaxant response (Emax= 79.1 ± 4.2 %), being without effect in CTR mice (Emax= 78.2 ± 3.3 %). Enhanced aortic ROS content is involved on endothelial dysfunction in SLE (Romero et al. 2017). We found a higher (≈ 62 %) red DHE signal in aortic ring from SLE mice, which it was abolished by DMB treatment (**Figure 27B**). When incubated with the NOX inhibitor VAS2870, improvement of endothelium-dependent relaxation to Ach was shown in IMQ aortic segments (**Figure 27A**), which suggest the partial involvement of NOX activity in the endothelial dysfunction found in aortic rings from IMQ mice. Furthermore, the NOX activity was roughly 1.8-fold higher in IMQ aortic rings than in CTR tissue samples (**Figure 27C**). Accordingly, mRNA levels of catalytic NOX-4 and regulatory p47phox subunits of NOX were also higher in rings from IMQ group in comparison with CTR (**Figure 27C**). DMB treatment reduced both NOX activity and NOX-4 transcript levels, suggesting that TMAO regulated NADPH-driven ROS production to induce endothelial dysfunction. The eNOS inhibitor L-NAME abolished the relaxant response induced by Ach aortic rings from CTR and IMQ groups, involving NO in this relaxation (Robles-Vera et al. 2020). Reduced NO production was detected in aortas from TMAO-supplemented mice, which led to high plasma levels of TMAO (31.5 μM) (Brunt et al. 2020), and by *in vitro* TMAO incubation (>50 μM). However, we did not find significant changes in eNOS mRNA levels among groups (**Figure 27D**), suggesting that NO destruction by ROS and reduced NO bioavailability is more relevant to induce endothelial dysfunction than reduced NO production.

Nuclear factor erythroid 2-related factor 2 (NRF-2) is a basic leucine zipper transcription factor and is essential for protecting cells against oxidative stress. NRF-2 acts through the antioxidant response element (ARE)/electrophile response element (EpRE) to regulate the expression of antioxidative enzymes, such as NADPH quinone oxidoreductase-1 (NQO-1) and heme oxygenase-1 (HO-1), and coordinate a wide range of responses to oxidative damage. A GWAS analysis defined the NRF-2 locus as a region associated with susceptibility to SLE (Xing et al. 2007). In addition, NRF-2 activation suppressed LN through inhibition of oxidative injury (Jiang et al. 2014). In aorta from IMQ mice we found reduced NRF-2 mRNA levels, associated to reduced levels of NQO-1 and HO-1 (**Figure 27E**).

By contrast, the transcript levels of NRF-2 inhibitor keap1 was unchanged. Interestingly, DMB treatment restored NRF-2 levels and down-stream antioxidant enzymes (**Figure 27E**), suggesting NRF-2 downregulation linked to plasma TMAO levels, which could be partially involved in the endothelial dysfunction induced by IMQ.

Previous studies have shown that TMAO induces vascular inflammation by activating the NLRP3 inflammasome and production of ROS (M.-L. Chen et al. 2017; Zhang et al. 2020). Activation of NLRP3 inflammasome with TMAO is critical for the secretion of IL-1β and ICAM1 gene expression (Zhang et al. 2020). We found increased mRNA levels of NLRP3 and down-stream IL-1β and ICAM1 (**Figure 28A**) in aorta from IMQ mice as compared to CTR group. Nonetheless, DMB did not affect the expression of the NLRP3 pathway, suggesting that plasma levels of TMAO in IMQ mice were insufficient to activate directly the NLRP3 pathway.

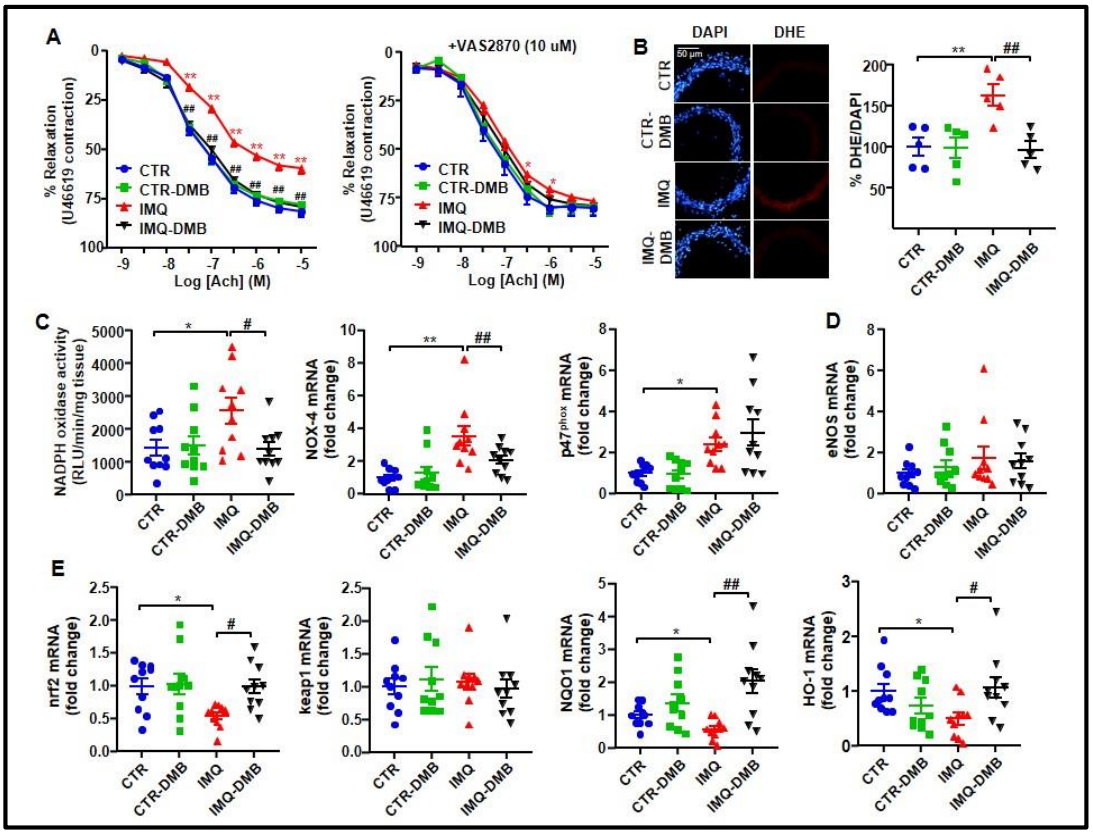

Figure 27. Effects of 3,3-dimethyl-1-butanol (DMB) treatment on SLE-linked endothelial dysfunction, NADPH oxidase activity, and NRF-2 pathway in imiquimod (IMQ) mice.

(**A**) Acetylcholine (Ach)-induced relaxation responses in aortas pre-contracted by U46619 (10 nM), with or without the specific pan-NOX inhibitor VAS2870 (10 µM). (**B**) ROS content measured by the ratio between red DHE and blue DAPI fluorescence. (**C**) Aortic NADPH oxidase activity determined using a lucigenin-enhanced chemiluminescence and aortic mRNA levels of NADPH oxidase subunits NOX-4 and p47phox, (**D**) eNOS, and (**E**) NRF-2- pathway, measured by RT-PCR. Groups: control (CTR), CTR-group treated with DMB (CTR-DMB), IMQ, and IMQ-group treated with DMB (IMQ-DMB). The data are shown in a means ±SEM structure. The concentration-response curves to Ach were analyzed by two-way ANOVA with the Tukey's multiple comparison test. One-way ANOVA and Tukey's post hoc test or Kruskal–Wallis test with Dunn's multiple comparisons were performed. * $p < 0.05$ and ** $p < 0.01$ when compared to CTR; # $p < 0.05$ and ## $p < 0.01$ when compared to IMQ.

Vascular infiltration of Th17 is an important element to consider when looking for subjacent mechanisms responsible for the endothelial dysfunction triggered by IMQ microbiota (de la Visitación et al. 2021). We found higher macrophage and Th17 accumulation in aorta from IMQ than in CTR mice, which were decreased by DMB treatment (**Figure 28B**), suggesting that TMAO increased vascular immune cells infiltration. The proinflammatory cytokine IL-17a causes Rho-kinase-mediated endothelial dysfunction (de la Visitación et al. 2021; de la Visitación et al. 2021), at least in part by NOX activation (Higashi et al. 2003) and NRF-2 inhibition (Guan, Liang, and Wang 2018). The Ach-induced response was also ameliorated in IMQ-treated animals post-Y27632 incubation (a Rho kinase inhibitor) (**Figure 28C**), pointing to Rho kinase activation as a cause for reduced relaxation.

Overall, our data suggest that endothelial dysfunction induced by TMAO under TLR-7 activation is mainly mediated by vascular Th17 infiltration, and the subsequent ROS levels increase, linked to increased NOX-driven ROS production and reduced NRF-2 antioxidant defense. These vascular changes seem to be produced by IL17/Rho kinase pathway activation.

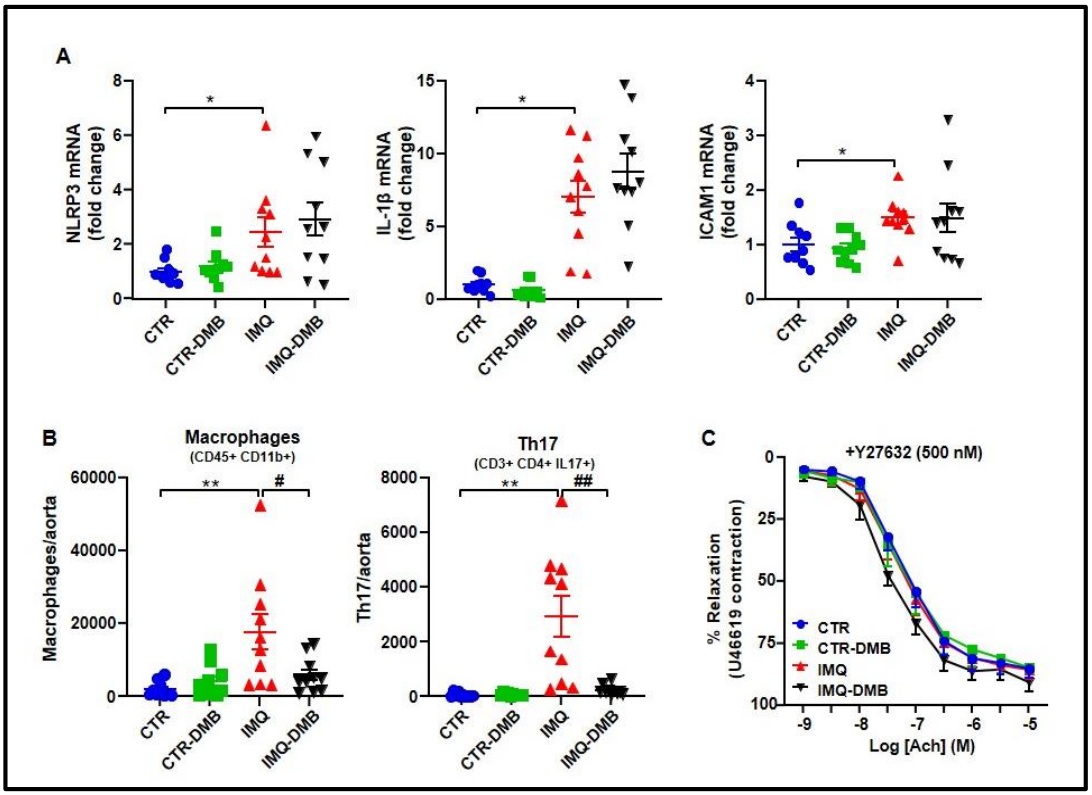

Figure 28. Role of NLRP3 pathway and immune cells infiltration in TMAO-induced endothelial dysfunction in imiquimod (IMQ) animals.

(**A**) Aortic mRNA levels of NLRP3 and downstream IL-1β and ICAM1 measured by RT-PCR. (**B**) Th17 and Th1 cells as detected with flow cytometry in aorta. (**C**) Acetylcholine (Ach)-induced relaxation responses in aortas pre-contracted by U46619 (10 nM), with or without the specific Rho kinase inhibitor Y27632 (500 nM). Groups: control (CTR), CTR-group treated with 3,3-dimethyl-1-butanol (DMB) (CTR-DMB), IMQ, and IMQ-group treated with DMB (IMQ-DMB). The data are represented as means ± SEM. The concentration–response curves to Ach were analyzed by two-way ANOVA with the Tukey's multiple comparison test. One-way ANOVA and Tukey's multiple comparison test were performed. * $p < 0.05$ and ** $p < 0.01$ when compared to CTR; # $p < 0.05$ and ## $p < 0.01$ when compared to IMQ.

3. Effects of SCFA on cardiovascular complications in TLR-7-induced lupus mice

3.1. SCFA prevented the increase in BP and target organ hypertrophy, but not disease activity in lupus-prone mice

We examined whether the administration of SCFA induced alterations in gut microbiota composition. Our findings revealed that IMQ treatment reduced various microecological parameters of alpha-diversity (Abundance-based coverage estimator, Shannon, and Simpson) (**Figure 29A**) and led to changes in beta-diversity (**Figure 29B**). However, neither ACE nor BUT administration modified these parameters or the relative abundance of bacteria belonging to different phyla (**Figure 29C**). SCFA induced minor changes in certain genera (both ACE and BUT reduced *Alkaliphilus*, *Akkermansia*, and *Faecalibacterium*; ACE increased *Bacillus*, and BUT increased *Selenomonas*) (**Figure 29D**) and bacterial metabolic pathways (BUT increased ribokinase and decreased penicillin-binding protein compared to the IMQ group; no significant changes were induced by ACE) (**Figure 29E**), suggesting that SCFA exert direct effects on host target organs rather than mediated by changes in gut microbiota.

As expected, TLR-7 activation with IMQ resulted in a gradual increase in SBP, with the IMQ group showing approximately 25 mmHg higher than control animals at the end of the experiment. Both ACE and BUT inhibited the development of high BP induced by IMQ by approximately 78.9% and 79.3%, respectively (**Figure 30A**). However, no significant differences in heart rate were found between the CTR and IMQ groups, and both SCFA treatments did not alter heart rate (**Figure 30B**). Sustained high BP is a crucial factor in the development of cardiac and renal hypertrophy (Frohlich et al. 1992). We observed that IMQ-treated mice exhibited higher left ventricular weight/tibia length and right kidney weight/tibia length (approximately 10% and 34%, respectively) than control mice, indicating that IMQ induced cardiac and renal hypertrophy. Both SCFA prevented left ventricular hypertrophy, but not renal hypertrophy (**Figure 30C**), suggesting that factors other than BP might be contributing to kidney hypertrophy in this lupus model, which appeared to be unaffected by SCFA.

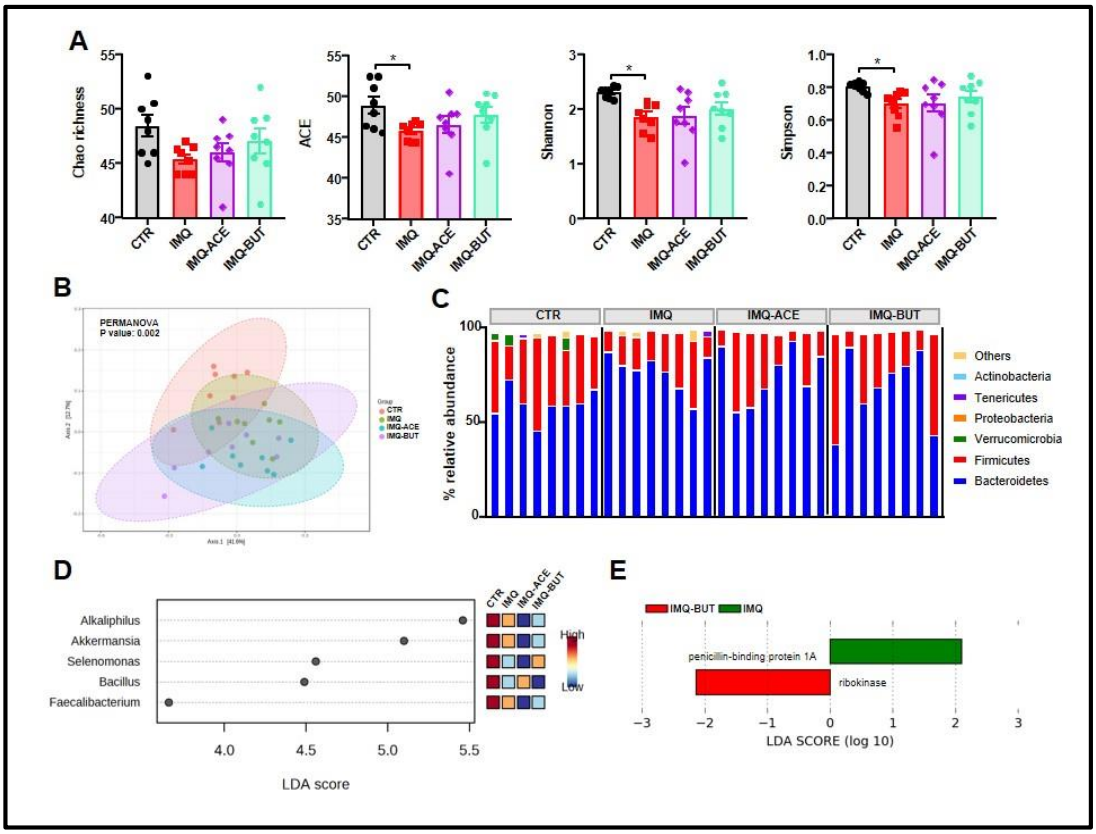

Figure 29. Effects of fiber treatments gut microbiota composition in mice with lupus induced by TLR-7 activation with imiquimod (IMQ).

(**A**) Ecological parameters of alpha diversity (Chao richness, Abundance-based coverage estimator (ACE), Shannon diversity and Simpson index). (**B**) Principal Coordinate Analysis (PCoA) in the gut microbiota, (**C**) proportion of bacterial phyla, (**D**) linear discriminant analysis (LDA) score at $p < 0.05$ was used to rank the ability of different genera to discriminate among groups, (**E**) LDA score of > 2 to separate KEGG genes by Picrust between IMQ and IMQ-treated with butyrate. Groups: control (CTR), IMQ and IMQ-groups treated with acetate (ACE) or butyrate (BUT). Values are expressed as means ± SEM (n = 8). The variables were tested with one-way ANOVA and Tukey post hoc test, or Kruskal-Wallis with Dunn's multiple comparisons. *P<0.05 compared to the CTR group.

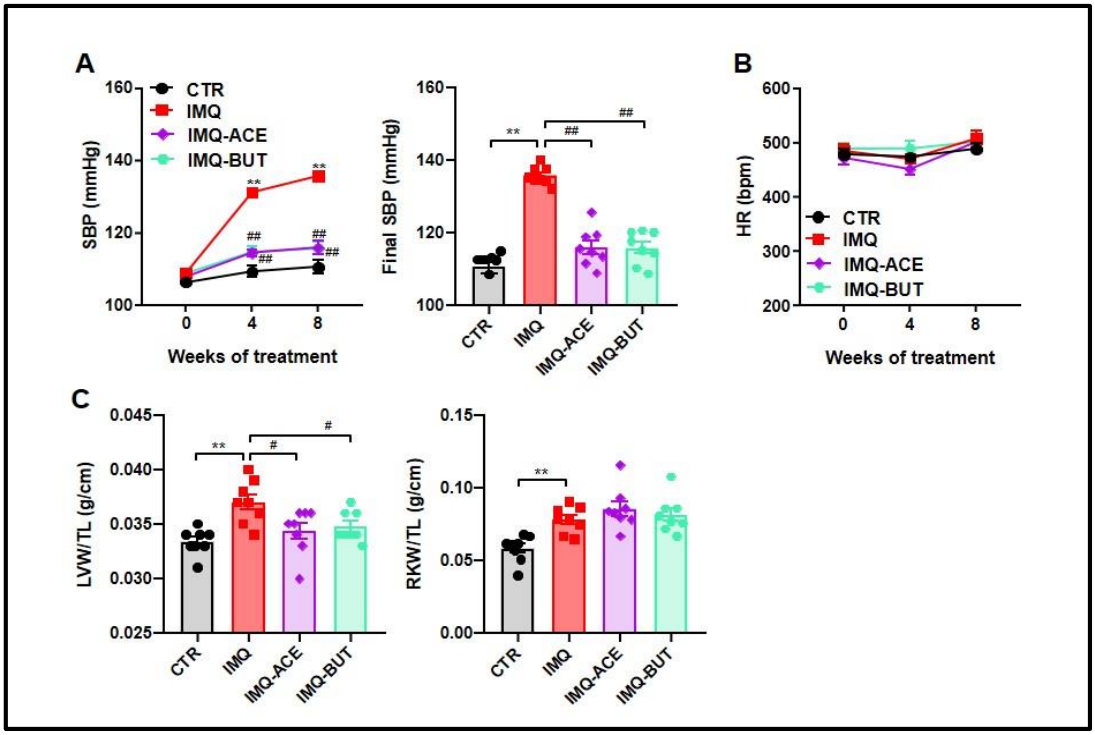

Figure 30. Effects of SCFA treatments on blood pressure and target organ hypertrophy in TLR-7-induced lupus mice.

(**A**) Time-course and final systolic blood pressure (SBP), and (**B**) heart rate (HR) measured through tail-cuff plethysmography. (**C**) Morphological parameters: left ventricle weight (LVW) and right kidney weight (RKW) normalized by tibia length (TL) in control (CTR), imiquimod (IMQ), and IMQ-treated mice with acetate (ACE) or butyrate (BUT). Data presented as means ± SEM (n = 8). Two-way ANOVA with Sidak's multiple comparisons test for SBP and HR. One-way ANOVA and Tukey's post hoc or Kruskal-Wallis with Dunn's multiple comparisons for final SBP and morphological variables. **P<0.01 vs. CTR; #P<0.05 and ##P<0.01 vs. untreated IMQ.

In this TLR-7-mediated autoimmunity model, increased plasma levels of autoantibodies, splenomegaly, hepatomegaly, and higher type-1 IFN expression in lymph organs were observed (Crow 2014; Yokogawa et al. 2014). In fact, we found elevated plasma levels of anti-dsDNA (**Figure 31A**), spleen weight/tibia length (**Figure 31B**), liver weight/tibia length (**Figure 31C**), and IFNα mRNA levels in MLN (**Figure 31D**) in IMQ mice compared to the CTR group. However, both SCFA were unable to reduce these signs of autoimmunity in IMQ mice. Additionally, we evaluated the immunomodulatory effects of SCFA by measuring the levels of B cells in MLN and spleens after TLR-7 activation. IMQ treatment increased the percentage of B cells in the spleen but not in MLN, and both SCFA treatments had no effect on B cell content (**Figure 31E**).

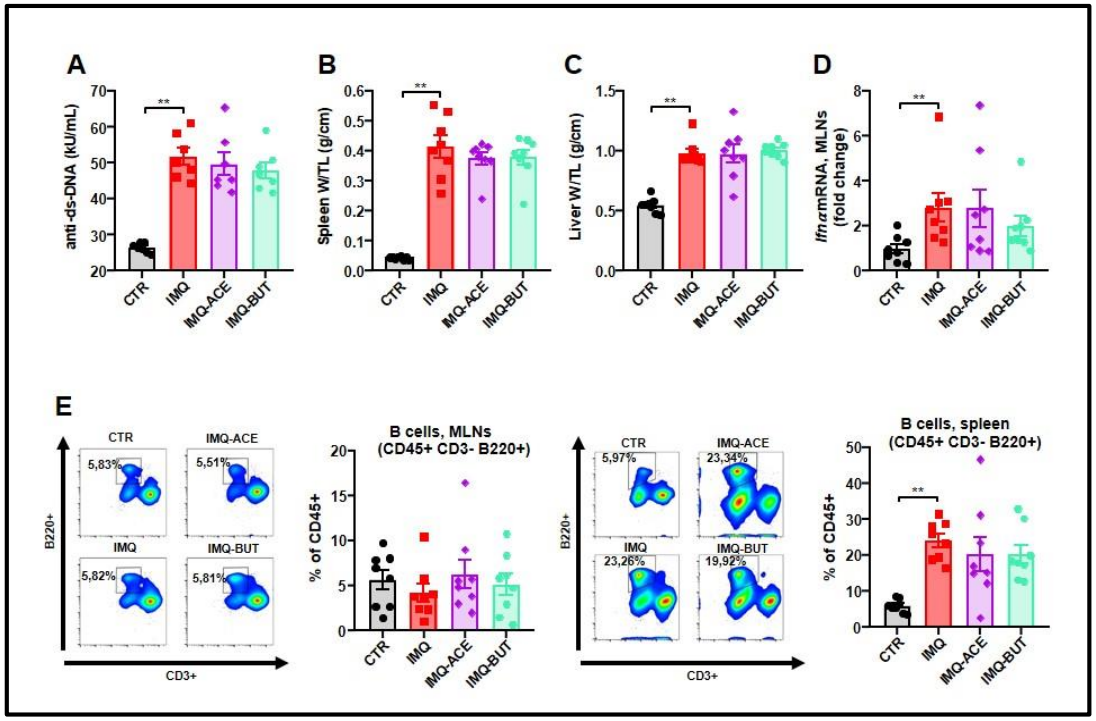

Figure 31. SCFA treatments did not change disease activity sings in mice with lupus induced by TLR-7 activation with imiquimod (IMQ).

(**A**) Circulating double-stranded DNA (anti-ds-DNA), (**B**) splenomegaly, (**C**) hepatomegaly, (**D**) IFNα mRNA levels in mesenteric lymph nodes (MLNs), and (**E**) percentage of B cells in MLNs and spleen. Groups: Control (CTR), IMQ and IMQ-groups treated with acetate (ACE) or butyrate (BUT). Values are expressed as means ± SEM (n = 8). Data were analyzed with one-way ANOVA and Tukey post hoc test, or Kruskal-Wallis with Dunn's multiple comparisons. **P<0.01 compared to the CTR group.

3.2. SCFA treatments prevented endothelial dysfunction, vascular oxidative stress and Th17 infiltration in aorta

Aortas from the IMQ group exhibited significantly reduced endothelium-dependent vasorelaxant responses to Ach compared to the CTR group (Emax reduced by 34%, P<0.01) (**Figure 32A**). However, treatment with both ACE and BUT reversed the impairment of Ach-induced relaxation. The Ach-induced response was also improved in the IMQ group after incubation with the pan-NOX inhibitor VAS2870, indicating mediation by NOX activation, and by the Rho kinase inhibitor Y27632 (**Figure 32A**), suggesting that the impaired Ach-induced relaxation is, at least in part, due to Rho kinase activation. Previous studies have indicated a link between ROS-dependent activation of RhoA/Rho kinase (MacKay et al. 2017). As the primary source of ROS in the vascular wall, NOX activity was approximately 4.5-fold higher in the aortic rings from the IMQ group compared to the CTR group, and both ACE and BUT reduced this increased activity by around 66% and 73%, respectively (**Figure 32B**). Inflammatory cells have been demonstrated to enhance vascular ROS synthesis (Pietrowski et al. 2011). We further investigated T lymphocyte extravasation in the aorta and observed that Th17 cells were approximately 10-fold higher in the aortas of the IMQ group compared to the CTR group; however, this increase was mitigated by both ACE and BUT treatment (**Figure 32C**).

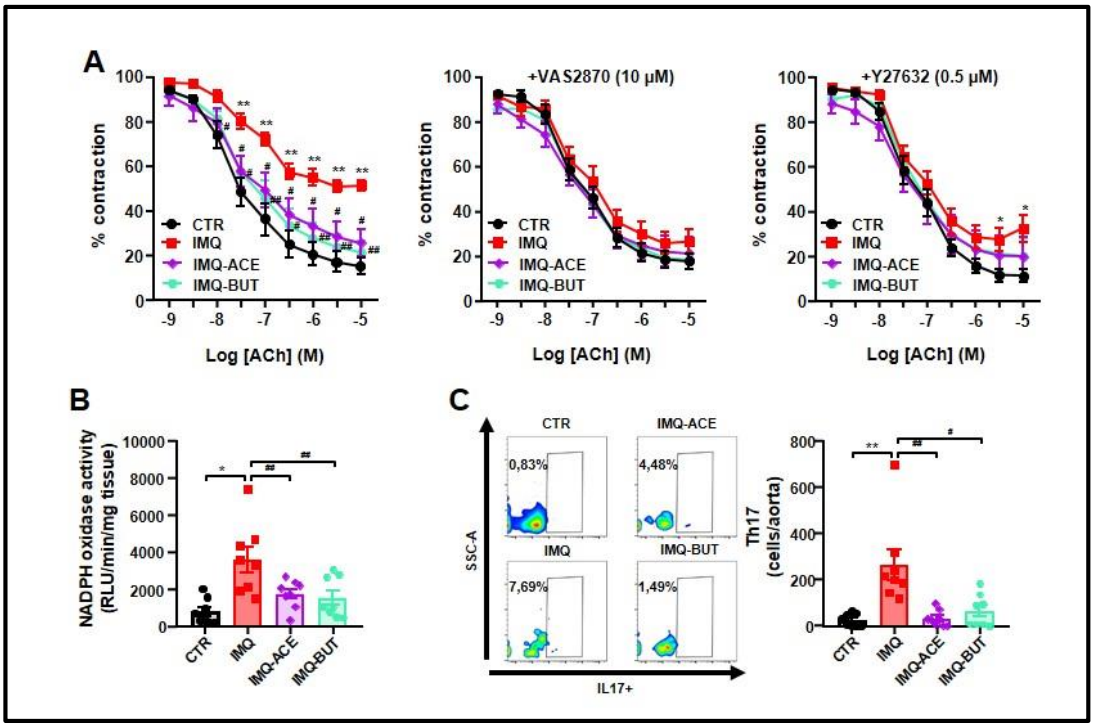

Figure 32. Effects of SCFA treatments on endothelial function, NADPH oxidase activity, and immune cell infiltration in TLR-7-induced lupus mice.

(**A**) Vascular relaxation responses induced by acetylcholine (Ach) in aortic rings pre-contracted by U46619, with or without NADPH oxidase inhibitor VAS2870 or Rho kinase inhibitor Y27632. (**B**) Aortic NADPH oxidase activity. (**C**) Aortic immune cell infiltration measured by flow cytometry. Groups: control (CTR), imiquimod (IMQ), and IMQ-treated mice with acetate (ACE) or butyrate (BUT). Data presented as means ± SEM (n = 8). Two-way ANOVA with Sidak's multiple comparisons for Ach concentration-response curves. One-way ANOVA and Tukey's post hoc or Kruskal-Wallis with Dunn's multiple comparisons for other variables. *P<0.05 and **P<0.01 vs. CTR; #P<0.05 and ##P<0.01 vs. untreated IMQ.

3.3. Fiber treatments increased SCFA production by remodeling the gut microbiota and prevented the rise in BP

The consumption of dietary fiber induced significant and profound changes in the composition of the gut microbiota. In IMQ mice, RS led to a reduction in Chao richness but a normalization of Shannon and Simpson diversity (**Figure 33A**). We conducted a two-dimensional PCA analysis of the bacterial community, which measures microorganism diversity among samples (β-diversity) at various taxonomic levels (phylum, class, order, family, genus, and species). The Permanova analysis showed a significant clustering of the animals into each group (**Figure 33B**). Specifically, bacteria belonging to *Actinobacteria*, *Firmicutes*, and *Verrucomicrobia* were reduced in the IMQ group compared to the CTR group, whereas those belonging to *Bacteroidetes* were increased (**Figure 33C, Figure 34**). RS treatment reduced the relative abundance of *Firmicutes* and increased *Bacteroidetes* and *Verrucomicrobia*, while ITF did not significantly change the microbiota composition at the phylum level (**Figure 33C, Figure 34**). Consequently, the *Firmicutes*/*Bacteroidetes* ratio, an index of gut dysbiosis, was reduced by IMQ and increased by RS treatment (**Figure 33D**). At the family level, we observed reduced *Bacillaceae* and *Verrumicrobiaceae* and increased *Porphyromonadaceae* relative abundance in the IMQ group compared to the CTR group (**Figure 34, Figure 35**). RS treatment increased *Bacillaceae* and *Verrucomicrobiaceae* proportions and reduced *Porphyromonadaceae* and *Prevotellaceae*, whereas ITF consumption increased *Bacteroidaceae* and reduced *Barnesiella* and *Porphyromonas* (**Figure 34, Figure 35**). At the genus level, we found a lower relative abundance of *Akkermansia* and *Bacillus* and a higher abundance of *Barnesiella* in the IMQ group compared to the CTR group (**Figure 34, Figure 36**). RS treatment increased *Akkermansia*, *Bacillus*, and *Clostridium*, and reduced *Alkaliphilus*, *Barnesiella*, *Porphyromonas*, and *Prevotella*, whereas ITF increased *Bacteroides* and reduced *Barnesiella* and *Porphyromonas* (**Figure 34, Figure 36**).

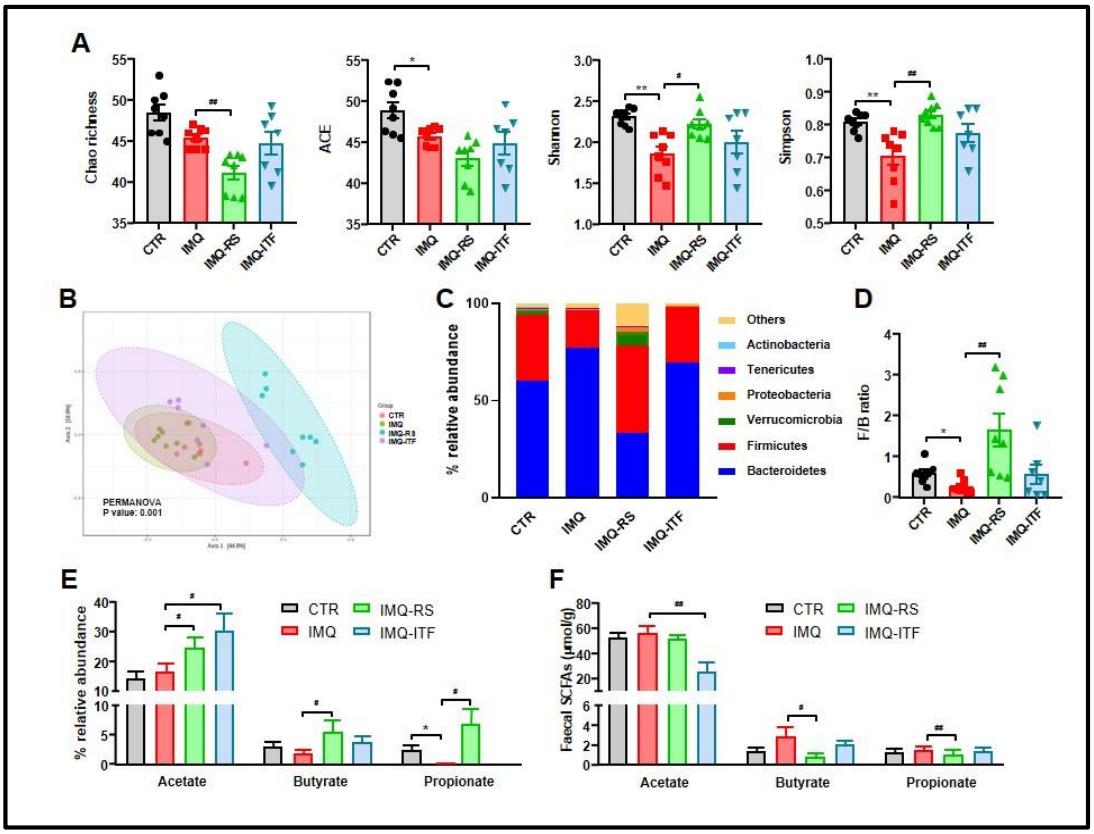

Figure 33. Effects of fiber treatments on gut microbiota composition in TLR-7-induced lupus mice.

(**A**) Alpha diversity indices, (**B**) Principal Coordinate Analysis (PCA) of gut microbiota, (**C**) Proportion of bacterial phyla, (**D**) Firmicutes/Bacteroidetes (F/B) ratio, and (**E**) Proportion of short-chain fatty acids (SCFA)-producing bacteria in feces using 16S rRNA analysis. (**F**) SCFA concentrations in feces measured by gas chromatography. Groups: control (CTR), imiquimod (IMQ), IMQ treated with resistant starch (RS) or inulin-type fructans (ITF). Data presented as means ± SEM (n = 8). One-way ANOVA and Tukey's post hoc or Kruskal-Wallis with Dunn's multiple comparisons for all variables.

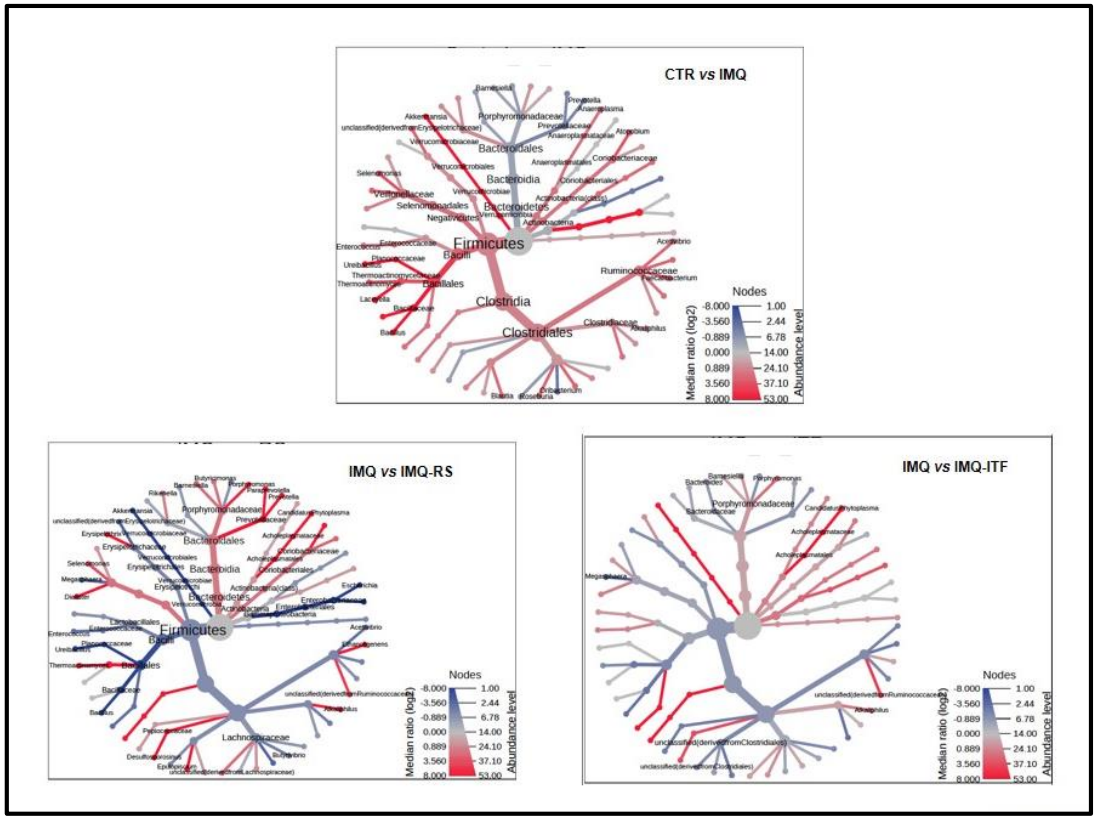

Figure 34. Analysis of gut microbiota differences between experimental groups.

Heat tree showing differences in the community structure, (n = 7-8). Size and color of nodes and edges are correlated with the abundance of organisms in each community. Significant taxon names are labeled (Wilcoxon Rank Sum test P-value < 0.05). Groups: Control (CTR), IMQ and IMQ-groups treated with acetate (ACE) or butyrate (BUT).

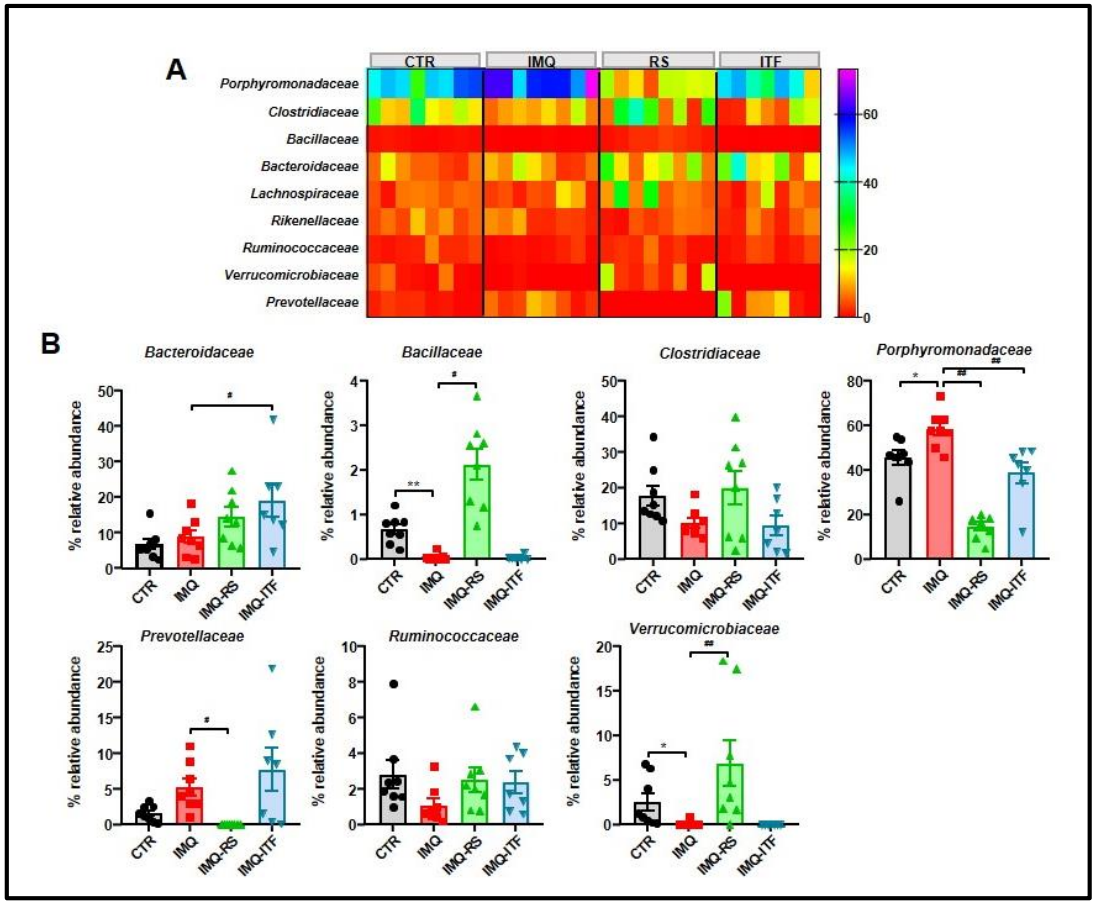

Figure 35. Family changes in the gut microbiota composition induced by fiber treatments in mice with lupus induced by TLR-7 activation with imiquimod (IMQ).

(**A**) Heat map of bacterial families. The heatmap colours represent the relative percentage of microbial genera assigned within each sample. (**B**) Relative abundance of bacterial families with a relative abundance > 1% in control (CTR), IMQ, and IMQ-groups treated with resistant starch (RS) or inulin-type fructans (ITF). Values are expressed as means ± SEM (n = 7-8). Data were analyzed with one-way ANOVA and Tukey post hoc test, or Kruskal-Wallis with Dunn's multiple comparisons. *P<0.05 and **P<0.01 compared to the CTR group, #P<0.05 and ##P<0.01 compared to the untreated IMQ group.

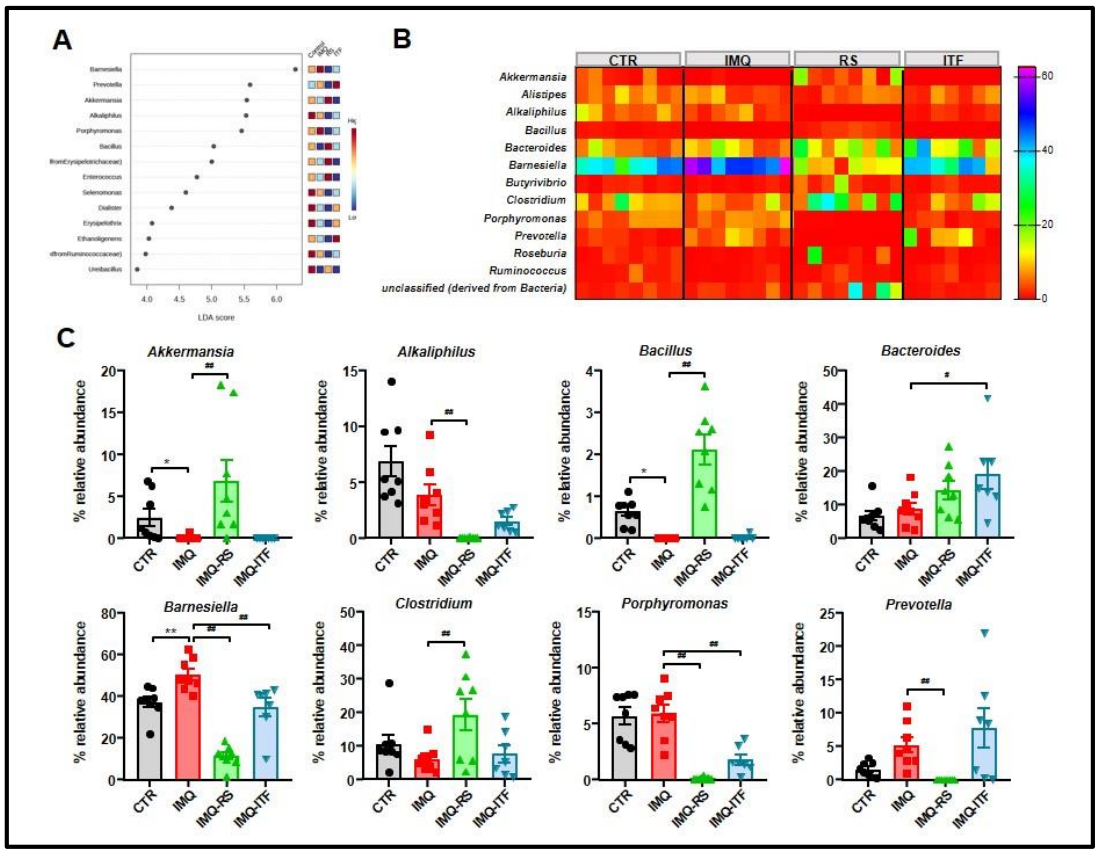

Figure 36. Genera changes in the gut microbiota composition induced by fiber treatments in mice with lupus induced by TLR-7 activation with imiquimod (IMQ).

(**A**) Linear discriminant analysis (LDA) score at $p < 0.05$ was used to rank the ability of different genera to discriminate among groups, (**B**) Heat map of bacterial genera. The heatmap colours represent the relative percentage of microbial genera assigned within each sample. (**C**) Relative abundance of bacterial genera with a relative abundance > 1% in control (CTR), IMQ, and IMQ-groups treated with resistant starch (RS) or inulin-type fructans (ITF). Values are expressed as means ± SEM (n = 7-8). Data were analyzed with one-way ANOVA and Tukey post hoc test, or Kruskal-Wallis with Dunn's multiple comparisons. *P<0.05 and **P<0.01 compared to the CTR group, #P<0.05 and ##P<0.01 compared to the untreated IMQ group.

As prebiotic fiber is fermented by gut bacteria, leading to the production of SCFA, we investigated the relative abundance of SCFA-producing bacteria. We observed no significant changes in ACE- and BUT-producing bacteria, but there was a decreased abundance of PROP-producing bacteria in the IMQ group compared to the CTR group (**Figure 33E**). However, the RS diet elevated the proportion of bacteria producing ACE, BUT, and PROP, while ITF increased only the proportion of ACE-producing bacteria (**Figure 33E**). Notably, the faecal content of PROP and BUT in the IMQ-RS group was lower compared to the IMQ group, although ACE content remained unchanged. Furthermore, in ITF-treated mice, the faecal ACE content was lower than that in IMQ mice (**Figure 33F**), indicating enhanced SCFA absorption in the fiber-treated groups.

SCFA possess the capability to enter the cytosol through passive diffusion and can also be absorbed by solute transporters, such as the proton-coupled monocarboxylate transporters (MCT)-1 and MCT-4, which are upregulated due to prolonged ACE or BUT consumption (Ritzhaupt et al. 1998). This elucidates our findings, as both fiber treatments increased the presence of SCFA-producing bacteria in IMQ mice and resulted in higher colonic mRNA levels of MCT-1 and MCT-4 (**Figure 37A**). Moreover, BUT within intestinal epithelial cells consumes local oxygen, stabilizing the hypoxia-inducible factor (HIF), a transcription factor that orchestrates barrier protection (Parada Venegas et al. 2019). In alignment with the augmented BUT production and absorption in the colon stemming from RS consumption, we observed elevated colonic Hif-1 mRNA levels in RS-treated mice compared to the IMQ group (**Figure 37B**).

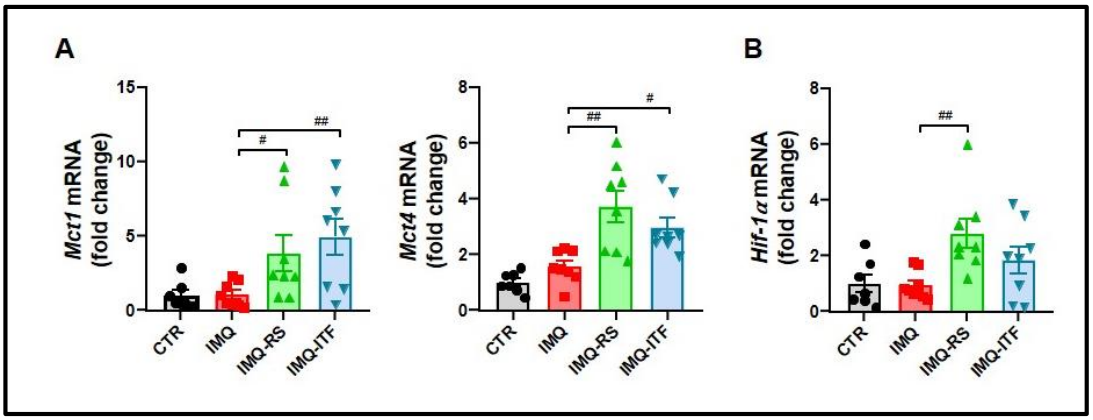

Figure 37. Fiber treatments increase de expression of colonic SCFAs transporters in mice with lupus induced by TLR-7 activation with imiquimod (IMQ).

(**A**) Colonic mRNA levels of monocarboxylate-transporter (MCT)1 and MCT4, and (**B**) hypoxia inducible factor (HIF)-1α. Groups: Control (CTR), IMQ, and IMQ-groups treated with resistant starch (RS) or inulin-type fructans (ITF). Values are expressed as means ± SEM (n = 7-8). Data were analyzed with one-way ANOVA and Tukey post hoc test, or Kruskal-Wallis with Dunn's multiple comparisons. #P<0.05 and ##P<0.01 compared to the untreated IMQ group.

Similar to SCFA treatments, both RS and ITF consumption effectively prevented the rise in SBP to a similar extent (approximately 69.4% and 66.4%, respectively) (**Figure 38A**). Additionally, both RS and ITF reduced left ventricular hypertrophy (**Figure 38B**), increased endothelium-dependent aortic relaxation in response to Ach (**Figure 40C**) and achieved these effects by reducing NOX activity (**Figure 38D**) and Th17 infiltration (**Figure 38E**). In contrast to the consumption of ACE or BUT alone, RS fiber, which increased the bacterial production of ACE, BUT, and PROP, showed greater efficacy in improving the main signs of autoimmunity in this model, such as high plasma anti-ds-DNA levels (**Figure 39A**), splenomegaly (**Figure 39B**), hepatomegaly (**Figure 39C**), and elevated mRNA levels of IFNα in MLN (**Figure 39D**). However, ITF fiber did not exhibit significant effects in these parameters. Moreover, neither RS nor ITF had any impact on B cell content in MLN and spleen (**Figure 39E**).

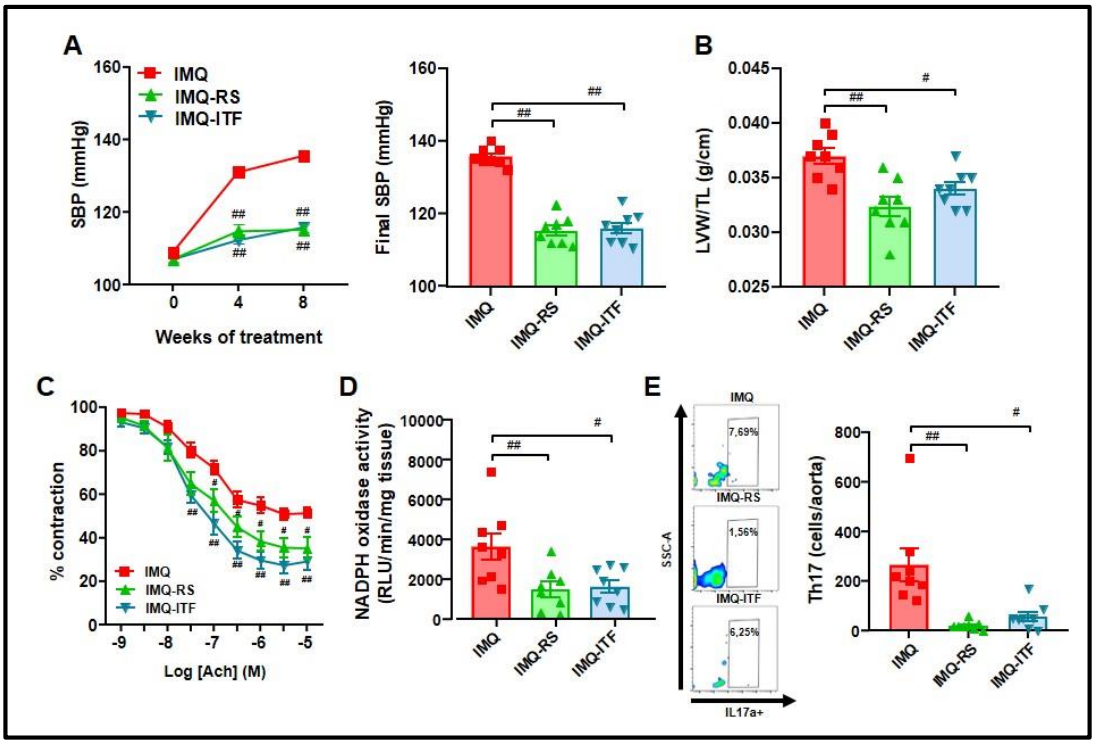

Figure 38. Effects of fiber treatments on blood pressure, organ hypertrophy, endothelial function, NADPH oxidase activity, and immune cell infiltration in TLR-7-induced lupus mice.

(**A**) Time-course and final systolic blood pressure (SBP), (**B**) left ventricular weight (LVW) normalized by tibia length (TL), (**C**) acetylcholine (Ach)-induced vascular relaxation, (**D**) aortic NADPH oxidase activity, and (**E**) aortic immune cell infiltration. Groups: control (CTR), imiquimod (IMQ), IMQ treated with resistant starch (RS) or inulin-type fructans (ITF). Data presented as means ± SEM (n = 8). Two-way ANOVA with Sidak's multiple comparisons for SBP time-course and Ach concentration-response curves. One-way ANOVA and Tukey's post hoc or Kruskal-Wallis with Dunn's multiple comparisons for other variables. #P<0.05 and ##P<0.01 vs. untreated IMQ.

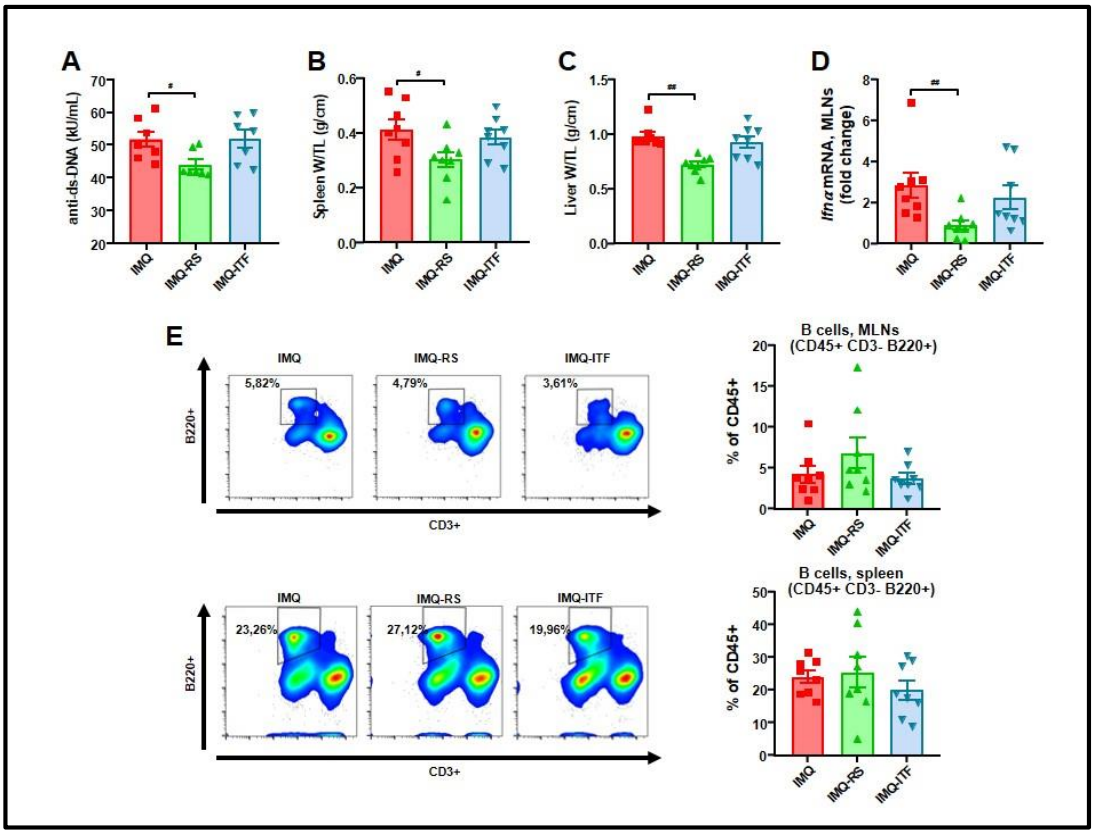

Figure 39. Effects of fiber treatments on disease activity sings in mice with lupus induced by TLR-7 activation with imiquimod (IMQ).

(**A**) Circulating double-stranded DNA (anti-ds-DNA), (**B**) splenomegaly, (**C**) hepatomegaly, (**D**) IFNα mRNA levels in mesenteric lymph nodes (MLNs), and (**E**) percentage of B cells in MLNs and spleen. Groups: IMQ and IMQ-groups treated with resistant starch (RS) or inulin-type fructans (ITF). Values are expressed as means ± SEM (n = 7-8). Data were analyzed with one-way ANOVA and Tukey post hoc test, or Kruskal-Wallis with Dunn's multiple comparisons. #P<0.05 and ##P<0.01 compared to the untreated IMQ group.

3.4. SCFA treatments improved intestinal integrity and inflammation

Recognizing the importance of the translocation of the structural bacterial component LPS in relation to autoimmunity and high BP (Liang et al. 2013), we proceeded to evaluate the integrity and permeability of the intestinal epithelium. We assessed gut barrier integrity by examining colonic mRNA expression of key junctional transcripts (**Figure 40A**), including occludin and ZO-1, along with MUC molecules (**Figure 40B**), such as MUC-2 and MUC-3. We found that mRNA levels of occludin were lower (approximately 54%) in the IMQ group compared to the CTR group, while no significant changes were observed in the other markers of gut integrity. This discrepancy resulted in an increase (approximately 47%) in plasma LPS levels (**Figure 40C**).

Under our experimental conditions, ACE treatment increased colonic mRNA levels of occludin, ZO-1, and MUC-3, leading to a reduction in plasma endotoxin levels. However, BUT did not demonstrate improvement in gut integrity or permeability. Furthermore, ACE treatment resulted in decreased mRNA levels of the proinflammatory cytokine IL-1ß (**Figure 40D**). In contrast, BUT acted as a primary energy source for colonocytes, consuming oxygen and stabilizing HIF-1α (**Figure 40E**). In both epithelial and immune cells, SCFA serve as ligands for GPRs, such as GPR43 and GPR41, which are upregulated by SCFA or have inhibitory effects on HDAC activity. This mechanism triggers histone acetylation and modulates gene regulation involved in cell proliferation, differentiation, and the inflammatory response, contributing to intestinal homeostasis (Parada Venegas et al. 2019). In line with this, we found elevated GPR41 and GPR43 mRNA levels in colonic samples from the IMQ-ACE and IMQ-BUT groups, respectively, compared to the IMQ mice (**Figure 40F**). Additionally, colonic HDAC3 transcript levels were downregulated in the IMQ-BUT group compared to the IMQ mice (**Figure 40G**). In summary, our findings indicate enhanced colonic integrity and reduced permeability and inflammation resulting from ACE treatment, which is associated with GPR43 activation. On the other hand, GPR41 activation and HDACs inhibition by BUT primarily might contribute to improved colonic metabolism.

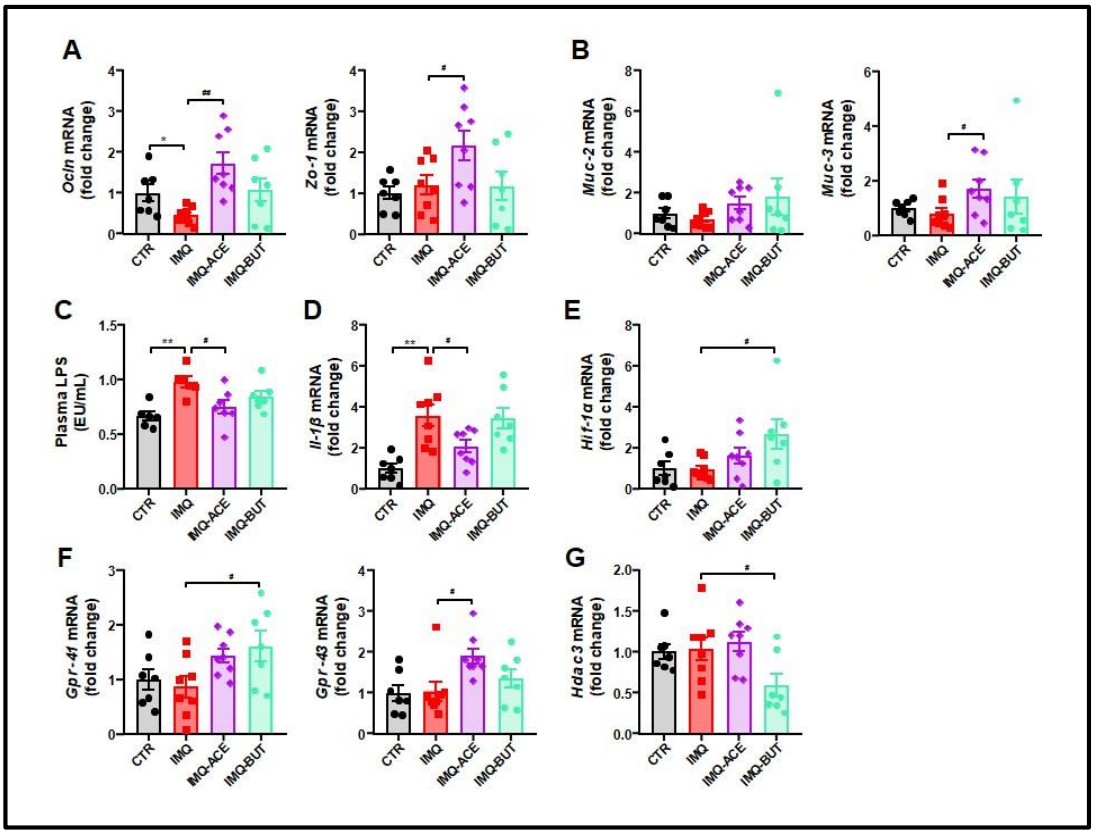

Figure 40. Effects of SCFA treatments on colonic integrity markers, permeability, and inflammation in TLR-7-induced lupus mice.

(**A**) Colonic mRNA expression of occludin (Ocln) and zonula occludens-1 (Zo-1), and (**B**) mucin (Muc)-2 and Muc-3 mucins. (**C**) Plasma LPS levels, (**D**) colonic interleukin (Il)-1ß mRNA expression, and (**E**) colonic hypoxia inducible factor (Hif)-1α mRNA expression. (**F**) Colonic G-protein-coupled receptor (Gpr)41, Gpr43, (**G**) and histone deacetylase (Hdac)3 mRNA levels. Groups: control (CTR), imiquimod (IMQ), and IMQ-treated mice with acetate (ACE) or butyrate (BUT). Data presented as means ± SEM (n = 8). One-way ANOVA and Tukey's post hoc or Kruskal-Wallis with Dunn's multiple comparisons for all variables. *P<0.05 and **P<0.01 vs. CTR; #P<0.05 and ##P<0.01 vs. untreated IMQ.

3.5. SCFA treatments attenuated T cells imbalance in MLN

Considering the critical role of Th17 polarization in secondary lymph organs and Th17 infiltration in the aorta, which contributes to vascular alterations caused by TLR-7 activation (de la Visitación et al. 2021; Robles-Vera et al. 2020) we investigated whether SCFA could modulate this Th imbalance in MLN, as previously described in systemic hypertension (Robles-Vera et al. 2020). In our study, we observed that the percentage of Th17 cells (CD4+ IL-17a+) and Th1 cells (CD4+ IFN-γ+) increased by approximately 3.2-fold and 2.5-fold, respectively, in IMQ mice, while Treg cells (CD4+ CD25+) remained unchanged (**Figure 41**). Both ACE and BUT consumption normalized the proportion of Th17 cells without affecting Th1 and Treg cells. To gain further insights into the immunomodulatory effects of SCFA in MLN, we investigated the cells and cytokines involved in the polarization of Th17 cells. In IMQ mice, the integrity of the colon was compromised, enabling bacterial translocation through the intestinal barrier and triggering the activation and migration of CX3CR1+ cells, such as DC or macrophages, towards the lower intestinal tract lymph nodes (Niess et al. 2005). These cells also present antigens to naïve CD4+ T lymphocytes, contributing to T cell priming. In alignment with this, we observed higher levels of CX3CR1 mRNA (approximately 3.6-fold increase) in MLN from the IMQ group compared to the CTR mice, which were brought back to normal levels by ACE consumption, although not by BUT consumption (**Figure 42A**). Additionally, DC, apart from their role as antigen-presenting cells, release mediators that promote T cell polarization. IL-6 induces the proliferation of Th17 cells and suppresses Treg cells (Kimura and Kishimoto 2010). Our analysis of transcript levels in MLN revealed that IL-6 levels were approximately 5.9-fold higher in the IMQ group than in the CTR group, and ACE treatment reduced this elevation by about 45% (**Figure 42B**). The activation of GPRs and inhibition of HDACs by SCFA in immune cells have been previously documented (Parada Venegas et al. 2019). We noted that ACE treatment upregulated GPR43 mRNA levels, while BUT increased GPR41 expression and downregulated HDAC3 (**Figure 42C**). It has been described that sodium BUT, acting as an HDACs inhibitor, regulates the balance between Th17 and Treg cells through the NRF-2/HO-1/IL-6 receptor pathway (X. Chen et al. 2017). In line with NRF-2 activation, the mRNA levels of the downstream antioxidant enzymes HO-1 and NQO-1 were increased by BUT, leading to a decreased expression of the IL-6 receptor (**Figure 42D**) and resulting in a reduced Th17 polarization.

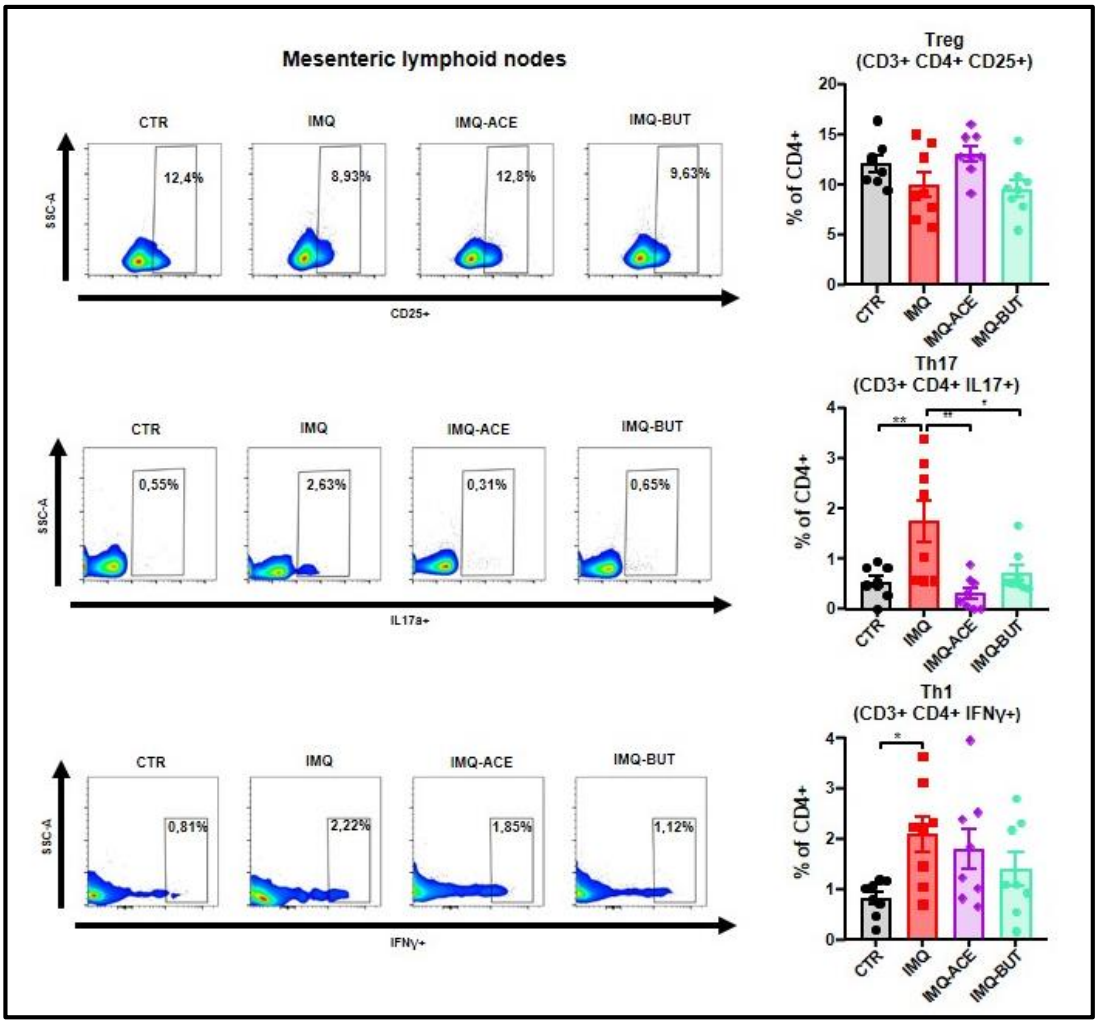

Figure 41. Effects of SCFA treatments on lymphocyte populations in mesenteric lymph nodes of TLR-7-induced lupus mice.

Regulatory T cells (Treg), Th17, and Th1 cells measured by flow cytometry in control (CTR), imiquimod (IMQ), and IMQ-treated mice with acetate (ACE) or butyrate (BUT) groups. Data presented as % of parent and means ± SEM (n = 8). One-way ANOVA and Tukey's post hoc or Kruskal-Wallis with Dunn's multiple comparisons. *P<0.05 and **P<0.01 vs. CTR; #P<0.05 and ##P<0.01 vs. untreated IMQ.

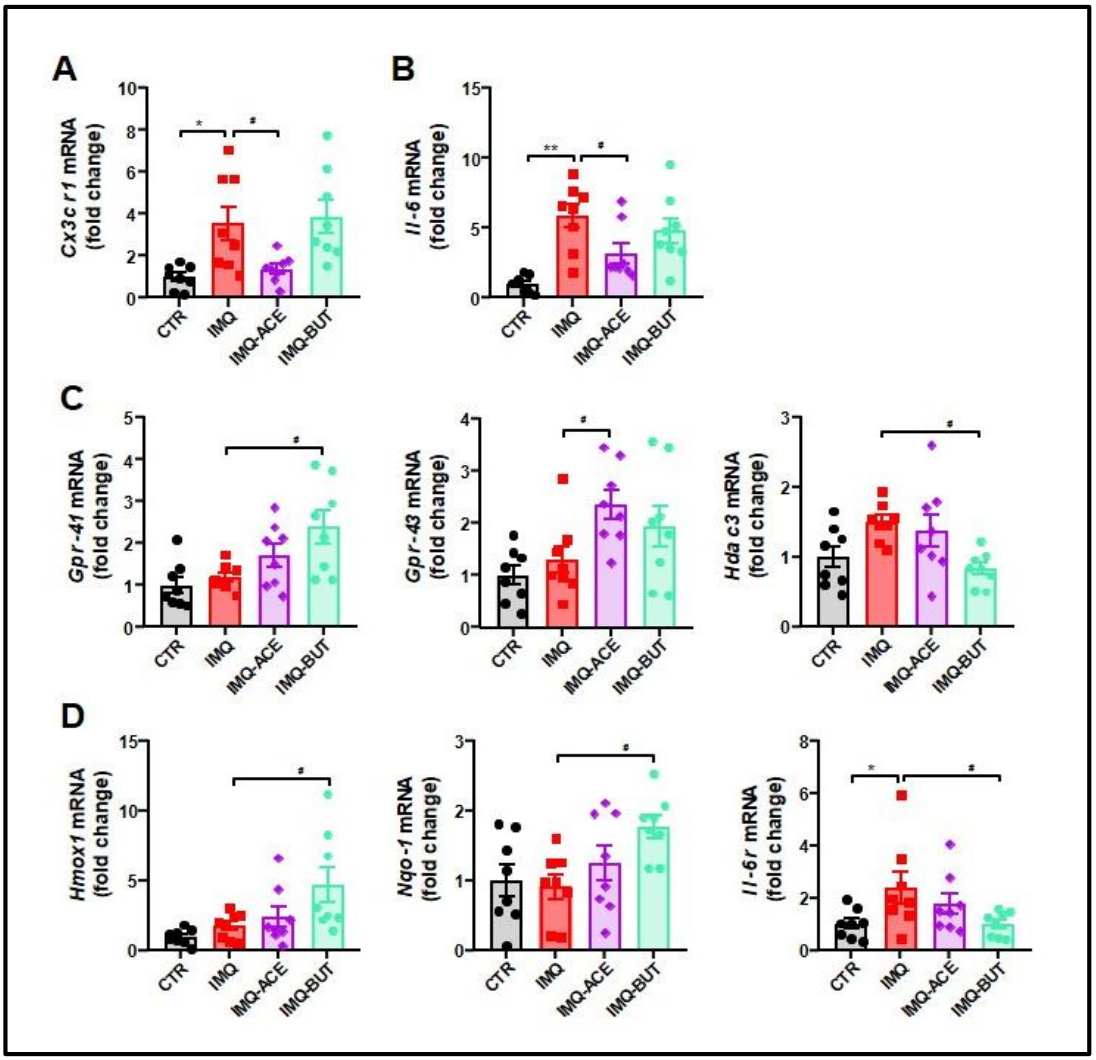

Figure 42. SCFA treatments prevented T cells activation in mesenteric lymph nodes in mice with lupus induced by TLR-7 activation with imiquimod (IMQ).

(**A**) mRNA levels of the marker of antigen presenting cells CX3CR1+. (**B**) mRNA levels of interleukin (IL)6. (**C**) Expression of G protein-coupled receptor (GPR)43, and histone deacetylase (HDAC)3. (**D**) Pathway nuclear factor erythroid 2-related factor 2 (NRF-2)/heme oxygenase 1 (HO-1)/IL-6 receptor measured by the mRNA levels of HO-1, NAD(P)H:quinone oxidoreductase 1 (NQO1), and IL-6 receptor (IL-6R). Groups: control (CTR), IMQ and IMQ-groups treated with acetate (ACE) or butyrate (BUT). Values are expressed as means ± SEM, n = 8. Data were analyzed with one-way ANOVA and Tukey post hoc test, or Kruskal-Wallis with Dunn's multiple comparisons. *P<0.05 and **P<0.01 compared to the CTR group, #P<0.05 compared to the untreated IMQ group.

3.6. GPR43 blockade prevented the protective effects induced by ACE

To investigate the potential role of GPR43 in the effects of SCFA, we utilized the GPR43 antagonist GLPG-0974. This drug counteracted the antihypertensive effects of ACE (**Figure 43A**) and attenuated its ability to reduce heart hypertrophy (**Figure 43B**), while having no impact on the effects of BUT. Moreover, blocking GPR43 abolished the improvement of endothelium-dependent relaxation to Ach induced by ACE, but not by BUT treatment (**Figure 43C**). The impaired relaxant response to Ach induced by GLPG-0974 was mitigated in the presence of the NOX inhibitor, VAS2870, or the Rho kinase inhibitor, Y27632 (**Figure 43C**), suggesting that ACE reduced NOX and Rho kinase activities through GPR43 activation. Indeed, GLPG-0974 increased NOX activity in IMQ mice treated with ACE, bringing it to levels comparable to untreated IMQ mice (**Figure 43D**). When aortic rings were incubated with an antibody to neutralize IL-17a, the reduced endothelium-dependent relaxation to Ach induced by GLPG-0974 in the presence of ACE was reversed (**Figure 43E**), suggesting that ACE improved this relaxant response by reducing IL-17a production in the vascular wall. This finding was further supported by the increased Th17 infiltration observed in aortic rings from the GLPG-IMQ-ACE group (**Figure 43F**). In contrast, GPR43 blockade had no effect on the protective responses induced by BUT in IMQ mice, suggesting the involvement of GPR43-independent mechanisms.

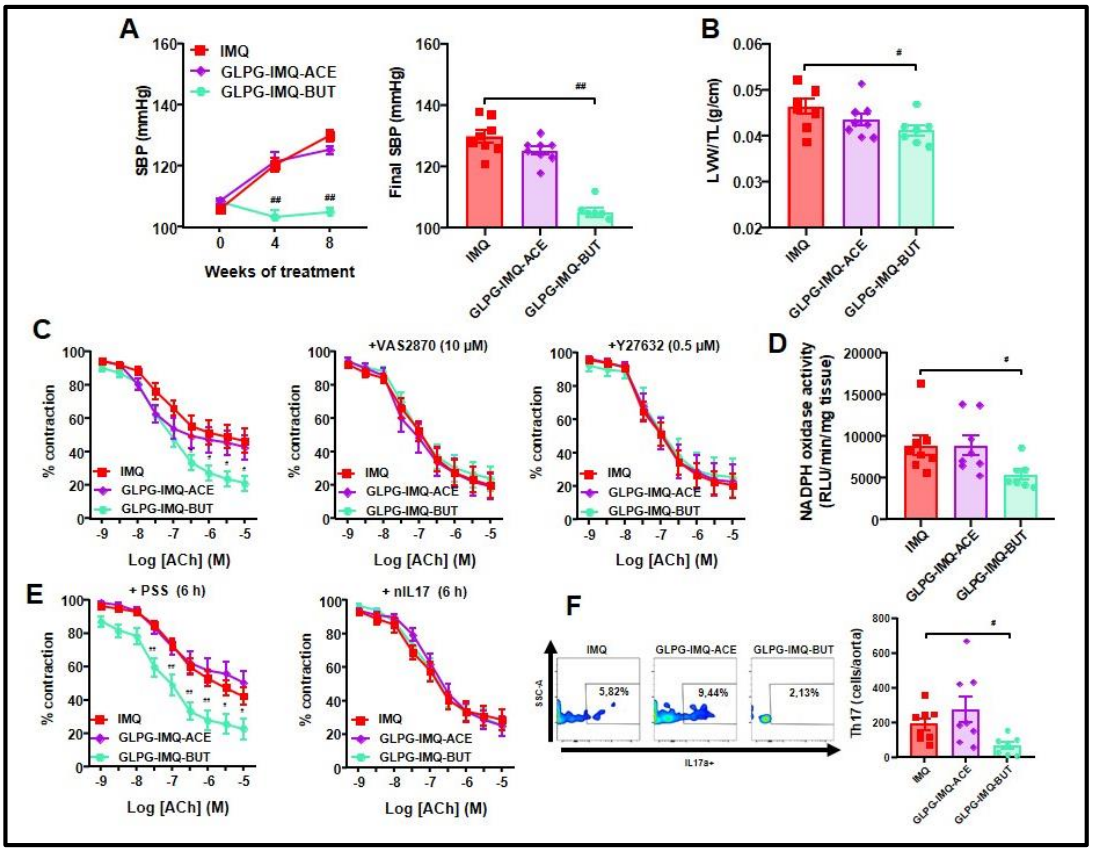

Figure 43. Effects of pharmacological GPR43 blockade on SCFA treatments in TLR-7-induced lupus mice.

(**A**) Time-course and final systolic blood pressure (SBP), (**B**) left ventricular weight (LVW) normalized by tibia length (TL), (**C**) acetylcholine (Ach)-induced vascular relaxation, (**D**) aortic NADPH oxidase activity, (**E**) Ach-induced vascular relaxation after IL-17 neutralization, and (**F**) aortic immune cell infiltration. Groups: IMQ, IMQ treated with GPR43 blockade (GLPG) and acetate (ACE) or butyrate (BUT). Data presented as means ± SEM (n = 7-8). Two-way ANOVA with Sidak's multiple comparisons for SBP time-course and Ach concentration-response curves. One-way ANOVA and Tukey's post hoc or Kruskal-Wallis with Dunn's multiple comparisons for other variables. #P<0.05 and ##P<0.01 vs. untreated IMQ.

3.7. SCFA abolished the transfer of hypertensive phenotype induced by gut microbiota from IMQ mice in GF mice

As anticipated, transferring the microbiota from donor IMQ group to recipient GF mice led to an increase in SBP by approximately 23 mmHg (**Figure 44A**), induced left ventricular and kidney hypertrophy (**Figure 44B**), impaired endothelium-dependent relaxation (**Figure 44C**) through elevated NOX activity (**Figure 44D**), and increased aortic Th17 infiltration (**Figure 44E**). This confirmed that the hypertensive phenotype can be transferred by the microbiota. In contrast, the signs of autoimmunity, such as plasma anti-ds-DNA (**Figure 45A**), splenomegaly (**Figure 45B**), hepatomegaly (**Figure 45C**), and blood B cell content (**Figure 45D**) were not transferred by microbiota inoculation for 3 weeks. Interestingly, both ACE and BUT treatments abolished the transfer of the hypertensive phenotype observed in mice inoculated with IMQ faeces. Furthermore, it was interesting to note that the hypertensive phenotype induced in GF mice by faecal inoculation from IMQ mice was associated with a higher proportion of Th17 cells in MLN and blood, with no significant changes in Treg and Th1 cell abundance (**Figure 46**). However, spleen showed no significant changes in the proportion of Th17, Treg, and Th1 cells after microbiota inoculation. ACE treatment reduced Th17 content in MLN and blood, whereas BUT increased MLN and circulating Treg cells while reducing Th17 cells in MLN. Overall, our data demonstrated that SCFA treatments restored the Th17/Treg balance in GF mice inoculated with faeces from IMQ mice, reducing vascular Th17 infiltration, which led to improved endothelial dysfunction and BP normalization.

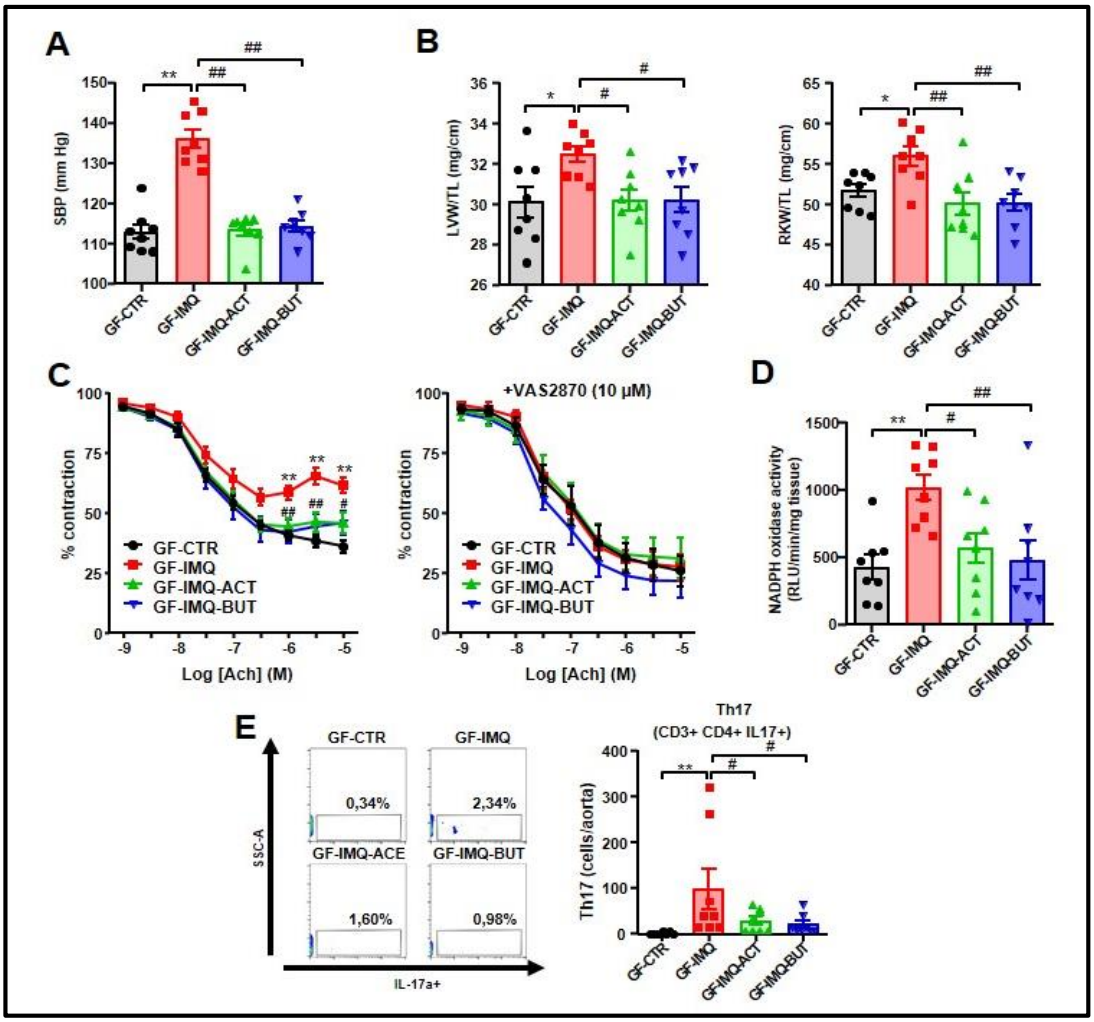

Figure 44. Effects of SCFA treatments on hypertension transfer to germ-free mice from TLR-7-induced lupus mice.

(**A**) Systolic blood pressure (SBP) measured by tail-cuff plethysmography, (**B**) left ventricular weight (LVW) and right kidney weight (RKW) normalized by tibia length (TL), (**C**) acetylcholine (Ach)-induced vascular relaxation, (**D**) aortic NADPH oxidase activity, and (**E**) aortic immune cell infiltration. Groups: germ-free (GF) mice inoculated with control faeces (GF-CTR), IMQ faeces (GF-IMQ), and IMQ faeces treated with acetate (GF-IMQ-ACE) or butyrate (GF-IMQ-BUT). Data presented as means ± SEM (n = 8). Two-way ANOVA with Sidak's multiple comparisons for SBP time-course and Ach concentration-response curves. One-way ANOVA and Tukey's post hoc or Kruskal-Wallis with Dunn's multiple comparisons for other variables. *P<0.05 and **P<0.01 vs. GF-CTR; #P<0.05 and ##P<0.01 vs. GF-IMQ.

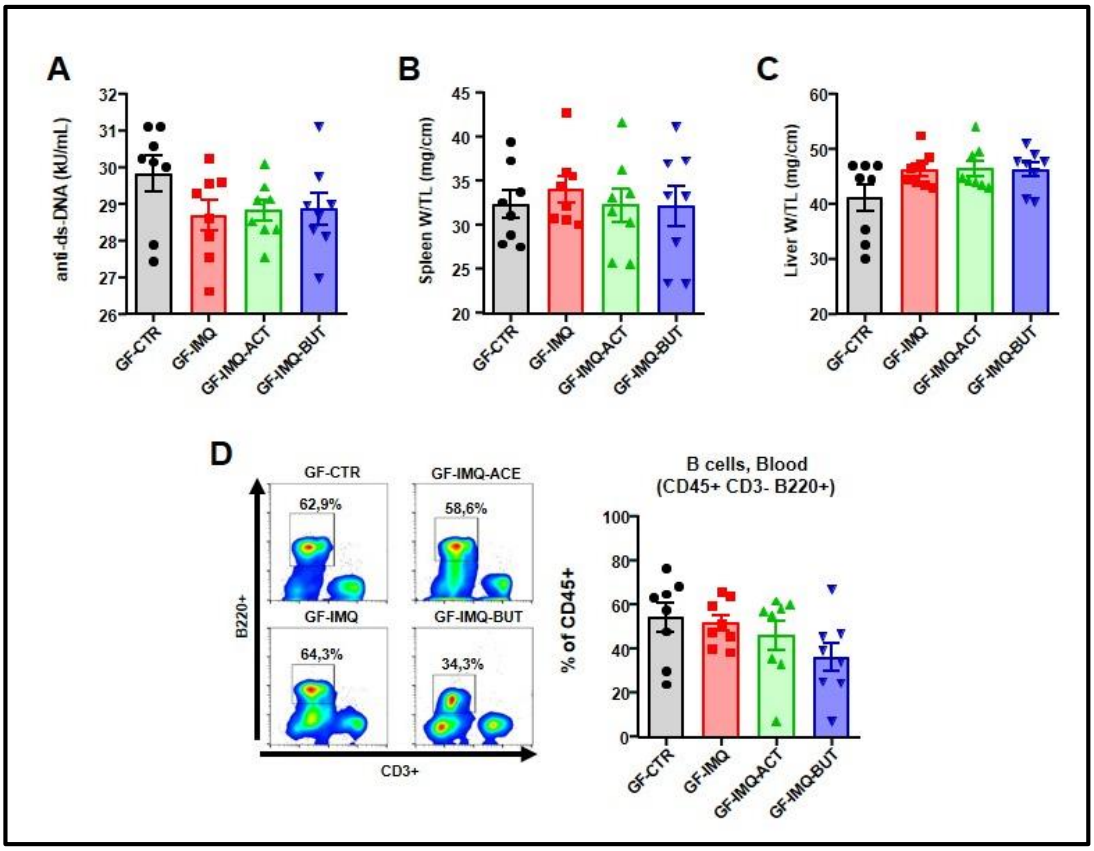

Figure 45. Effects of SCFA treatments on autoimmunity signs in germ-free (GF) mice inoculated with faeces from mice with lupus induced by TLR-7 activation with imiquimod (IMQ).

(**A**) Circulating double-stranded DNA (anti-ds-DNA), (**B**) splenomegaly, (**C**) hepatomegaly, and (**D**) percentage of B cells in blood. Groups: germ-free (GF) inoculated with control faeces (GF-CTR), GF inoculated with IMQ faeces (GF-IMQ) and GF inoculated with IMQ faeces and treated with acetate (GF-IMQ-ACE) or with butyrate (GF-IMQ-BUT). Values are expressed as means ± SEM, n = 8. Data were analyzed with one-way ANOVA and Tukey post hoc test, or Kruskal-Wallis with Dunn's multiple comparisons.

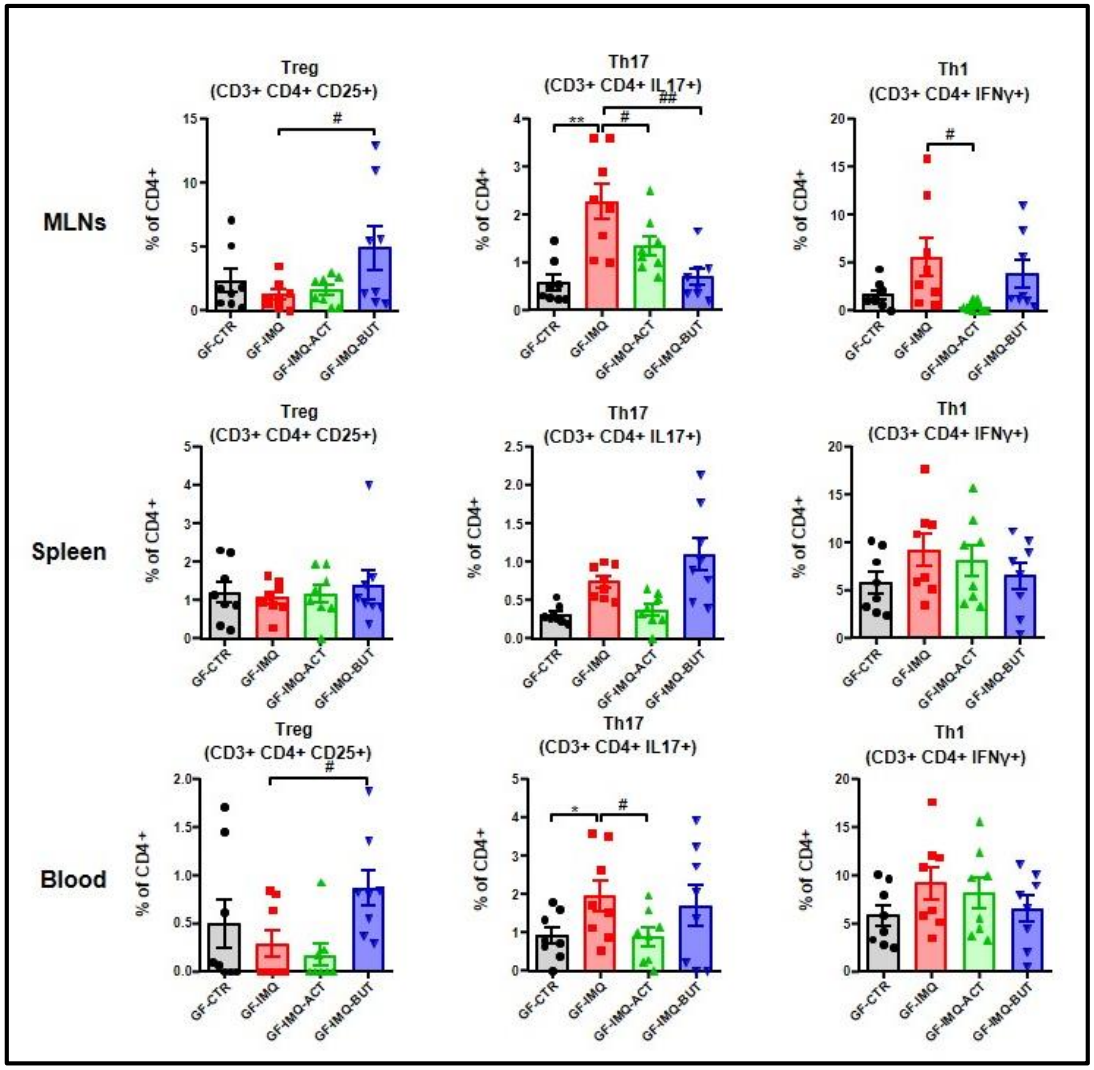

Figure 46. SCFA treatments prevented the immune imbalance induced by inoculation of faeces from mice with lupus induced by TLR-7 activation with imiquimod (IMQ) to germ-free (GF) mice.

Proportion of different immune cell types (Regulatory T cells (Tregs), Th17, and Th1 cells) measured by flow cytometry in mesenteric lymph nodes (MLNs), spleen, and blood. All data are expressed as % of parent. Groups: germ-free (GF) inoculated with control faeces (GF-CTR), GF inoculated with IMQ faeces (GF-IMQ) and GF inoculated with IMQ faeces and treated with acetate (GF-IMQ-ACE) or with butyrate (GF-IMQ-BUT). Values are expressed as means ± SEM, n = 8. Data were analyzed with one-way ANOVA and Tukey post hoc test, or Kruskal-Wallis with Dunn's multiple comparisons. *P<0.05 and **P<0.01 compared to the GF-CTR group, #P<0.05 and ##P<0.01 compared to the GF-IMQ group.

4. Role of dietary fiber intake in the raise of BP in NZBWF1 mice

4.1. Fiber treatments prevented the increase in BP, targeting organ hypertrophy, renal injury but not disease activity in lupus-prone mice

The mouse mortality rate in each group was the following: CTR group, 0%; SLE group, 10%, 1 dead mouse out of 10; RS group, 0%; and ITF group, 10%, 1 dead mouse out of 10. At the end of the experiment, a significant increase in the body weight of SLE mice in comparison to body weight of CTR animals was found, and neither RS, nor ITF significantly changed body weight in SLE mice (**Figure 47A**). In addition, no change in drink, food and energy intake were observed among all experimental groups (**Figure 47B**). At twenty-five weeks of age, SBP values were similar for all experimental groups. At thirty-three weeks of age, we detected the characteristic rise in SBP in SLE by approximately 29 mmHg from CTR values, which was partially prevented by ITF (≈ 43 %, $P<0.05$) and totally by RS ($P<0.01$) (**Figure 48A, 48B**). Sustained high BP is one of the most powerful determinants of the development of cardiac and renal hypertrophy (Frohlich et al. 1992). Absolute heart weight and left ventricle weight were higher in SLE than in CTR group (166.7 ± 9.8 mg vs. 132.5 ± 3.6 mg, $P < 0.001$; 121.0 ± 7.6 mg vs. 95.5 ± 2.5 mg, $P < 0.01$, respectively), which were unaffected by both fiber treatments. Left ventricle weight/tibia length, right and left kidney weight/tibia length indices were increased in SLE compared to CTR values (≈ 21 %, ≈ 30%, and ≈ 31%, respectively) (**Figure 48C**). RS treatment suppressed the observed cardiac hypertrophy but was unable to change the SLE high renal index. ITF did not change these morphological parameters (**Figure 48C**). SLE disease activity was determined at the experimental endpoint measuring plasma levels of anti-dsDNA autoantibodies, which revealed higher levels in SLE in relation to CTR (**Figure 48D**), as previously reported (Gómez-Guzmán et al. 2014; de la Visitación et al. 2021). Both fiber treatments did not significantly change disease activity, compared to SLE group. Likewise, splenomegaly has been used as a marker of disease progression, which can be associated to the development of a lymphoproliferative disorder (Wofsy et al. 1988). We have also detected this phenotypic characteristic in SLE (increase ≈ 2.4 times in spleen weight/tibia length compared to CTR group), and neither RS nor ITF treatments were able to change splenomegaly compared to SLE mice (**Figure 48E**).

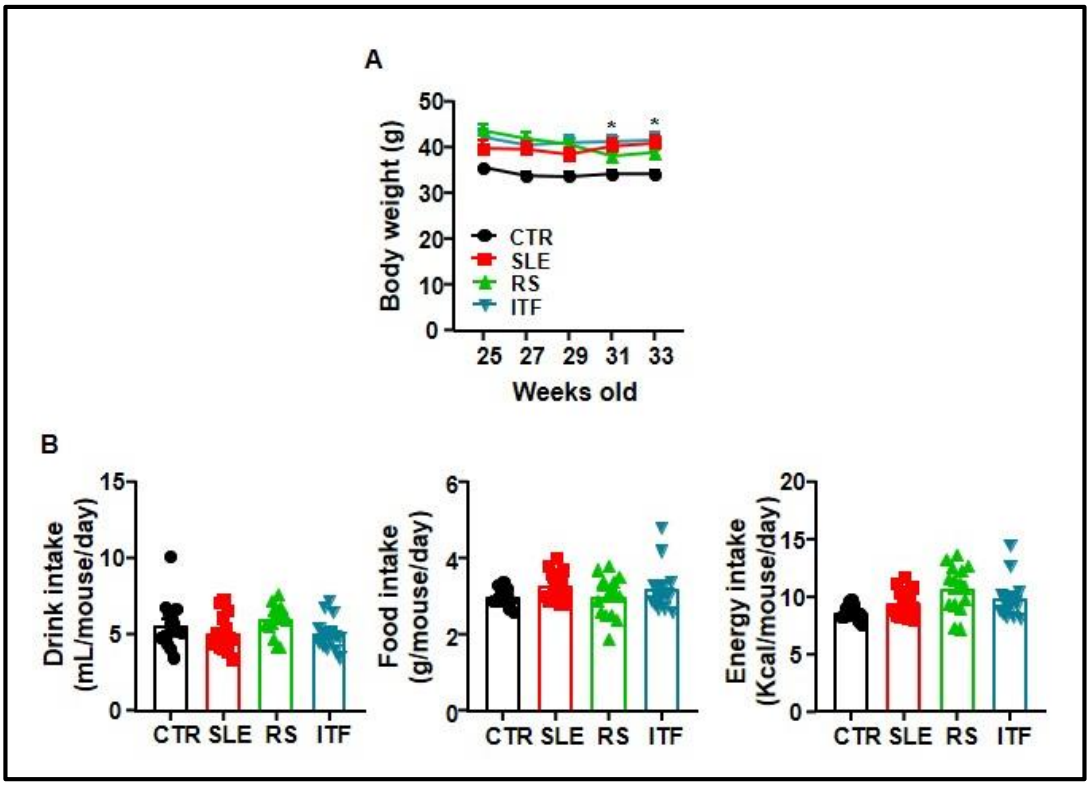

Figure 47. Effects of fiber treatments on general parameters of systemic lupus erythematosus (SLE) mice.

(**A**) Time course of body weight (n=9-10, data are shown as means ± SEM, *P<0.05 compared to the CTR group, two-way ANOVA, Sidak's multiple comparisons test) (**B**) Mean of dairy drink, food, and energy intake in all experimental groups: control (CTR), SLE, and SLE-groups treated with resistant starch (RS) or inulin-type fructans (ITF). Values are expressed as means ± SEM at different timepoint.

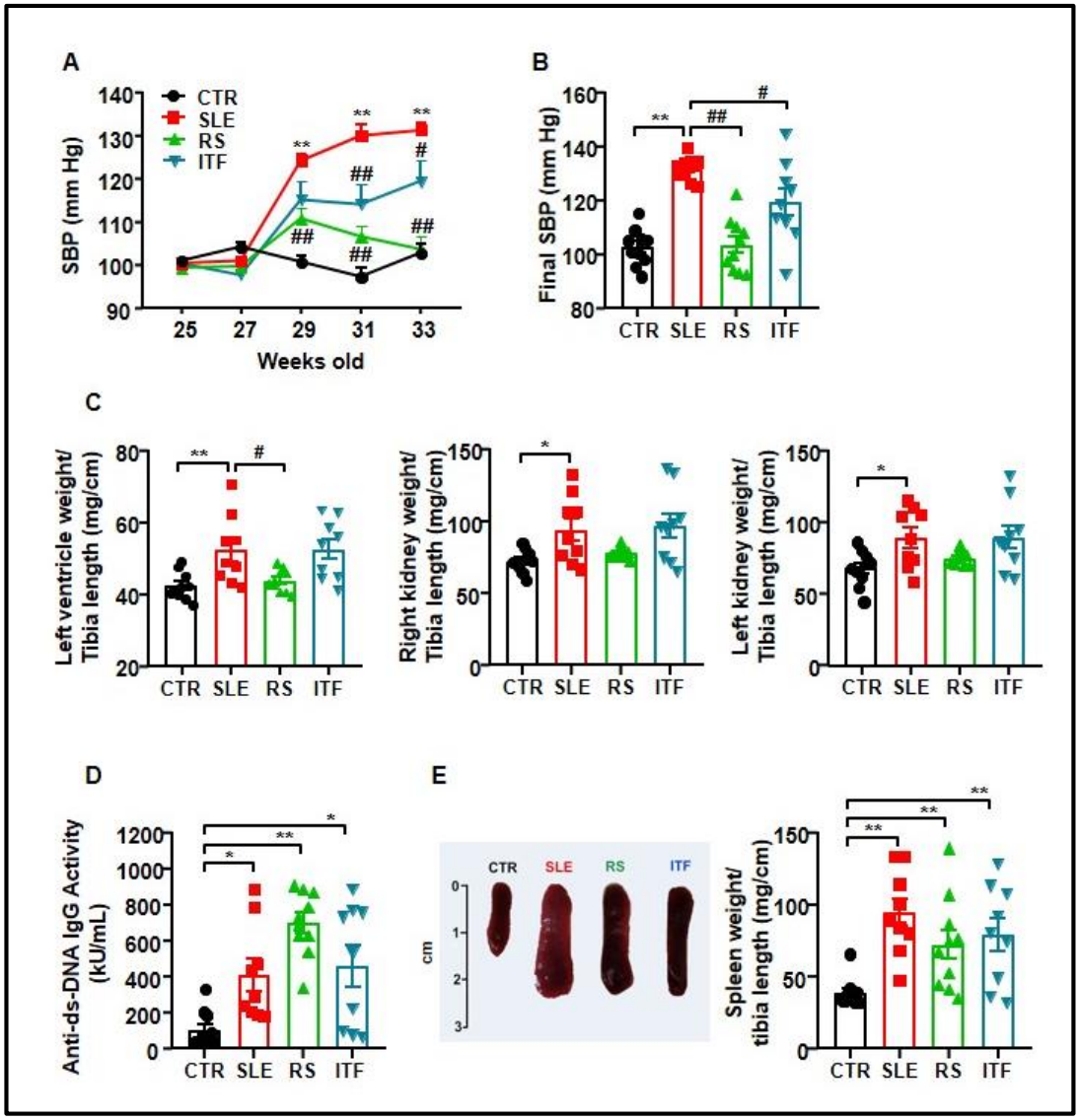

Figure 48. Fiber treatments inhibited the increase of blood pressure, target organ hypertrophy but not disease activity in systemic lupus erythematosus (SLE) mice.

(**A**) Time-course of systolic blood pressure (SBP) (n=9-10, data are shown as means ± SEM, **P<0.01 compared to the CTR group, #P<0.05 and ##P<0.01 compared to the untreated SLE group, two-way ANOVA, Sidak's multiple comparisons test) and (**B**) final SBP measured by tail-cuff plethysmography, (**C**) morphological parameters, (**D**) circulating double-stranded DNA autoantibodies levels, and (**E**) splenomegaly in control (CTR), SLE and SLE-groups treated with resistant starch (RS) or inulin-type fructans (ITF). Values are expressed as means ± SEM, n = 9-10, *P<0.05 and **P<0.01 compared to the CTR group, #P<0.05 and ##P<0.01 compared to the untreated SLE group, one-way ANOVA.

Renal injury is one of the characteristics most frequently associated to kidney inflammation in SLE (Gómez-Guzmán et al. 2014) The main evidence for differences in renal injuries, their analyses, and representative images to illustrate them are shown (**Figure 49, Table 5**). The kidneys of mice in the CTR group showed no remarkable glomerular, vascular, or tubulointerstitial lesions. Morphological examination of the glomeruli in SLE mice group revealed variable grades of intracapillary proliferation, mesangial sclerosis, wire loops, hyaline thrombi as well as very scan extracapillary proliferation (cellular crescent), fucsinophils deposits, and fibrous crescent formation. The quantification of glomerular cells showed an increased number of cells per glomerulus in SLE mice compared with CTR mice, which were reduced by RS supplementation but not ITF diet. Diffuse and global mesangial sclerosis, and intracapillary proliferation were significantly higher in SLE and ITF mice groups compared with RS mice and CTR groups. Glomerular activity scores were increased ≈ 5.8 fold in SLE as compared to CTR mice, and were reduced by both types of diet (**Figure 49B**). In tubulointerstitial in renal papilla is evident a moderate intensity of Tertiary Lymphoid Structures (TLS) (**Figure 49A**) and scan tubular casts. Kidney TLS have a similar cell composition, structure, and gene signature as lymph nodes and therefore may function as a kidney-specific type of lymph node (Dorraji et al. 2020). Lymphatic tissue swelling is one of the characteristics of lupus mice and is associated with SLE activity (Cohen and Eisenberg 1991). TLS in renal papilla were unchanged by both RS and ITF (**Figure 49A**). Tubulointerstitial scores were ≈ 16-fold higher in SLE than in CTR group but were unchanged by both types of diet (**Figure 49B**). The group of SLE mice shows glomerular chronic lesions (**Figure 49A**), which increased the chronic lesion score (**Figure 49B**). The RS diet significantly reduces glomerular lesions, while the use of ITF diet does not modify the lesions.

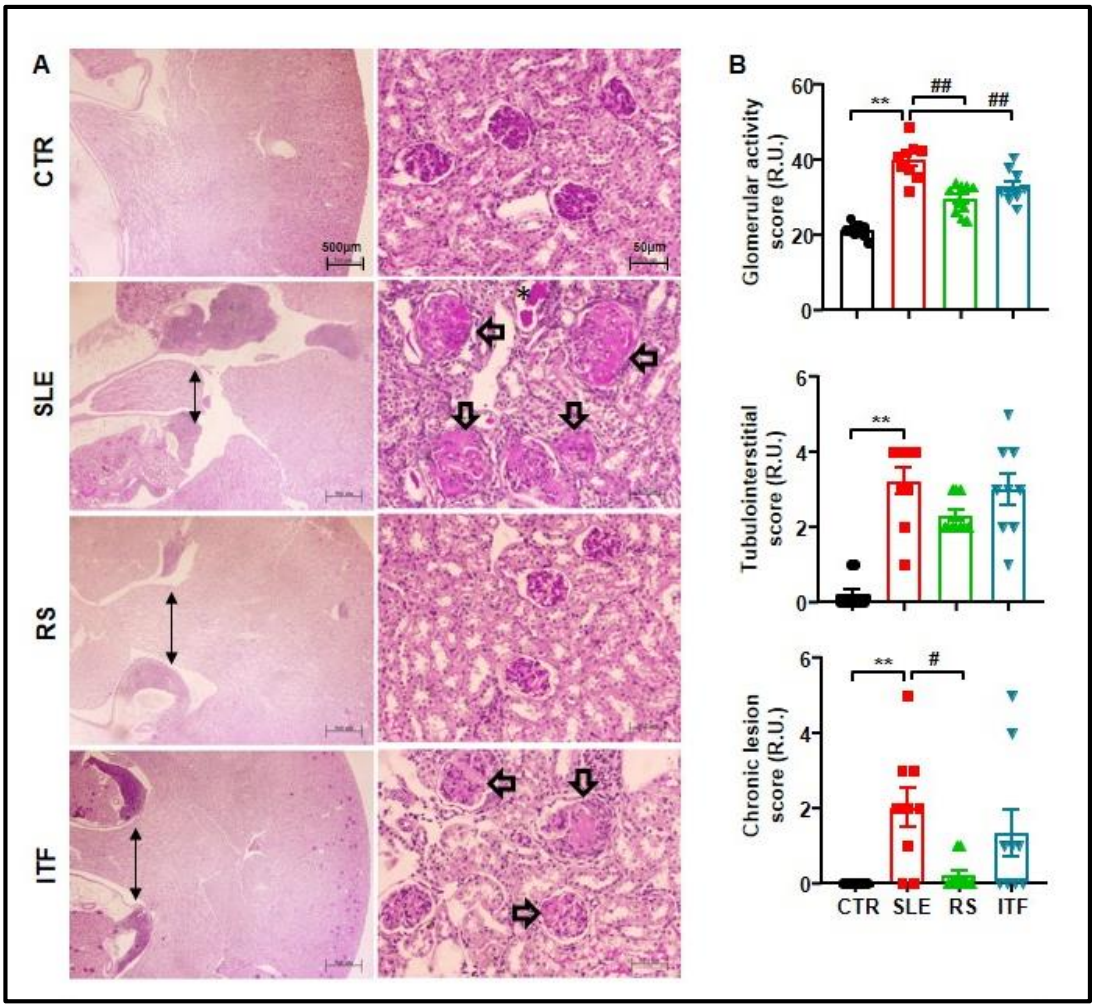

Figure 49. Fiber treatments improved morphological renal cortex features in systemic lupus erythematosus (SLE) mice.

(**A**) Kidney sections in control (CTR), SLE and SLE-groups treated with resistant starch (RS) or inulin-type fructans (ITF) were stained with hematoxylin-eosin and representative images are shown. Bar scale: 500 µm (left panels). Kidney sections were stained with periodic acid-Schiff and glomerular representative images are shown. Bar scale: 50 µm (right panels). Chronic inflammatory infiltrate in medullary area of kidney (black arrows), mesangial matrix expansion of glomeruli (white arrows), and hialyne tubular casts (asterisk). (**B**) The mean scores for individual pathological features were summed to obtain the three main scores (the glomerular activity score, the tubulointerstitial activity score, and the chronic lesion score). Values are expressed as means ± SEM of relative units (R.U.). **P<0.01 compared to the CTR group, #P<0.05 and ##P<0.01 compared to the untreated SLE group,one-way ANOVA.

Variables	CTR (n = 10)	SLE (n = 9)	RS (n = 10)	ITF (n = 9)
Glomerulosclerosis (0-3) (%)	0.00±0.00 [0]	0.44±0.15 [33]	0.0±0.0 [0]	0.33±0.25 [22]
Crescents (0-3) (%)	0.00±0.00 [0]	0.33±0.10 [33]	0.00±0.00 [0]	0.22±0.16 [22]
Wire loops (0-3) (%)	0.00±0.00 [0]	0.89±0.16** [78]	0.20±0.14# [20]	0.56±0.19 [56]
Mesangial sclerosis (0-3) (%)	0.00±0.00 [0]	1.22±0.22** [78]	0.20±0.14# [20]	0.78±0.29 [56]
Cells/Glomerulus	21.3±0.6	34.2±2.3**	28.1±1.2#	29.4±1.0
Hyaline casts (0-3) %	0.00±0.00 [10]	0.78±0.13** [78]	0.10±0.11# [10]	0.78±0.29 [56]

Table 5. Quantification of renal lesions.

Values are expressed as means ± SEM of percentage of affected glomeruli (n=50/mouse). The percentage of mice with lesion is expressed in brackets [mice %]. **P<0.01 compared to the CTR group, #P<0.05 and ##P<0.01 compared to the untreated SLE group,one-way ANOVA.

4.2. Fiber treatments induced remodeling of gut microbiota composition

CTR and SLE did not present significant changes at the end of the experiment 1.4.1 for Chao richness (estimating the total operational taxonomic units in each given community), Pielou evenness (showing how individuals in the community are distributed over different operational taxonomic units), and Shannon diversity (that combines richness and evenness) (**Figure 50A**). We performed a two- and three-dimensional PLS-DA of the bacterial community, which measures microorganism diversity among samples, i.e. β-diversity, at the level of the different taxa (phylum, class, order, family, genus and species), in an unsupervised manner. This analysis showed a no significative clustering of the animals into the CTR and SLE groups. However, well separated populations were seen for PLS-DA between the clusters for SLE vs SLE-RS or SLE vs SLE-ITF (**Figure 51**). We did not detect changes in the proportion of bacteria from several phyla (**Figure 50B**), *Firmicutes/Bacteroidetes* was also unchanged (**Figure 50C**). ITF supplementation to SLE mice increased evenness. However, RS diet induced more profound changes in phyla proportion, increasing *Verrucomicrobia* reads. Interestingly, both types of fibers also increased strict anaerobes bacteria content in faeces (**Figure 50D**). At family level, reduced *Clostridiaceae* and increased *Lactobacillaceae* proportions were found in SLE as compared to CTR (**Figure 52**).

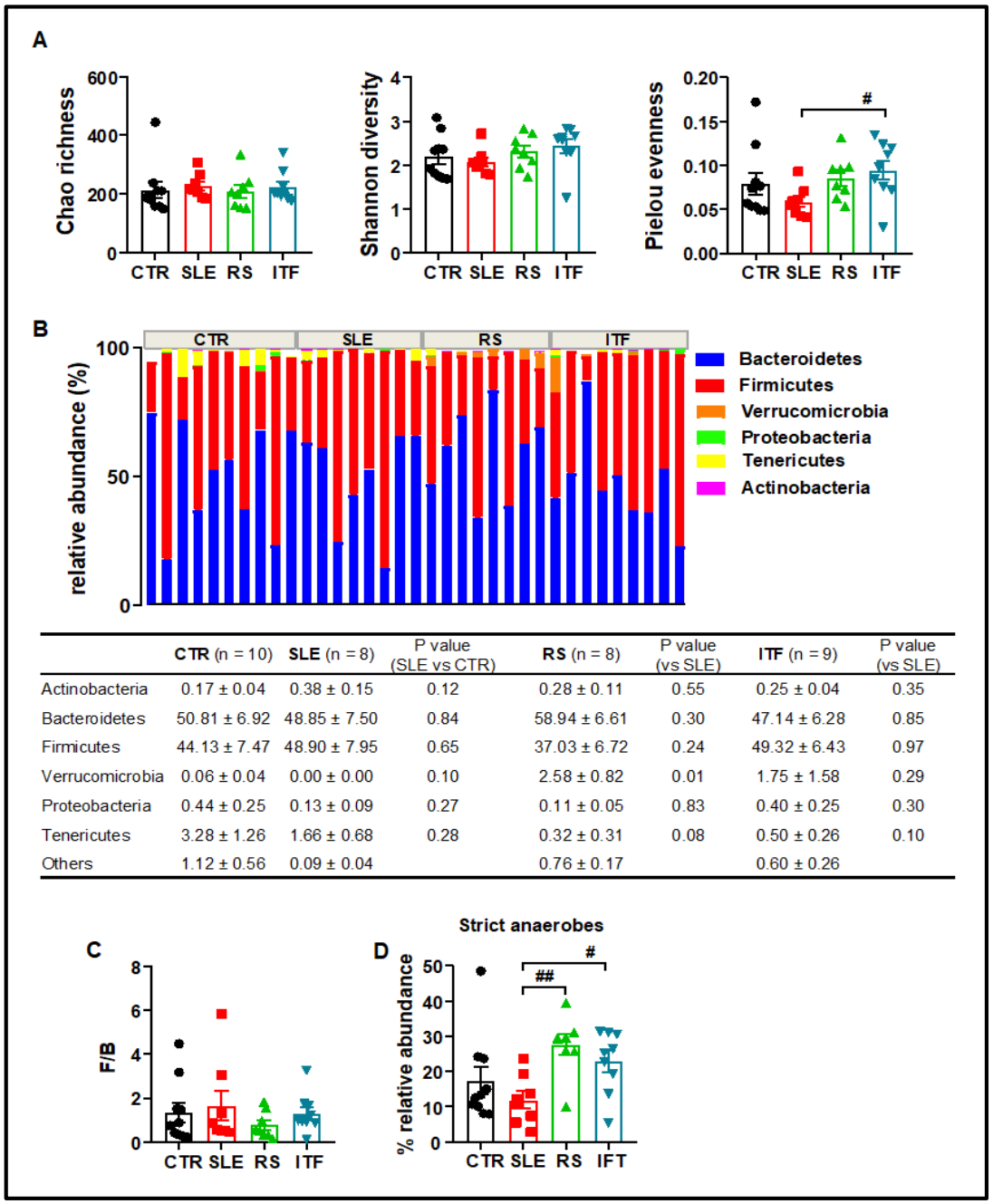

	CTR (n = 10)	**SLE** (n = 8)	P value (SLE vs CTR)	**RS** (n = 8)	P value (vs SLE)	**ITF** (n = 9)	P value (vs SLE)
Actinobacteria	0.17 ± 0.04	0.38 ± 0.15	0.12	0.28 ± 0.11	0.55	0.25 ± 0.04	0.35
Bacteroidetes	50.81 ± 6.92	48.85 ± 7.50	0.84	58.94 ± 6.61	0.30	47.14 ± 6.28	0.85
Firmicutes	44.13 ± 7.47	48.90 ± 7.95	0.65	37.03 ± 6.72	0.24	49.32 ± 6.43	0.97
Verrucomicrobia	0.06 ± 0.04	0.00 ± 0.00	0.10	2.58 ± 0.82	0.01	1.75 ± 1.58	0.29
Proteobacteria	0.44 ± 0.25	0.13 ± 0.09	0.27	0.11 ± 0.05	0.83	0.40 ± 0.25	0.30
Tenericutes	3.28 ± 1.26	1.66 ± 0.68	0.28	0.32 ± 0.31	0.08	0.50 ± 0.26	0.10
Others	1.12 ± 0.56	0.09 ± 0.04		0.76 ± 0.17		0.60 ± 0.26	

Figure 50. Effects of fiber treatments in alpha diversity parameters and phyla composition of gut microbiota in systemic lupus erythematosus (SLE) mice.

(**A**) Ecological parameters (**B**), proportion of bacterial phyla, (**C**) ratio of bacteria belonging to Firmicutes/Bacteroidetes (F/B) phyla, and (**D**) proportion of strict anaerobes bacteria in control (CTR), SLE, and SLE-groups treated with resistant starch (RS) or inulin-type fructans (ITF). Values are expressed as means ± SEM, n = 8-10, #P<0.05 and ##P<0.01 compared to the untreated SLE group, one-way ANOVA.

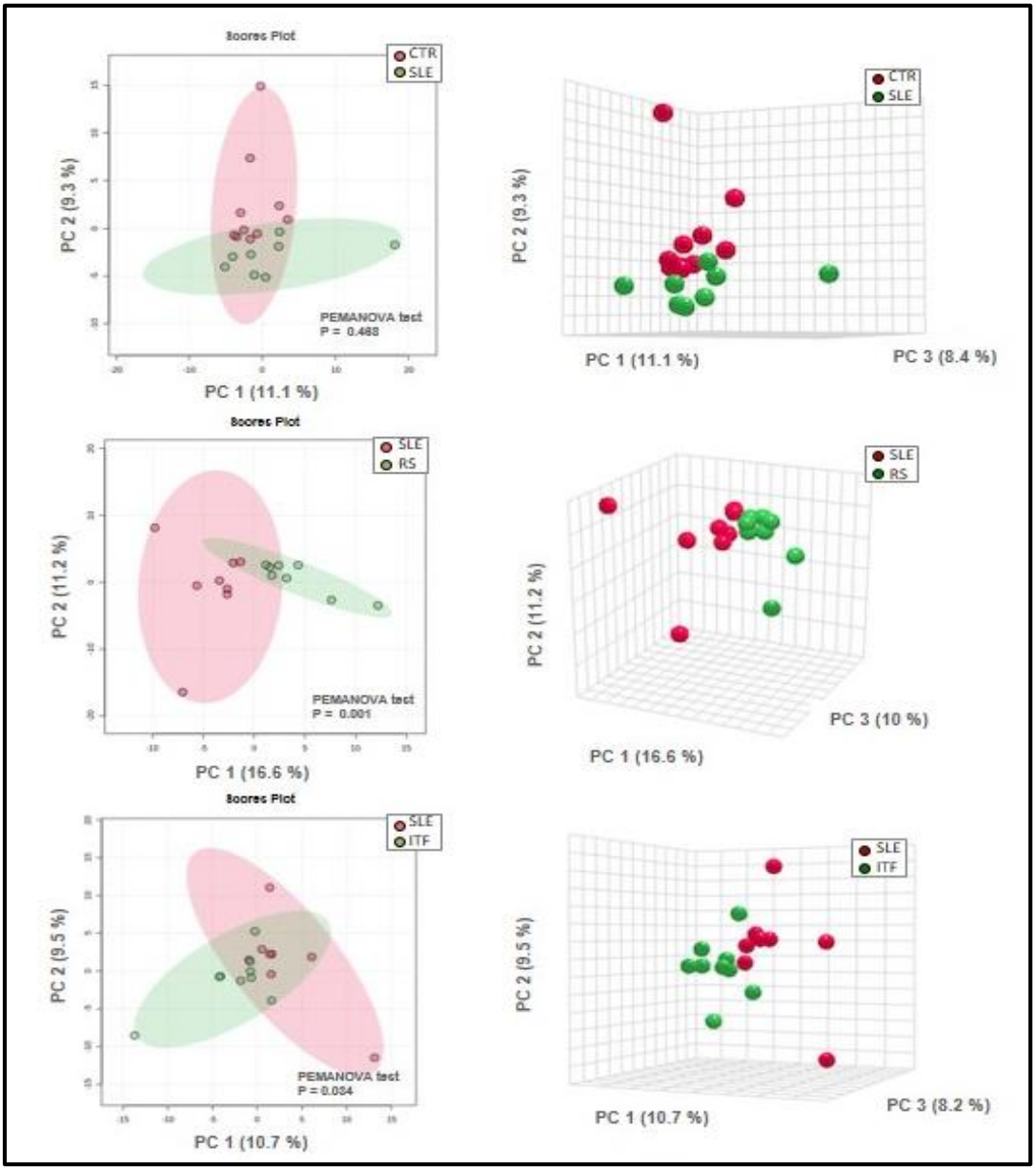

Figure 51. Effects of fiber treatments in beta diversity parameters of gut microbiota in systemic lupus erythematosus (SLE) mice.

Two- and three-dimensional partial least square discriminant analysis (PLS-DA) of the bacterial community, which measures microorganism diversity between samples, at the level of the different taxa (phylum, class, order, family, genus, and species) (n = 8-10 mice per treatment group for each comparison). Groups: control (CTR), SLE, and SLE-groups treated with resistant starch (RS) or inulin-type fructans (ITF).

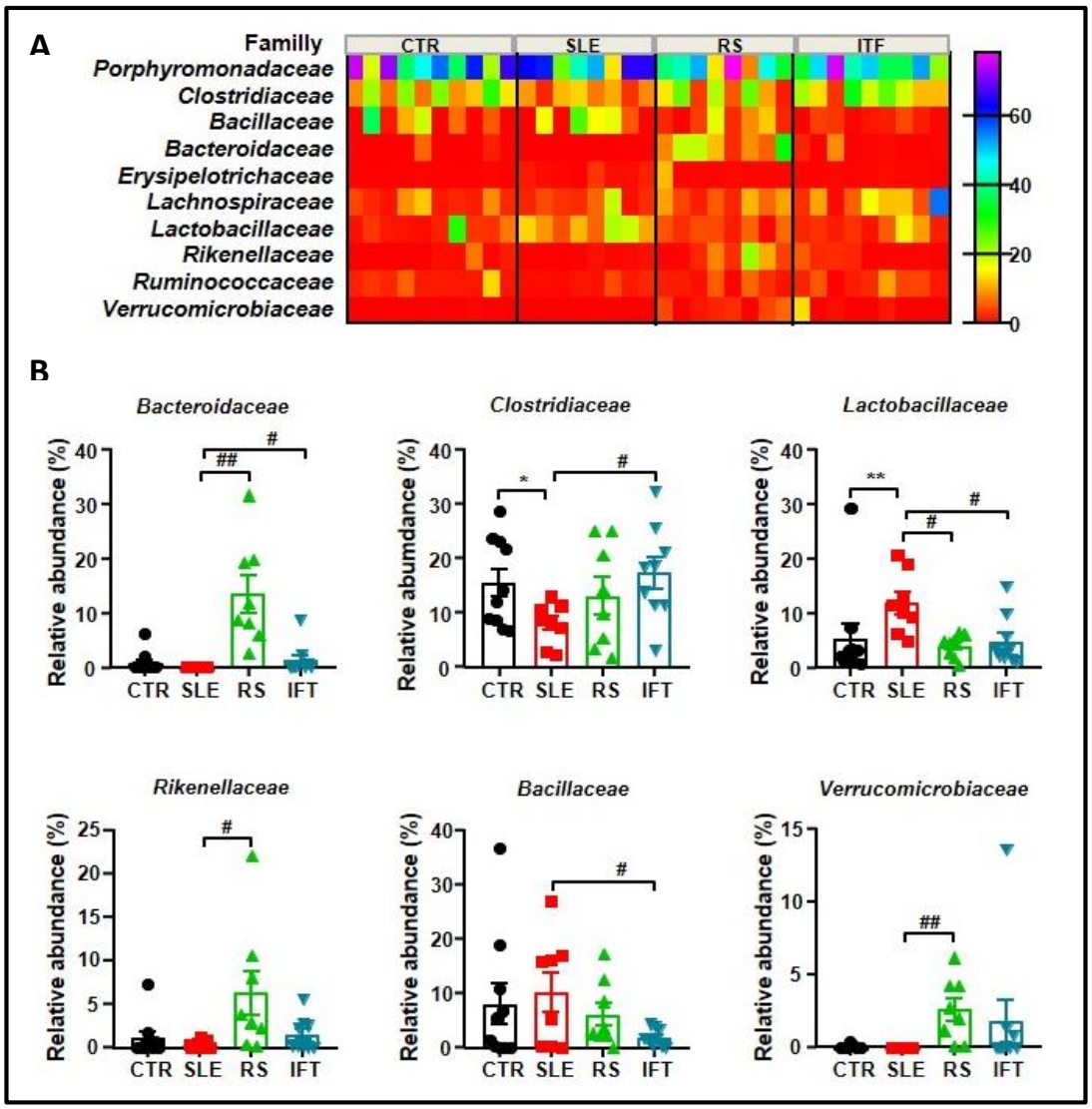

Figure 52. Family changes in the gut microbiota composition induced by fiber treatments in systemic lupus erythematosus (SLE) mice.

(**A**) Heat map of bacterial families. The heatmap colours represent the relative percentage of microbial genera assigned within each sample. (**B**) Relative abundance of bacterial families with a relative abundance > 1% in control (CTR), SLE, and SLE-groups treated with resistant starch (RS) or inulin-type fructans (ITF). Values are expressed as means ± SEM, n = 8-10, *P<0.05 and **P<0.01 compared to the CTR group, #P<0.05 and ##P<0.01 compared to the untreated SLE group, one-way ANOVA.

RS treatment increased *Bacteroidaceae*, *Rikenellaceae*, and *Verrucomicrobiaceae* proportions (**Figure 52**), mainly due to a significative expansion of genera *Bacteroides* (*Bacteroidaceae*), *Parabacteroides* (*Porphyromanadaceae*), *Alistipes* (*Rikenellaceae*), and *Akkermansia* (*Verrucomicrobiaceae*) (**Figure 53**). In addition, RS diet reduced *Lactobacillus* (*Lactobacillaceae*), *Barnesiella* (*Porphyromanadaceae*), and *Roseburia* (*Lachnospiraceae*). By contrast, the changes induced by soluble fiber focus mainly on inducing an expansion of *Clostridiaceae*, especially *Clostridium* genus, and a contraction in *Bacteroidaceae* (*Bacteroides* genus), *Lactobacillaceae* (*Lactobacillus* genus), and *Bacillaceae*, and *Roseburia*. Species, such as *Akkermansia muciniphila* and *Bacteriodes acidifaciens* were increased by RS treatment. Both fiber treatments were unable to change *Lactobacillus reuterii* content (**Figure 54**).

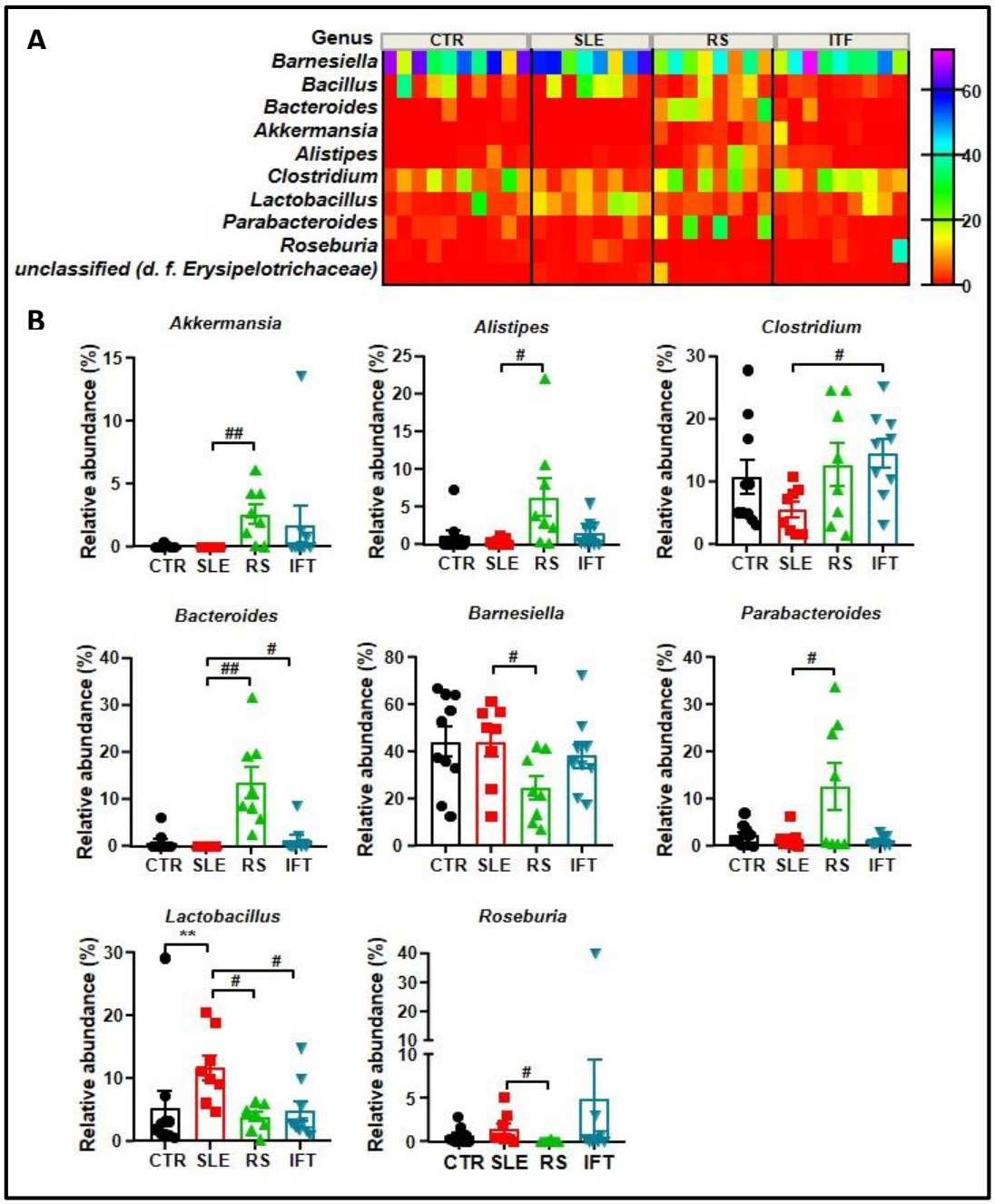

Figure 53. Genera changes in the gut microbiota composition induced by fiber treatments in systemic lupus erythematosus (SLE) mice.

(**A**) Heat map of bacterial genus. The heatmap colours represent the relative percentage of microbial genera assigned within each sample. (**B**) Relative abundance of bacterial genus with a relative abundance > 1% in control (CTR), SLE, and SLE-groups treated with resistant starch (RS) or inulin-type fructans (ITF). Values are expressed as means ± SEM, n = 8-10, **P<0.01 compared to the CTR group, #P<0.05 and ##P<0.01 compared to the untreated SLE group, one-way ANOVA.

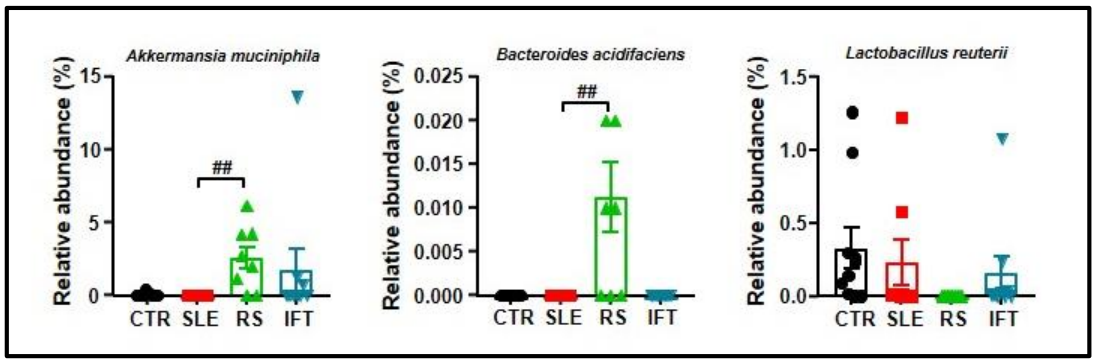

Figure 54. Changes in significant species in the gut microbiota composition induced by fiber treatments in systemic lupus erythematosus (SLE) mice.

Groups: control (CTR), SLE, and SLE-groups treated with resistant starch (RS) or inulin-type fructans (ITF). Values are expressed as means ± SEM, n = 8-10, ##P<0.01 compared to the untreated SLE group, one-way ANOVA.

Considering that fermentation of prebiotic fiber by the gut bacteria leads to the production of SCFA we analyzed the relative abundance of SCFA-producing bacteria. As described previously (de la Visitación et al. 2021), no significant change in SCFA-producing bacteria were found between CTR and SLE. However, ACE-producing bacteria were increased by RS diet whereas ITF increased the proportion of BUT-producing bacteria (**Figure 55A**). When we measured SCFA content in faeces we found reduced ACE and BUT content in SLE-RS group as compared to SLE mice, being unchanged in ITF-treated mice (**Figure 55B**) suggesting increased absorption of SCFA in fiber-treated groups. In general, bacteria-produced SCFA may follow a colonic-hepatic-periphery distribution. Colonic levels were followed by a significant drop, around 10-fold, in the liver, reaching the periphery in the µM range (Cummings et al. 1987). SCFA might be able to enter the cytosol by passive diffusion, but additionally they can be absorbed by solute transporters, such as MCT-1 and MCT-4 (Ritzhaupt et al. 1998), which are upregulated by chronic ACE or BUT consumption (Robles-Vera et al. 2020). MCT-1 is the principal transporter for BUT in intestinal epithelial cells and it is upregulated by BUT and fermentable carbohydrates (Parada Venegas et al. 2019). This justifies our findings by which ITF treatment increased BUT-producing bacteria in SLE mice, also increased the colonic mRNA levels of MCT-1, whereas RS, which increased ACE-producing bacteria, increased the mRNA levels of MCT-4 (**Figure 55C**). Treatment with SCFA induces a higher proliferative activity and turnover in GF or antibiotic-treated SPF mice (Park et al. 2016). In agreement with this, we found that colonic weight/length ratio, an index of epithelial cells proliferation was similar between CTR and SLE group (14.4 ± 0.4 vs.15.5 ± 1.4 mg/cm, respectively,

P>0.05), but was ≈ 60% higher in RS-treated mice as compared to SLE group, showing promotion of intestinal epithelial cells turnover. Additionally, BUT in intestinal epithelial cells consumes (local) O_2, stabilizing the HIF, a transcription factor coordinating barrier protection (Kelly and Colgan 2016). We also found increased colonic HIF-1 mRNA levels in ITF treated SLE mice as compared to SLE group (**Figure 55D**). In addition, increased contents of ACE, BUT and PROP in the RS group and BUT in the ITF group as compared to SLE mice were detected in colon tissue (**Figure 55E**), possibly due to increased uptake. These SCFA are absorbed from the gut into the hepatic portal circulation and/or lacteal lymphatic system to the liver. In the liver tissue, lower BUT and higher PROP levels were found in the RS group than in SLE group (**Figure 56**). BUT and PROP, mostly metabolized by hepatocytes, appear at low concentration in the systemic circulation (González-Bosch et al. 2021). In agreement with this information and despite higher production and absorption of SCFA in fiber-treated mice we found similar plasma levels of ACE and PROP in all experimental groups (**Figure 55F**). Plasma level of BUT were below the detection limit (0.2 µM) using a LC-QqQ-MS determination. Overall, our data demonstrated that fiber treatments induced modifications in gut microbiota composition characterized by increased ACE- or BUT-producing bacteria. These SCFA upregulate colonic MCTs transporters increasing their absorption into intestinal epithelial cells, lending to improved colonic homeostasis and reaching the liver, where they were metabolized resulting in similar plasma levels between groups.

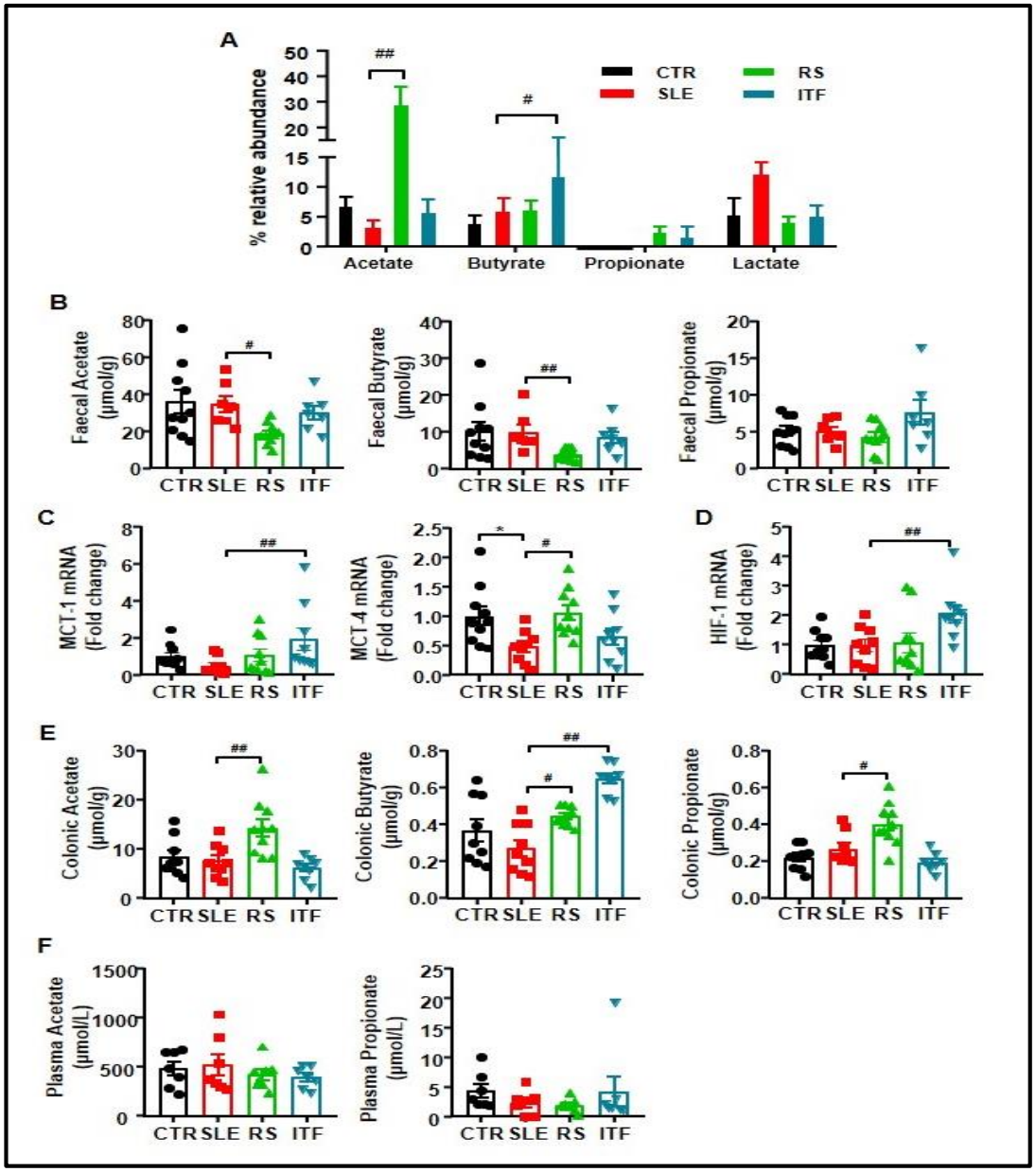

Figure 55. Fiber treatments changed short chain fatty acids (SCFA) bioavailability in systemic lupus erythematosus (SLE) mice.

(**A**) Proportion of SCFA producing- bacteria in faeces from control (CTR), SLE and SLE-groups treated with resistant starch (RS) or inulin-type fructans (ITF) measured by 16S rRNA analysis (n = 8-10). (**B**) Concentrations of SCFA in faeces by HPLC-ESI-MS expressed as µmol/g of lyophilized faeces. (**C**) Colonic mRNA levels of monocarboxylate-transporter (MCT)1 and MCT4, and (**D**) hypoxia inducible factor (HIF)-1. (**E**) Concentrations of SCFA in colonic tissue expressed as µmol/g of lyophilized colon, and (**F**) in plasma from all experimental groups measured by HPLC-ESI-MS and expressed as µmol/L. Values are expressed as means ± SEM, n = 9-10, *P<0.05 compared to the CTR group, #P<0.05 and ##P<0.01 compared to the untreated SLE group, one-way ANOVA.

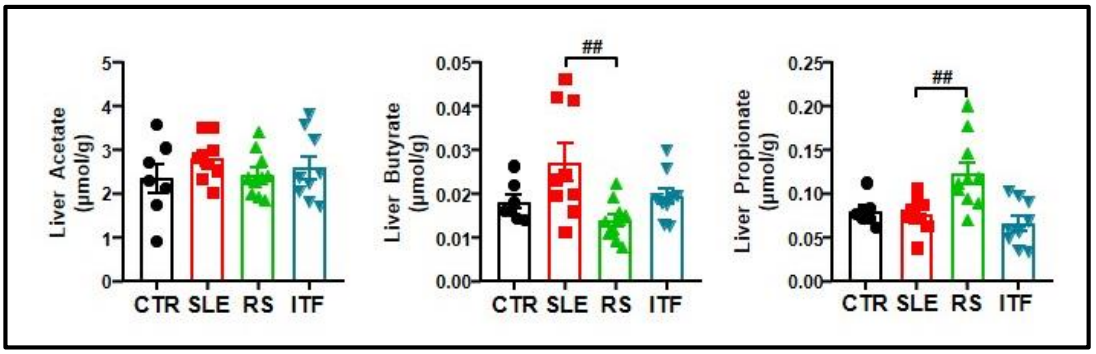

Figure 56. Changes in the liver concentration of SCFAs induced by fiber treatments in systemic lupus erythematosus (SLE) mice measured by HPLC-ESI-MS and expressed as µmol/g of lyophilized liver.

Groups: control (CTR), SLE, and SLE-groups treated with resistant starch (RS) or inulin-type fructans (ITF). Values are expressed as means ± SEM, n = 7-10, ##P<0.01 compared to the untreated SLE group, one-way ANOVA.

4.3. Fiber treatments improved intestinal integrity and inflammation

Given the importance of gut commensal translocation in autoimmunity (Manfredo Vieira et al. 2018), we next assessed the integrity of the intestinal epithelium. We studied the gut barrier integrity through colonic mRNA levels and protein expression of barrier-forming junction transcripts (**Figure 57A**), such as occludin and ZO-1 and the MUC-2 and MUC-3 (**Figure 57B**). Reduced mRNA levels of ZO-1, MUC-2 and MUC-3 were observed in SLE group as compared to CTR and treated groups. However, protein expression of occludin was lower in SLE than in CTR, being without change ZO-1. Consistent with this reduced intestinal integrity in SLE mice we found increased (≈ 5.4-fold) plasma LPS levels (**Figure 57C**). In agreement with previous data (Zegarra-Ruiz et al. 2019), RS diet improved these markers of gut integrity and reduced plasma endotoxin levels. By contrast, ITF only significantly increase colonic occludin expression, but was unable to change endotoxemia. These results suggest that intestinal permeability is high for SLE mice allowing bacterial components (e.g., LPS) into the blood stream. Moreover, both fibers reduced mRNA levels of proinflammatory cytokines IL-1ß and TNF-α (**Figure 57D**). In epithelial and immune cells SCFA behave like ligands for GPRs, such as GPR43, and GPR41, which are upregulated by SCFA. Moreover, SCFA (mainly BUT) have direct inhibitory effects over HDACs activity triggering histone acetylation, modulating gene regulation of cell proliferation, differentiation, and the inflammatory response, contributing to intestinal homeostasis (Parada Venegas et al. 2019). In agreement with this, we found higher GPR43 and GPR41 mRNA level in colonic samples from RS and ITF groups, respectively, as compared to SLE mice (**Figure 57E**). Moreover, colonic HDAC3 transcript was downregulated in the ITF group as compared to SLE mice (**Figure 57E**). Overall, our results are consistent with increased colonic integrity and reduced inflammation induced by fiber treatments, linked to GPR43 activation in RS-treated mice, and GPR41 activation and HDACs inhibition in ITF-treated mice.

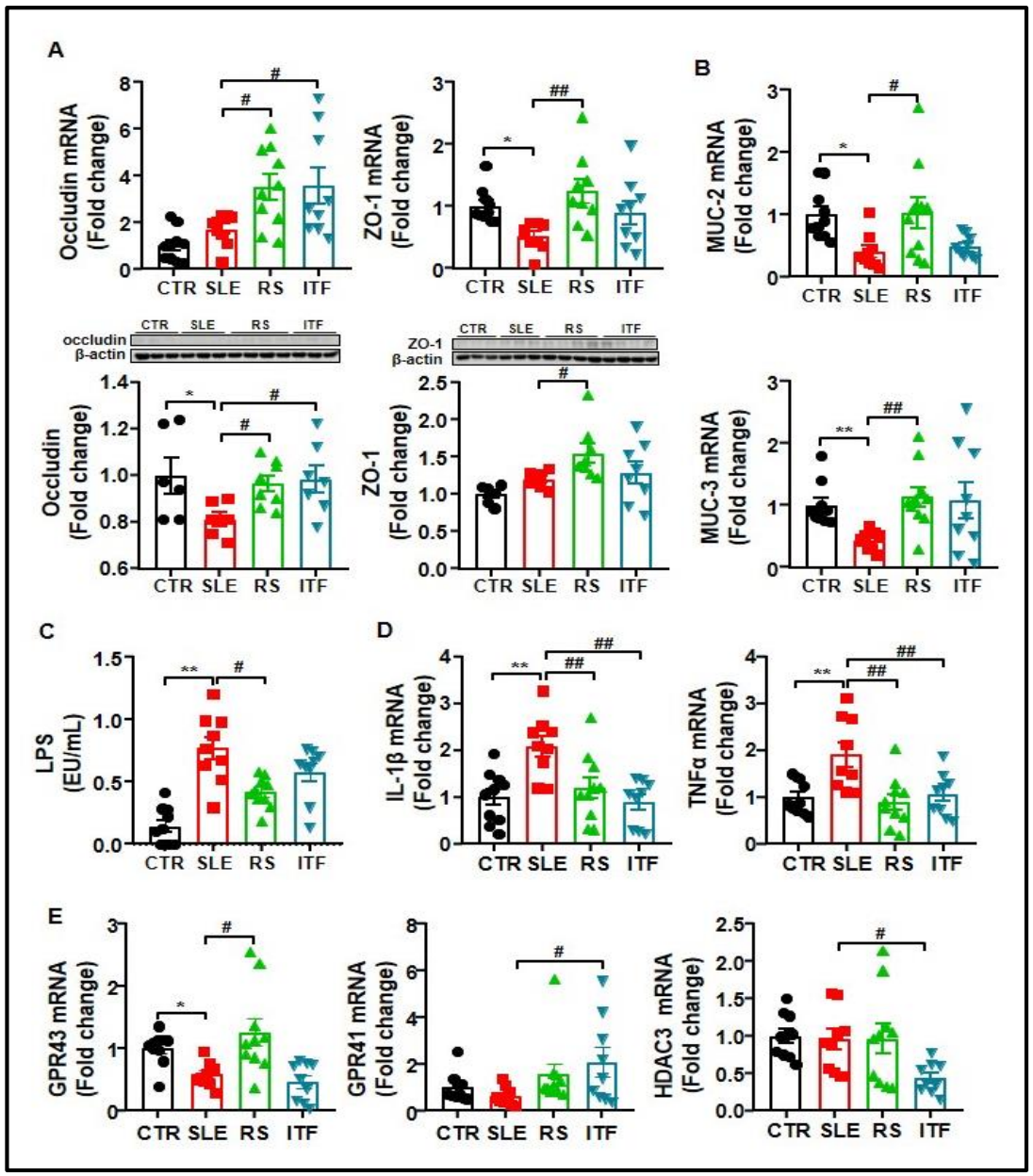

Figure 57. Fiber treatments improved colonic epithelial integrity markers, permeability, and inflammation in systemic lupus erythematosus (SLE) mice.

(**A**) Colonic mRNA levels and protein expression of occludin and zonula occludens-1 (ZO-1), and (**B**) mucins (MUC)-2 and MUC-3. (**C**) Plasma LPS levels measured as endotoxin units (EU). (**D**) Colonic mRNA expression levels of proinflammatory cytokines interleukin (IL)-1ß and tumour necrosis factor (TNF)α. (**E**) Colonic mRNA levels of G-protein coupled receptors (GPR)43, and histone deacetylases (HDAC)3. Groups: control (CTR), SLE, and SLE-groups treated with resistant starch (RS) or inulin-type fructans (ITF). Values are expressed as means ± SEM, n = 9-10, *P<0.05 and **P<0.01 compared to the CTR group, #P<0.05 and ##P<0.01 compared to the untreated SLE group, one-way ANOVA.

4.4. Fiber treatments attenuated T cells imbalance

Increased autoantibody production and lupus-like autoimmune disease progression are associated with a T cell imbalance and high B cells levels (Dar et al. 1988; Talaat et al. 2015). We assessed B and T cell populations from MLN, spleen, and blood. Levels for B cells were increased in the secondary lymphoid organs from SLE compared to CTR. Meanwhile, T cells were unchanged (**Figure 58A, 58B**). Fiber treatments produced no changes on the levels of B and Th cells in either lymphatic organ. In conditions of disrupted gut mucosal integrity, such as those found in SLE, bacteria translocate through the intestinal barrier triggering the activation and migration of CX3CR1+ cells, such as DC or macrophages, towards drain lower intestinal tract lymph nodes (Niess et al. 2005). These cells additionally present antigens to naïve CD4+ T lymphocytes, lending to T cell priming. In correlation with the results of intestinal integrity described above, we found high levels of CX3CR1 mRNA in MLN from SLE group as compared CTR mice, which were reduced by RS treatment, but not by ITF (**Figure 59A**). DC from hypertensive mice $CD80^{high}$ and $CD86^{high}$ (common B7 ligands), which points to DC maturation and activation (Vinh et al. 2010). In our experiment, MLN from SLE mice showed higher CD80 and CD86 mRNA levels as compared to CTR mice, and only RS treatment restored their levels like CTR group (**Figure 59B**). MLN T lymphocytes upregulate integrinα4β7 (Mora and von Andrian 2008). We observed that Itga4, but not Itgb7 expression were higher in MLN from SLE mice than CTR group (**Figure 59C**), pointing to an increased activation of T cells. RS consumption reduced both integrin subunits, showing reduced T cells activation. Beyond their role as antigen presenting cells, DC release mediators promoting T cell polarization. IL-6 induces Th17 cell proliferation and inhibits Treg cell differentiation (Kimura and Kishimoto 2010). We analyzed its transcript levels in MLN and observed that were significantly augmented in SLE group when compared to those found in CTR group and were only normalized by RS treatment (**Figure 59D**). In consequence, the percentage of Th17 cells (CD4+/IL-17a+) increased ≈ 2.8-fold in SLE mice in MLN (**Figure 58A**), being Treg (Treg, CD4+/CD25+) and Th1 (CD4+/IFN-γ+) unchanged. Interestingly, both RS and ITF treatments normalized Th17 content, suggesting that ITF exert immunoregulatory effect independently of IL-6 levels. Consistent with higher ACE production and absorption in RS group, GPR43 level was increased by RS treatment in MLN (**Figure 59E**). It has been described that sodium BUT, acting as HDACs inhibitor, regulates Th17/Treg cell balance to ameliorate via the NRF-2/HO-1/IL-6 receptor pathway (X. Chen et al. 2017). We found that mRNA levels of HDAC3 in MLN were reduced by ITF treatment, whereas RS mice were without effect (**Figure 59F**).

Consistent with NRF-2 activation, the mRNA levels of the down-stream antioxidant enzymes HO-1 and NQO-1 mRNA levels were increased by ITF (**Figure 59G**), lending to reduced expression of IL-6 receptor (**Figure 59G**). When we analyzed Th17 and Treg cell content in colonic lamina propria by immunofluorescence, we found higher Th17 cells in SLE as compared with CTR mice, which was reduced by both RS and ITF treatments, whereas no significant changes in Treg content were observed among all experimental groups (**Figure 60**). In spleen, irrigated by systemic circulation, no significant changes in Treg, Th17, and Th1 were induced by RS or ITF treatment (**Figure 61A**). Circulating B, Treg, Th1, and Th17 cells were increased in SLE compared to CTR (**Figure 61B**). Following the trends observed in MLN, RS and ITF diets decreased the proportion of circulating Th17 cells.

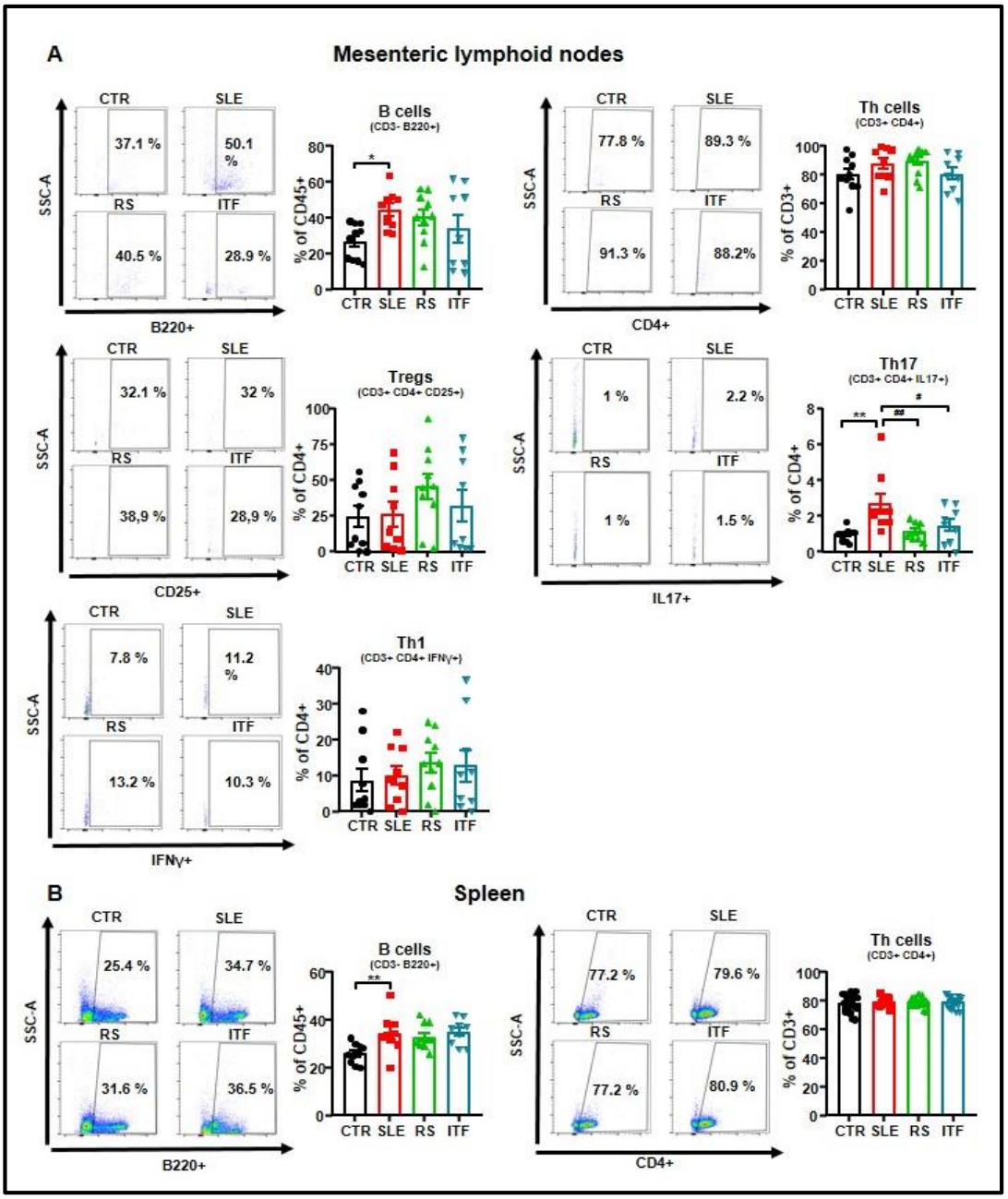

Figure 58. Effects of fiber treatments on lymphocytes populations in systemic lupus erythematosus (SLE) mice.

(**A**) Total B lymphocytes, T helper (Th) cells, Regulatory T cells (Treg), Th17, and Th1 cells measured by flow cytometry in mesenteric lymphoid nodes, and (**B**) B and Th cells in spleen from control (CTR), SLE and SLE-groups treated with resistant starch (RS) or inulin-type fructans (ITF). All data are expressed as % of parent, except for B cells, that are represented as % of grandparent (% of CD45+). Values are expressed as means ± SEM, n = 9-10, *P<0.05 and **P<0.01 compared to the CTR group, #P<0.05 and ##P<0.01 compared to the untreated SLE group, one-way ANOVA.

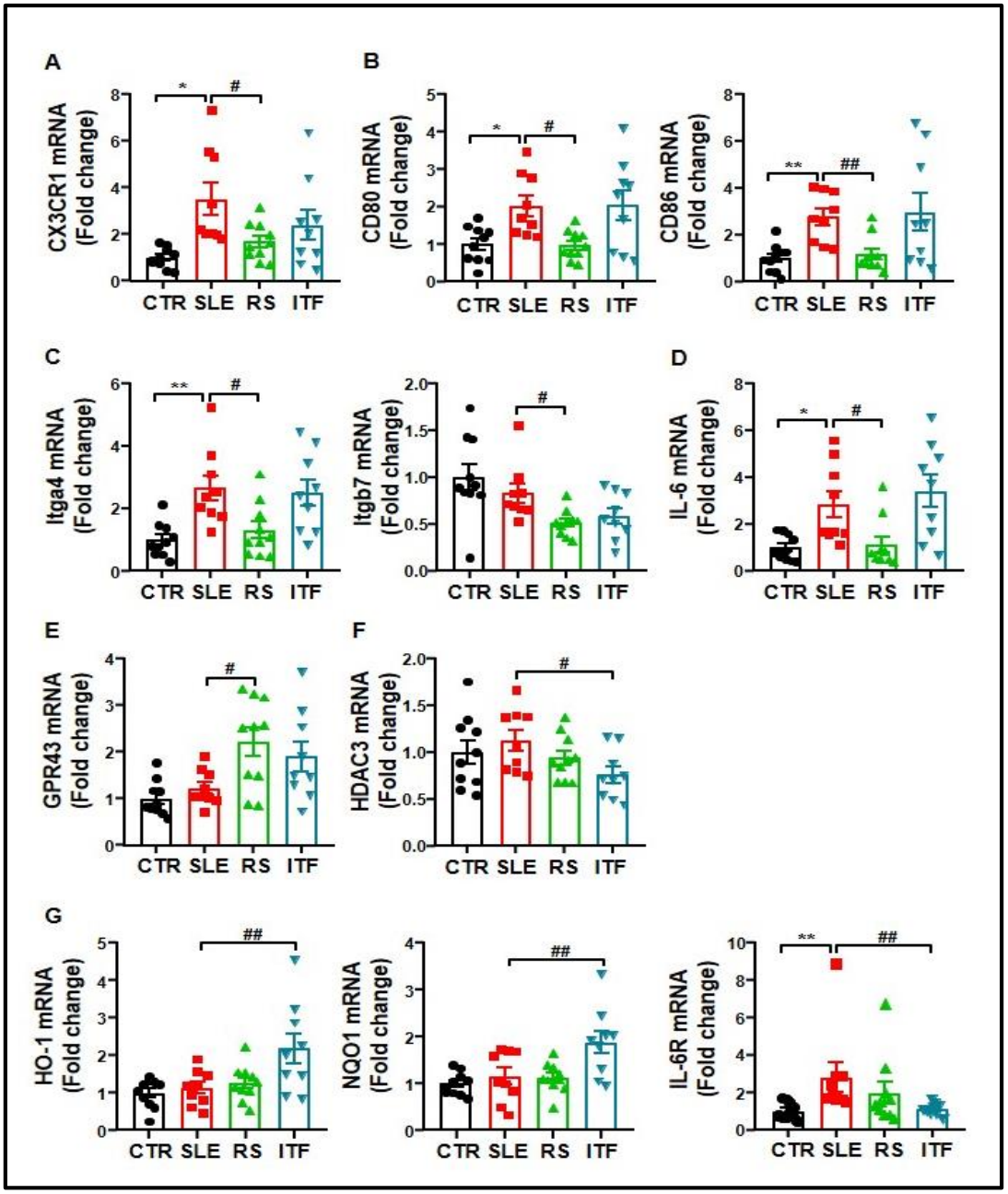

Figure 59. Fiber treatments prevented T cells activation in mesenteric lymph nodes in systemic lupus erythematosus (SLE) mice.

(**A**) mRNA levels of CX3CR1+, (**B**) CD80 and CD86, (**C**) integrinα4β7 (Itga4, Itgb7), (**D**) interleukin (IL)6, (**E**) G protein-coupled receptor (GPR)43 and (**F**) histone deacetylase (HDAC)3. (**G**) mRNA levels of HO-1, NAD(P)H:quinone oxidoreductase 1 (NQO1), and IL-6 receptor (IL-6R). Groups: control (CTR), SLE and SLE-groups treated with resistant starch (RS) or inulin-type fructans (ITF). Values are expressed as means ± SEM, n = 9-10, *P<0.05 and **P<0.01 compared to the CTR group, #P<0.05 and ##P<0.01 compared to the untreated SLE group, one-way ANOVA.

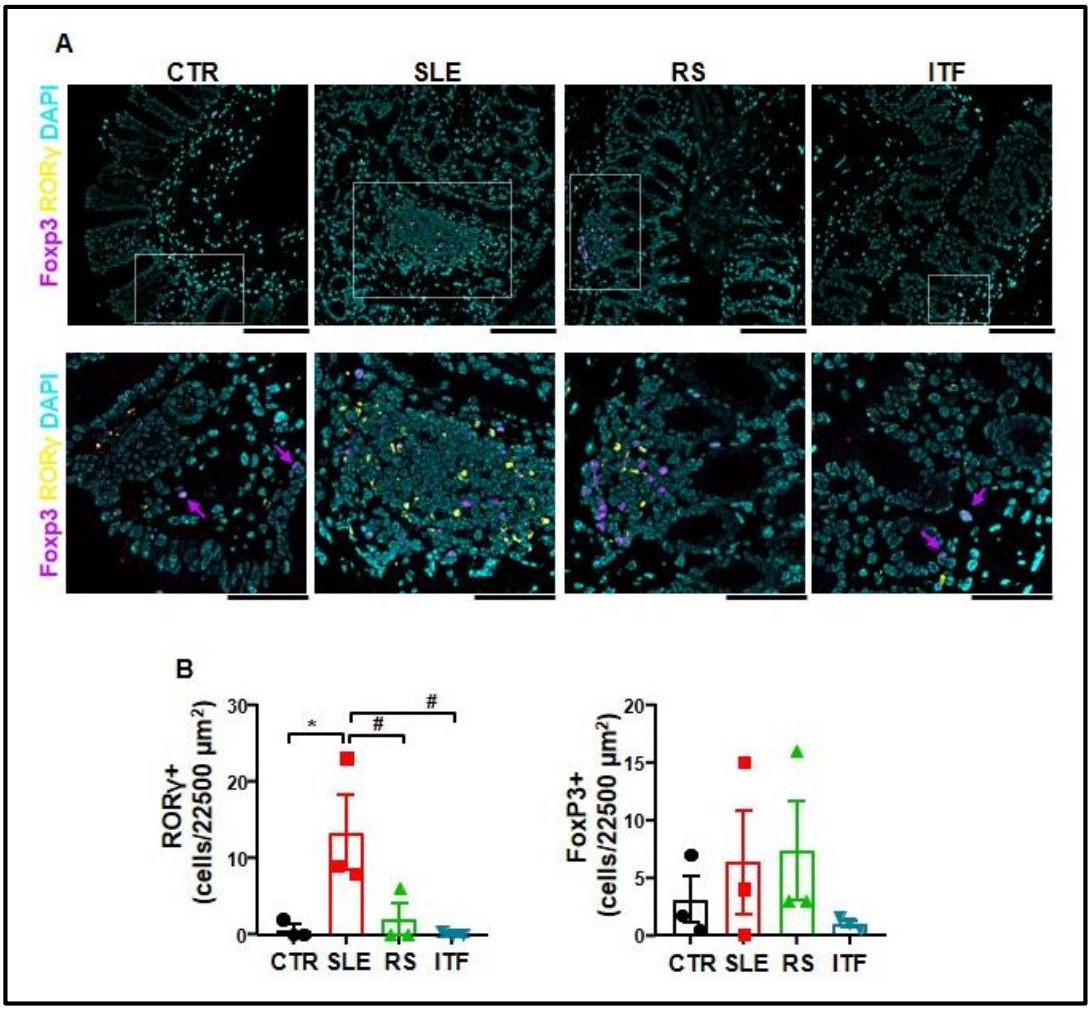

Figure 60. Fiber treatments prevented T cells polarization in lamina propria in systemic lupus erythematosus (SLE) mice.

(**A**) Representative images of RORγ immunofluorescence (yellow), FoxP3 (magenta) and DAPI-stained nuclei (cyan). Scale bar 100 µm (top), and 50 µm (bottom). (**B**) Quantification of RORγ and Foxp3 immunofluorescence in colonic sections from all experimental groups. Groups: control (CTR), SLE and SLE-groups treated with resistant starch (RS) or inulin-type fructans (ITF). Values are expressed as means ± SEM, n = 3, *P<0.05 compared to the CTR group, #P<0.05 compared to the untreated SLE group, one-way ANOVA.

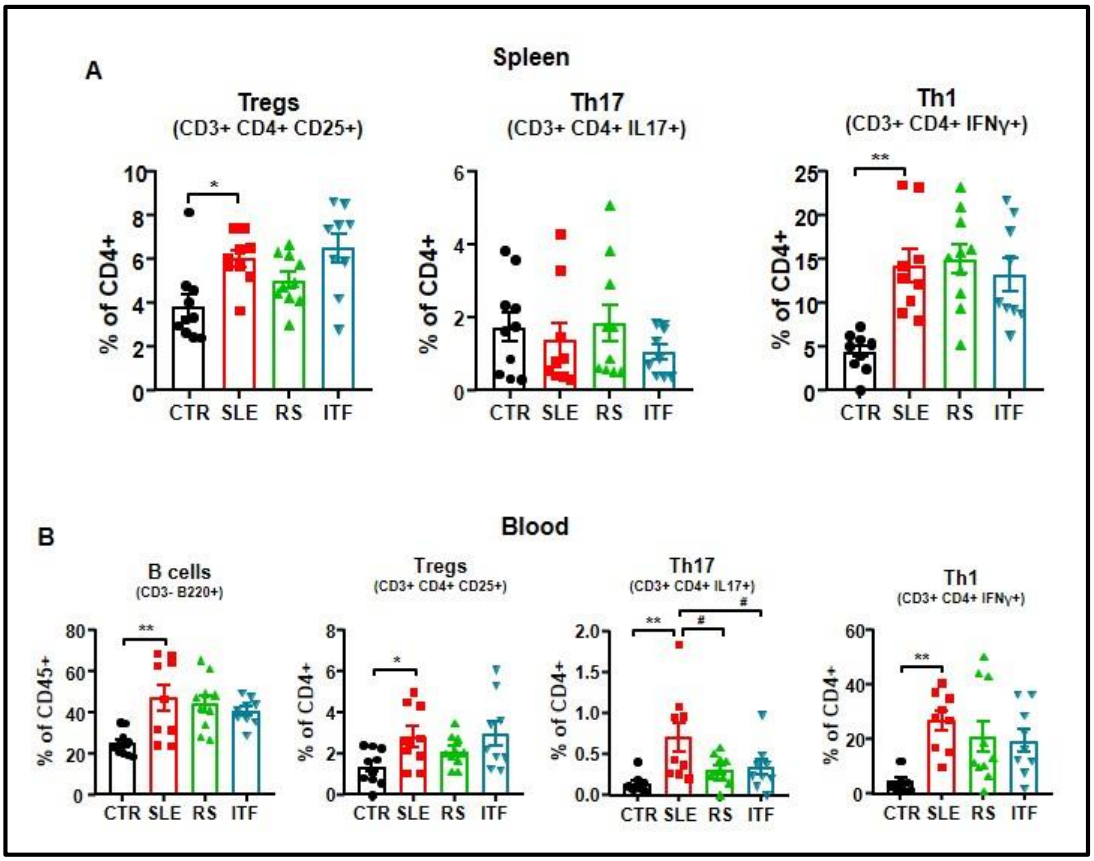

Figure 61. Effects of fiber treatments on lymphocytes populations in systemic lupus erythematosus (SLE) mice.

(**A**) Regulatory T cells (Treg), Th17, and Th1 cells measured by flow cytometry in spleen, and (**B**) B cells, Tregs, Th17, and Th1 cells measured by flow cytometry in blood from control (CTR), SLE and SLE-groups treated with resistant starch (RS) or inulin-type fructans (ITF). All data are expressed as % of parent, except for B cells, that are represented as % of grandparent (% of CD45+). Values are expressed as means ± SEM, n = 9-10, *P<0.05 and **P<0.01 compared to the CTR group, #P<0.05 compared to the untreated SLE group, one-way ANOVA.

4.5. Fiber treatments prevented endothelial dysfunction, vascular oxidative stress and Th17 infiltration in aorta

SLE aortas showed diminished endothelium-dependent vasorelaxant responses to Ach compared to CTR (Emax= 38.3 ± 5.4 % and 56.4 ± 4.4 %, respectively, P<0.01) (**Figure 62A**). RS and ITF fibers improved the impairment of Ach-induced relaxation. This Ach-induced response was also improved in SLE after incubation with the pan-NOX inhibitor VAS2870 or the Rho kinase inhibitor Y27632 (**Figure 62A**), suggesting that the impairment in Ach-induced relaxation is mediated, at least in part, by NOX and Rho kinase activation. ROS-dependent activation of RhoA/Rho kinase has been previously described (MacKay et al. 2017). NOX is the main source of ROS in the vascular wall, we quantitated NOX activity. NOX activity (**Figure 62B**) was ≈ 1.7-fold higher in aortic rings from SLE than CTR group, and both type of fiber inhibited this activity. Considering that inflammatory cells boosted vascular ROS synthesis, we studied T lymphocyte extravasation in aorta. Th17 cells were higher in aorta from SLE as compared to CTR, we did not observe significative changes in Treg and Th1 cells (**Figure 62C**). Both RS and ITF treatments reduced the infiltration of Th17 in aorta. In addition, LPS stimulates and increase the expression of TLR-4 in the vasculature, which resulted in increased NOX activity (Liang et al. 2013). In correlation with plasma LPS levels, mRNA levels of TLR-4 were higher in SLE compared to CTR group, which were significantly reduced by RS treatment (**Figure 62D**). SCFA reduced NOX activity through activation of GPRs or HDACs inhibition (Robles-Vera et al. 2020). However, no significant changes in aortic GPR43 (**Figure 62E**) or HDAC3 (**Figure 62F**) were found among all experimental groups, ruling out that a direct action of SCFA in vascular wall was involved on the vasculo-protective effect induced by both fiber treatments.

To address the question whether changes in gut microbiota induced by fiber intervention in lupus mice play a role in their protective effects on gut, immune system, BP and endothelial function, we inoculated microbiota from all experimental groups to recipient normotensive female C57Bl/6J GF mice, which were maintained for 3 weeks.

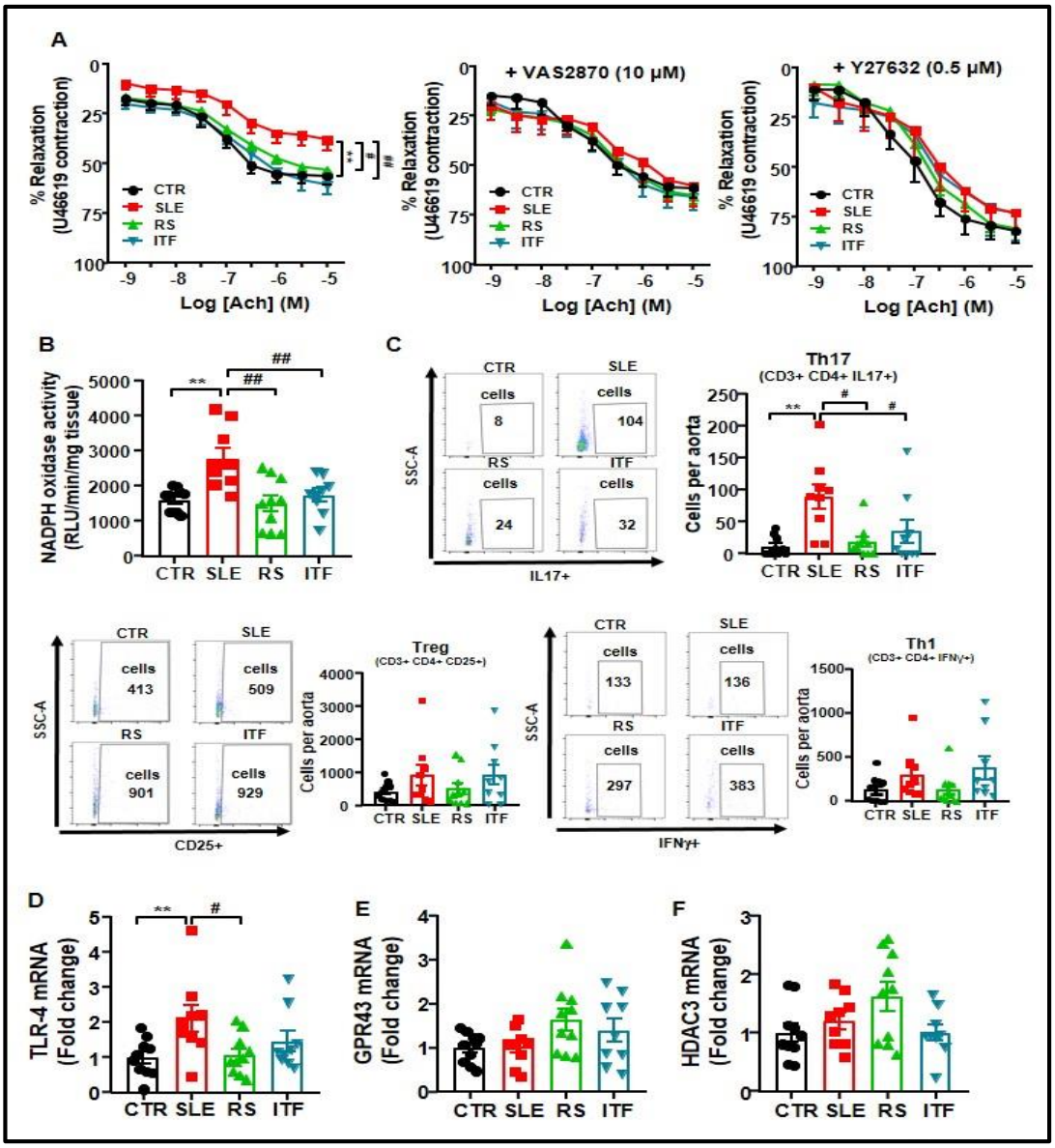

Figure 62. Fiber treatments improved endothelial function, NADPH oxidase activity and aortic infiltration of immune cells in systemic lupus erythematosus (SLE) mice.

(**A**) Vascular relaxation responses induced by acetylcholine (Ach) in endothelium-intact aortas pre-contracted by U46619 (3 nM), in the absence or in the presence of the NADPH oxidase inhibitor VAS2870 (10 µM) or the Rho kinase inhibitor Y27632 (0.5 µM) (n=9-10, data are shown as means ± SEM, *P<0.05 compared to the CTR group, #P<0.05 compared to the untreated SLE group, two-way ANOVA, Dunnett's multiple comparisons test). (**B**) Aortic NOX activity measured by lucigenin-enhanced chemiluminescence. (**C**) Aortic infiltration of immune cells measured by flow cytometry. (**D**) Aortic mRNA levels of toll-like receptor (TLR)4, G protein-coupled receptor (GPR)43, and histone deacetylase (HDAC)3. Groups: control (CTR), SLE and SLE-groups treated with resistant starch (RS) or inulin-type fructans (ITF). Values are expressed as means ± SEM, n = 9-10, **P<0.01 compared to the CTR group, #P<0.05 and ##P<0.01 compared to the untreated SLE group, one-way ANOVA.

4.6. Fiber treatments abolished hypertensive phenotype induced by gut microbiota from female NZBWF1 mice in GF mice

As expected, donor SLE microbiota increased SBP in recipient GF mice to a maximum of ≈ 22 mmHg, as compared to faecal inoculation of donor CTR mice (**Figure 63A**). Interestingly, a significant reduction in SBP was observed in mice inoculated to SLE feces from mice treated with fibers, showing that changes in gut microbiota induced by fiber treatments disrupt the hypertensive phenotype of microbiota from SLE mice. Intra-arterial mean BP (MBP) was recorded to confirm the effects of faecal transfer on BP (**Figure 63B**). However, SLE microbiota transplantation for 3 weeks was unable to evoke higher protein excretion (**Figure 63C**) or to induce significant morphological changes in left ventricle (**Figure 63D**). Interestingly, a low degree of splenomegaly was induced by gut microbiota from SLE mice (increase ≈ 41% in spleen weight/tibia length compared to GF-CTR group), which disappeared in GF-RS and GF-ITF mice (**Figure 63E**). Despite this, no significant changes in plasma levels of anti-dsDNA were observed among all experimental groups (**Figure 63F**), showing no change in lupus activity induced by microbiota from SLE mice.

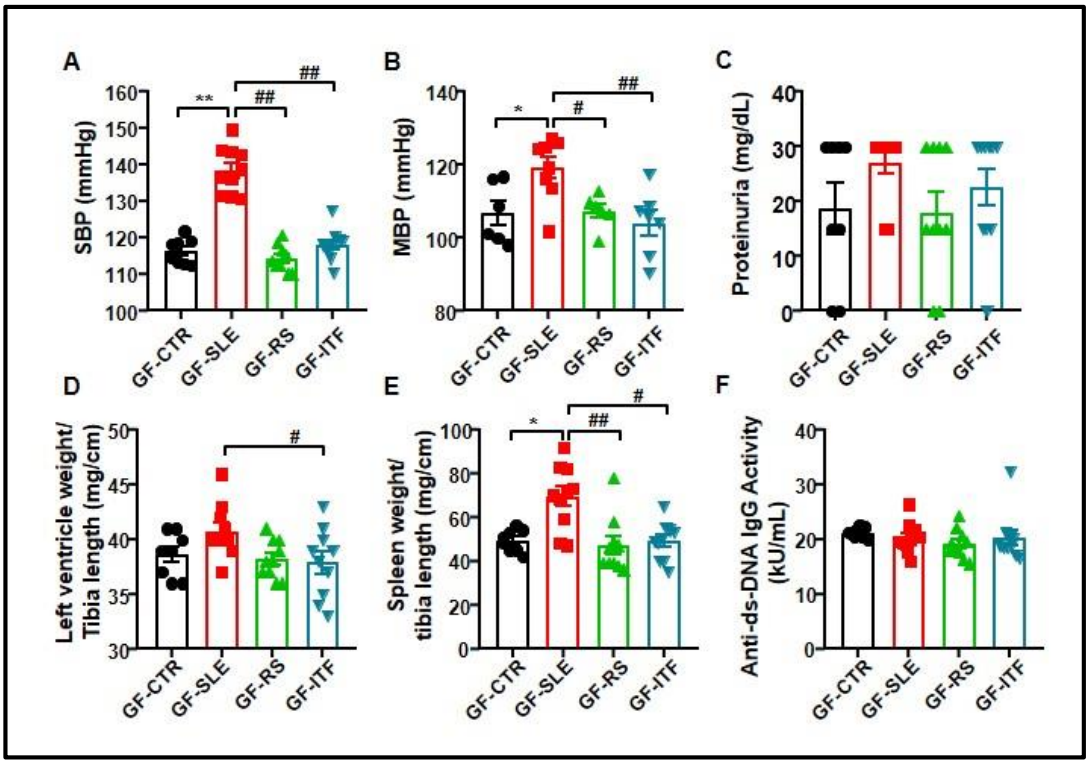

Figure 63. Fiber treatments prevented the transfer of hypertensive phenotype to germ-free mice induced by inoculation of faeces from systemic lupus erythematosus (SLE) mice.

(**A**) Systolic blood pressure (SBP) measured by tail-cuff plethysmography. (**B**) Mean arterial blood pressure (SBP) measured by direct register in carotid artery. (**C**) Urine protein concentration measured by Combur test strips. (**D**) Left ventricular weight/tibia length ratio was measured as morphological parameter in the heart. (**E**) Spleen weight/tibia length ratio, and (**F**) autoantibody levels were measured as markers of the pathology. Groups: germ-free (GF) inoculated with control faeces (GF-CTR), GF inoculated with SLE faeces (GF-SLE) and GF inoculated with faeces from SLE-groups treated with resistant starch (GF-RS) or with inulin-type fructans (GF-ITF). Values are expressed as means ± SEM, n = 8-10, *P<0.05 and **P<0.01 compared to the GF-CTR group, #P<0.05 and ##P<0.01 compared to the GF-SLE group, one-way ANOVA.

4.7. Fiber treatments inhibited the impaired gut integrity and immune imbalance induced by gut microbiota from female NZBWF1 mice in GF mice

Inoculation of SLE microbiota to GF mice reduced colonic mRNA levels of ZO1, without significant changes in occludin (**Figure 64A**), MUC-2 and MUC-3 (**Figure 64B**). Gut microbiota transplantation from SLE-RS group to GF mice increased occludin, ZO-1 and mucins mRNA levels, whereas feces from SLE mice treated with ITF fiber showed similar profile than untreated SLE mice. Plasma LPS levels were increased slightly (≈ 34 %) in GF-SLE group as compared to GF-CTR group (**Figure 64C**). Moreover, microbiota inoculation from RS and ITF to GF mice reduced colonic mRNA levels of TNFα and IL1ß expression (**Figure 64D**). Interestingly, the SCFA receptor GPR43 transcript was increased GF-RS (**Figure 64E**) whereas mRNA levels of HDAC3 were reduced in GF-ITF as compared to GF-SLE (**Figure 64F**), showing a role of SCFA in the colonic effects of the microbiota from fiber-treated SLE mice inoculated into GF, despite GF mice fed standard diet.

In MLN, the higher transcript levels of CD80, Itga7 and IL-6 found in GF inoculated with SLE microbiota, as compared to mice inoculated with feces from CTR group, were normalized in GF-RS group (**Figure 65A**). By contract, no change was observed in GF-ITF mice (**Figure 65A**). This data showed that protective effects of RS fiber on T cell activation in gut secondary lymph nodes was transferred by the microbiota. Moreover, GPR43 and HDAC3 expression were increased in GF-RS and reduced in GF-ITF, respectively (**Figure 65B**), involving SCFA. NRF-2 activation was detected in GF-ITF group, since HO-1 and NQO-1 mRNA levels were higher than GF-SLE group, and IL-6 receptor expression where lower (**Figure 65C**). According to IL-6 or IL-6 receptor levels, the transplantation of microbiota from SLE to recipient GF mice increased the Th17 proportion in MLN as compared to CTR microbiota transfer (**Figure 66A**). Interestingly, reduced proportion of Th17 population was found in MLN and blood from GF-RS and GF-ITF groups, as compared to GF-SLE mice, being unaltered in spleen (**Figure 66A, 66B, 66C**). Other changes in B, and Treg cells induced by SLE microbiota inoculation were unaffected by both fiber interventions (**Figure 66A, 66B, 66C**). Overall, our data demonstrated that fiber treatments restored Th17/Treg balance in SLE mice, at least in part, by changing gut microbiota composition.

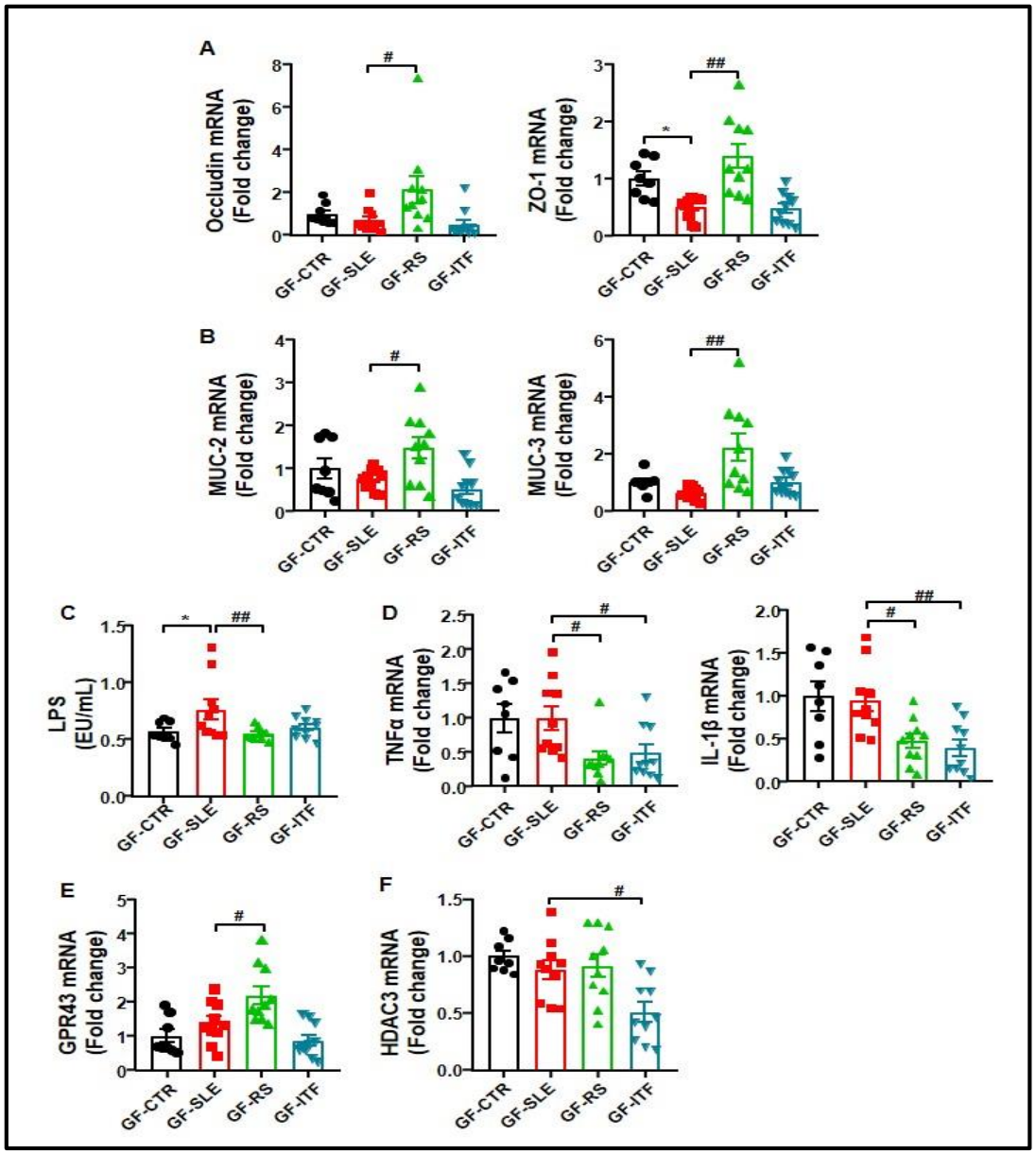

Figure 64. Fiber treatments prevented the transfer of altered gut permeability phenotype to germ-free mice induced by inoculation of faeces from systemic lupus erythematosus (SLE) mice.

(**A**) Colonic mRNA expression levels of occludin and zonula occludens-1 (ZO-1), and (**B**) mucins (MUC)-2 and MUC-3. (**C**) Plasma LPS levels measured as endotoxin units (EU). (**D**) Colonic mRNA expression levels of proinflammatory cytokines interleukin (IL)-1ß and tumour necrosis factor (TNF)α, (**E**) G-protein coupled receptors (GPR)43 and (**F**) histone deacetylases (HDAC)3. Groups: germ-free (GF) inoculated with control faeces (GF-CTR), GF inoculated with SLE faeces (GF-SLE) and GF inoculated with faeces from SLE-groups treated with resistant starch (GF-RS) or with inulin-type fructans (GF-ITF). Values are expressed as means ± SEM, n = 8-10, *P<0.05 compared to the GF-CTR group, #P<0.05 and ##P<0.01 compared to the GS-SLE group, one-way ANOVA.

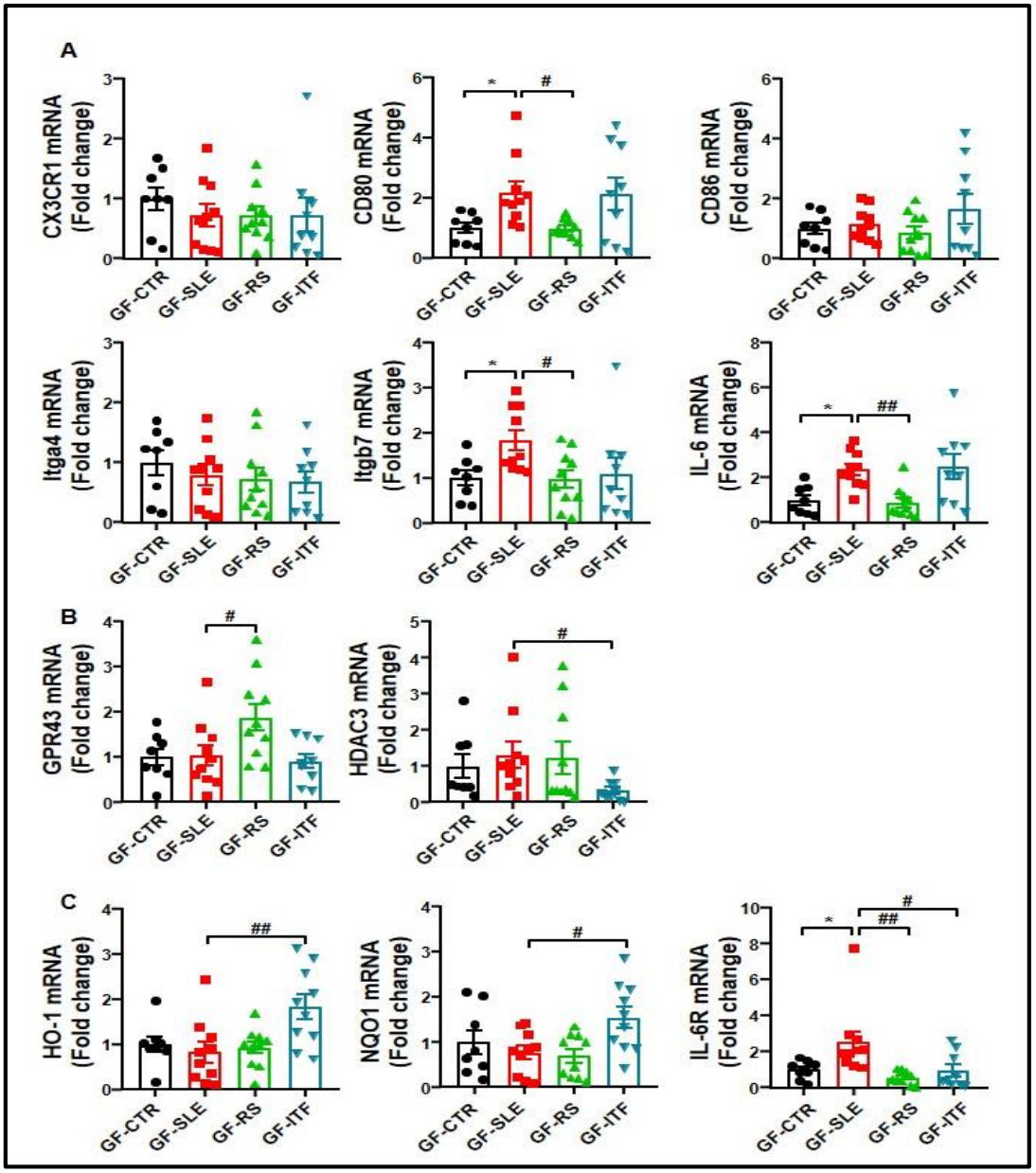

Figure 65. Fiber treatments prevented the transfer T cells activation in mesenteric lymph nodes phenotype to germ-free mice induced by inoculation of faeces from systemic lupus erythematosus (SLE) mice.

(**A**) mRNA levels of CX3CR1+, CD80, CD86, integrinα4β7 (Itga4, Itgb7), and the interleukin (IL)6. (**B**) Expression of G protein-coupled receptor (GPR)43 and histone deacetylase (HDAC)3. (**C**) mRNA levels of HO-1, NAD(P)H:quinone oxidoreductase 1 (NQO1), and IL-6 receptor (IL-6R). Groups: germ-free (GF) inoculated with control faeces (GF-CTR), GF inoculated with SLE faeces (GF-SLE) and GF inoculated with faeces from SLE-groups treated with resistant starch (GF-RS) or with inulin-type fructans (GF-ITF). Values are expressed as means ± SEM, n = 8-10, *P<0.05 compared to the GF-CTR group, #P<0.05 and ##P<0.01 compared to the GS-SLE group, one-way ANOVA.

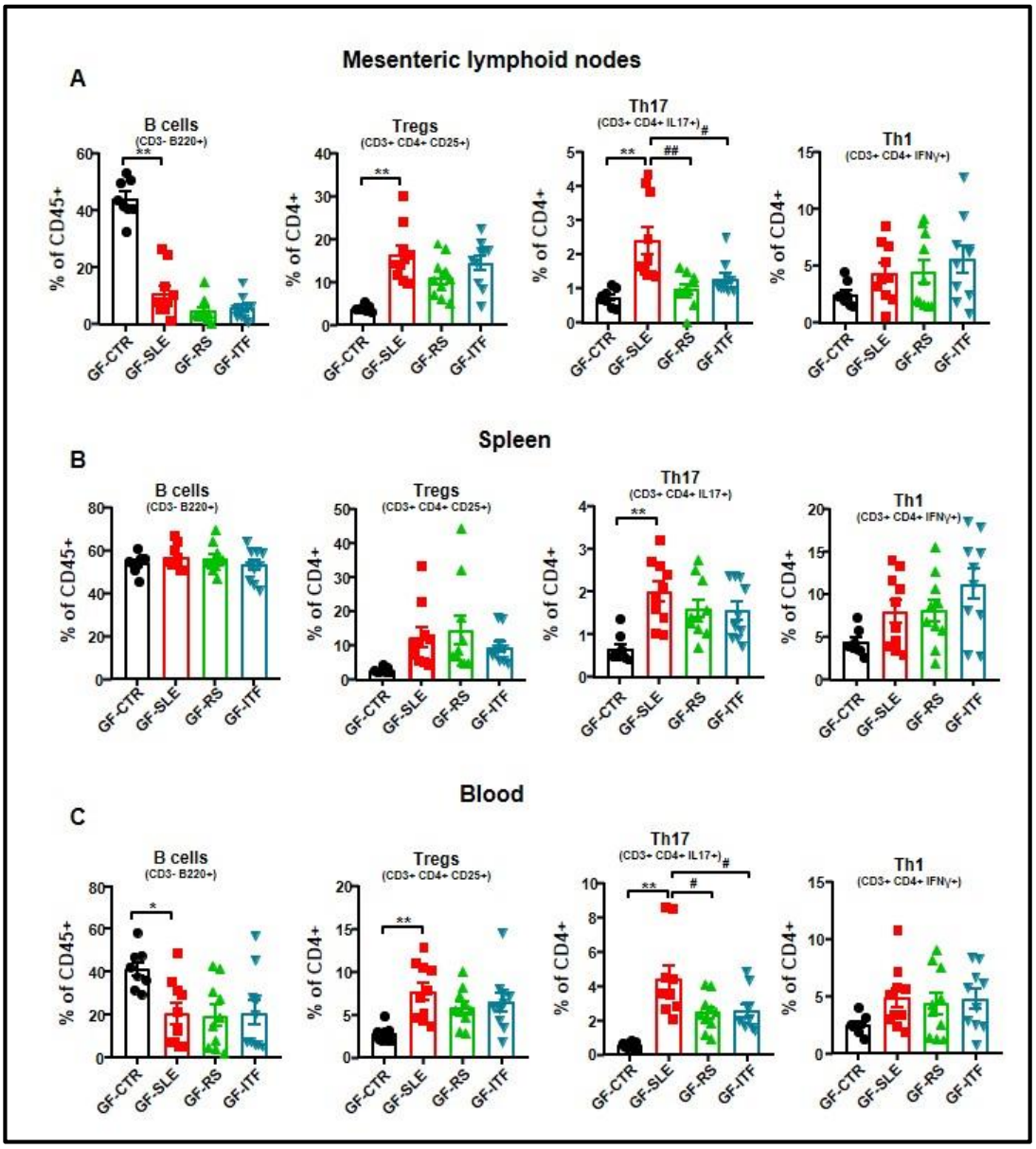

Figure 66. Fiber treatments prevented the transfer of Th17 differentiation phenotype to germ-free mice induced by inoculation of faeces from systemic lupus erythematosus (SLE) mice.

Proportion of different immune cell types (Total B lymphocytes, Regulatory T cells (Tregs), Th17, and Th1 cells measured by flow cytometry in (**A**) mesenteric lymph nodes, (**B**) spleen, and (**C**) blood. All data are expressed as % of parent, except for B cells, that are represented as % of grandparent (% of CD45+). Groups: germ-free (GF) inoculated with control faeces (GF-CTR), GF inoculated with SLE faeces (GF-SLE) and GF inoculated with faeces from SLE-groups treated with resistant starch (GF-RS) or with inulin-type fructans (GF-ITF). Values are expressed as means ± SEM, n = 8-10, *P<0.05 and **P<0.01 compared to the GF-CTR group, #P<0.05 and ##P<0.01 compared to the GS-SLE group, one-way ANOVA.

4.8. Fiber treatments abolished gut microbiota-induced endothelial dysfunction in female NZBWF1 mice in GF mice

Endothelium-dependent relaxant curves to Ach in U46619-precontracted GF-SLE aortas were highly impaired when compared to GF-CTR group (Emax: 52.8 ± 2.9% vs. 66.6 ± 1.1%, P<0.01, respectively) (**Figure 67A**), showing that endothelial dysfunction found in SLE mice was, at least in part, mediated by gut microbiota, and that this vascular phenotype was transferred to mice without SLE background by microbiota inoculation. However, this impaired of Ach relaxation was absent in aorta from GF mice inoculated with feces from SLE mice treated with RS or ITF. Incubation for 30 min with the pan-NOX inhibitor VAS2870 or the Rho kinase inhibitor Y27632 abolished differences between groups in relaxation to Ach, showing the involvement of NOX and Rho kinase in this impaired relaxant response induced by SLE microbiota (**Figure 67A**). In fact, the faecal transplant from SLE caused an increase in aortic NOX activity (**Figure 67B**), as compared to CTR microbiota inoculation. Remarkably, Th17 infiltration in aorta was higher in GF-SLE than GF-CTR group, being without changes in Treg and Th1 (**Figure 67C**). Again, inoculation with feces from SLE mice treated with RS or ITF reduced both aortic NOX activity and Th17 infiltration. Overall, our data showed that fiber treatments improved vascular oxidative stress and endothelial disfunction in SLE mice by inducing changes in gut microbiota which led to reduced vascular Th17 infiltration.

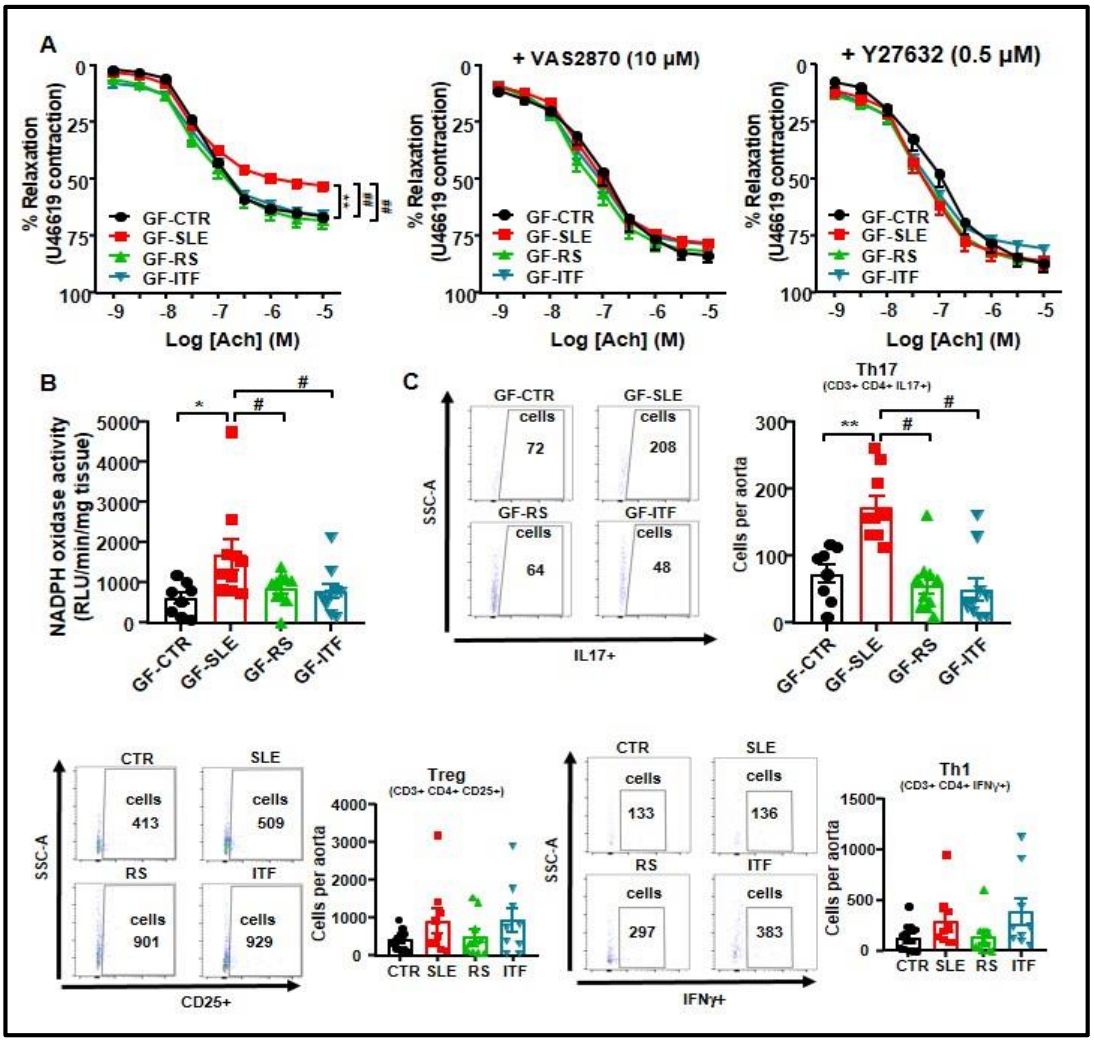

Figure 67. Fiber treatments prevented the transfer of endothelial dysfunction phenotype to germ-free mice induced by inoculation of faeces from systemic lupus erythematosus (SLE) mice.

(**A**) Vascular relaxation responses induced by acetylcholine (Ach) in endothelium-intact aortas pre-contracted by U46619 (3 nM), in the absence or in the presence of the NADPH oxidase inhibitor VAS2870 (10 µM) or the Rho kinase inhibitor Y27632 (0.5 µM) in all experimental groups (n=8-10, data are shown as means ± SEM, **P<0.01 compared to the CTR group, ##P<0.01 compared to the untreated SLE group, two-way ANOVA, Dunnett's multiple comparisons test). (**B**) Aortic NADPH oxidase activity measured by lucigenin-enhanced chemiluminescence. (**C**) Aortic infiltration of immune cells measured by flow cytometry. Groups: germ-free (GF) inoculated with control faeces (GF-CTR), GF inoculated with SLE faeces (GF-SLE) and GF inoculated with faeces from SLE-groups treated with resistant starch (GF-RS) or with inulin-type fructans (GF-ITF). Values are expressed as means ± SEM, n = 8-10, *P<0.05 and **P<0.01 compared to the GF-CTR group, #P<0.05 compared to the GF-SLE group, one-way ANOVA.

DISCUSSION

DISCUSSION

1. Role of gut microbiota in the development of hypertension in a TLR-7-dependent lupus mouse model

With the present experiments, we have demonstrated the relevance of gut microbiota in as a regulating agent for endothelial function and BP in a systemic autoimmunity model induced by TLR-7 activation, which mimicked SLE patients with high IFN signature (> 80% patients). This is especially suggested by the observed changes in endothelial dysfunction, vascular oxidative stress, and SBP induced by shifts in gut microbiota composition after both chronic VANCO treatment and stool transplantation of microbiota from control mice to IMQ-treated mice. The beneficial effects of both interventions were associated with reduced polarization of Th cells to Th17 in MLN, with the subsequent reduced Th17 cells/IL17a in blood and reduced Th17 infiltration in the aorta. It is interesting to note that a profound decrease in colonic biomass in MIX mice, reduced autoimmunity, improved kidney function, as described previously using two different TLR-7-dependent lupus models (Zegarra-Ruiz et al. 2019), but did not prevent endothelial dysfunction and the raise of SBP, showing a clear dissociation between autoimmunity and BP. In addition, MIX treatment was unable to reduce Th17 polarization in secondary lymph organs and Th17 infiltration in aorta, confirming the key role of IL17 in the vascular alterations induced by TLR-7 activation. IL-17a has also been implicated as a pathogenicity factor in a number of chronic inflammatory diseases, including multiple sclerosis, arthritis, and psoriasis. However, our present data are in agreement with that showing that IL-17a are not a direct mediator of autoimmunity (Regen et al. 2021), but it controls microbiota-mediated vascular dysfunction induced by TLR-7-activation.

Profiling colonic microbiomes from TLR-7-dependent lupus mice showed an enrichment of mainly three bacterial taxa: the genera *Bacteroides* and *Macellibacteroides*, and the family *Bacteroidaceae*, whereas *Acetobacteroides* was enriched in CTR group. However, these genera were reduced by MIX treatment, which was unable to reduce BP, suggesting that they do not contribute to increase BP in IMQ-treated mice. Dysbiosis in hypertension is mainly associated with reduced proportions of SCFA-producing bacteria, mainly ACE- and BUT-producing bacteria (Robles-Vera, Toral, and Duarte 2020). However, no significant changes in SCFA-producing bacteria were found between CTR and IMQ group suggesting that

these SCFA are not involved in the development of high BP. Interestingly, VANCO treatment increased ACE- and PROP-producing bacteria associated to BP reduction, whereas MIX treatment was without effect in the proportion of SCFA-producing bacteria. These data suggest that regulating bacterial SCFA production, such as increasing ACE and PROP, could be involved in BP regulation in IMQ-treated mice. In fact, we demonstrated recently that chronic oral ACE consumption could prevent the increase in BP in spontaneously hypertensive rats, reducing Th17 population in MLN, and restoring Th17/Treg balance in aorta (Robles-Vera et al. 2020). Similarly, PROP attenuated vascular dysfunction and hypertension by increasing splenic Treg cells and reducing Th17 cells (Bartolomaeus et al. 2019). Unfortunately, we did not measure plasma levels of SCFA. Taken into account that SCFA have direct vasculoprotective effects in vascular wall (Robles-Vera et al. 2020), we cannot exclude whether lower plasma SCFA levels in the IMQ group are involved in high BP, and if VANCO improved endothelial function and reduced BP by increasing plasma ACE or PROP concentrations.

VANCO, but not MIX, treatment enriched *Akkermansia* and *Parasutterella*. *A. muciniphila*, which was 53.56 % of all species found in gut microbiota from VANCO group, induces intestinal adaptive immune responses during homeostasis. T cell responses to *A. muciniphila* appear to be context dependent (Ansaldo et al. 2019). In fact, *A. muciniphila*, which was increased in patients with multiple sclerosis (Berer et al. 2017), induced proinflammatory responses in human peripheral blood mononuclear cells and in monocolonized mice (Cekanaviciute et al. 2017). However, this microorganism improves the metabolism of obese and diabetic mice (Plovier et al. 2017), and immune system in hyperlipidemic E3L.CETP mice (Katiraei et al. 2020). In our experiment, in the setting of TLR-7-activation, *A. muciniphila* is associated with reduced Th17 cells in MLN and spleen. Among the potential mechanisms, it has been shown that *A. muciniphila* expresses specific proteins on its outer membrane, such as the protein Amuc_1100. This protein binds and activates TLR-2, which potently inhibits TLR-4- and TLR-7/8-induced cytokine production by DC (Wenink et al. 2009). Moreover, enrichment of *Parasutterella* has beneficial effects in immune function (Chen et al. 2018). Most notably, when transplanted to a control mice, microbiota from IMQ mice during 2 weeks induced a significantly increase in SBP and reduced endothelium-dependent relaxation to Ach, without change in autoimmunity and proteinuria as compared to the healthy control microbiota transplantation. Our data implies that the modified microbiota has a crucial part in the onset and progression of hypertension and is one of the triggering elements for SLE hypertension, instead of being a result and accompanying phenomenon in the development of lupus after TLR-7 activation.

In addition, VANCO treatment reduced BP, whereas a more aggressive microbiota depletion using a broad-spectrum antibiotic mixture, which also contained a lower dose of VANCO, was unable to change the development of hypertension in IMQ mice. This is consistent with the finding that the interaction between the gut microbiome and BP is very complex and depends on multiple host factors as well as the environment.

The microbial profiles of the colonized mice showed several differences, including lower *Sutterella*, an organism shown to induce a protective immunoregulatory profile *in vitro* (Berer et al. 2017), and *Anaerovibrio* proportion. These microbial changes were also associated to increased Th17 proportions in MLN, plasma IL-17a levels, and Th17 infiltration in aorta in control mice transplanted with IMQ microbiota. Interestingly, control stool transplantation to IMQ-treated mice enriched *Sutterella* and *Anaerovibrio* in faeces, associated with reduced Th17 polarization and improvement of endothelial function and hypertension, suggesting a role of these bacteria in BP control in this model of autoimmunity.

Several studies have shown that multiple elements partake to the onset of SLE hypertension, including the inflammatory cytokines, and oxidative stress, as well as B-cell hyperactivity and autoantibody production (Taylor and Ryan 2016). These elements, that mediate in local inflammation and the subsequent renal and vascular dysfunction, are likely downstream of the initial immune system dysregulation (de la Visitación et al. 2019). In line with these findings, we detected high plasma concentrations of pro-inflammatory cytokines (IL-17a and IFNα), in IMQ mice, besides vascular oxidative stress, and increased plasma anti-ds-DNA. Remarkably, interventions reducing plasma IL17a levels, such as, VANCO treatment and transplantation of control microbiota, reduced high BP induced by TLR-7 activation. In addition, FMT from IMQ group to control mice increased plasma IL-17a, suggesting the key role of IL17a as a mediator in the pro-hypertensive impact of microbiota in IMQ mice. These data are similar to that described after FMT transplantation from NZBWF1 mice, which composition is quite different to IMQ group, to germ-free or germ-depleted mice (de la Visitación et al. 2021), showing that the polarization of naïve T cells toward Th17 cells induced by several bacteria is a key event to increase BP. The involvement of B-cell hyperactivity and autoantibody synthesis as mediator of vascular changes brought by microbiota was ruled out, since MIX treatment reduced plasma autoantibody but did not prevent BP increase and faecal transplant from IMQ-treated animals to CTR mice raised BP but not anti-ds-DNA antibodies.

Hypertension is often associated with impaired endothelial function, but if this is causative in the progression of hypertension is difficult to prove. Recently, it has been shown impaired endothelium-dependent relaxation responses to Ach in aortas from TLR-7-activated mice (Liu et al. 2018; Robles-Vera et al. 2020). High NOX ROS synthesis can be linked to the loss of endothelial function and the increase in BP in female IMQ-treated animals (Robles-Vera et al. 2020). Consistently, in these experiments we also detected a decreased Ach-dependent relaxation and high NOX activity in aortic rings from IMQ group in comparison with CTR. Curiously, VANCO or transplantation of healthy microbiota prevented both pathological effects, linking the microbiota to oxidative stress and endothelial function. In accordance, faecal transplant from IMQ to CTR had the opposite effect, impairing Ach-induced vasorelaxation and increasing NOX activity. NOX ROS synthesis has a crucial part in endothelial dysfunction caused by microbiota since the selective NOX inhibitor VAS2870 improved the vasorelaxation to Ach induced by stool transplantation of donor IMQ.

Proinflammatory cytokines in plasma, or local production in the vascular tissues, due to infiltrating inflammatory cells, control NOX activity (Kelley and Wuthrich 1999; Ryan 2013). Both VANCO treatment and FMT from control mice decreased Th17 maturation and proliferation in MLN, circulation, and infiltration in aorta. The pro-inflammatory cytokine IL-17a is known to cause a loss of endothelial function due to Rho kinase activation in the vascular wall (Nguyen et al. 2013), at least partially, by raising NOX-generated ROS (Pietrowski et al. 2011). Moreover, the Rho-kinase inhibitor Y27632 improved the response to Ach in CTR-IMQ group, which suggests that the IL-17-Rho kinase pathway is regulated by the microbiota from IMQ mice. Consistently, the faecal transplant from IMQ to CTR raised Th17 cell levels in MLN, and its infiltration in aorta. Furthermore, nIL-17 reverted Ach relaxation in CTR with IMQ microbiota to values similar to those of CTR-CTR. Overall, these data showed that regulation of naïve T cells maturation to Th17 in secondary lymphoid tissues at the gut, with the subsequent Th17 infiltration at vascular tissues, is a crucial component of subjacent causes behind the endothelial dysfunction induced by IMQ microbiota.

These experiments show that: 1) there are differences between gut microbiota from hypertensive IMQ-treated mice and their appropriate controls, 2) this gut microbiota triggers changes in BP regulation, as proved by reduced BP induced by VANCO treatment and stool transplantation from control mice, and 3) this can be linked to the activation of pro-inflammatory Th17 lymphocytes (**Figure 68**). Lupus is a female-biased disease with that affects females nearly 9:1 over males. Our data were obtained from female mice.

Since proof exists supporting differences in gut microbiota composition between the sexes (Beale, Kaye, and Marques 2019), the role of gut microbiota in BP regulation using male mice should be studied. Targeting the IL-17a/IL-17receptor pathway may present an intriguing therapeutic strategy for Th17-induced hypertension in SLE patients. However, several adverse events for drugs blocking the IL-17a pathway, such as bacterial infections, mucocutaneous candidiasis, and neutropaenia have been reported. The present results open new possibilities to the prevention of SLE-associated cardiovascular complications by modulating of the gut microbiota composition, such as with the consumption of probiotics (de la Visitación et al. 2021). Nonetheless, caution should be taken when extrapolating these findings to humans due to the potential differences in the features of the animal and human gut microbiota. Moreover, the translation of the use of strategies of faecal transplantation performed in the present experimental model into the clinic, in example FTM from non-SLE human to SLE patients, needs further research, taken into account the specificity of the observed microbiota changes in this model, which were different than those observed in genetic SLE mouse (de la Visitación et al. 2021), and possibly in human SLE patients. Despite FMT gaining considerable interest as a therapeutic approach in autoimmune diseases, their use in clinical practice may be limited due to practical objections in these chronic conditions. In addition, FMT from control to IMQ-treated mice reduced vascular alterations but did not reduce autoimmunity.

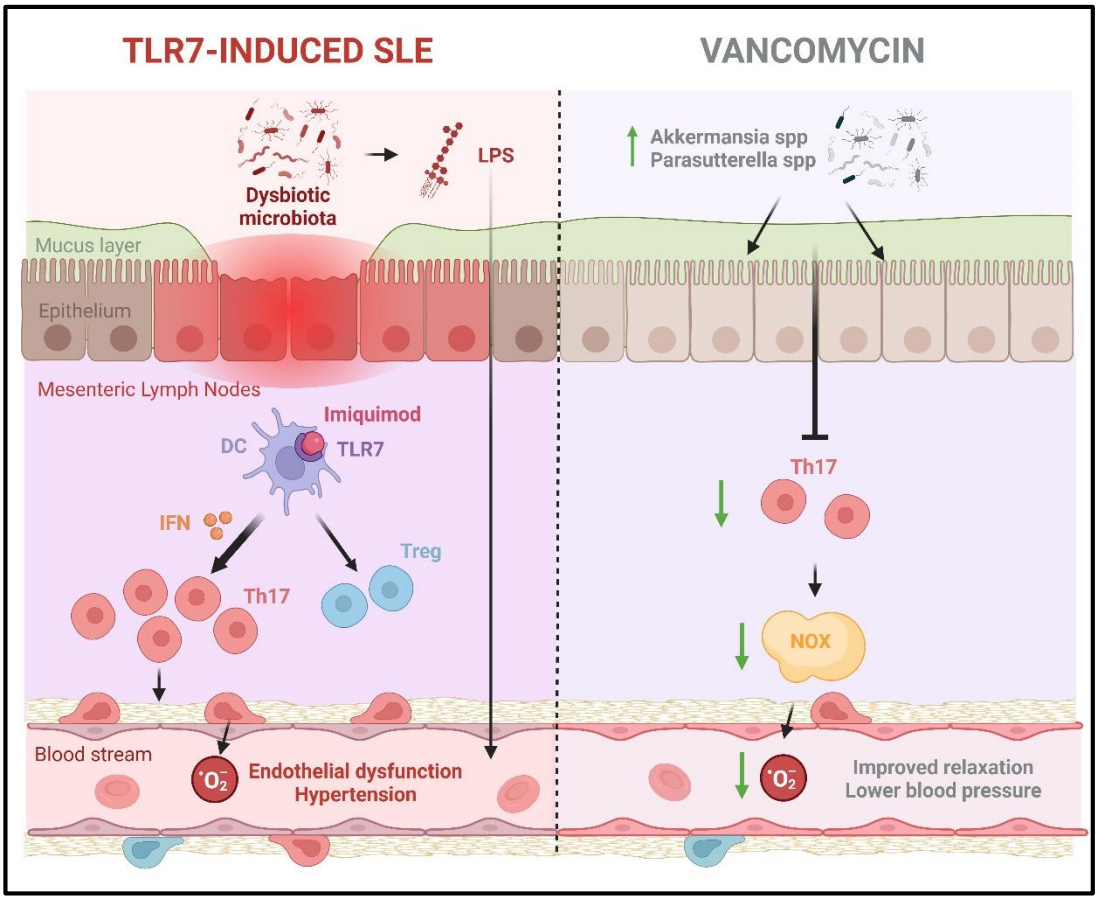

Figure 68. Role of gut microbiota in the development of hypertension in a TLR-7-dependent lupus mouse model.

Abbreviations: DC, dendritic cell; IFN, interferon; LPS, lipopolysaccharide; NOX, NADPH oxidase; TLR, toll-like receptor.

2. Role of TMAO in SLE development and cardiovascular complications in a lupus mouse model induced by TLR-7 activation

It has been previously demonstrated that gut microbiota has a crucial role in vascular complications associated to SLE (de la Visitación et al. 2021; de la Visitación et al. 2021). Microbial metabolites, the gut microorganism-produced repertoire, mainly include SCFA, TMAO, LPS, H_2S, uremic toxins, and bile acids (Robles-Vera, Toral, and Duarte 2020). In the present study we have demonstrated the importance of the gut microbiota metabolite TMAO as a regulating agent for autoimmunity, endothelial function and BP in a TLR-7 activation-induced mouse SLE model. This model simulates more than 80% SLE patients, who have a high IFN signature. This is mainly supported by the reduction in plasma anti-dsDNA levels, the improvement of endothelial-mediated vasorelaxation, and the SBP reduction induced by DMB supplementation to IMQ-treated mice. Growing evidence indicates that living microbial therapy, including FMT (de la Visitación et al. 2021) and probiotics (de la Visitación et al. 2021), might be able to improve the microbial dysbiosis and to reduce SLE cardiovascular complications. However, the translation of these strategies that involve faecal transplantation into the clinic, such as FMT from healthy human to SLE patients, is in need of more research. In spite of FMT gaining interest as a therapeutic alternative for autoimmune diseases, their use in clinical practice might be scarce due to practical objections in these chronic pathologies. Moreover, FMT from CTR to IMQ-treated mice decreased vascular alterations but was not able to affect autoimmunity (de la Visitación et al. 2021). In our experiment DMB was able to reduce disease activity and BP suggesting as a potential therapeutic drug for SLE.

Plasma TMAO levels were higher in SLE patients as compared to healthy human (Yuhua Li et al. 2019). We showed for the first time that plasma TMAO levels increased after TLR-7 activation, and gut bacterial TMA liase inhibition with DMB reduced plasma TMAO levels. Interestingly, this reduction led to lower autoimmunity, since lower plasma anti-dsDNA levels, splenomegaly and hepatomegaly were found in IMQ-DMB group as compared to IMQ mice. The mechanisms involved in the progression of SLE activity induced by TMAO are unknown. Humoral immune system components play a crucial role in lupus onset as shown by evidence suggesting that B cell populations, which are differentiated into antibody-producing plasma cells, are higher in SLE (Dar et al. 1988).

Accordingly, we found a higher number of B cells in spleen and blood in IMQ mice than in the CTR group, which was normalized with DMB treatment. It is possible that TMAO sensitizes B cells to the binding of antigens and the activation of intracellular transduction pathways, such as protein kinase C, which lead to the differentiation of B lymphocytes (Ye et al. 2019). In fact, TMAO elevated protein kinase C activity in a dose-dependent manner in endothelial cells (Ma et al. 2017). Furthermore, in spite of the high proportion of Treg in lupus mice, these cells cannot control the cumulative impact of multiple genetic triggers of lymphocyte activation and autoreactivity (Zhang et al. 2015). However, DMB was unable to reduce circulating Treg cell counts ruling out a possible role of Treg to lessen autoantibody levels. The administration of a mouse anti-CD20 antibody to deplete B cells ostensibly mitigates autoantibody production and prevents the development of high BP in female NZBWF1 mice (Mathis et al. 2014). Thus, decreased anti-dsDNA antibody concentration by B cell depletion and lower activation levels, may be linked to the antihypertensive effects of DMB supplementation. Additionally, an imbalance between anti-inflammatory Treg and pro-inflammatory Th17 cells is generally seen as a relevant element in both human SLE and murine lupus (Alunno et al. 2012). We found increased Th17 population in secondary lymph organs from IMQ mice and lower Th17 count induced by TMAO reduction with DMB supplementation, which might be involved in lower autoimmunity induced by DMB. Our results in SLE disease are in agreement to that previously reported indicating that TMAO control macrophage M1 polarization by NLRP3 inflammasome activation, which provide the cytokines microenvironment in which naive CD4+ T cells subsequently differentiated into Th1 and Th17 subsets (Wu et al. 2020). However, if this polarization towards Th1 and Th17 is mediated by the polarized M1 macrophage requiring NLRP3 inflammasome activation in our experimental conditions is unknown.

Hypertension can be linked to impaired endothelial function. In recent years, impaired endothelium-dependent relaxation responses to Ach in aortas from TLR-7-activated mice have been demonstrated repeatedly (de la Visitación et al. 2021; Liu et al. 2018; Robles-Vera et al. 2020). High vascular ROS levels might be associated with the damage to the endothelial function and the raise in BP in female IMQ-treated animals (Robles-Vera et al. 2020). In accordance to this, in our experiments we also detected a poor Ach-dependent relaxation and high ROS content linked to increased NOX activity and reduced NRF-2-antioxidant defense in IMQ aortic segments when compared to CTR. Interestingly, DMB suppressed NOX over-activity and normalized NRF-2 pathway improving endothelial dysfunction. High TMAO concentration induced loss of Ach-induced relaxation.

Moreover, treatment with DMB for 8 to 10 weeks to suppress TMA selectively ameliorated endothelium-dependent dilation in old mice to young levels by normalizing vascular superoxide anion production, improving NO-mediated dilation, and impeding superoxide-related blocking of endothelium-dependent dilation (Brunt et al. 2020). Moreover, high TMAO concentrations can induce oxidative stress in cultured endothelial cells via activation of the NLRP3 inflammasome. However, no significant changes in NLRP3 pathway was induced by DMB, suggesting that plasma TMAO levels found in IMQ mice were not sufficient to induce NLRP3 inflammasome at the vascular tissue.

Th17 polarization in secondary lymph organs and Th17 infiltration in aorta plays a crucial part in the vascular alterations caused via TLR-7 activation. In fact, FMT from IMQ mice to control mice caused an increase in plasma IL-17a, which led to endothelial function impairment, since IL-17a neutralization restored endothelium-dependent relaxation (de la Visitación et al. 2021). We found both reduced Th17 polarization in lymph nodes and vascular infiltration after DMB supplementation linked to improvement of endothelial dysfunction. The pro-inflammatory cytokine IL-17a has been shown to be detrimental to the endothelial function, activating the Rho kinase in the vascular wall (Nguyen et al. 2013), at least partially, increasing NOX-generated ROS (Pietrowski et al. 2011) and reducing NRF-2 pathway (Guan et al. 2018). In addition to this, the Rho-kinase inhibitor Y27632 restored the response to Ach in IMQ mice similar to CTR. Targeting the IL-17a/IL-17receptor pathway could be an innovative and effective therapeutic approach for Th17-induced hypertension in SLE patients. However, a few critical but severe adverse events for IL-17a-blocking strategies, such as bacterial infections, mucocutaneous candidiasis, and neutropenia are known to appear. In our experiment DMB, acting in gut microbiota, reduce this pathway and suggest new pathways to the prevention of SLE-associated cardiovascular complications. However, caution is imperative to extrapolate these findings to humans because of all the potential dissimilitude in the features of the animal and human gut microbiota.

These experiments show that the gut microbiome metabolic product TMAO increases TLR-7 induced autoimmunity and vascular dysfunction. This can be linked to increased B cells differentiation and activation of pro-inflammatory Th17 lymphocytes. Our study provides the missing link between bacterial metabolite derived of choline and lupus severity, revealing the potential to alleviate cardiovascular complications by blockage of the TMAO pathway (**Figure 69**).

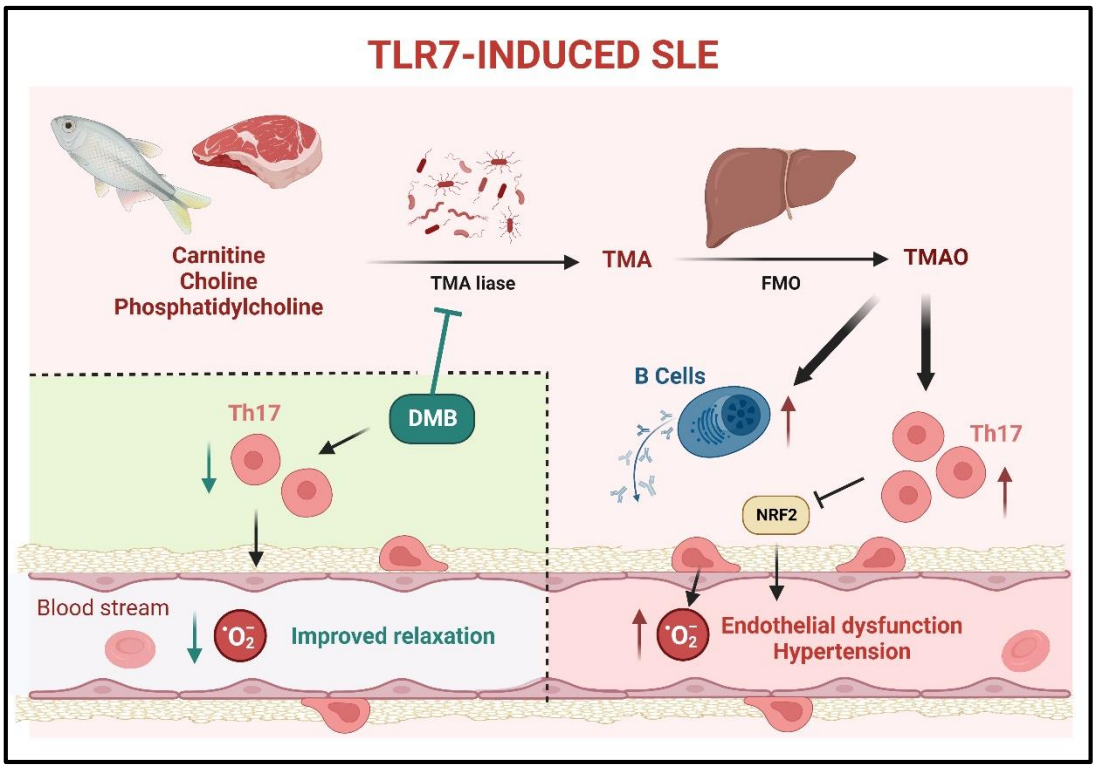

Figure 69. Role of TMAO in SLE development and cardiovascular complications in a lupus mouse model induced by TLR-7 activation.

Abbreviations: DMB, 3,3-dimethyl-1-butanol; FMO, flavin monooxygenase; NRF-2, Nuclear factor erythroid 2-related factor 2; TMA, trimethylamine; TMAO, trimethylamine N-oxide.

3. Effects of SCFA on cardiovascular complications in TLR-7-induced lupus mice

In this study, we have demonstrated the significance of SCFA derived from gut microbiota in preventing cardiovascular complications associated with lupus induced by TLR-7 activation. Specifically, we have identified GPR43-dependent immune modulation in gut secondary lymph nodes induced by ACE, which is linked to the improvement of endothelial dysfunction and reduction of BP. On the other hand, the preventive effect of BUT in vascular dysfunction seems to be related to the rebalancing of Th17/Treg polarization through GPR41 activation and/or HDACs inhibition. However, neither BUT nor ACE were able to prevent the development of systemic autoimmunity. Furthermore, we have found that the chronic consumption of insoluble (RS) or soluble (ITF) fibers, acting as dietary sources of SCFA, exerted similar cardiovascular protective effects as ACE or BUT supplementation alone. Moreover, we have demonstrated through faecal inoculation of dysbiotic microbiota from donor IMQ mice to recipient GF mice that gut microbiota plays a key role in the generation of endothelial dysfunction and high BP, mediated by the increase in Th17 cells in MLN, blood, and vascular wall. SCFA treatment effectively abolished the transfer of this hypertensive phenotype.

Gut leakiness was found to be TLR-7 dependent, as demonstrated in studies with TLR-7 knockout mice (Zegarra-Ruiz et al. 2019) and in autoimmune conditions induced by TLR-7 activation (González-Correa et al. 2021; de la Visitación et al. 2021). However, the physiological function of TLR-7 in the gut, particularly on the gut epithelium, remains poorly understood. In our current study, we have observed that gut leakiness is involved in Th17 differentiation in MLN, as it facilitates the accumulation of antigen-presenting cells, activates T CD4+ naïve cells, and increases IL-6 production. This supports the notion that gut integrity plays a critical role in gut immune modulation. We have demonstrated that ACE, which reduces colonic leakiness, also inhibits the accumulation of CX3CR1+ cells in MLN and reduces IL-6-driven Th17 polarization. Moreover, we found that the reduction in Th17 proportion in MLN induced by ACE was abolished by the blockade of GPR43, highlighting the key role of GPR43 activation in the immune modulatory effects of ACE. In contrast, BUT was unable to improve gut leakiness or reduce CX3CR1+ cells and IL-6 levels in MLN. However, BUT was effective in reducing IL-6 receptor expression, thereby preventing Th17 polarization. This effect seems to be mediated by the reduction in HDAC3 mRNA levels, leading to the activation of the NRF-2/HO-1 pathway in MLN, as described previously (Chen et al. 2017).

Endothelial dysfunction plays a key role in the development of hypertension, where decreased NO bioavailability connects oxidative stress to endothelial dysfunction and elevated BP. Both innate and adaptive immune responses contribute to the generation of ROS and inflammatory changes in the kidneys, blood vessels, and brain during hypertension (Zhang et al. 2021). In the context of SLE mice, dysfunctional communication between the immune system and vascular wall is involved in endothelial dysfunction (Romero et al. 2017; Toral et al. 2019). Our current findings support the critical role of IL-17a derived from Th17 cells in vascular wall dysfunction and elevated BP observed in autoimmunity induced by TLR-7 activation (de la Visitación et al. 2021; de la Visitación et al. 2021; Robles-Vera et al. 2020). Importantly, SCFA treatments and fiber consumption reduced Th17 infiltration in the vascular wall, resulting in improved vascular NOX-driven ROS production and restoration of impaired endothelium-dependent relaxation. ROS production by vascular NOX is considered crucial in endothelial dysfunction, as demonstrated by the beneficial effects of the selective NOX inhibitor VAS2870, which improved aortic endothelium-dependent relaxation to Ach. NOX activity can be modulated by local and circulating cytokines (Kelley and Wuthrich 1999; Ryan 2013). IL-17a, a pro-inflammatory cytokine, has been shown to induce Rho-kinase-mediated endothelial dysfunction in the vasculature, likely due to increased ROS generation through NOX activation (Nguyen et al. 2013; Pietrowski et al. 2011). Our results in this SLE model suggest that the IL-17-Rho-kinase pathway is significantly influenced by SCFA. This is supported by the restoration of Ach relaxation observed with SCFA or fiber treatments, similar to the effects of the Rho-kinase inhibitor Y27632. Additionally, neutralizing IL-17a in aortic rings from IMQ mice also improved endothelial dysfunction. Interestingly, the reduction in aortic Th17 infiltration and improvement of endothelium-dependent relaxation induced by ACE were abolished by GLPG-0974, confirming the crucial role of GPR43 activation in its vasculo-protective effects. An important limitation of our study is the lack of confirmation of these results in GPR43-/- mice.

Activation of TLR-4 in blood vessels by bacterial products such as LPS leads to increased NOX-dependent superoxide anion production and inflammation (Liang et al. 2013). In the case of IMQ mice, plasma endotoxin levels were elevated, and interventions aimed at reducing endotoxemia normalized vascular TLR-4 expression, thereby improving both vascular oxidative stress and inflammation (de la Visitación et al. 2021; Toral et al. 2019). Our study observed heightened plasma levels of LPS in IMQ mice, which correlated with decreased colonic integrity. Notably, administration of ACE effectively reduced endotoxemia and improved endothelial dysfunction.

This suggests that the decrease in aortic TLR-4 activation by LPS also contributed to the attenuation of vascular oxidative stress induced by ACE.

Previous reports have demonstrated that preventing autoimmunity through anti-CD20 therapy (Mathis et al. 2014) or depleting plasma cells with bortezomib (Taylor et al. 2018) guards against the development of SLE-induced hypertension. As expected, we noted elevated B cell populations in the spleens of IMQ mice compared to the CTR group. However, neither ACE nor BUT treatments reduced B cell generation or plasma anti-ds-DNA levels, indicating that B cells and autoantibodies are not implicated in the BP regulation induced by SCFA. Moreover, FMT from IMQ mice to GF mice did not elevate the proportion of B cells in blood, yet it impaired endothelial function and heightened BP. Interestingly, SCFA treatments managed to ameliorate these cardiovascular abnormalities. Among them, only a diet rich in RS, which augmented the production of ACE, BUT, and PROP by gut bacteria, thwarted signs of autoimmunity by modulating the TLR-7-IFN axis, a vital factor in human SLE (Crow 2014).

In summary, our study demonstrates that SCFA interventions partially thwarted hypertension development and mitigated cardiac hypertrophy and endothelial dysfunction in TLR-7-activated SLE-induced mice. These effects correlated with enhanced gut integrity, reduced endotoxemia, and decreased Th17 infiltration in the vascular wall. Additionally, dietary fiber interventions, which bolstered SCFA production by gut microbiota in IMQ mice, rebalanced the gut-immune system, counteracted endothelial dysfunction, and provided protection against hypertension (**Figure 70**). Given that individuals with SLE have reported lower fiber intake compared to healthy individuals (Elkan et al. 2012; Schäfer et al. 2021)s, and considering the observed inverse correlation between dietary fiber intake and active SLE risk (Minami et al. 2011), our findings suggest a potential role for RS-rich fiber treatment in preventing autoimmunity and SLE-related cardiovascular complications. This is especially relevant for patients exhibiting SLE phenotypes associated with increased TLR-7 signaling, elevated IgD-CD27-double-negative B cells in peripheral blood (Jenks et al. 2018), and excessive accumulation of extrafollicular helper T cells (Caielli et al. 2019).

Importantly, dietary interventions such as fiber-rich diets or SCFA treatments may provide a more targeted and potentially safer approach compared to broad-spectrum antibiotics, which can lead to side effects ranging from diarrheal events, disruption of the native microbiota, to more serious concerns like antibiotic resistance and systemic toxicities (de la Visitación et al. 2021).

However, it is vital to exercise caution when extrapolating our findings to humans due to documented differences between animal and human microbiota features.

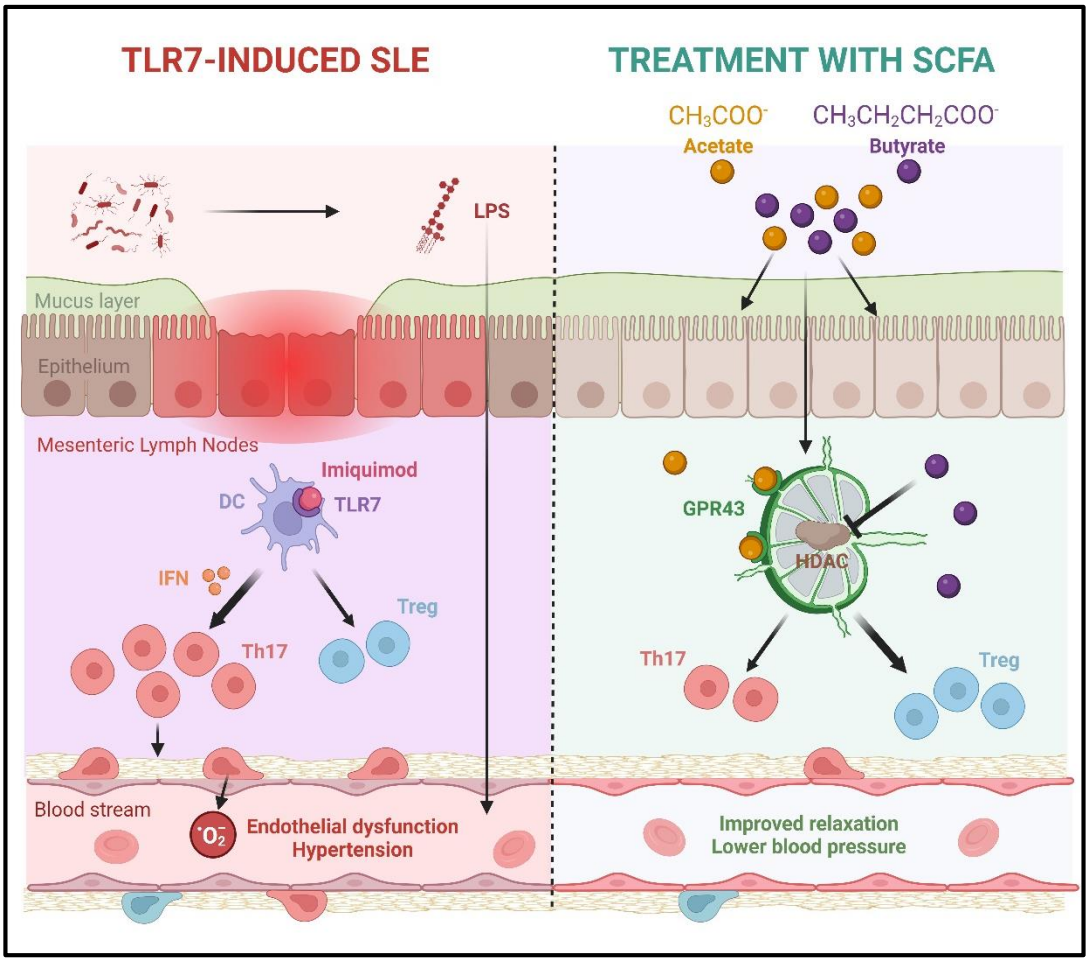

Figure 70. Effects of SCFA on cardiovascular complications in TLR-7-induced lupus mice.

Abbreviations: DC, dendritic cell; GPR43, G-protein coupled receptor 43; HDAC, histone deacetylases; IFN, interferon; LPS, lipopolysaccharide; TLR, toll-like receptor.

4. Role of dietary fiber intake in the raise of BP in NZBWF1 mice

The most important information from this study is that preventive cardiovascular effects of fiber interventions in SLE mice were associated to the rebalancing of dysfunctional gut-immune system-vascular wall axis. This was supported by several pieces of evidence: (i) increasing SCFA producing bacteria; (ii) normalization of gut integrity and leakiness; (iii) reduction of Th17 polarization in MLN and lamina propria and lower vascular Th17 infiltration; (iv) dampened endothelial dysfunction and high BP, and (v) feces inoculation from SLE mice treated with RS or ITF to GF transferred the improved gut-immune system-vascular wall axis.

Gut microbiota-host genetics interaction plays an important role in the progression of autoimmune diseases, like SLE. It has been previously demonstrated that gut microbiota and gut-immune system communication are crucial in the development of endothelial dysfunction and hypertension in female NZBWF1 mice (de la Visitación et al. 2021). We must highlight that the PLS-DA of gut microbiota in NZBWF1 mice and age-matched control mice did not demonstrate highly differentiated microbial communities. In agreement with previous evidence (de la Visitación et al. 2021; Toral et al. 2019) the main characteristics of gut microbiota remodeling in SLE were: (i) No significant changes in α-diversity parameters (richness, diversity, and evenness), in *Firmicutes/Bacteroidetes* ratio, in SCFA-producing bacteria and in strict anaerobic bacteria proportion; (ii) The main changes happen within the sublevel categories as family and genera, with reduced content in *Clostridiaceae* and increased *Lactobacillus* (*Lactobacillaceae*). NZB/WF1 mice displayed a higher abundance of *Lactobacilli* in the gut microbiota, which may be associated with more severe clinical signs, especially the impairment of systemic autoimmunity and renal function (Luo et al. 2018). Our results agree with the key role of *Lactobacilli* in the development renal dysfunction in SLE since RS and ITF interventions, which reduce *Lactobacillus* proportion, improved renal injury. Interestingly, the faecal content of *Lactobacillus reuteri*, a SCFA-sensitive bacteria, and its translocation to secondary lymph nodes and liver seems to be involved in SLE autoimmunity (Zegarra-Ruiz et al. 2019). However, in our experimental conditions the proportion of *L. reuteri* in faeces from CTR and SLE mice was similar and was unaffected by either RS or ITF, suggesting that translocation of this bacteria is not involved in autoimmunity in NZB/WF1 mice.

Prebiotic fiber fermentative metabolization by the gut microbiota produces metabolites known as SCFA, which have been demonstrated to be relevant regulators of pro-hypertensive components in SLE, such as inflammatory and immune processes (de la Visitación et al. 2019; Taylor and Ryan 2016). As expected, fiber supplementation promoted the growth of ACE-producing bacteria (RS fiber) and BUT-producing bacteria (ITF fiber). *Bacteroides acidifacients* (*Bacteroidaceae*, phylum *Bacteroidetes*), an ACE-producing bacteria, which was associated to reduced BP in hypertensive animals, was increased by RS fiber consumption (Marques et al. 2017).

SCFA are relevant metabolites for the maintenance of intestinal homeostasis. SCFA can act as fuel for intestinal epithelial cells and intervene in the strengthening of the gut barrier function (Parada Venegas et al. 2019). In our experimental conditions, reduced colonic integrity was found in SLE mice, associated with increased translocation of LPS into the circulation. RS increased the expression of TJ proteins and reduced endotoxemia. Interestingly, colonic upregulation of SCFA receptor GPR43 was induced by RS fiber, suggesting that binding of ACE to GPR43 is a possible mechanism to improve gut integrity in SLE, whereas BUT induced HDACs inhibition seems to be involved in the protective effect of ITF fiber. In addition, RS fiber significantly increased colonic mRNA levels of mucins, associated with a significant increase of *Akkermansia muciniphila*. This is a gram-negative, strictly anaerobic bacterium belonging to the *Verrucomicrobia* phylum. It is capable of degrading mucin. These mucolytic properties seem to stimulate mucus renewal by a positive feedback loop (Derrien et al. 2004). In addition, *A. muciniphila* was associated with improved endothelial dysfunction, an early marker of CVD, in apolipoprotein E knockout (Apoe−/−) mice (Catry et al. 2018) and reduced endotoxemia (Li et al. 2016).

Recent publications that study female NZBWF1 mice have demonstrated that there is a broad arrange of factors playing a role in the onset of hypertension besides B-cell hyperactivity and autoantibody synthesis, such as pro-inflammatory cytokines or oxidative stress (Taylor and Ryan 2016). These are elements that mainly mediate local inflammation and can be linked to renal and vascular dysfunction. They can be found with a high probability downstream of the initial genetically-determined immune system dysregulation (de la Visitación et al. 2019). Previous studies demonstrated that dysfunctional polarization of naïve T cells to Th17 in MLN and Th17 infiltration in the vascular wall are crucial events involved in the gut microbiota-mediated higher BP in SLE mice (de la Visitación et al. 2021; Toral et al. 2019). The present study agrees with this hypothesis and demonstrated that fiber treatments reshaped gut-immune system axis, reducing Th17 polarization in MLN.

In fact, stool inoculation from SLE mice treated with RS or ITF was unable to increase Th17 content in GF MLN as compared to faecal inoculation from untreated SLE mice. SCFA, such as ACE or BUT, might mediate this gut-immune system communication in this part of the intestine, as previously described (Robles-Vera et al. 2020). As expected, B cell populations were higher in secondary lymph organs from SLE mice as compared to CTR in our results, and neither RS nor ITF treatments reduced B cell generation and circulating B cells, discarding the involvement of B cells in the BP regulation induced by microbiota. Likewise, FMT from SLE mice to GF mice did not increase the proportion of B cells in MLN. As per these results, we did not gather sufficient evidence to prove a hypothetical pathogenic role of anti-ds-DNA, as mediator of BP increase induced by microbiota. In fact, both fiber treatments decreased BP but were not able to reduce plasma anti-ds-DNA. Also, faecal inoculation from hypertensive SLE mice to GF mice induced an increase in BP but could not alter circulating anti-ds-DNA.

Endothelial dysfunction plays a seminal part in the pathogenesis of hypertension. Decreased NO bioavailability is the central factor that links oxidative stress to endothelial dysfunction and hypertension. Both innate and adaptive immune responses participate in the generation of ROS and inflammatory changes in the kidneys, blood vessels and brain in hypertension (Wenzel et al. 2008). A dysfunctional communication between immune system and vascular wall is involved in endothelial dysfunction in SLE mice (Romero et al. 2017; Toral et al. 2019). High NOX-driven ROS synthesis is linked to both endothelial dysfunction and high BP in female NZB/WF1 mice (Gómez-Guzmán et al. 2014; de la Visitación et al. 2021; Toral et al. 2019). Accordingly, we too have detected a reduction in Ach-induced relaxation and an increase in NOX activity in aorta from SLE as compared to CTR. It is interesting that chronic fiber treatments were able to prevent the impoverished responses to Ach and the increase in NOX activity. We were able to corroborate these effects through FMT to GF mice, involving gut microbiota in oxidative stress and endothelial dysfunction. ROS production by the vascular NOX has been seen as a crucial part of microbiota-induced endothelial dysfunction since incubation with the selective NOX inhibitor VAS2870 suppresses the impairment of aortic endothelium-dependent relaxation to Ach. Local and circulating cytokines can modulate NOX activity (Kelley and Wuthrich 1999; Ryan 2013; Toral et al. 2019). Both RS and ITF decreased Th17 maturation in MLN, circulation and vascular infiltration (as seen in aorta). It has already been established that the pro-inflammatory cytokine IL-17a induces Rho-kinase-mediated endothelial dysfunction in the vasculature (Nguyen et al. 2013), presumably partially because of an increase in ROS generation by NOX activation (Pietrowski et al. 2011).

Thus, the Rho-kinase inhibitor Y27632 restored Ach relaxation similarly to what we observed with the fiber treatments, which suggest that the IL-17-Rho-kinase-pathway is highly regulated by gut microbiota in our genetic SLE model. Additionally, stool inoculation from SLE mice treated with RS or ITF to GF was unable to induce Th17 populations in MLN, Th17 infiltration in aorta and impaired Ach relaxation, as compared to faecal inoculation from untreated SLE mice. Overall, fibers intervention improved immune system-vascular axis, reducing Th17 polarization in secondary lymph nodes and restoring endothelial function in SLE mice.

Activating TLR-4 in vessels with bacterial products like LPS increases NOX dependent superoxide anion production and inflammation (Liang et al. 2013). In SLE mice, plasma endotoxin levels were increased, and intervention addressed to reduce endotoxemia normalized vascular TLR-4 expression and improved both vascular oxidative stress and inflammation (de la Visitación et al. 2021; Toral et al. 2019). In addition, we were able to find increased LPS plasma levels in SLE mice associated to lower colonic integrity. Fiber interventions, especially RS, reduced endotoxemia, vascular TLR-4 expression and improved endothelial dysfunction.

Renal function plays a crucial role in the long-term control of BP, impaired activity in the kidney is undoubtedly involved in the prevalence of hypertension in SLE patients and murine models. Moreover, in this experiment both fiber treatments decreased renal damage and BP concomitantly. Nonetheless, SLE-linked hypertension has been detected without displaying nephritis (Petrin et al. 1993; Ward and Studenski 1992). Around 53% of SLE patients in one cohort suffered from hypertension but not nephritis (Shaharir et al. 2015). Remarkably, faecal transplant from SLE induced an increase in BP that was not accompanied by changes in protein excretion, pointing to a kidney-independent BP regulatory role for the microbiota.

In conclusion, our study demonstrated that fiber interventions partially prevented the development of hypertension and ameliorated cardiac hypertrophy and kidney damage in a genetic model of SLE. These effects were associated with changes in the gut microbiota (increasing SCFA-producing bacteria), improvement of gut integrity, and decreased endothelial dysfunction. Additionally, faecal inoculation from SLE mice treated with RS of ITF donor mice into recipients GF mice suppressed gut-immune system disbalance, endothelial dysfunction, and protects against hypertension. Overall, preventive BP effects and hypertensive cardiac damage induced by RS and ITF are partially attributed to improvement of the gut-immune system-vascular wall axis (**Figure 71**).

Women get SLE approximately 9:1 over men. Due to this, our results for this experiment and in most of the preceding bibliography were obtained using female models of the disease. Considering the evidence that supports significant differences in gut microbiota for both sexes (Beale et al. 2019), the possible effects of gut microbiota and its difference in BP regulation in males should be studied. Our results help rethink the current paradigm on the prevention of SLE-linked cardiovascular complications, suggesting modulation of the gut microbiota composition using fiber treatment. Nonetheless, caution is advisable for future extrapolations of our findings to humans since there are documented differences between the features of animal and human microbiota.

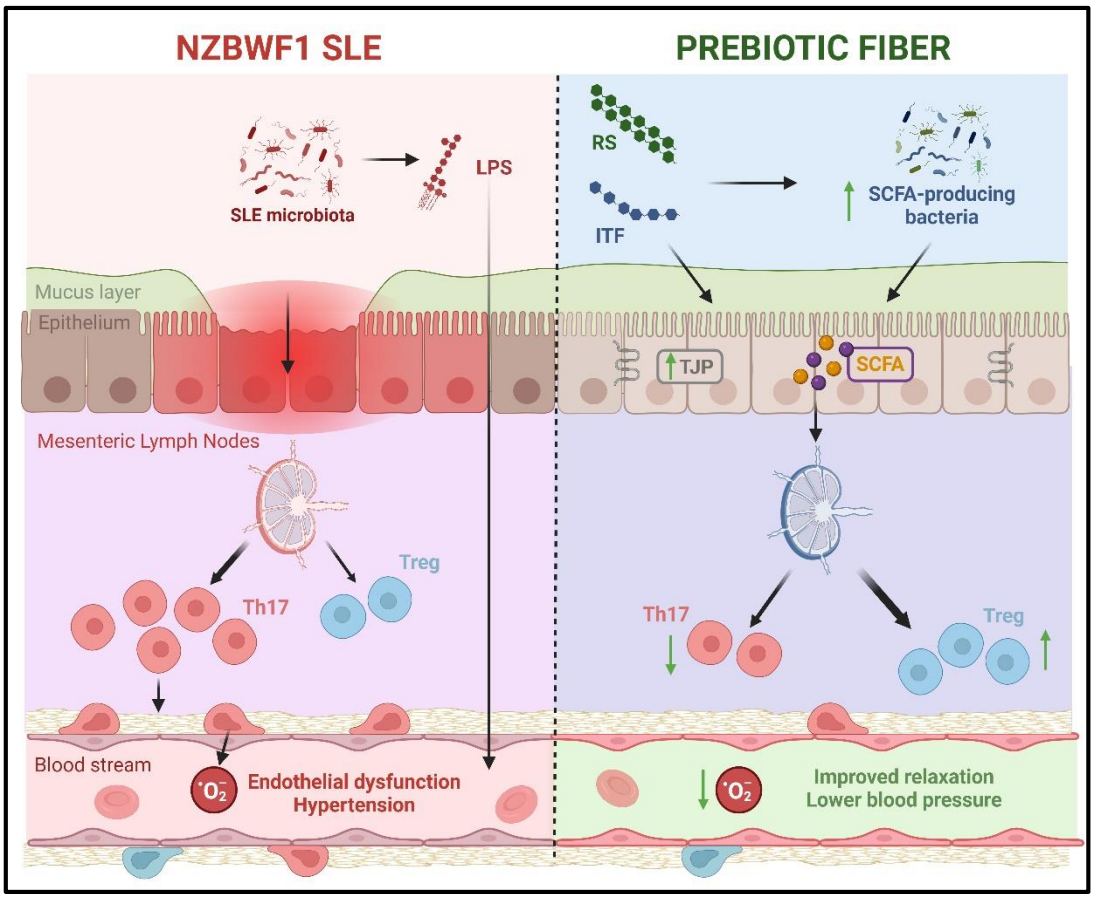

Figure 71. Role of dietary fiber intake in the raise of BP in NZBWF1 mice.

Abbreviations: ITF, inulin-type fructans; LPS, lipopolysaccharide; RS, resistant starch; SCFA, short chain fatty acids; TJP, tight junction proteins.

CONCLUSIONS

CONCLUSIONS

1. Gut microbiota from IMQ-mice is different to healthy controls and it triggers changes in blood pressure regulation, as proved by vancomycin treatment and stool transplantation from control mice, and this can be linked to the activation of pro-inflammatory Th17 lymphocytes.

2. Gut microbiome metabolic product TMAO increases TLR-7 induced autoimmunity and vascular dysfunction. This can be associated with increased B cells differentiation and activation of pro-inflammatory Th17 lymphocytes, revealing the potential to alleviate cardiovascular complications by blockage of the TMAO pathway.

3. Microbiota-derived SCFA have a protective effect on vascular dysfunction in TLR-7-driven SLE. Acetate and butyrate exert this regulatory action through GPR43 and HDACs, respectively, lowering Th17 proliferation and infiltration. Therefore, fiber-rich diets or SCFA treatments may provide an alternative intervention in preventing autoimmunity and SLE-related complications.

4. Dietary interventions with prebiotic fibers are able to prevent the development of hypertension linked to SLE. This effect can be explained by gut microbiota modulation and SCFA production, leading to immunomodulatory regulation. Thus, fiber consumption might be a novel approach to prevent cardiovascular complications in SLE.

REFERENCES

REFERENCES

Ahmad, R., M. F. Sorrell, S. K. Batra, P. Dhawan, and A. B. Singh. 2017. “Gut Permeability and Mucosal Inflammation: Bad, Good or Context Dependent.” *Mucosal Immunology* 10(2):307–17.

Al-Herz, Adeeba, Stephanie Ensworth, Kamran Shojania, and John M. Esdaile. 2003. “Cardiovascular Risk Factor Screening in Systemic Lupus Erythematosus.” *The Journal of Rheumatology* 30(3):493–96.

Alarcón, G. S., A. W. Friedman, K. V Straaton, J. M. Moulds, J. Lisse, H. M. Bastian, G. Jr McGwin, A. A. Bartolucci, J. M. Roseman, and J. D. Reveille. 1999. “Systemic Lupus Erythematosus in Three Ethnic Groups: III. A Comparison of Characteristics Early in the Natural History of the LUMINA Cohort. LUpus in MInority Populations: NAture vs. Nurture.” *Lupus* 8(3):197–209.

Alunno, Alessia, Elena Bartoloni, Onelia Bistoni, Giuseppe Nocentini, Simona Ronchetti, Sara Caterbi, Valentina Valentini, Carlo Riccardi, and Roberto Gerli. 2012. “Balance between Regulatory T and Th17 Cells in Systemic Lupus Erythematosus: The Old and the New.” *Clinical and Developmental Immunology* 2012.

Ansaldo, Eduard, Leianna C. Slayden, Krystal L. Ching, Meghan A. Koch, Natalie K. Wolf, Damian R. Plichta, Eric M. Brown, Daniel B. Graham, Ramnik J. Xavier, James J. Moon, and Gregory M. Barton. 2019. “Akkermansia Muciniphila Induces Intestinal Adaptive Immune Responses during Homeostasis.” *Science (New York, N.Y.)* 364(6446):1179–84.

Aringer, Martin, Karen Costenbader, David Daikh, Ralph Brinks, Marta Mosca, Rosalind Ramsey-Goldman, Josef S. Smolen, David Wofsy, Dimitrios T. Boumpas, Diane L. Kamen, David Jayne, Ricard Cervera, Nathalie Costedoat-Chalumeau, Betty Diamond, Dafna D. Gladman, Bevra Hahn, Falk Hiepe, Søren Jacobsen, Dinesh Khanna, Kirsten Lerstrøm, Elena Massarotti, Joseph McCune, Guillermo Ruiz-Irastorza, Jorge Sanchez-Guerrero, Matthias Schneider, Murray Urowitz, George Bertsias, Bimba F. Hoyer, Nicolai Leuchten, Chiara Tani, Sara K. Tedeschi, Zahi Touma, Gabriela Schmajuk, Branimir Anic, Florence Assan, Tak Mao Chan, Ann Elaine Clarke, Mary K. Crow, László Czirják, Andrea Doria, Winfried Graninger, Bernadett Halda-Kiss, Sarfaraz Hasni, Peter M. Izmirly, Michelle Jung, Gábor Kumánovics, Xavier Mariette, Ivan Padjen, José M. Pego-Reigosa, Juanita Romero-Diaz, Íñigo

Rúa-Figueroa Fernández, Raphaèle Seror, Georg H. Stummvoll, Yoshiya Tanaka, Maria G. Tektonidou, Carlos Vasconcelos, Edward M. Vital, Daniel J. Wallace, Sule Yavuz, Pier Luigi Meroni, Marvin J. Fritzler, Ray Naden, Thomas Dörner, and Sindhu R. Johnson. 2019. “2019 European League Against Rheumatism/American College of Rheumatology Classification Criteria for Systemic Lupus Erythematosus.” *Arthritis & Rheumatology (Hoboken, N.J.)* 71(9):1400–1412.

Arpaia, Nicholas, Clarissa Campbell, Xiying Fan, Stanislav Dikiy, Joris van der Veeken, Paul deRoos, Hui Liu, Justin R. Cross, Klaus Pfeffer, Paul J. Coffer, and Alexander Y. Rudensky. 2013. “Metabolites Produced by Commensal Bacteria Promote Peripheral Regulatory T-Cell Generation.” *Nature* 504(7480):451–55.

Asarat, M., V. Apostolopoulos, T. Vasiljevic, and O. Donkor. 2016. “Short-Chain Fatty Acids Regulate Cytokines and Th17/Treg Cells in Human Peripheral Blood Mononuclear Cells in Vitro.” *Immunological Investigations* 45(3):205–22.

Ascher, Stefanie and Christoph Reinhardt. 2018. “The Gut Microbiota: An Emerging Risk Factor for Cardiovascular and Cerebrovascular Disease.” *European Journal of Immunology* 48(4):564–75.

Ayano, Masahiro and Takahiko Horiuchi. 2023. “Complement as a Biomarker for Systemic Lupus Erythematosus.” *Biomolecules* 13(2).

Azzouz, Doua F., Ze Chen, Peter M. Izmirly, Lea Ann Chen, Zhi Li, Chongda Zhang, David Mieles, Kate Trujillo, Adriana Heguy, Alejandro Pironti, Greg G. Putzel, Dominik Schwudke, David Fenyo, Jill P. Buyon, Alexander V Alekseyenko, Nicolas Gisch, and Gregg J. Silverman. 2023. “Longitudinal Gut Microbiome Analyses and Blooms of Pathogenic Strains during Lupus Disease Flares.” *Annals of the Rheumatic Diseases* 82(10):1315–27.

Azzouz, Doua, Aidana Omarbekova, Adriana Heguy, Dominik Schwudke, Nicolas Gisch, Brad H. Rovin, Roberto Caricchio, Jill P. Buyon, Alexander V Alekseyenko, and Gregg J. Silverman. 2019. “Lupus Nephritis Is Linked to Disease-Activity Associated Expansions and Immunity to a Gut Commensal.” *Annals of the Rheumatic Diseases* 78(7):947–56.

Barrat, Franck J., Thea Meeker, Jean H. Chan, Cristiana Guiducci, and Robert L. Coffman. 2007. “Treatment of Lupus-Prone Mice with a Dual Inhibitor of TLR7 and TLR9 Leads to Reduction of Autoantibody Production and Amelioration of Disease Symptoms.” *European Journal of Immunology* 37(12):3582–86.

Bartels, Christie M., Kevin A. Buhr, Jerry W. Goldberg, Carolyn L. Bell, Maja Visekruna, Swapna Nekkanti, and Robert T. Greenlee. 2014. “Mortality and Cardiovascular Burden of Systemic Lupus Erythematosus in a US Population-Based Cohort.” *The Journal of Rheumatology* 41(4):680–87.

Bartolomaeus, Hendrik, András Balogh, Mina Yakoub, Susanne Homann, Lajos Markó, Sascha Höges, Dmitry Tsvetkov, Alexander Krannich, Sebastian Wundersitz, Ellen G. Avery, Nadine Haase, Kristin Kräker, Lydia Hering, Martina Maase, Kristina Kusche-Vihrog, Maria Grandoch, Jens Fielitz, Stefan Kempa, Maik Gollasch, Zhaxybay Zhumadilov, Samat Kozhakhmetov, Almagul Kushugulova, Kai-Uwe Eckardt, Ralf Dechend, Lars Christian Rump, Sofia K. Forslund, Dominik N. Müller, Johannes Stegbauer, and Nicola Wilck. 2019. “Short-Chain Fatty Acid Propionate Protects From Hypertensive Cardiovascular Damage.” *Circulation* 139(11):1407–21.

Beale, Anna L., David M. Kaye, and Francine Z. Marques. 2019. “The Role of the Gut Microbiome in Sex Differences in Arterial Pressure.” *Biology of Sex Differences* 10(1):22.

Belkaid, Yasmine and Oliver J. Harrison. 2017. “Homeostatic Immunity and the Microbiota.” *Immunity* 46(4):562–76.

Berer, Kerstin, Lisa Ann Gerdes, Egle Cekanaviciute, Xiaoming Jia, Liang Xiao, Zhongkui Xia, Chuan Liu, Luisa Klotz, Uta Stauffer, Sergio E. Baranzini, Tania Kümpfel, Reinhard Hohlfeld, Gurumoorthy Krishnamoorthy, and Hartmut Wekerle. 2017. “Gut Microbiota from Multiple Sclerosis Patients Enables Spontaneous Autoimmune Encephalomyelitis in Mice.” *Proceedings of the National Academy of Sciences of the United States of America* 114(40):10719–24.

Brown, Andrew J., Susan M. Goldsworthy, Ashley A. Barnes, Michelle M. Eilert, Lili Tcheang, Dion Daniels, Alison I. Muir, Mark J. Wigglesworth, Ian Kinghorn, Neil J. Fraser, Nicholas B. Pike, Jay C. Strum, Klaudia M. Steplewski, Paul R. Murdock, Julie C. Holder, Fiona H. Marshall, Philip G. Szekeres, Shelagh Wilson, Diane M. Ignar, Steve M. Foord, Alan Wise, and Simon J. Dowell. 2003. “The Orphan G Protein-Coupled Receptors GPR41 and GPR43 Are Activated by Propionate and Other Short Chain Carboxylic Acids.” *The Journal of Biological Chemistry* 278(13):11312–19.

Brown, Grant J., Pablo F. Cañete, Hao Wang, Arti Medhavy, Josiah Bones, Jonathan A. Roco, Yuke He, Yuting Qin, Jean Cappello, Julia I. Ellyard, Katharine Bassett, Qian Shen, Gaetan Burgio, Yaoyuan Zhang, Cynthia Turnbull, Xiangpeng Meng, Phil Wu, Eun Cho, Lisa A. Miosge, T. Daniel

Andrews, Matt A. Field, Denis Tvorogov, Angel F. Lopez, Jeffrey J. Babon, Cristina Aparicio López, África Gónzalez-Murillo, Daniel Clemente Garulo, Virginia Pascual, Tess Levy, Eric J. Mallack, Daniel G. Calame, Timothy Lotze, James R. Lupski, Huihua Ding, Tomalika R. Ullah, Giles D. Walters, Mark E. Koina, Matthew C. Cook, Nan Shen, Carmen de Lucas Collantes, Ben Corry, Michael P. Gantier, Vicki Athanasopoulos, and Carola G. Vinuesa. 2022. "TLR7 Gain-of-Function Genetic Variation Causes Human Lupus." *Nature* 605(7909):349–56.

Brunt, Vienna E., Rachel A. Gioscia-Ryan, Abigail G. Casso, Nicholas S. VanDongen, Brian P. Ziemba, Zachary J. Sapinsley, James J. Richey, Melanie C. Zigler, Andrew P. Neilson, Kevin P. Davy, and Douglas R. Seals. 2020. "Trimethylamine-N-Oxide Promotes Age-Related Vascular Oxidative Stress and Endothelial Dysfunction in Mice and Healthy Humans." *Hypertension (Dallas, Tex. : 1979)* 76(1):101–12.

Brunt, Vienna E., Rachel A. Gioscia-Ryan, James J. Richey, Melanie C. Zigler, Lauren M. Cuevas, Antonio Gonzalez, Yoshiki Vázquez-Baeza, Micah L. Battson, Andrew T. Smithson, Andrew D. Gilley, Gail Ackermann, Andrew P. Neilson, Tiffany Weir, Kevin P. Davy, Rob Knight, and Douglas R. Seals. 2019. "Suppression of the Gut Microbiome Ameliorates Age-Related Arterial Dysfunction and Oxidative Stress in Mice." *The Journal of Physiology* 597(9):2361–78.

Buie, Joy Jones, Ludivine L. Renaud, Robin Muise-Helmericks, and Jim C. Oates. 2017. "IFN-α Negatively Regulates the Expression of Endothelial Nitric Oxide Synthase and Nitric Oxide Production: Implications for Systemic Lupus Erythematosus." *Journal of Immunology (Baltimore, Md. : 1950)* 199(6):1979–88.

Caielli, Simone, Shruti Athale, Bojana Domic, Elise Murat, Manjari Chandra, Romain Banchereau, Jeanine Baisch, Kate Phelps, Sandra Clayton, Mei Gong, Tracey Wright, Marilynn Punaro, Karolina Palucka, Cristiana Guiducci, Jacques Banchereau, and Virginia Pascual. 2016. "Oxidized Mitochondrial Nucleoids Released by Neutrophils Drive Type I Interferon Production in Human Lupus." *The Journal of Experimental Medicine* 213(5):697–713.

Caielli, Simone, Diogo Troggian Veiga, Preetha Balasubramanian, Shruti Athale, Bojana Domic, Elise Murat, Romain Banchereau, Zhaohui Xu, Manjari Chandra, Cheng-Han Chung, Lynnette Walters, Jeanine Baisch, Tracey Wright, Marilynn Punaro, Lorien Nassi, Katie Stewart, Julie Fuller, Duygu Ucar, Hideki Ueno, Joseph Zhou, Jacques Banchereau, and Virginia Pascual. 2019.

"A CD4(+) T Cell Population Expanded in Lupus Blood Provides B Cell Help through Interleukin-10 and Succinate." *Nature Medicine* 25(1):75–81.

Caporaso, J. Gregory, Christian L. Lauber, William A. Walters, Donna Berg-Lyons, Catherine A. Lozupone, Peter J. Turnbaugh, Noah Fierer, and Rob Knight. 2011. "Global Patterns of 16S RRNA Diversity at a Depth of Millions of Sequences per Sample." *Proceedings of the National Academy of Sciences of the United States of America* 108 Suppl(Suppl 1):4516–22.

Catry, Emilie, Laure B. Bindels, Anne Tailleux, Sophie Lestavel, Audrey M. Neyrinck, Jean-François Goossens, Irina Lobysheva, Hubert Plovier, Ahmed Essaghir, Jean-Baptiste Demoulin, Caroline Bouzin, Barbara D. Pachikian, Patrice D. Cani, Bart Staels, Chantal Dessy, and Nathalie M. Delzenne. 2018. "Targeting the Gut Microbiota with Inulin-Type Fructans: Preclinical Demonstration of a Novel Approach in the Management of Endothelial Dysfunction." *Gut* 67(2):271–83.

Cekanaviciute, Egle, Bryan B. Yoo, Tessel F. Runia, Justine W. Debelius, Sneha Singh, Charlotte A. Nelson, Rachel Kanner, Yadira Bencosme, Yun Kyung Lee, Stephen L. Hauser, Elizabeth Crabtree-Hartman, Ilana Katz Sand, Mar Gacias, Yunjiao Zhu, Patrizia Casaccia, Bruce A. C. Cree, Rob Knight, Sarkis K. Mazmanian, and Sergio E. Baranzini. 2017. "Gut Bacteria from Multiple Sclerosis Patients Modulate Human T Cells and Exacerbate Symptoms in Mouse Models." *Proceedings of the National Academy of Sciences of the United States of America* 114(40):10713–18.

Celhar, Teja and Anna-Marie Fairhurst. 2017. "Modelling Clinical Systemic Lupus Erythematosus: Similarities, Differences and Success Stories." *Rheumatology (Oxford, England)* 56(suppl_1):i88–99.

Chan, Vera Sau-Fong, Helen Hoi-Lun Tsang, Rachel Chun-Yee Tam, Liwei Lu, and Chak-Sing Lau. 2013. "B-Cell-Targeted Therapies in Systemic Lupus Erythematosus." *Cellular & Molecular Immunology* 10(2):133–42.

Chang, Ling-Sai, Po-Yu Huang, Ho-Chang Kuo, Yu-Kang Tu, Ping-Tao Tseng, Chih-Sung Liang, and Chih-Wei Hsu. 2022. "Diagnostic Accuracy of the American College of Rheumatology-1997, the Systemic Lupus International Collaborating Clinics-2012, and the European League Against Rheumatism-2019 Criteria for Juvenile Systemic Lupus Erythematosus: A Systematic Review and Net." *Autoimmunity Reviews* 21(9):103144.

Chang, Pamela V, Liming Hao, Stefan Offermanns, and Ruslan Medzhitov. 2014. "The Microbial Metabolite Butyrate Regulates Intestinal Macrophage Function via Histone Deacetylase Inhibition." *Proceedings of the National Academy of Sciences of the United States of America* 111(6):2247–52.

Chen, Jiaxuan, Shuzhen Liao, Huimin Zhou, Lawei Yang, Fengbiao Guo, Shuxian Chen, Aifen Li, Quanren Pan, Chen Yang, Hua-Feng Liu, and Qingjun Pan. 2021. "Humanized Mouse Models of Systemic Lupus Erythematosus: Opportunities and Challenges." *Frontiers in Immunology* 12:816956.

Chen, Ling, Shuang Li, Jie Zheng, Wentao Li, Xuemei Jiang, Xilun Zhao, Jian Li, Lianqiang Che, Yan Lin, Shengyu Xu, Bin Feng, Zhengfeng Fang, and De Wu. 2018. "Effects of Dietary Clostridium Butyricum Supplementation on Growth Performance, Intestinal Development, and Immune Response of Weaned Piglets Challenged with Lipopolysaccharide." *Journal of Animal Science and Biotechnology* 9:62.

Chen, Ming-Liang, Xiao-Hui Zhu, Li Ran, He-Dong Lang, Long Yi, and Man-Tian Mi. 2017. "Trimethylamine-N-Oxide Induces Vascular Inflammation by Activating the NLRP3 Inflammasome Through the SIRT3-SOD2-MtROS Signaling Pathway." *Journal of the American Heart Association* 6(9).

Chen, Xiaoqing, Wenru Su, Taoshang Wan, Jianfeng Yu, Wenjie Zhu, Fen Tang, Guangming Liu, Nancy Olsen, Dan Liang, and Song Guo Zheng. 2017. "Sodium Butyrate Regulates Th17/Treg Cell Balance to Ameliorate Uveitis via the Nrf2/HO-1 Pathway." *Biochemical Pharmacology* 142:111–19.

Chia, Stanley, Motaz Qadan, Richard Newton, Christopher A. Ludlam, Keith A. A. Fox, and David E. Newby. 2003. "Intra-Arterial Tumor Necrosis Factor-Alpha Impairs Endothelium-Dependent Vasodilatation and Stimulates Local Tissue Plasminogen Activator Release in Humans." *Arteriosclerosis, Thrombosis, and Vascular Biology* 23(4):695–701.

Choi, Seung-Chul, Josephine Brown, Minghao Gong, Yong Ge, Mojgan Zadeh, Wei Li, Byron P. Croker, George Michailidis, Timothy J. Garrett, Mansour Mohamadzadeh, and Laurence Morel. 2020. "Gut Microbiota Dysbiosis and Altered Tryptophan Catabolism Contribute to Autoimmunity in Lupus-Susceptible Mice." *Science Translational Medicine* 12(551).

Christensen, Sean R. and Mark J. Shlomchik. 2007. "Regulation of Lupus-Related Autoantibody Production and Clinical Disease by Toll-like Receptors." *Seminars in Immunology* 19(1):11–23.

Christovich, Anna and Xin M. Luo. 2022. “Gut Microbiota, Leaky Gut, and Autoimmune Diseases.” *Frontiers in Immunology* 13:946248.

Cohen, P. L. and R. A. Eisenberg. 1991. “Lpr and Gld: Single Gene Models of Systemic Autoimmunity and Lymphoproliferative Disease.” *Annual Review of Immunology* 9:243–69.

Cotillard, Aurélie, Sean P. Kennedy, Ling Chun Kong, Edi Prifti, Nicolas Pons, Emmanuelle Le Chatelier, Mathieu Almeida, Benoit Quinquis, Florence Levenez, Nathalie Galleron, Sophie Gougis, Salwa Rizkalla, Jean-Michel Batto, Pierre Renault, Joel Doré, Jean-Daniel Zucker, Karine Clément, and Stanislav Dusko Ehrlich. 2013. “Dietary Intervention Impact on Gut Microbial Gene Richness.” *Nature* 500(7464):585–88.

Crispín, José C., Mohamed Oukka, George Bayliss, Robert A. Cohen, Christine A. Van Beek, Isaac E. Stillman, Vasileios C. Kyttaris, Yuang-Taung Juang, and George C. Tsokos. 2008. “Expanded Double Negative T Cells in Patients with Systemic Lupus Erythematosus Produce IL-17 and Infiltrate the Kidneys.” *Journal of Immunology (Baltimore, Md. : 1950)* 181(12):8761–66.

Crow, Mary K. 2014. “Type I Interferon in the Pathogenesis of Lupus.” *Journal of Immunology (Baltimore, Md. : 1950)* 192(12):5459–68.

Crow, Mary K. 2023. “Pathogenesis of Systemic Lupus Erythematosus: Risks, Mechanisms and Therapeutic Targets.” *Annals of the Rheumatic Diseases* 82(8):999–1014.

Cui, Yong, Yujun Sheng, and Xuejun Zhang. 2013. “Genetic Susceptibility to SLE: Recent Progress from GWAS.” *Journal of Autoimmunity* 41:25–33.

Cummings, J. H., E. W. Pomare, W. J. Branch, C. P. Naylor, and G. T. Macfarlane. 1987. “Short Chain Fatty Acids in Human Large Intestine, Portal, Hepatic and Venous Blood.” *Gut* 28(10):1221–27.

D’Cruz, David P., Munther A. Khamashta, and Graham R. V Hughes. 2007. “Systemic Lupus Erythematosus.” *Lancet (London, England)* 369(9561):587–96.

Dar, O., M. R. Salaman, M. H. Seifert, and D. A. Isenberg. 1988. “B Lymphocyte Activation in Systemic Lupus Erythematosus: Spontaneous Production of IgG Antibodies to DNA and Environmental Antigens in Cultures of Blood Mononuclear Cells.” *Clinical and Experimental Immunology* 73(3):430–35.

Deane, Jonathan A., Prapaporn Pisitkun, Rebecca S. Barrett, Lionel Feigenbaum, Terrence Town, Jerrold M. Ward, Richard A. Flavell, and Silvia Bolland. 2007. “Control of Toll-like Receptor 7 Expression Is Essential to Restrict Autoimmunity and Dendritic Cell Proliferation.” *Immunity* 27(5):801–10.

Deanfield, John, Ann Donald, Claudio Ferri, Cristina Giannattasio, Julian Halcox, Sean Halligan, Amir Lerman, Giuseppe Mancia, James J. Oliver, Achille C. Pessina, Damiano Rizzoni, Gian Paolo Rossi, Antonio Salvetti, Ernesto L. Schiffrin, Stefano Taddei, and David J. Webb. 2005. “Endothelial Function and Dysfunction. Part I: Methodological Issues for Assessment in the Different Vascular Beds: A Statement by the Working Group on Endothelin and Endothelial Factors of the European Society of Hypertension.” *Journal of Hypertension* 23(1):7–17.

Derrien, Muriel, Elaine E. Vaughan, Caroline M. Plugge, and Willem M. de Vos. 2004. “Akkermansia Muciniphila Gen. Nov., Sp. Nov., a Human Intestinal Mucin-Degrading Bacterium.” *International Journal of Systematic and Evolutionary Microbiology* 54(Pt 5):1469–76.

Docampo, Melissa D., Marina B. da Silva, Amina Lazrak, Katherine B. Nichols, Sophia R. Lieberman, Ann E. Slingerland, Gabriel K. Armijo, Yusuke Shono, Chi Nguyen, Sebastien Monette, Emmanuel Dwomoh, Nicole Lee, Clair D. Geary, Suelen M. Perobelli, Melody Smith, Kate A. Markey, Santosha A. Vardhana, Anastasia I. Kousa, Eli Zamir, Itamar Greenfield, Joseph C. Sun, Justin R. Cross, Jonathan U. Peled, Robert R. Jenq, Christoph K. Stein-Thoeringer, and Marcel R. M. van den Brink. 2022. “Alloreactive T Cells Deficient of the Short-Chain Fatty Acid Receptor GPR109A Induce Less Graft-versus-Host Disease.” *Blood* 139(15):2392–2405.

Dole, Vandana S., Kenneth S. Henderson, Richard D. Fister, Michael T. Pietrowski, Geomaris Maldonado, and Charles B. Clifford. 2013. “Pathogenicity and Genetic Variation of 3 Strains of Corynebacterium Bovis in Immunodeficient Mice.” *Journal of the American Association for Laboratory Animal Science : JAALAS* 52(4):458–66.

Dorraji, Seyed Esmaeil, Premasany Kanapathippillai, Aud-Malin Karlsson Hovd, Mikael Ryan Stenersrød, Kjersti Daae Horvei, Anita Ursvik, Stine Linn Figenschau, Dhivya Thiyagarajan, Christopher Graham Fenton, Hege Lynum Pedersen, and Kristin Andreassen Fenton. 2020. “Kidney Tertiary Lymphoid Structures in Lupus Nephritis Develop into Large Interconnected Networks and Resemble Lymph Nodes in Gene Signature.” *The American Journal of Pathology* 190(11):2203–25.

Du, Yong, Soomro Sanam, Krause Kate, and Chandra Mohan. 2015. “Animal Models of Lupus and Lupus Nephritis.” *Current Pharmaceutical Design* 21(18):2320–49.

Durcan, Laura, Tom O’Dwyer, and Michelle Petri. 2019. “Management Strategies and Future Directions for Systemic Lupus Erythematosus in Adults.” *Lancet (London, England)* 393(10188):2332–43.

Edgar, Robert C. and Henrik Flyvbjerg. 2015. “Error Filtering, Pair Assembly and Error Correction for next-Generation Sequencing Reads.” *Bioinformatics (Oxford, England)* 31(21):3476–82.

Edwards, C. J. and K. H. Costenbader. 2014. “Epigenetics and the Microbiome: Developing Areas in the Understanding of the Aetiology of Lupus.” *Lupus*, 505–6.

Edwards, Jonnelle M., Shaunak Roy, Jeremy C. Tomcho, Zachary J. Schreckenberger, Saroj Chakraborty, Nicole R. Bearss, Piu Saha, Cameron G. McCarthy, Matam Vijay-Kumar, Bina Joe, and Camilla F. Wenceslau. 2020. “Microbiota Are Critical for Vascular Physiology: Germ-Free Status Weakens Contractility and Induces Sex-Specific Vascular Remodeling in Mice.” *Vascular Pharmacology* 125–126:106633.

Eisenberg, R. A. and F. J. Dixon. 1980. “Effect of Castration on Male-Determined Acceleration of Autoimmune Disease in BXSB Mice.” *Journal of Immunology (Baltimore, Md. : 1950)* 125(5):1959–61.

Elkan, A. C., C. Anania, T. Gustafsson, T. Jogestrand, I. Hafström, and J. Frostegård. 2012. “Diet and Fatty Acid Pattern among Patients with SLE: Associations with Disease Activity, Blood Lipids and Atherosclerosis.” *Lupus* 21(13):1405–11.

Eloranta, Maija-Leena and Lars Rönnblom. 2016. “Cause and Consequences of the Activated Type I Interferon System in SLE.” *Journal of Molecular Medicine (Berlin, Germany)* 94(10):1103–10.

Frohlich, E. D., C. Apstein, A. V Chobanian, R. B. Devereux, H. P. Dustan, V. Dzau, F. Fauad-Tarazi, M. J. Horan, M. Marcus, and B. Massie. 1992. “The Heart in Hypertension.” *The New England Journal of Medicine* 327(14):998–1008.

Frostegård, J. 2008. “Systemic Lupus Erythematosus and Cardiovascular Disease.” *Lupus* 17(5):364–67.

Frostegård, Johan. 2023. “Systemic Lupus Erythematosus and Cardiovascular Disease.” *Journal of Internal Medicine* 293(1):48–62.

Fujisaka, Shiho, Siegfried Ussar, Clary Clish, Suzanne Devkota, Jonathan M. Dreyfuss, Masaji Sakaguchi, Marion Soto, Masahiro Konishi, Samir Softic, Emrah Altindis, Ning Li, Georg Gerber, Lynn Bry, and C. Ronald Kahn. 2016. “Antibiotic Effects on Gut Microbiota and Metabolism Are Host Dependent.” *The Journal of Clinical Investigation* 126(12):4430–43.

Geng, Linyu, Jian Zhao, Yun Deng, Ivan Molano, Xue Xu, Lingxiao Xu, Phillip Ruiz, Quanzhen Li, Xuebing Feng, Miaojia Zhang, Wenfeng Tan, Diane L. Kamen, Sang-Cheol Bae, Gary S. Gilkeson, Lingyun Sun, and Betty P. Tsao. 2022. “Human SLE Variant NCF1-R90H Promotes Kidney Damage and Murine Lupus through Enhanced Tfh2 Responses Induced by Defective Efferocytosis of Macrophages.” *Annals of the Rheumatic Diseases* 81(2):255–67.

Gentile, Christopher L. and Tiffany L. Weir. 2018. “The Gut Microbiota at the Intersection of Diet and Human Health.” *Science (New York, N.Y.)* 362(6416):776–80.

Giannelou, Mayra and Clio P. Mavragani. 2017. “Cardiovascular Disease in Systemic Lupus Erythematosus: A Comprehensive Update.” *Journal of Autoimmunity* 82:1–12.

Gladman, Dafna D., Dominique Ibañez, and Murray B. Urowitz. 2002. “Systemic Lupus Erythematosus Disease Activity Index 2000.” *The Journal of Rheumatology* 29(2):288–91.

Gomes, Aline Corado, Christian Hoffmann, and João Felipe Mota. 2018. “The Human Gut Microbiota: Metabolism and Perspective in Obesity.” *Gut Microbes* 9(4):308–25.

Gómez-Guzmán, Manuel, Rosario Jiménez, Miguel Romero, Manuel Sánchez, María José Zarzuelo, Mercedes Gómez-Morales, Francisco O’Valle, Antonio José López-Farré, Francesca Algieri, Julio Gálvez, Francisco Pérez-Vizcaino, José Mario Sabio, and Juan Duarte. 2014. “Chronic Hydroxychloroquine Improves Endothelial Dysfunction and Protects Kidney in a Mouse Model of Systemic Lupus Erythematosus.” *Hypertension (Dallas, Tex.: 1979)* 64(2):330–37.

González-Bosch, Carmen, Emily Boorman, Patricia A. Zunszain, and Giovanni E. Mann. 2021. “Short-Chain Fatty Acids as Modulators of Redox Signaling in Health and Disease.” *Redox Biology* 47:102165.

González-Correa, Cristina, Javier Moleón, Sofía Miñano, Iñaki Robles-Vera, Marta Toral, Natividad Martín-Morales, Francisco O'Valle, Manuel Sánchez, Manuel Gómez-Guzmán, Rosario Jiménez, Miguel Romero, and Juan Duarte. 2023. "Mineralocorticoid Receptor Blockade Improved Gut Microbiota Dysbiosis by Reducing Gut Sympathetic Tone in Spontaneously Hypertensive Rats." *Biomedicine & Pharmacotherapy = Biomedecine & Pharmacotherapie* 158:114149.

González-Correa, Cristina, Javier Moleón, Sofía Miñano, Néstor de la Visitación, Iñaki Robles-Vera, Manuel Gómez-Guzmán, Rosario Jiménez, Miguel Romero, and Juan Duarte. 2021. "Trimethylamine N-Oxide Promotes Autoimmunity and a Loss of Vascular Function in Toll-like Receptor 7-Driven Lupus Mice." *Antioxidants (Basel, Switzerland)* 11(1).

De Groof, Aurélie, Patrice Hémon, Olivier Mignen, Jacques-Olivier Pers, Edward K. Wakeland, Yves Renaudineau, and Bernard R. Lauwerys. 2017. "Dysregulated Lymphoid Cell Populations in Mouse Models of Systemic Lupus Erythematosus." *Clinical Reviews in Allergy & Immunology* 53(2):181–97.

Guan, Peng, Yingran Liang, and Na Wang. 2018. "Fasudil Alleviates Pressure Overload-Induced Heart Failure by Activating Nrf2-Mediated Antioxidant Responses." *Journal of Cellular Biochemistry* 119(8):6452–60.

Guzik, Tomasz J., Nyssa E. Hoch, Kathryn A. Brown, Louise A. McCann, Ayaz Rahman, Sergey Dikalov, Jorg Goronzy, Cornelia Weyand, and David G. Harrison. 2007. "Role of the T Cell in the Genesis of Angiotensin II Induced Hypertension and Vascular Dysfunction." *The Journal of Experimental Medicine* 204(10):2449–60.

Hak, A. Elisabeth, Elizabeth W. Karlson, Diane Feskanich, Meir J. Stampfer, and Karen H. Costenbader. 2009. "Systemic Lupus Erythematosus and the Risk of Cardiovascular Disease: Results from the Nurses' Health Study." *Arthritis and Rheumatism* 61(10):1396–1402.

Halkom, Alya, Haijing Wu, and Qianjin Lu. 2020. "Contribution of Mouse Models in Our Understanding of Lupus." *International Reviews of Immunology* 39(4):174–87.

He, Jingquan, Tianlong Chan, Xiaoping Hong, Fengping Zheng, Chengxin Zhu, Lianghong Yin, Weier Dai, Donge Tang, Dongzhou Liu, and Yong Dai. 2020. "Microbiome and Metabolome Analyses Reveal the Disruption of Lipid Metabolism in Systemic Lupus Erythematosus." *Frontiers in Immunology* 11:1703.

He, Zhixing, Tiejuan Shao, Haichang Li, Zhijun Xie, and Chengping Wen. 2016. “Alterations of the Gut Microbiome in Chinese Patients with Systemic Lupus Erythematosus.” *Gut Pathogens* 8:64.

Hennessy, Elizabeth J., Andrew E. Parker, and Luke A. J. O’Neill. 2010. “Targeting Toll-like Receptors: Emerging Therapeutics?” *Nature Reviews. Drug Discovery* 9(4):293–307.

Hevia, Arancha, Christian Milani, Patricia López, Adriana Cuervo, Silvia Arboleya, Sabrina Duranti, Francesca Turroni, Sonia González, Ana Suárez, Miguel Gueimonde, Marco Ventura, Borja Sánchez, and Abelardo Margolles. 2014. “Intestinal Dysbiosis Associated with Systemic Lupus Erythematosus.” *MBio* 5(5).

Higashi, Midoriko, Hiroaki Shimokawa, Tsuyoshi Hattori, Junko Hiroki, Yasushi Mukai, Keiko Morikawa, Toshihiro Ichiki, Shosuke Takahashi, and Akira Takeshita. 2003. “Long-Term Inhibition of Rho-Kinase Suppresses Angiotensin II-Induced Cardiovascular Hypertrophy in Rats in Vivo: Effect on Endothelial NAD(P)H Oxidase System.” *Circulation Research* 93(8):767–75.

Hill, Gary S., Michel Delahousse, Dominique Nochy, and Jean Bariéty. 2005. “Class IV-S versus Class IV-G Lupus Nephritis: Clinical and Morphologic Differences Suggesting Different Pathogenesis.” *Kidney International* 68(5):2288–97.

Hochberg, M. C. 1997. “Updating the American College of Rheumatology Revised Criteria for the Classification of Systemic Lupus Erythematosus.” *Arthritis and Rheumatism* 40(9):1725.

Hong, Yeon-Hee, Yukihiko Nishimura, Daisuke Hishikawa, Hiroaki Tsuzuki, Hisae Miyahara, Chizu Gotoh, Ki-Choon Choi, Dan Dan Feng, Chen Chen, Hong-Gu Lee, Kazuo Katoh, Sang-Gun Roh, and Shinichi Sasaki. 2005. “Acetate and Propionate Short Chain Fatty Acids Stimulate Adipogenesis via GPCR43.” *Endocrinology* 146(12):5092–99.

Iatcu, Camelia Oana, Aimee Steen, and Mihai Covasa. 2021. “Gut Microbiota and Complications of Type-2 Diabetes.” *Nutrients* 14(1).

Ikdahl, Eirik, Grunde Wibetoe, Silvia Rollefstad, Anne Salberg, Kjetil Bergsmark, Tore K. Kvien, Inge C. Olsen, Dag Magnar Soldal, Gunnstein Bakland, Åse Lexberg, Bjørg Tilde Svanes Fevang, Hans Christian Gulseth, Glenn Haugeberg, and Anne Grete Semb. 2019. “Guideline Recommended Treatment to Targets of Cardiovascular Risk Is Inadequate in Patients with Inflammatory Joint Diseases.” *International Journal of Cardiology* 274:311–18.

Islam, Md Asiful, Shahad Saif Khandker, Przemysław J. Kotyla, and Rosline Hassan. 2020. “Immunomodulatory Effects of Diet and Nutrients in Systemic Lupus Erythematosus (SLE): A Systematic Review.” *Frontiers in Immunology* 11:1477.

Ito, K. and D. Murphy. 2013. “Application of Ggplot2 to Pharmacometric Graphics.” *CPT: Pharmacometrics & Systems Pharmacology* 2(10):e79.

Jama, Hamdi A., Dakota Rhys-Jones, Michael Nakai, Chu K. Yao, Rachel E. Climie, Yusuke Sata, Dovile Anderson, Darren J. Creek, Geoffrey A. Head, David M. Kaye, Charles R. Mackay, Jane Muir, and Francine Z. Marques. 2023. “Prebiotic Intervention with HAMSAB in Untreated Essential Hypertensive Patients Assessed in a Phase II Randomized Trial.” *Nature Cardiovascular Research* 2(1):35–43.

Jenks, Scott A., Kevin S. Cashman, Esther Zumaquero, Urko M. Marigorta, Aakash V Patel, Xiaoqian Wang, Deepak Tomar, Matthew C. Woodruff, Zoe Simon, Regina Bugrovsky, Emily L. Blalock, Christopher D. Scharer, Christopher M. Tipton, Chungwen Wei, S. Sam Lim, Michelle Petri, Timothy B. Niewold, Jennifer H. Anolik, Greg Gibson, F. Eun-Hyung Lee, Jeremy M. Boss, Frances E. Lund, and Ignacio Sanz. 2018. “Distinct Effector B Cells Induced by Unregulated Toll-like Receptor 7 Contribute to Pathogenic Responses in Systemic Lupus Erythematosus.” *Immunity* 49(4):725-739.e6.

Jiang, Tao, Fei Tian, Hongting Zheng, Samantha A. Whitman, Yifeng Lin, Zhigang Zhang, Nong Zhang, and Donna D. Zhang. 2014. “Nrf2 Suppresses Lupus Nephritis through Inhibition of Oxidative Injury and the NF-KB-Mediated Inflammatory Response.” *Kidney International* 85(2):333–43.

Jin, Jiajia, Liaomei Gao, Xiuli Zou, Yun Zhang, Zhijian Zheng, Xinjie Zhang, Jiaxuan Li, Zhenyu Tian, Xiaowei Wang, Junfei Gu, Cheng Zhang, Tiejun Wu, Zhe Wang, and Qunye Zhang. 2022. “Gut Dysbiosis Promotes Preeclampsia by Regulating Macrophages and Trophoblasts.” *Circulation Research* 131(6):492–506.

Johansson, Malin E. V and Gunnar C. Hansson. 2016. “Immunological Aspects of Intestinal Mucus and Mucins.” *Nature Reviews. Immunology* 16(10):639–49.

Karbach, Susanne H., Tanja Schönfelder, Ines Brandão, Eivor Wilms, Nives Hörmann, Sven Jäckel, Rebecca Schüler, Stefanie Finger, Maike Knorr, Jeremy Lagrange, Moritz Brandt, Ari Waisman, Sabine Kossmann, Katrin Schäfer, Thomas Münzel, Christoph Reinhardt, and Philip Wenzel. 2016. “Gut Microbiota Promote Angiotensin II-Induced Arterial Hypertension and Vascular

Dysfunction." *Journal of the American Heart Association* 5(9).

Katiraei, Saeed, Margreet R. de Vries, Alice H. Costain, Kathrin Thiem, Lisa R. Hoving, Janna A. van Diepen, Hermelijn H. Smits, Kristien E. Bouter, Patrick C. N. Rensen, Paul H. A. Quax, Max Nieuwdorp, Mihai G. Netea, Willem M. de Vos, Patrice D. Cani, Clara Belzer, Ko Willems van Dijk, Jimmy F. P. Berbée, and Vanessa van Harmelen. 2020. "Akkermansia Muciniphila Exerts Lipid-Lowering and Immunomodulatory Effects without Affecting Neointima Formation in Hyperlipidemic APOE*3-Leiden.CETP Mice." *Molecular Nutrition & Food Research* 64(15):e1900732.

Katz-Agranov, Nurit and Gisele Zandman-Goddard. 2017. "The Microbiome and Systemic Lupus Erythematosus." *Immunologic Research* 65(2):432–37.

Kaul, Arvind, Caroline Gordon, Mary K. Crow, Zahi Touma, Murray B. Urowitz, Ronald van Vollenhoven, Guillermo Ruiz-Irastorza, and Graham Hughes. 2016. "Systemic Lupus Erythematosus." *Nature Reviews. Disease Primers* 2:16039.

Kaye, David M., Waled A. Shihata, Hamdi A. Jama, Kirill Tsyganov, Mark Ziemann, Helen Kiriazis, Duncan Horlock, Amrita Vijay, Beverly Giam, Antony Vinh, Chad Johnson, April Fiedler, Daniel Donner, Matthew Snelson, Melinda T. Coughlan, Sarah Phillips, Xiao-Jun Du, Assam El-Osta, Grant Drummond, Gavin W. Lambert, Tim D. Spector, Ana M. Valdes, Charles R. Mackay, and Francine Z. Marques. 2020. "Deficiency of Prebiotic Fiber and Insufficient Signaling Through Gut Metabolite-Sensing Receptors Leads to Cardiovascular Disease." *Circulation* 141(17):1393–1403.

Kelley, V. R. and R. P. Wuthrich. 1999. "Cytokines in the Pathogenesis of Systemic Lupus Erythematosus." *Seminars in Nephrology* 19(1):57–66.

Kelly, Caleb J. and Sean P. Colgan. 2016. "Breathless in the Gut: Implications of Luminal O2 for Microbial Pathogenicity." *Cell Host & Microbe* 19(4):427–28.

Khoryati, Liliane, Jean-François Augusto, Emilie Shipley, Cécile Contin-Bordes, Isabelle Douchet, Stéphane Mitrovic, Marie-Elise Truchetet, Estibaliz Lazaro, Pierre Duffau, Lionel Couzi, Clément Jacquemin, Thomas Barnetche, Pierre Vacher, Thierry Schaeverbeke, Patrick Blanco, and Christophe Richez. 2016. "IgE Inhibits Toll-like Receptor 7- and Toll-like Receptor 9-Mediated Expression of Interferon-α by Plasmacytoid Dendritic Cells in Patients With Systemic Lupus Erythematosus." *Arthritis & Rheumatology (Hoboken, N.J.)* 68(9):2221–31.

Kim, Ji-Won, Seung-Ki Kwok, Jung-Yoon Choe, and Sung-Hwan Park. 2019. “Recent Advances in Our Understanding of the Link between the Intestinal Microbiota and Systemic Lupus Erythematosus.” *International Journal of Molecular Sciences* 20(19).

Kim, S., R. Goel, A. Kumar, Y. Qi, G. Lobaton, K. Hosaka, M. Mohammed, E. M. Handberg, E. M. Richards, C. J. Pepine, and M. K. Raizada. 2018. “Imbalance of Gut Microbiome and Intestinal Epithelial Barrier Dysfunction in Patients with High Blood Pressure.” *Clin Sci (Lond)*.

Kimura, Akihiro and Tadamitsu Kishimoto. 2010. “IL-6: Regulator of Treg/Th17 Balance.” *European Journal of Immunology* 40(7):1830–35.

Kinashi, Yusuke and Koji Hase. 2021. “Partners in Leaky Gut Syndrome: Intestinal Dysbiosis and Autoimmunity.” *Frontiers in Immunology* 12:673708.

Kiriakidou, Marianthi and Cathy Lee Ching. 2020. “Systemic Lupus Erythematosus.” *Annals of Internal Medicine* 172(11):ITC81–96.

Krasselt, Marco and Christoph Baerwald. 2019. “Sex, Symptom Severity, and Quality of Life in Rheumatology.” *Clinical Reviews in Allergy & Immunology* 56(3):346–61.

de la Visitación, Néstor, Iñaki Robles-Vera, Javier Moleón-Moya, Manuel Sánchez, Rosario Jiménez, Manuel Gómez-Guzmán, Cristina González-Correa, Mónica Olivares, Marta Toral, Miguel Romero, and Juan Duarte. 2021. “Probiotics Prevent Hypertension in a Murine Model of Systemic Lupus Erythematosus Induced by Toll-Like Receptor 7 Activation.” *Nutrients* 13(8).

de la Visitación, Néstor, Iñaki Robles-Vera, Javier Moleón, Cristina González-Correa, Nazaret Aguilera-Sánchez, Marta Toral, Manuel Gómez-Guzmán, Manuel Sánchez, Rosario Jiménez, Natividad Martin-Morales, Francisco O’Valle, Miguel Romero, and Juan Duarte. 2021. “Gut Microbiota Has a Crucial Role in the Development of Hypertension and Vascular Dysfunction in Toll-like Receptor 7-Driven Lupus Autoimmunity.” *Antioxidants (Basel, Switzerland)* 10(9).

de la Visitación, Néstor, Iñaki Robles-Vera, Marta Toral, and Juan Duarte. 2019. “Protective Effects of Probiotic Consumption in Cardiovascular Disease in Systemic Lupus Erythematosus.” *Nutrients* 11(11).

de la Visitación, Néstor, Iñaki Robles-Vera, Marta Toral, Manuel Gómez-Guzmán, Manuel Sánchez, Javier Moleón, Cristina González-Correa, Natividad Martín-Morales, Francisco O’Valle, Rosario Jiménez, Miguel Romero, and Juan

Duarte. 2021. “Gut Microbiota Contributes to the Development of Hypertension in a Genetic Mouse Model of Systemic Lupus Erythematosus.” *British Journal of Pharmacology* 178(18):3708–29.

Lavin, Richard, Nicholas DiBenedetto, Vladimir Yeliseyev, Mary Delaney, and Lynn Bry. 2018. “Gnotobiotic and Conventional Mouse Systems to Support Microbiota Based Studies.” *Current Protocols in Immunology* 121(1):e48.

Lee, Tai-Ping, Shye-Jye Tang, Ming-Fang Wu, Ying-Chyi Song, Chia-Li Yu, and Kuang-Hui Sun. 2010. “Transgenic Overexpression of Anti-Double-Stranded DNA Autoantibody and Activation of Toll-like Receptor 4 in Mice Induce Severe Systemic Lupus Erythematosus Syndromes.” *Journal of Autoimmunity* 35(4):358–67.

Li, Jin, Shaoqiang Lin, Paul M. Vanhoutte, Connie W. Woo, and Aimin Xu. 2016. “Akkermansia Muciniphila Protects Against Atherosclerosis by Preventing Metabolic Endotoxemia-Induced Inflammation in Apoe-/- Mice.” *Circulation* 133(24):2434–46.

Li, Jing, Xiaohui Wang, Fengchun Zhang, and Hang Yin. 2013. “Toll-like Receptors as Therapeutic Targets for Autoimmune Connective Tissue Diseases.” *Pharmacology & Therapeutics* 138(3):441–51.

Li, Jing, Fangqing Zhao, Yidan Wang, Junru Chen, Jie Tao, Gang Tian, Shouling Wu, Wenbin Liu, Qinghua Cui, Bin Geng, Weili Zhang, Ryan Weldon, Kelda Auguste, Lei Yang, Xiaoyan Liu, Li Chen, Xinchun Yang, Baoli Zhu, and Jun Cai. 2017. “Gut Microbiota Dysbiosis Contributes to the Development of Hypertension.” *Microbiome* 5(1):14.

Li, Li and Chandra Mohan. 2007. “Genetic Basis of Murine Lupus Nephritis.” *Seminars in Nephrology* 27(1):12–21.

Li, Yao, Hai-Fang Wang, Xin Li, Hai-Xia Li, Qiong Zhang, Hong-Wei Zhou, Yan He, Pan Li, Chen Fu, Xiao-He Zhang, Yu-Rong Qiu, and Ji-Liang Li. 2019. “Disordered Intestinal Microbes Are Associated with the Activity of Systemic Lupus Erythematosus.” *Clinical Science (London, England : 1979)* 133(7):821–38.

Li, Yuhua, Ling Liang, Xiaoli Deng, and Lijun Zhong. 2019. “Lipidomic and Metabolomic Profiling Reveals Novel Candidate Biomarkers in Active Systemic Lupus Erythematosus.” *International Journal of Clinical and Experimental Pathology* 12(3):857–66.

Liang, Chao Fan, Jacky Tc Liu, Yu Wang, Aimin Xu, and Paul M. Vanhoutte. 2013. "Toll-like Receptor 4 Mutation Protects Obese Mice against Endothelial Dysfunction by Decreasing NADPH Oxidase Isoforms 1 and 4." *Arteriosclerosis, Thrombosis, and Vascular Biology* 33(4):777–84.

Liu, Yudong and Mariana J. Kaplan. 2018. "Cardiovascular Disease in Systemic Lupus Erythematosus: An Update." *Current Opinion in Rheumatology* 30(5):441–48.

Liu, Yudong, Nickie L. Seto, Carmelo Carmona-Rivera, and Mariana J. Kaplan. 2018. "Accelerated Model of Lupus Autoimmunity and Vasculopathy Driven by Toll-like Receptor 7/9 Imbalance." *Lupus Science & Medicine* 5(1):e000259.

Liu, Zheng and Anne Davidson. 2012. "Taming Lupus-a New Understanding of Pathogenesis Is Leading to Clinical Advances." *Nature Medicine* 18(6):871–82.

López, Patricia, Borja Sánchez, Abelardo Margolles, and Ana Suárez. 2016. "Intestinal Dysbiosis in Systemic Lupus Erythematosus: Cause or Consequence?" *Current Opinion in Rheumatology* 28(5):515–22.

Lu, Jing, Yujuan Li, Xinyue Wang, and Min Wu. 2022. "Immune Mechanism of Gut Microbiota and Its Metabolites in the Occurrence and Development of Cardiovascular Diseases." (December).

Luo, Xin M., Michael R. Edwards, Qinghui Mu, Yang Yu, Miranda D. Vieson, Christopher M. Reilly, S. Ansar Ahmed, and Adegbenga A. Bankole. 2018. "Gut Microbiota in Human Systemic Lupus Erythematosus and a Mouse Model of Lupus." *Applied and Environmental Microbiology* 84(4).

Luu, Maik and Alexander Visekruna. 2019. "Short-Chain Fatty Acids: Bacterial Messengers Modulating the Immunometabolism of T Cells." *European Journal of Immunology* 49(6):842–48.

Ma, GuoHua, Bing Pan, Yue Chen, CaiXia Guo, MingMing Zhao, LeMin Zheng, and BuXing Chen. 2017. "Trimethylamine N-Oxide in Atherogenesis: Impairing Endothelial Self-Repair Capacity and Enhancing Monocyte Adhesion." *Bioscience Reports* 37(2).

Ma, Yiyangzi, Ruru Guo, Yiduo Sun, Xin Li, Lun He, Zhao Li, Gregg J. Silverman, Guobing Chen, Feng Gao, Jiali Yuan, Qiang Wei, Mengtao Li, Liangjing Lu, and Haitao Niu. 2021. "Lupus Gut Microbiota Transplants Cause Autoimmunity and Inflammation." *Clinical Immunology (Orlando, Fla.)* 233:108892.

Ma, Yiyangzi, Xiaoxue Xu, Mengtao Li, Jun Cai, Qiang Wei, and Haitao Niu. 2019. “Gut Microbiota Promote the Inflammatory Response in the Pathogenesis of Systemic Lupus Erythematosus.” *Molecular Medicine (Cambridge, Mass.)* 25(1):35.

Macia, Laurence, Jian Tan, Angelica T. Vieira, Katie Leach, Dragana Stanley, Suzanne Luong, Mikako Maruya, Craig Ian McKenzie, Atsushi Hijikata, Connie Wong, Lauren Binge, Alison N. Thorburn, Nina Chevalier, Caroline Ang, Eliana Marino, Remy Robert, Stefan Offermanns, Mauro M. Teixeira, Robert J. Moore, Richard A. Flavell, Sidonia Fagarasan, and Charles R. Mackay. 2015. “Metabolite-Sensing Receptors GPR43 and GPR109A Facilitate Dietary Fibre-Induced Gut Homeostasis through Regulation of the Inflammasome.” *Nature Communications* 6:6734.

MacKay, Charles E., Yasin Shaifta, Vladimir V Snetkov, Asvi A. Francois, Jeremy P. T. Ward, and Greg A. Knock. 2017. “ROS-Dependent Activation of RhoA/Rho-Kinase in Pulmonary Artery: Role of Src-Family Kinases and ARHGEF1.” *Free Radical Biology & Medicine* 110:316–31.

Mackensen, Andreas, Fabian Müller, Dimitrios Mougiakakos, Sebastian Böltz, Artur Wilhelm, Michael Aigner, Simon Völkl, David Simon, Arnd Kleyer, Luis Munoz, Sascha Kretschmann, Soraya Kharboutli, Regina Gary, Hannah Reimann, Wolf Rösler, Stefan Uderhardt, Holger Bang, Martin Herrmann, Arif Bülent Ekici, Christian Buettner, Katharina Marie Habenicht, Thomas H. Winkler, Gerhard Krönke, and Georg Schett. 2022. “Anti-CD19 CAR T Cell Therapy for Refractory Systemic Lupus Erythematosus.” *Nature Medicine* 28(10):2124–32.

Madhur, Meena S., Heinrich E. Lob, Louise A. McCann, Yoichiro Iwakura, Yelena Blinder, Tomasz J. Guzik, and David G. Harrison. 2010. “Interleukin 17 Promotes Angiotensin II-Induced Hypertension and Vascular Dysfunction.” *Hypertension (Dallas, Tex. : 1979)* 55(2):500–507.

Manfredo Vieira, S., M. Hiltensperger, V. Kumar, D. Zegarra-Ruiz, C. Dehner, N. Khan, F. R. C. Costa, E. Tiniakou, T. Greiling, W. Ruff, A. Barbieri, C. Kriegel, S. S. Mehta, J. R. Knight, D. Jain, A. L. Goodman, and M. A. Kriegel. 2018. “Translocation of a Gut Pathobiont Drives Autoimmunity in Mice and Humans.” *Science (New York, N.Y.)* 359(6380):1156–61.

Manzi, Susan, Elaine N. Meilahn, Joan E. Rairie, Claudia G. Conte, Thomas A. Medsger, Linda Jansen-Mcwilliams, Ralph B. D’agostino, and Lewis H. Kuller. 1997. *Age-Specific Incidence Rates of Myocardial Infarction and Angina in Women with Systemic Lupus Erythematosus: Comparison with the Framingham Study*. Vol. 145.

Marques, Francine Z., Hamdi A. Jama, Kirill Tsyganov, Paul A. Gill, Dakota Rhys-Jones, Rikeish R. Muralitharan, Jane Muir, Andrew Holmes, and Charles R. Mackay. 2019. “Guidelines for Transparency on Gut Microbiome Studies in Essential and Experimental Hypertension.” *Hypertension (Dallas, Tex. : 1979)* 74(6):1279–93.

Marques, Francine Z., Erin Nelson, Po-Yin Chu, Duncan Horlock, April Fiedler, Mark Ziemann, Jian K. Tan, Sanjaya Kuruppu, Niwanthi W. Rajapakse, Assam El-Osta, Charles R. Mackay, and David M. Kaye. 2017. “High-Fiber Diet and Acetate Supplementation Change the Gut Microbiota and Prevent the Development of Hypertension and Heart Failure in Hypertensive Mice.” *Circulation* 135(10):964–77.

Martel, Jan, Shih-Hsin Chang, Yun-Fei Ko, Tsong-Long Hwang, John D. Young, and David M. Ojcius. 2022. “Gut Barrier Disruption and Chronic Disease.” *Trends in Endocrinology and Metabolism: TEM* 33(4):247–65.

Maslowski, Kendle M., Angelica T. Vieira, Aylwin Ng, Jan Kranich, Frederic Sierro, Di Yu, Heidi C. Schilter, Michael S. Rolph, Fabienne Mackay, David Artis, Ramnik J. Xavier, Mauro M. Teixeira, and Charles R. Mackay. 2009. “Regulation of Inflammatory Responses by Gut Microbiota and Chemoattractant Receptor GPR43.” *Nature* 461(7268):1282–86.

Mathis, K. W., M. Venegas-Pont, C. W. Masterson, N. J. Stewart, K. L. Wasson, and M. J. Ryan. 2012. “Oxidative Stress Promotes Hypertension and Albuminuria During the Autoimmune Disease Systemic Lupus Erythematosus.” *Hypertension* 59(3):673–79.

Mathis, Keisa W., Kedra Wallace, Elizabeth R. Flynn, Christine Maric-Bilkan, Babbette LaMarca, and Michael J. Ryan. 2014. “Preventing Autoimmunity Protects against the Development of Hypertension and Renal Injury.” *Hypertension (Dallas, Tex. : 1979)* 64(4):792–800.

McCallum, Giselle and Carolina Tropini. 2023. “The Gut Microbiota and Its Biogeography.” *Nature Reviews. Microbiology*.

van der Meulen, Taco A., Hermie J. M. Harmsen, Arnau Vich Vila, Alexander Kurilshikov, Silvia C. Liefers, Alexandra Zhernakova, Jingyuan Fu, Cisca Wijmenga, Rinse K. Weersma, Karina de Leeuw, Hendrika Bootsma, Fred K. L. Spijkervet, Arjan Vissink, and Frans G. M. Kroese. 2019. “Shared Gut, but Distinct Oral Microbiota Composition in Primary Sjögren’s Syndrome and Systemic Lupus Erythematosus.” *Journal of Autoimmunity* 97:77–87.

Milligan, Graeme, Leigh A. Stoddart, and Nicola J. Smith. 2009. “Agonism and Allosterism: The Pharmacology of the Free Fatty Acid Receptors FFA2 and FFA3.” *British Journal of Pharmacology* 158(1):146–53.

Minami, Yuko, Yasuhiko Hirabayashi, Chisato Nagata, Tomonori Ishii, Hideo Harigae, and Takeshi Sasaki. 2011. “Intakes of Vitamin B6 and Dietary Fiber and Clinical Course of Systemic Lupus Erythematosus: A Prospective Study of Japanese Female Patients.” *Journal of Epidemiology* 21(4):246–54.

Moleón, Javier, Cristina González-Correa, Iñaki Robles-Vera, Sofía Miñano, Néstor de la Visitación, Antonio Manuel Barranco, Natividad Martín-Morales, Francisco O’Valle, Laura Mayo-Martínez, Antonia García, Marta Toral, Rosario Jiménez, Miguel Romero, and Juan Duarte. 2023. “Targeting the Gut Microbiota with Dietary Fibers: A Novel Approach to Prevent the Development Cardiovascular Complications Linked to Systemic Lupus Erythematosus in a Preclinical Study.” *Gut Microbes* 15(2):2247053.

Mora, J. R. and U. H. von Andrian. 2008. “Differentiation and Homing of IgA-Secreting Cells.” *Mucosal Immunology* 1(2):96–109.

Mouries, Juliette, Paola Brescia, Alessandra Silvestri, Ilaria Spadoni, Marcel Sorribas, Reiner Wiest, Erika Mileti, Marianna Galbiati, Pietro Invernizzi, Luciano Adorini, Giuseppe Penna, and Maria Rescigno. 2019. “Microbiota-Driven Gut Vascular Barrier Disruption Is a Prerequisite for Non-Alcoholic Steatohepatitis Development.” *Journal of Hepatology* 71(6):1216–28.

Mu, Qinghui, Michael R. Edwards, Brianna K. Swartwout, Xavier Cabana Puig, Jiangdi Mao, Jing Zhu, Joe Grieco, Thomas E. Cecere, Meeta Prakash, Christopher M. Reilly, Christopher Puglisi, Prathyusha Bachali, Amrie C. Grammer, Peter E. Lipsky, and Xin M. Luo. 2020. “Gut Microbiota and Bacterial DNA Suppress Autoimmunity by Stimulating Regulatory B Cells in a Murine Model of Lupus.” *Frontiers in Immunology* 11:593353.

Mu, Qinghui, Vincent J. Tavella, Jay L. Kirby, Thomas E. Cecere, Matthias Chung, Jiyoung Lee, Song Li, S. Ansar Ahmed, Kristin Eden, Irving Coy Allen, Christopher M. Reilly, and Xin M. Luo. 2017. “Antibiotics Ameliorate Lupus-like Symptoms in Mice.” *Scientific Reports* 7(1):13675.

Mu, Qinghui, Husen Zhang, Xiaofeng Liao, Kaisen Lin, Hualan Liu, Michael R. Edwards, S. Ansar Ahmed, Ruoxi Yuan, Liwu Li, Thomas E. Cecere, David B. Branson, Jay L. Kirby, Poorna Goswami, Caroline M. Leeth, Kaitlin A. Read, Kenneth J. Oestreich, Miranda D. Vieson, Christopher M. Reilly, and Xin M. Luo. 2017. “Control of Lupus Nephritis by Changes of Gut Microbiota.” *Microbiome* 5(1):73.

Murphy, E D and J. B. Roths. 1978. “New Inbred Strains.” *Mouse News Lett* 58:51–52.

Murphy, Edwin D and John B. Roths. 1978. “A Single Gene Model for Massive Lymphoproliferation with Immune Complex Disease in New Mouse Strain MRL.”

Namour, Florence, René Galien, Tim Van Kaem, Annegret Van der Aa, Frédéric Vanhoutte, Johan Beetens, and Gerben Van’t Klooster. 2016. “Safety, Pharmacokinetics and Pharmacodynamics of GLPG0974, a Potent and Selective FFA2 Antagonist, in Healthy Male Subjects.” *British Journal of Clinical Pharmacology* 82(1):139–48.

Nandakumar, Kutty Selva and Kerstin Nündel. 2022. “Editorial: Systemic Lupus Erythematosus - Predisposition Factors, Pathogenesis, Diagnosis, Treatment and Disease Models.” *Frontiers in Immunology* 13:1118180.

Nguyen, Hoanglan, Valorie L. Chiasson, Piyali Chatterjee, Shelley E. Kopriva, Kristina J. Young, and Brett M. Mitchell. 2013. “Interleukin-17 Causes Rho-Kinase-Mediated Endothelial Dysfunction and Hypertension.” *Cardiovascular Research* 97(4):696–704.

Niess, Jan Hendrik, Stephan Brand, Xiubin Gu, Limor Landsman, Steffen Jung, Beth A. McCormick, Jatin M. Vyas, Marianne Boes, Hidde L. Ploegh, James G. Fox, Dan R. Littman, and Hans-Christian Reinecker. 2005. “CX3CR1-Mediated Dendritic Cell Access to the Intestinal Lumen and Bacterial Clearance.” *Science (New York, N.Y.)* 307(5707):254–58.

Nosalski, Ryszard and Tomasz J. Guzik. 2017. “Perivascular Adipose Tissue Inflammation in Vascular Disease.” *British Journal of Pharmacology* 174(20):3496–3513.

Oliveira, Christopher B. and Mariana J. Kaplan. 2022. “Cardiovascular Disease Risk and Pathogenesis in Systemic Lupus Erythematosus.” *Seminars in Immunopathology* 44(3):309–24.

La Paglia, Giuliana Maria Concetta, Maria Comasia Leone, Gemma Lepri, Roberta Vagelli, Eleonora Valentini, Alessia Alunno, and Chiara Tani. 2017. “One Year in Review 2017: Systemic Lupus Erythematosus.” *Clinical and Experimental Rheumatology* 35(4):551–61.

Pan, Quanren, Fengbiao Guo, Yanyan Huang, Aifen Li, Shuxian Chen, Jiaxuan Chen, Hua-Feng Liu, and Qingjun Pan. 2021. “Gut Microbiota Dysbiosis in Systemic Lupus Erythematosus: Novel Insights into Mechanisms and Promising Therapeutic Strategies.” *Frontiers in Immunology* 12:799788.

Parada Venegas, Daniela, Marjorie K. De la Fuente, Glauben Landskron, María Julieta González, Rodrigo Quera, Gerard Dijkstra, Hermie J. M. Harmsen, Klaas Nico Faber, and Marcela A. Hermoso. 2019. “Corrigendum: Short Chain Fatty Acids (SCFAs)-Mediated Gut Epithelial and Immune Regulation and Its Relevance for Inflammatory Bowel Diseases.” *Frontiers in Immunology* 10:1486.

Park, Jung-Ha, Takenori Kotani, Tasuku Konno, Jajar Setiawan, Yasuaki Kitamura, Shinya Imada, Yutaro Usui, Naoya Hatano, Masakazu Shinohara, Yasuyuki Saito, Yoji Murata, and Takashi Matozaki. 2016. “Promotion of Intestinal Epithelial Cell Turnover by Commensal Bacteria: Role of Short-Chain Fatty Acids.” *PloS One* 11(5):e0156334.

Patrick, David M., Néstor de la Visitación, Jaya Krishnan, Wei Chen, Michelle J. Ormseth, C. Michael Stein, Sean S. Davies, Venkataraman Amarnath, Leslie J. Crofford, Jonathan M. Williams, Shilin Zhao, Charles D. Smart, Sergey Dikalov, Anna Dikalova, Liang Xiao, Justin P. Van Beusecum, Mingfang Ao, Agnes B. Fogo, Annet Kirabo, and David G. Harrison. 2022. “Isolevuglandins Disrupt PU.1-Mediated C1q Expression and Promote Autoimmunity and Hypertension in Systemic Lupus Erythematosus.” *JCI Insight* 7(13).

Percie du Sert, Nathalie, Viki Hurst, Amrita Ahluwalia, Sabina Alam, Marc T. Avey, Monya Baker, William J. Browne, Alejandra Clark, Innes C. Cuthill, Ulrich Dirnagl, Michael Emerson, Paul Garner, Stephen T. Holgate, David W. Howells, Natasha A. Karp, Stanley E. Lazic, Katie Lidster, Catriona J. MacCallum, Malcolm Macleod, Esther J. Pearl, Ole H. Petersen, Frances Rawle, Penny Reynolds, Kieron Rooney, Emily S. Sena, Shai D. Silberberg, Thomas Steckler, and Hanno Würbel. 2020. “The ARRIVE Guidelines 2.0: Updated Guidelines for Reporting Animal Research.” *British Journal of Pharmacology* 177(16):3617–24.

Peterson, Lance W. and David Artis. 2014. “Intestinal Epithelial Cells: Regulators of Barrier Function and Immune Homeostasis.” *Nature Reviews. Immunology* 14(3):141–53.

Petrin, J., B. Rozman, P. Dolenc, D. Logar, B. Bozic, A. Vizjak, D. Ferluga, and P. Jezersek. 1993. “The Dissociation of Arterial Hypertension and Lupus Glomerulonephritis in Systemic Lupus Erythematosus.” *Blood Pressure* 2(2):108–12.

Pietrowski, Eweline, Bianca Bender, Jula Huppert, Robin White, Heiko J. Luhmann, and Christoph R. W. Kuhlmann. 2011. “Pro-Inflammatory Effects of Interleukin-17A on Vascular Smooth Muscle Cells Involve NAD(P)H- Oxidase Derived Reactive Oxygen Species.” *Journal of Vascular Research* 48(1):52–58.

Plovier, Hubert, Amandine Everard, Céline Druart, Clara Depommier, Matthias Van Hul, Lucie Geurts, Julien Chilloux, Noora Ottman, Thibaut Duparc, Laeticia Lichtenstein, Antonis Myridakis, Nathalie M. Delzenne, Judith Klievink, Arnab Bhattacharjee, Kees C. H. van der Ark, Steven Aalvink, Laurent O. Martinez, Marc-Emmanuel Dumas, Dominique Maiter, Audrey Loumaye, Michel P. Hermans, Jean-Paul Thissen, Clara Belzer, Willem M. de Vos, and Patrice D. Cani. 2017. “A Purified Membrane Protein from Akkermansia Muciniphila or the Pasteurized Bacterium Improves Metabolism in Obese and Diabetic Mice.” *Nature Medicine* 23(1):107–13.

Pluznick, Jennifer L. 2013. “Renal and Cardiovascular Sensory Receptors and Blood Pressure Regulation.” *American Journal of Physiology. Renal Physiology* 305(4):F439-44.

Regen, Tommy, Sandrine Isaac, Ana Amorim, Nicolás Gonzalo Núñez, Judith Hauptmann, Arthi Shanmugavadivu, Matthias Klein, Roman Sankowski, Ilgiz A. Mufazalov, Nir Yogev, Jula Huppert, Florian Wanke, Michael Witting, Alexandra Grill, Eric J. C. Gálvez, Alexei Nikolaev, Michaela Blanfeld, Immo Prinz, Philippe Schmitt-Kopplin, Till Strowig, Christoph Reinhardt, Marco Prinz, Tobias Bopp, Burkhard Becher, Carles Ubeda, and Ari Waisman. 2021. “IL-17 Controls Central Nervous System Autoimmunity through the Intestinal Microbiome.” *Science Immunology* 6(56).

Reynolds, Andrew, Jim Mann, John Cummings, Nicola Winter, Evelyn Mete, and Lisa Te Morenga. 2019. “Carbohydrate Quality and Human Health: A Series of Systematic Reviews and Meta-Analyses.” *Lancet (London, England)* 393(10170):434–45.

Ritzhaupt, A., I. S. Wood, A. Ellis, K. B. Hosie, and S. P. Shirazi-Beechey. 1998. “Identification and Characterization of a Monocarboxylate Transporter (MCT1) in Pig and Human Colon: Its Potential to Transport L-Lactate as Well as Butyrate.” *The Journal of Physiology* 513 (Pt 3(Pt 3):719–32.

Robles-Vera, Iñaki, Marta Toral, and Juan Duarte. 2020. “Microbiota and Hypertension: Role of the Sympathetic Nervous System and the Immune System.” *American Journal of Hypertension* 33(10):890–901.

Robles-Vera, Iñaki, Marta Toral, Néstor de la Visitación, Nazaret Aguilera-Sánchez, Juan Miguel Redondo, and Juan Duarte. 2020. “Protective Effects of Short-Chain Fatty Acids on Endothelial Dysfunction Induced by Angiotensin II.” *Frontiers in Physiology* 11:277.

Robles-Vera, Iñaki, Marta Toral, Néstor de la Visitación, Manuel Sánchez, Manuel Gómez-Guzmán, Miguel Romero, Tao Yang, José L. Izquierdo-Garcia, Rosario Jiménez, Jesús Ruiz-Cabello, Eduardo Guerra-Hernández, Mohan K. Raizada, Francisco Pérez-Vizcaíno, and Juan Duarte. 2020. “Probiotics Prevent Dysbiosis and the Rise in Blood Pressure in Genetic Hypertension: Role of Short-Chain Fatty Acids.” *Molecular Nutrition & Food Research* 64(6):e1900616.

Robles-Vera, Iñaki, Néstor De La Visitación, Marta Toral, Manuel Sánchez, Manuel Gómez-Guzmán, Francisco O’valle, Rosario Jiménez, Juan Duarte, and Miguel Romero. 2020. “Toll-like Receptor 7-Driven Lupus Autoimmunity Induces Hypertension and Vascular Alterations in Mice.” *Journal of Hypertension* 38(7):1322–35.

Romero, Miguel, Marta Toral, Inaki Robles-Vera, Manuel Sanchez, Rosario Jimenez, Francisco O’Valle, Alba Rodriguez-Nogales, Francisco Perez-Vizcaino, Julio Galvez, and Juan Duarte. 2017. “Activation of Peroxisome Proliferator Activator Receptor Beta/Delta Improves Endothelial Dysfunction and Protects Kidney in Murine Lupus.” *Hypertension (Dallas, Tex.: 1979)* 69(4):641–50.

Rosser, Elizabeth C. and Claudia Mauri. 2016. “A Clinical Update on the Significance of the Gut Microbiota in Systemic Autoimmunity.” *Journal of Autoimmunity* 74:85–93.

Ruff, William E., Teri M. Greiling, and Martin A. Kriegel. 2020. “Host-Microbiota Interactions in Immune-Mediated Diseases.” *Nature Reviews. Microbiology* 18(9):521–38.

Ryan, Michael J. 2009. “The Pathophysiology of Hypertension in Systemic Lupus Erythematosus.” *American Journal of Physiology. Regulatory, Integrative and Comparative Physiology* 296(4):R1258-67.

Ryan, Michael J. 2013. “An Update on Immune System Activation in the Pathogenesis of Hypertension.” *Hypertension* 62(2):226–30.

Sacre, Karim, Brigitte Escoubet, Blandine Pasquet, Marie-Paule Chauveheid, Maria-Christina Zennaro, Florence Tubach, and Thomas Papo. 2014. “Increased Arterial Stiffness in Systemic Lupus Erythematosus (SLE) Patients at Low Risk for Cardiovascular Disease: A Cross-Sectional Controlled Study.” *PloS One* 9(4):e94511.

Santisteban, Monica M., Seungbum Kim, Carl J. Pepine, and Mohan K. Raizada. 2016. “Brain-Gut-Bone Marrow Axis: Implications for Hypertension and Related Therapeutics.” *Circulation Research* 118(8):1327–36.

Satoh, M. and W. H. Reeves. 1994. “Induction of Lupus-Associated Autoantibodies in BALB/c Mice by Intraperitoneal Injection of Pristane.” *The Journal of Experimental Medicine* 180(6):2341–46.

Savarese, Emina, Ohk-wha Chae, Simon Trowitzsch, Gert Weber, Berthold Kastner, Shizuo Akira, Hermann Wagner, Roland M. Schmid, Stefan Bauer, and Anne Krug. 2006. “U1 Small Nuclear Ribonucleoprotein Immune Complexes Induce Type I Interferon in Plasmacytoid Dendritic Cells through TLR7.” *Blood* 107(8):3229–34.

Schäfer, Anna-Lena, Alexandra Eichhorst, Carolin Hentze, Antoine N. Kraemer, Anaïs Amend, Dalina T. L. Sprenger, Cara Fluhr, Stephanie Finzel, Christoph Daniel, Ulrich Salzer, Marta Rizzi, Reinhard E. Voll, and Nina Chevalier. 2021. “Low Dietary Fiber Intake Links Development of Obesity and Lupus Pathogenesis.” *Frontiers in Immunology* 12:696810.

Segata, Nicola, Jacques Izard, Levi Waldron, Dirk Gevers, Larisa Miropolsky, Wendy S. Garrett, and Curtis Huttenhower. 2011. “Metagenomic Biomarker Discovery and Explanation.” *Genome Biology* 12(6):R60.

Seibold, J. R., L. R. Wechsler, and R. J. Cammarata. 1980. “LE Cells in Intermittent Hydrarthrosis.” *Arthritis and Rheumatism* 23(8):958–59.

Shafeghat, Melika, Sina Kazemian, Arya Aminorroaya, Zahra Aryan, and Nima Rezaei. 2022. “Toll-like Receptor 7 Regulates Cardiovascular Diseases.” *International Immunopharmacology* 113(Pt A):109390.

Shaharir, Syahrul Syazliana, Ruslinda Mustafar, Rozita Mohd, Mohd Shahrir Mohd Said, and Halim A. Gafor. 2015. “Persistent Hypertension in Lupus Nephritis and the Associated Risk Factors.” *Clinical Rheumatology* 34(1):93–97.

Shanahan, Fergus, Tarini S. Ghosh, and Paul W. O’Toole. 2021. “The Healthy Microbiome-What Is the Definition of a Healthy Gut Microbiome?” *Gastroenterology* 160(2):483–94.

Shirakashi, Mirei, Mikako Maruya, Keiji Hirota, Tatsuaki Tsuruyama, Takashi Matsuo, Ryu Watanabe, Koichi Murata, Masao Tanaka, Hiromu Ito, Hajime Yoshifuji, Koichiro Ohmura, Dirk Elewaut, Shimon Sakaguchi, Sidonia Fagarasan, Tsuneyo Mimori, and Motomu Hashimoto. 2022. “Effect of Impaired T Cell Receptor Signaling on the Gut Microbiota in a Mouse Model of Systemic Autoimmunity.” *Arthritis & Rheumatology (Hoboken, N.J.)* 74(4):641–53.

Silverman, Gregg J., Jing Deng, and Doua F. Azzouz. 2022. “Sex-Dependent Lupus Blautia (Ruminococcus) Gnavus Strain Induction of Zonulin-Mediated Intestinal Permeability and Autoimmunity.” *Frontiers in Immunology* 13:897971.

Sindhava, Vishal J., Michael A. Oropallo, Krishna Moody, Martin Naradikian, Lauren E. Higdon, Lin Zhou, Arpita Myles, Nathaniel Green, Kerstin Nündel, William Stohl, Amanda M. Schmidt, Wei Cao, Stephanie Dorta-Estremera, Taku Kambayashi, Ann Marshak-Rothstein, and Michael P. Cancro. 2017. “A TLR9-Dependent Checkpoint Governs B Cell Responses to DNA-Containing Antigens.” *The Journal of Clinical Investigation* 127(5):1651–63.

Singh, Nagendra, Ashish Gurav, Sathish Sivaprakasam, Evan Brady, Ravi Padia, Huidong Shi, Muthusamy Thangaraju, Puttur D. Prasad, Santhakumar Manicassamy, David H. Munn, Jeffrey R. Lee, Stefan Offermanns, and Vadivel Ganapathy. 2014. “Activation of Gpr109a, Receptor for Niacin and the Commensal Metabolite Butyrate, Suppresses Colonic Inflammation and Carcinogenesis.” *Immunity* 40(1):128–39.

Small, Heather Y., Serena Migliarino, Marta Czesnikiewicz-Guzik, and Tomasz J. Guzik. 2018. “Hypertension: Focus on Autoimmunity and Oxidative Stress.” *Free Radical Biology & Medicine* 125:104–15.

Smith, Patrick M., Michael R. Howitt, Nicolai Panikov, Monia Michaud, Carey Ann Gallini, Mohammad Bohlooly-Y, Jonathan N. Glickman, and Wendy S. Garrett. 2013. “The Microbial Metabolites, Short-Chain Fatty Acids, Regulate Colonic Treg Cell Homeostasis.” *Science (New York, N.Y.)* 341(6145):569–73.

Somers, Emily C., Wenpu Zhao, Emily E. Lewis, Lu Wang, Jeffrey J. Wing, Baskaran Sundaram, Ella A. Kazerooni, W. Joseph McCune, and Mariana J. Kaplan. 2012. “Type I Interferons Are Associated with Subclinical Markers of Cardiovascular Disease in a Cohort of Systemic Lupus Erythematosus Patients.” *PloS One* 7(5):e37000.

Souyris, Mélanie, José E. Mejía, Julie Chaumeil, and Jean-Charles Guéry. 2019. “Female Predisposition to TLR7-Driven Autoimmunity: Gene Dosage and the Escape from X Chromosome Inactivation.” *Seminars in Immunopathology* 41(2):153–64.

Stoddart, Leigh A., Nicola J. Smith, and Graeme Milligan. 2008. “International Union of Pharmacology. LXXI. Free Fatty Acid Receptors FFA1, -2, and -3: Pharmacology and Pathophysiological Functions.” *Pharmacological Reviews* 60(4):405–17.

Szabó, Csaba, Harry Ischiropoulos, and Rafael Radi. 2007. “Peroxynitrite: Biochemistry, Pathophysiology and Development of Therapeutics.” *Nature Reviews. Drug Discovery* 6(8):662–80.

Talaat, Roba M., Sara F. Mohamed, Iman H. Bassyouni, and Ahmed A. Raouf. 2015. “Th1/Th2/Th17/Treg Cytokine Imbalance in Systemic Lupus Erythematosus (SLE) Patients: Correlation with Disease Activity.” *Cytokine* 72(2):146–53.

Tan, Jian K., Craig McKenzie, Eliana Mariño, Laurence Macia, and Charles R. Mackay. 2017. “Metabolite-Sensing G Protein-Coupled Receptors-Facilitators of Diet-Related Immune Regulation.” *Annual Review of Immunology* 35:371–402.

Tang, W. H. Wilson, Zeneng Wang, Bruce S. Levison, Robert A. Koeth, Earl B. Britt, Xiaoming Fu, Yuping Wu, and Stanley L. Hazen. 2013. “Intestinal Microbial Metabolism of Phosphatidylcholine and Cardiovascular Risk.” *The New England Journal of Medicine* 368(17):1575–84.

Taylor, Erin B., Michelle T. Barati, David W. Powell, Hannah R. Turbeville, and Michael J. Ryan. 2018. “Plasma Cell Depletion Attenuates Hypertension in an Experimental Model of Autoimmune Disease.” *Hypertension (Dallas, Tex. : 1979)* 71(4):719–28.

Taylor, Erin B. and Michael J. Ryan. 2016. “Understanding Mechanisms of Hypertension in Systemic Lupus Erythematosus.” *Therapeutic Advances in Cardiovascular Disease* 11(1):20–32.

Taylor, Erin B. and Michael J. Ryan. 2017. “Understanding Mechanisms of Hypertension in Systemic Lupus Erythematosus.” *Therapeutic Advances in Cardiovascular Disease* 11(1):20–32.

Tedeschi, Sara K., Bonnie Bermas, and Karen H. Costenbader. 2013. “Sexual Disparities in the Incidence and Course of SLE and RA.” *Clinical Immunology (Orlando, Fla.)* 149(2):211–18.

Toral, Marta, Inaki Robles-Vera, Nestor de la Visitacion, Miguel Romero, Manuel Sanchez, Manuel Gomez-Guzman, Alba Rodriguez-Nogales, Tao Yang, Rosario Jimenez, Francesca Algieri, Julio Galvez, Mohan K. Raizada, and Juan Duarte. 2019. “Role of the Immune System in Vascular Function and Blood Pressure Control Induced by Faecal Microbiota Transplantation in Rats.” *Acta Physiologica (Oxford, England)* e13285.

Toral, Marta, Inaki Robles-Vera, Miguel Romero, Nestor de la Visitacion, Manuel Sanchez, Francisco O’Valle, Alba Rodriguez-Nogales, Julio Galvez, Juan Duarte, and Rosario Jimenez. 2019. “Lactobacillus Fermentum CECT5716: A Novel Alternative for the Prevention of Vascular Disorders in a Mouse Model of Systemic Lupus Erythematosus.” *FASEB Journal : Official Publication of the Federation of American Societies for Experimental Biology* 33(9):10005–18.

Toral, Marta, Miguel Romero, Alba Rodriguez-Nogales, Rosario Jimenez, Inaki Robles-Vera, Francesca Algieri, Natalia Chueca-Porcuna, Manuel Sanchez, Nestor de la Visitacion, Monica Olivares, Federico Garcia, Francisco Perez-Vizcaino, Julio Galvez, and Juan Duarte. 2018. “Lactobacillus Fermentum Improves Tacrolimus-Induced Hypertension by Restoring Vascular Redox State and Improving ENOS Coupling.” *Molecular Nutrition & Food Research* e1800033.

Troldborg, Anne, Lisbeth Jensen, Bent Deleuran, Kristian Stengaard-Pedersen, Steffen Thiel, and Jens Christian Jensenius. 2018. “The C3dg Fragment of Complement Is Superior to Conventional C3 as a Diagnostic Biomarker in Systemic Lupus Erythematosus.” *Frontiers in Immunology* 9:581.

Tselios, Konstantinos, Charalampos Koumaras, Murray B. Urowitz, and Dafna D. Gladman. 2014. “Do Current Arterial Hypertension Treatment Guidelines Apply to Systemic Lupus Erythematosus Patients? A Critical Appraisal.” *Seminars in Arthritis and Rheumatism* 43(4):521–25.

Tsokos, George C. 2011. “Systemic Lupus Erythematosus.” *The New England Journal of Medicine* 365(22):2110–21.

Tsokos, George C. 2020. “Autoimmunity and Organ Damage in Systemic Lupus Erythematosus.” *Nature Immunology* 21(6):605–14.

Tunnicliffe, David J., Davinder Singh-Grewal, Siah Kim, Jonathan C. Craig, and Allison Tong. 2015. “Diagnosis, Monitoring, and Treatment of Systemic Lupus Erythematosus: A Systematic Review of Clinical Practice Guidelines.” *Arthritis Care & Research* 67(10):1440–52.

Uramoto, K. M., C. J. Jr Michet, J. Thumboo, J. Sunku, W. M. O’Fallon, and S. E. Gabriel. 1999. “Trends in the Incidence and Mortality of Systemic Lupus Erythematosus, 1950-1992.” *Arthritis and Rheumatism* 42(1):46–50.

Valiente, Giancarlo R., Armin Munir, Marcia L. Hart, Perry Blough, Takuma T. Wada, Emma E. Dalan, William L. Willis, Lai-Chu Wu, Aharon G. Freud, and Wael N. Jarjour. 2022. “Gut Dysbiosis Is Associated with Acceleration of Lupus Nephritis.” *Scientific Reports* 12(1):152.

Vera-Recabarren, M. A., M. García-Carrasco, M. Ramos-Casals, and C. Herrero. 2010. “Comparative Analysis of Subacute Cutaneous Lupus Erythematosus and Chronic Cutaneous Lupus Erythematosus: Clinical and Immunological Study of 270 Patients.” *The British Journal of Dermatology* 162(1):91–101.

Vinh, Antony, Wei Chen, Yelena Blinder, Daiana Weiss, W. Robert Taylor, Jörg J. Goronzy, Cornelia M. Weyand, David G. Harrison, and Tomasz J. Guzik. 2010. “Inhibition and Genetic Ablation of the B7/CD28 T-Cell Costimulation Axis Prevents Experimental Hypertension.” *Circulation* 122(24):2529–37.

Vinolo, Marco A. R., Hosana G. Rodrigues, Renato T. Nachbar, and Rui Curi. 2011. “Regulation of Inflammation by Short Chain Fatty Acids.” *Nutrients* 3(10):858–76.

Virdis, Agostino, Chiara Tani, Emiliano Duranti, Sabrina Vagnani, Linda Carli, Anja A. Kühl, Anna Solini, Chiara Baldini, Rosaria Talarico, Stefano Bombardieri, Stefano Taddei, and Marta Mosca. 2015. “Early Treatment with Hydroxychloroquine Prevents the Development of Endothelial Dysfunction in a Murine Model of Systemic Lupus Erythematosus.” *Arthritis Research & Therapy* 17:277.

Walker, J. M. 1994. “The Bicinchoninic Acid (BCA) Assay for Protein Quantitation.” *Methods in Molecular Biology (Clifton, N.J.)* 32:5–8.

Wang, P., Z. F. Ba, and I. H. Chaudry. 1994. “Administration of Tumor Necrosis Factor-Alpha in Vivo Depresses Endothelium-Dependent Relaxation.” *The American Journal of Physiology* 266(6 Pt 2):H2535-41.

Wang, Zeneng, Elizabeth Klipfell, Brian J. Bennett, Robert Koeth, Bruce S. Levison, Brandon Dugar, Ariel E. Feldstein, Earl B. Britt, Xiaoming Fu, Yoon-Mi Chung, Yuping Wu, Phil Schauer, Jonathan D. Smith, Hooman Allayee, W. H. Wilson Tang, Joseph A. DiDonato, Aldons J. Lusis, and Stanley L. Hazen. 2011. “Gut Flora Metabolism of Phosphatidylcholine Promotes Cardiovascular Disease.” *Nature* 472(7341):57–63.

Wang, Zeneng, Bruce S. Levison, Jennie E. Hazen, Lillian Donahue, Xin-Min Li, and Stanley L. Hazen. 2014. “Measurement of Trimethylamine-N-Oxide by Stable Isotope Dilution Liquid Chromatography Tandem Mass Spectrometry.” *Analytical Biochemistry* 455:35–40.

Ward, M. M. and S. Studenski. 1992. “Clinical Prognostic Factors in Lupus Nephritis. The Importance of Hypertension and Smoking.” *Archives of Internal Medicine* 152(10):2082–88.

Wenink, Mark H., Kim C. M. Santegoets, Jacobus C. A. Broen, Lenny van Bon, Shahla Abdollahi-Roodsaz, Calin Popa, Richard Huijbens, Thijs Remijn, Erik Lubberts, Piet L. C. M. van Riel, Wim B. van den Berg, and Timothy R. D. J. Radstake. 2009. “TLR2 Promotes Th2/Th17 Responses via TLR4 and TLR7/8 by Abrogating the Type I IFN Amplification Loop.” *Journal of Immunology (Baltimore, Md. : 1950)* 183(11):6960–70.

Wenzel, Katrin, Hannelore Haase, Gerd Wallukat, Wolfgang Derer, Sabine Bartel, Volker Homuth, Florian Herse, Norbert Hubner, Herbert Schulz, Marion Janczikowski, Carsten Lindschau, Christoph Schroeder, Stefan Verlohren, Ingo Morano, Dominik N. Muller, Friedrich C. Luft, Rainer Dietz, Ralf Dechend, and Peter Karczewski. 2008. “Potential Relevance of Alpha(1)-Adrenergic Receptor Autoantibodies in Refractory Hypertension.” *PloS One* 3(11):e3742.

Wofsy, David, Nancy Y. Chiang, John S. Greenspan, and Thomas H. Ermak. 1988. “Treatment of Murine Lupus with Monoclonal Antibody to L3T4. I. Effects on the Distribution and Function of Lymphocyte Subsets and on the Histopathology of Autoimmune Disease.” *Journal of Autoimmunity* 1(5):415–31.

Wolf, Victoria L. and Michael J. Ryan. 2019. “Autoimmune Disease-Associated Hypertension.” *Current Hypertension Reports* 21(1):10.

Wu, Jing, Mohamed A. Saleh, Annet Kirabo, Hana A. Itani, Kim Ramil C. Montaniel, Liang Xiao, Wei Chen, Raymond L. Mernaugh, Hua Cai, Kenneth E. Bernstein, Jörg J. Goronzy, Cornelia M. Weyand, John A. Curci, Natalia R. Barbaro, Heitor Moreno, Sean S. Davies, L. Jackson 2nd Roberts, Meena S. Madhur,

and David G. Harrison. 2016. “Immune Activation Caused by Vascular Oxidation Promotes Fibrosis and Hypertension.” *The Journal of Clinical Investigation* 126(1):50–67.

Wu, Kunpeng, Yan Yuan, Huihui Yu, Xin Dai, Shu Wang, Zhengxu Sun, Fen Wang, He Fei, Qiwang Lin, Hua Jiang, and Tong Chen. 2020. “The Gut Microbial Metabolite Trimethylamine N-Oxide Aggravates GVHD by Inducing M1 Macrophage Polarization in Mice.” *Blood* 136(4):501–15.

Xia, Wen-Jie, Meng-Lu Xu, Xiao-Jing Yu, Meng-Meng Du, Xu-Hui Li, Tao Yang, Lu Li, Ying Li, Kai B. Kang, Qing Su, Jia-Xi Xu, Xiao-Lian Shi, Xiao-Min Wang, Hong-Bao Li, and Yu-Ming Kang. 2021. “Antihypertensive Effects of Exercise Involve Reshaping of Gut Microbiota and Improvement of Gut-Brain Axis in Spontaneously Hypertensive Rat.” *Gut Microbes* 13(1):1–24.

Xing, Chao, Andrea L. Sestak, Jennifer A. Kelly, Kim L. Nguyen, Gail R. Bruner, John B. Harley, and Courtney Gray-McGuire. 2007. “Localization and Replication of the Systemic Lupus Erythematosus Linkage Signal at 4p16: Interaction with 2p11, 12q24 and 19q13 in European Americans.” *Human Genetics* 120(5):623–31.

Yang, John Jackson, Minh Tan Pham, Adelia Riezka Rahim, Tsung-Hsien Chuang, Ming-Fa Hsieh, and Chun-Ming Huang. 2020. “Mouse Abdominal Fat Depots Reduced by Butyric Acid-Producing Leuconostoc Mesenteroides.” *Microorganisms* 8(8).

Ye, Yan, Mei Liu, Longhai Tang, Fang Du, Yuanhua Liu, Pei Hao, Qiong Fu, Qiang Guo, Qingran Yan, Xiaoming Zhang, and Chunde Bao. 2019. “Iguratimod Represses B Cell Terminal Differentiation Linked with the Inhibition of PKC/EGR1 Axis.” *Arthritis Research & Therapy* 21(1):92.

Yokogawa, Maki, Mikiro Takaishi, Kimiko Nakajima, Reiko Kamijima, Chisa Fujimoto, Sayo Kataoka, Yoshio Terada, and Shigetoshi Sano. 2014. “Epicutaneous Application of Toll-like Receptor 7 Agonists Leads to Systemic Autoimmunity in Wild-Type Mice: A New Model of Systemic Lupus Erythematosus.” *Arthritis & Rheumatology (Hoboken, N.J.)* 66(3):694–706.

Zegarra-Ruiz, Daniel F., Asmaa El Beidaq, Alonso J. Iniguez, Martina Lubrano Di Ricco, Silvio Manfredo Vieira, William E. Ruff, Derek Mubiru, Rebecca L. Fine, John Sterpka, Teri M. Greiling, Carina Dehner, and Martin A. Kriegel. 2019. “A Diet-Sensitive Commensal Lactobacillus Strain Mediates TLR7-Dependent Systemic Autoimmunity.” *Cell Host & Microbe* 25(1):113-127.e6.

Zeng, Qiang, Dongfang Li, Yuan He, Yinhu Li, Zhenyu Yang, Xiaolan Zhao, Yanhong Liu, Yu Wang, Jing Sun, Xin Feng, Fei Wang, Jiaxing Chen, Yuejie Zheng, Yonghong Yang, Xuelin Sun, Ximing Xu, Daxi Wang, Toby Kenney, Yiqi Jiang, Hong Gu, Yongli Li, Ke Zhou, Shuaicheng Li, and Wenkui Dai. 2019. “Discrepant Gut Microbiota Markers for the Classification of Obesity-Related Metabolic Abnormalities.” *Scientific Reports* 9(1):13424.

Zhang, Husen, Xiaofeng Liao, Joshua B. Sparks, and Xin M. Luo. 2014. “Dynamics of Gut Microbiota in Autoimmune Lupus.” *Applied and Environmental Microbiology* 80(24):7551–60.

Zhang, Lingshu, Pingying Qing, Hang Yang, Yongkang Wu, Yi Liu, and Yubin Luo. 2021. “Gut Microbiome and Metabolites in Systemic Lupus Erythematosus: Link, Mechanisms and Intervention.” *Frontiers in Immunology* 12:686501.

Zhang, Ming, Gang Yu, Brian Chan, Joshua T. Pearson, Palaniswami Rathanaswami, John Delaney, Ai Ching Lim, John Babcook, Hailing Hsu, and Marc A. Gavin. 2015. “Interleukin-21 Receptor Blockade Inhibits Secondary Humoral Responses and Halts the Progression of Preestablished Disease in the (NZB × NZW)F1 Systemic Lupus Erythematosus Model.” *Arthritis & Rheumatology (Hoboken, N.J.)* 67(10):2723–31.

Zhang, Rong M., Kyle P. McNerney, Amy E. Riek, and Carlos Bernal-Mizrachi. 2021. “Immunity and Hypertension.” *Acta Physiologica (Oxford, England)* 231(1):e13487.

Zhang, Xiuli, Yining Li, Pingzhen Yang, Xiaoyu Liu, Lihe Lu, Yanting Chen, Xinglong Zhong, Zehua Li, Hailin Liu, Caiwen Ou, Jianyun Yan, and Minsheng Chen. 2020. “Trimethylamine-N-Oxide Promotes Vascular Calcification Through Activation of NLRP3 (Nucleotide-Binding Domain, Leucine-Rich-Containing Family, Pyrin Domain-Containing-3) Inflammasome and NF-KB (Nuclear Factor KB) Signals.” *Arteriosclerosis, Thrombosis, and Vascular Biology* 40(3):751–65.

Zhao, Shuang and Liang Li. 2018. “Dansylhydrazine Isotope Labeling LC-MS for Comprehensive Carboxylic Acid Submetabolome Profiling.” *Analytical Chemistry* 90(22):13514–22.

Zheng, Xia-xia, Tian Zhou, Xin-An Wang, Xiao-hong Tong, and Jia-wang Ding. 2015. “Histone Deacetylases and Atherosclerosis.” *Atherosclerosis* 240(2):355–66.

Zhou, Hong-Wei, Dong-Fang Li, Nora Fung-Yee Tam, Xiao-Tao Jiang, Hai Zhang, Hua-Fang Sheng, Jin Qin, Xiao Liu, and Fei Zou. 2011. “BIPES, a Cost-Effective High-Throughput Method for Assessing Microbial Diversity.” *The ISME Journal* 5(4):741–49.

Zhu, Weifei, Jill C. Gregory, Elin Org, Jennifer A. Buffa, Nilaksh Gupta, Zeneng Wang, Lin Li, Xiaoming Fu, Yuping Wu, Margarete Mehrabian, R. Balfour Sartor, Thomas M. McIntyre, Roy L. Silverstein, W. H. Wilson Tang, Joseph A. DiDonato, J. Mark Brown, Aldons J. Lusis, and Stanley L. Hazen. 2016. “Gut Microbial Metabolite TMAO Enhances Platelet Hyperreactivity and Thrombosis Risk.” *Cell* 165(1):111–24.

Zhu, Weifei, Zeneng Wang, W. H. Wilson Tang, and Stanley L. Hazen. 2017. “Gut Microbe-Generated Trimethylamine N-Oxide From Dietary Choline Is Prothrombotic in Subjects.” *Circulation* 135(17):1671–73.